

IL
NUOVO CIMENTO
ORGANO DELLA SOCIETÀ ITALIANA DI FISICA
SOTTO GLI AUSPICI DEL CONSIGLIO NAZIONALE DELLE RICERCHE

VOL. VII, N. 6

Serie decima

16 Marzo 1958

Fotoprotoni dall'ossigeno.

C. MILONE, S. MILONE-TAMBURINO, R. RINZIVILLO e A. RUBBINO

*Istituto di Fisica dell'Università - Catania
Centro Siciliano di Fisica Nucleare - Catania*

C. TRIBUNO

*Istituto di Fisica dell'Università - Torino
Istituto Nazionale di Fisica Nucleare - Sezione di Torino*

(ricevuto il 21 Settembre 1957)

Riassunto. — Si studia lo spettro dei fotoprotoni dall'Ossigeno esponendo targhette gassose ai raggi γ del betatron di 31 MeV dell'Istituto di Fisica dell'Università di Torino. Sono stati eseguiti irraggiamenti ad energia massima di 23, 26, 30 MeV. L'incertezza nell'energia dei protoni per quanto riguarda lo spessore della targhetta va da 0.15 MeV per protoni di 2 MeV a 0.02 MeV per protoni di 15 MeV. Gli spettri a 23 e 26 MeV mostrano una struttura fine con delle risonanze in assorbimento per $E_\gamma = 18.8, 19.3, 20.6$ e 22.2 MeV, in buon accordo con le risonanze trovate da altri autori. Gli spettri a 30 MeV mettono inoltre in evidenza altre risonanze a 24 (e 25.5) MeV. La resa/mole/roentgen fino a 30 MeV risulta \sim il 20% più alta della resa fino a 26 MeV. Si dà l'andamento della sezione d'urto per protoni che lasciano ^{15}N solo nello stato fondamentale; si mette in evidenza il contributo dei protoni che lasciano ^{15}N in livelli eccitati, e si dà l'andamento della sezione d'urto tenendo conto anche di questi protoni.

1. - Introduzione.

Diversi autori (1-4) hanno mostrato che lo spettro dei fotoprotoni dall'Ossigeno presenta una struttura fine. Alcune misure (2) sono state eseguite con fotoni aventi energia massima di 21 MeV, e quindi non comprendono la zona della risonanza gigante, la quale presenta il massimo sopra i 22 MeV.

Altre misure (1-3,4), sono state eseguite con fotoni aventi energia massima di $25 \div 26$ MeV (*). Poiché in un precedente lavoro (5) avevamo trovato che la resa per processi $O(\gamma, p)$ sopra i 25 MeV non è trascurabile, abbiamo ritenuto opportuno studiare lo spettro dei fotoprotoni dall'Ossigeno sperimentando con fotoni fino ad energia massima di 30 MeV.

I primi risultati di questo lavoro sono stati comunicati all'Accademia Gioenia di Catania (6).

2. - Dispositivo sperimentale.

Per avere informazioni dirette sullo spettro dei fotoprotoni è essenziale che lo spessore della targhetta bombardata dai raggi γ sia « piccolo » rispetto al percorso dei protoni.

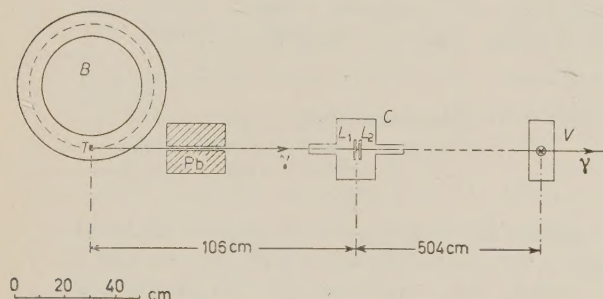


Fig. 1a. - Dispositivo sperimentale: B = betatrone; T = targhetta del betatrone; C = « camera » di esposizione contenente ossigeno; L = lastre per la rivelazione dei protoni; V = Victoreen per la misura di dose.

Nel nostro caso lo spessore della targhetta gasosa era di 1.8 mg/cm^2 cui corrisponde una incertezza nella energia dei protoni rivelati, che va da $\pm 0.15 \text{ MeV}$ per protoni di 2 MeV a $\pm 0.02 \text{ MeV}$ per protoni di 15 MeV.

Sono state eseguite tre esposizioni ai fotoni del betatrone B.B.C. di Torino irradiando successiva-

(1) W. E. STEPHENS, A. K. MANN, B. J. PATTON and E. J. WINHOLD: *Phys. Rev.*, **98**, 839 (1955).

(2) S. A. E. JOHANSON e B. FORKMAN: *Phys. Rev.*, **99**, 1031 (1955).

(3) L. COHEN, A. K. MANN, B. J. PATTON, K. REEBEL, W. E. STEPHENS e E. J. WINHOLD: *Phys. Rev.*, **104**, 108 (1956).

(4) S. A. E. JOHANSON e B. FORKMAN: Comunicazione privata.

(*) Di queste misure siano venuti a conoscenza quando il presente lavoro era già stato iniziato.

(5) C. MILONE, R. RICAMO e R. RINZIVILLO: *Nuovo Cimento*, **5**, 532 (1957).

(6) C. MILONE, S. MILONE-TAMBURINO, R. RINZIVILLO, A. RUBBINO e C. TRIBUNO: *Boll. Acc. Gioenia*, **69**, 434 (1957).

mente alle energie massime di 23, di 26 e di 30 MeV. I protoni venivano rivelati mediante emulsioni nucleari Ilford C₂ di 200 μ m di spessore, aventi dimensioni di 75 mm \times 75 mm ed un foro centrale di 25 mm di diametro, attraverso il quale passava con largo margine il fascio di fotoni collimato mediante un canale praticato entro uno schermo di piombo di 24 cm di spessore (Fig. 1). Tali emulsioni, disposte normalmente al fascio dei fotoni, erano racchiuse entro una «camera» contenente ossigeno e distavano 106 cm dalla sorgente dei fotoni.

Gli spettri ottenuti si riferiscono ai protoni emessi con un angolo θ compreso fra 90° e 115° rispetto alla direzione dei fotoni (Fig. 1b). Le dosi di esposizione sono state misurate mediante una camera Victoreen posta entro un blocco di plexiglas a 608 cm dalla sorgente dei fotoni.

I dati sperimentali sono riassunti nella Tabella I.

TABELLA I.

Energia massima dei fotoni (MeV) . . .	23	26	30	30
Röntgen (alla posizione della targhetta) . . .	4600	4900	5100	5200
Pressione dell'Ossigeno (atmosfere) . . .	1.20	1.20	1.02	3.00
Superficie esplorata (cm ²)	3.6	3.4	4.2	0.76
Numero di tracce di protoni osservate . .	406	902	1136	609
Resa/mole/röntgen relativa alla resa a 30 MeV (esposizione con $p=1$ atmosfera)	0.38	0.85	1	—

Ogni lastra è stata esplorata secondo corone circolari i cui centri coincidevano col centro geometrico della lastra stessa (Fig. 1b). A tal fine sono stati impiegati dei microscopi con tavolino girevole attorno al centro della lastra. I raggi delle corone esplorate variavano da 30 mm a 32 mm. La regione della targhetta gassosa da cui potevano provenire tracce di protoni sulle corone circolari esplorate era molto ben definita geometricamente sicché le tracce dovevano avere nelle lastre direzione quasi radiale e inclinazione ben determinata. Pertanto le tracce potevano essere sottoposte ad un controllo piuttosto rigoroso: non venivano accettate tracce aventi una dispersione angolare maggiore di $\Delta\varphi$ (Fig. 1b). Una analoga condizione di accettazione veniva imposta per l'angolo di inclinazione. Tali condizioni peraltro,

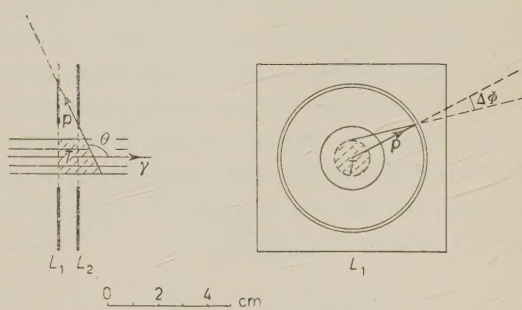


Fig. 1b. – Disposizione delle lastre per la rivelazione dei fotoprotoni: T = Targhetta gassosa bombardata dai fotoni; p = fotoprotone.

risultavano soddisfatte dalla quasi totalità delle tracce. Di conseguenza il fondo risultava trascurabile ($< 3\%$ per tutte le energie considerate e $\ll 1\%$ sopra 5 MeV).

Gli spettri di energia sono stati ottenuti dalla distribuzione in «range» (R) delle tracce di protoni osservate dentro l'emulsione aggiungendo ad ogni traccia uno spessore costante ΔR di emulsione equivalente al percorso medio del protone nel gas; $\Delta R = 15 \mu\text{m}$ nelle esposizioni ad una atmosfera.

Le tracce di protoni aventi in emulsione un «range» inferiore a $25 \mu\text{m}$ sono state trascurate, per cui — tenendo conto dei $15 \pm 4 \mu\text{m}$ equivalenti al percorso del protone nel gas — si ha un taglio nello spettro dei protoni per energia inferiore a 2 MeV.

3. — Risultati.

I risultati ottenuti sono riassunti nelle Fig. 2, 3, 4. In tali figure in ascisse, accanto all'energia E_p dei protoni in MeV, è riportata una seconda scala in cui è indicata una energia E_γ dedotta dalla relazione: $E_\gamma = (16/15)E_p + E_s$

essendo $E_s = 12.1 \text{ MeV}$ l'energia di soglia del processo $O(\gamma, p)$. Pertanto, nel caso in cui i protoni emessi lasciano il nucleo residuo ^{15}N nello stato fondamentale, E_γ rappresenta l'energia dei fotoni che hanno dato luogo ad emissione di protoni di energia E_p .

Nel caso generale, se E_x è l'energia del livello in cui viene lasciato il nucleo residuo ^{15}N , l'energia E_γ del fotone che ha dato luogo al protone di energia E_p è: $E_\gamma = (16/15)E_p + E_s + E_x$.

Per $E_p > 8 \text{ MeV}$ una piccola percentuale (10%) di protoni attraversava tutto lo spessore dell'emulsione e penetrava nel vetro. Tale percentuale è stata

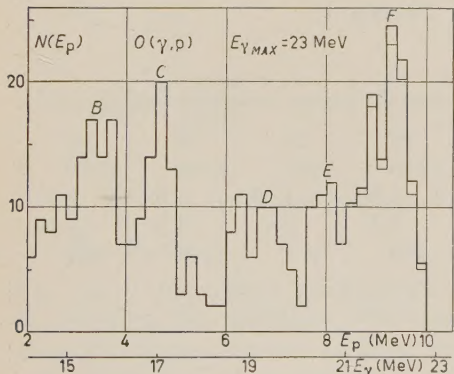


Fig. 2. — Spettro dei fotoprotoni dall'ossigeno nelle esposizioni ad $E_{\gamma\text{max}} = 23 \text{ MeV}$.

distribuita nello spettro col procedimento seguente: un primo spettro «non corretto» è stato desunto dalle sole tracce terminanti in emulsione. Successivamente, per ogni intervallo di energia, in base alle condizioni geometriche, è stata calcolata la probabilità che il percorso dei protoni finisca fuori dell'emulsione. In base a tale probabilità si è ricavato uno spettro «corretto». La correzione (del resto molto piccola) porta ad aggiungere un numero totale di tracce che coincide ottimamente con quello delle tracce uscenti. Nelle Fig. 2, 3, 4, è

riportato a tratto grosso lo spettro « corretto » e a tratto sottile lo spettro « non corretto ».

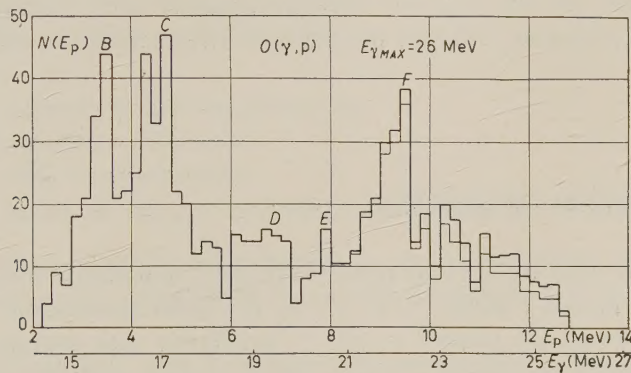


Fig. 3. — Spettro dei fotoprotoni dall'ossigeno nelle esposizioni ad $E_{\gamma_{\max}} = 26$ MeV.

Lo spettro riportato nella Fig. 4b è stato ottenuto, come quello riportato nella Fig. 4a, irradiando con fotoni aventi $E_{\gamma_{\max}} = 30$ MeV; le condizioni sperimentali differivano soltanto per il valore della pressione dell'ossigeno la

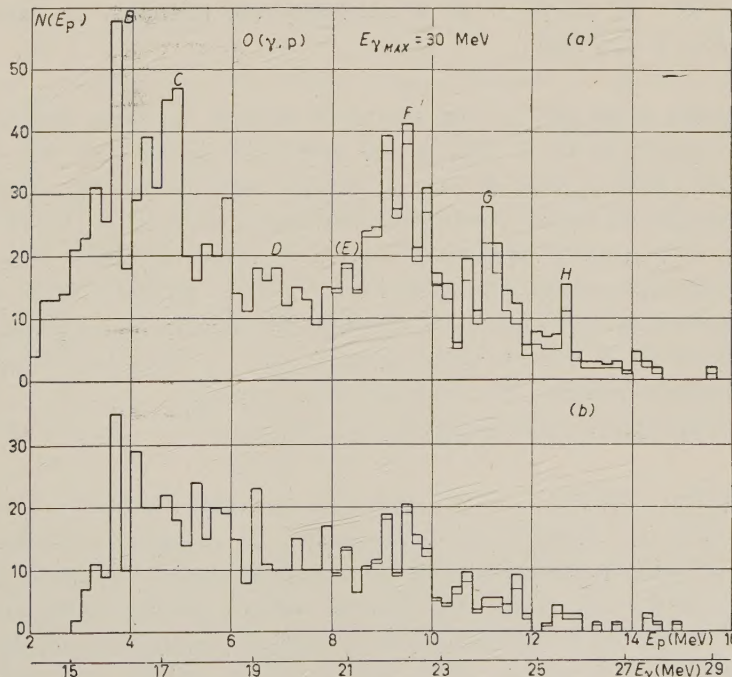


Fig. 4. — Spettro dei fotoprotoni dall'ossigeno nelle esposizioni ad $E_{\gamma_{\max}} = 30$ MeV.
a) pressione dell'ossigeno = 1 atmosfera; b) pressione dell'ossigeno = 3 atmosfere.

quale era di 3 atmosfere nel caso della Fig. 4b. Di conseguenza, a causa della maggiore perdita di energia nel gas, nello spettro della Fig. 4b si ha un taglio per $E_p < 3$ MeV ed una maggiore indeterminazione nella energia dei protoni. L'accordo fra i risultati ottenuti nei due casi risulta tuttavia abbastanza soddisfacente.

4. – Interpretazione dei risultati.

4.1. *Spettri a 23 MeV.* – Gli spettri ottenuti irradiando con $E_{\gamma_{\max}} = 23$ MeV mettono in evidenza i picchi *B*, *C*, *D*, *E*, *F* i quali concordano ottimamente con quelli ottenuti da COHEN e coll. (3) irradiando alla energia massima di 25 MeV. Si osservi che poichè il primo livello eccitato del ^{15}N è $E_{x1} = 5.3$ MeV, essendo $E_{\gamma_{\max}} = 23$ MeV ed $E_s = 12.1$ MeV, i protoni con energia $E_p > 15/16 \cdot (E_{\gamma_{\max}} - E_s - E_{x1}) = 5.2$ MeV lasciano il nucleo residuo ^{15}N nello stato fondamentale. Ne segue che ai picchi nello spettro di energia dei protoni per $E_p > 5.2$ MeV corrispondono picchi nell'assorbimento dei fotoni di energia $E_{\gamma} = (16/15)E_p + 12.1$ MeV. In particolare al massimo per $E_p = 9.3$ MeV (picco *F*) corrisponde un massimo nell'assorbimento dei fotoni di energia $E_{\gamma} \geq 22.1$ MeV. Ai picchi *D* ed *E* corrispondono risonanze in assorbimento per $E_{\gamma} \sim 19.3$ e 20.6 MeV.

4.2. *Spettri a 26 MeV.* – Gli spettri a 26 MeV mettono chiaramente in evidenza i picchi *B*, *C*, *F* (Fig. 3). Il picco *F* è dovuto ad una risonanza intorno a 22.2 MeV. I picchi *B* e *C* non possono essere attribuiti esclusivamente ad assorbimento di fotoni aventi rispettivamente energia $E_{\gamma_1} = 16$ ed $E_{\gamma_2} = 17$ MeV in quanto a circa pari numero di fotoni incidenti essi risultano molto più alti nelle esposizioni a 26 che in quelle a 23 MeV. Dalla differenza fra i due spettri si ricava che detti massimi derivano in buona parte da assorbimento di fotoni di energia superiore a 22 MeV con emissione di protoni che lasciano il nucleo residuo ^{15}N nei primi livelli eccitati.

Discuteremo più in esteso questa parte nel seguito.

4.3. *Spettro a 30 MeV.* – Negli spettri dei protoni ottenuti con irradiazioni a 30 MeV (Fig. 4) esistono protoni con energia E_p maggiore di 13 MeV, la cui emissione è dovuta ad assorbimento di fotoni di energia E_{γ} maggiore di 26 MeV ($(16/15)13 + 12.1 = 26$). Si ha così evidenza di una sezione d'urto non trascurabile al di sopra dei 26 MeV. Gli spettri, oltre ai gruppi *B*, *C*, *D*, *E*, *F* precedenti mettono in evidenza degli altri gruppi *G* (ed *H*) cui corrispondono risonanze in assorbimento per $E_{\gamma} = 24$ MeV (ed $E_{\gamma} = 25.5$ MeV).

Poichè le condizioni geometriche erano le stesse nelle tre esposizioni ad

$E_{\gamma \text{ max}} = 23, 26, 30 \text{ MeV}$, la resa Y in numero di protoni/mole/röntgen è proporzionale ad

$$\frac{N}{S \cdot D \cdot p}$$

in cui: N = numero di protoni osservati;

S = superficie esplorata;

D = dose di esposizione;

p = pressione del gas contenuto nella « camera » di esposizione.

Segue, in base ai valori della Tabella I, che posta eguale ad 1 la resa a 30 MeV, le rese a 23 e 26 MeV risultano rispettivamente 0.38 e 0.85.

4.4. Sezione d'urto. — Per il calcolo della sezione d'urto è necessario conoscere lo spettro $N(E_{\gamma}, E_{\gamma \text{ max}})$ dei fotoni emessi dal Betatron. Nota la dose in röntgen si può calcolare il numero dei fotoni/cm²/MeV in base ai valori riportati

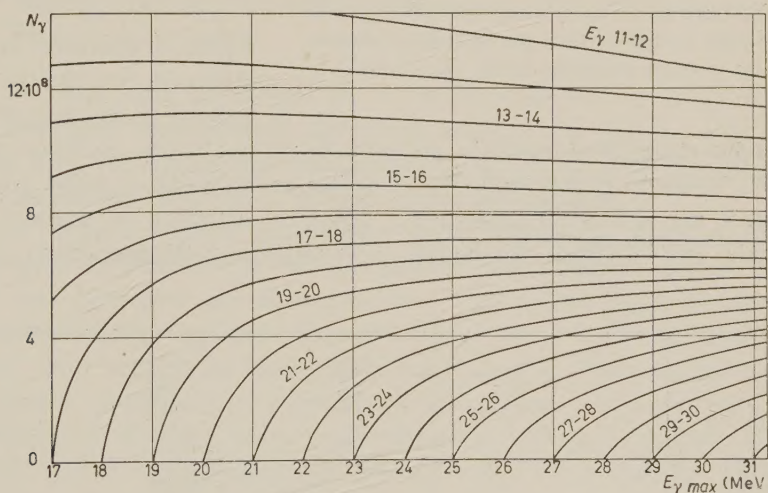


Fig. 5. — N = numero di fotoni/cm² per E_{γ} compreso nell'intervallo di energia di 1 MeV indicato nelle varie curve e per 100 röntgen in funzione della energia massima $E_{\gamma \text{ max}}$ di funzionamento del betatron.

da vari autori (7,8) fino ad energie massime di 27 MeV. Per estrapolazione abbiamo ottenuto dai dati predetti i grafici riportati nella Fig. 5, dai quali abbiamo ricavato le distribuzioni dei fotoni emessi dal Betatron quando lavora rispettivamente alle energie di 23, 26, 30 MeV (Fig. 6).

(7) H. E. JOHNS, L. KATZ, R. DOUGLAS e R. HASLAM: *Phys. Rev.*, **40**, 1062 (1950).

(8) L. KATZ e A. G. W. CAMERON: *Canad. Journ. Phys.*, **29**, 518 (1951).

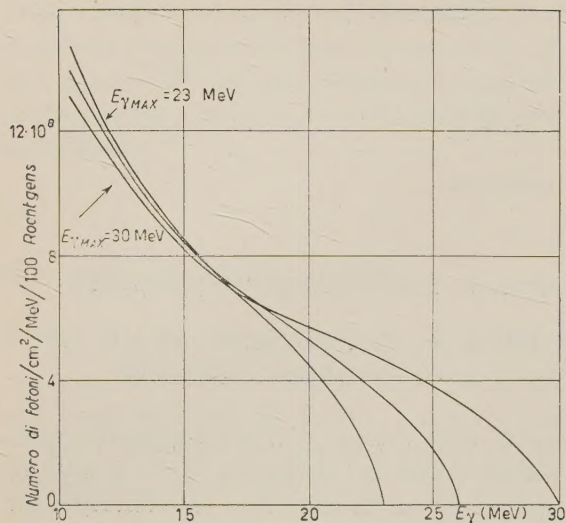


Fig. 6. – Numero di fotoni per cm^2 per MeV e per una dose totale di 100 röntgen per betatrone funzionante alle energie massime di 23, 26, 30 MeV.

4.4.1. – Un calcolo della sezione d'urto nell'ipotesi che i fotoni assorbiti provochino l'emissione di protoni che lasciano il nucleo residuo ^{15}N solo nello stato fondamentale è stato eseguito da diversi autori (1,2). Noi abbiamo voluto eseguire un calcolo di questo tipo mediante gli spettri sperimentali ottenuti con le irradiazioni a 23, 26, 30 MeV utilizzando però, di tali spettri, *soltanto* i protoni con energia E_p compresa tra ($E_{\gamma\text{max}} - E_s - 5.2$ MeV) ed ($E_{\gamma\text{max}} - E_s$). I protoni compresi in questo intervallo energetico hanno *certamente* lasciato il nucleo

residuo nello stato fondamentale essendo il primo livello eccitato del ^{15}N a 5.3 MeV. Tenendo conto degli spettri di bremsstrahlung e delle condizioni sperimentali nei diversi irraggiamenti, abbiamo ottenuto la sezione d'urto differenziale in funzione dell'energia E_γ riportata nell'istogramma A) della

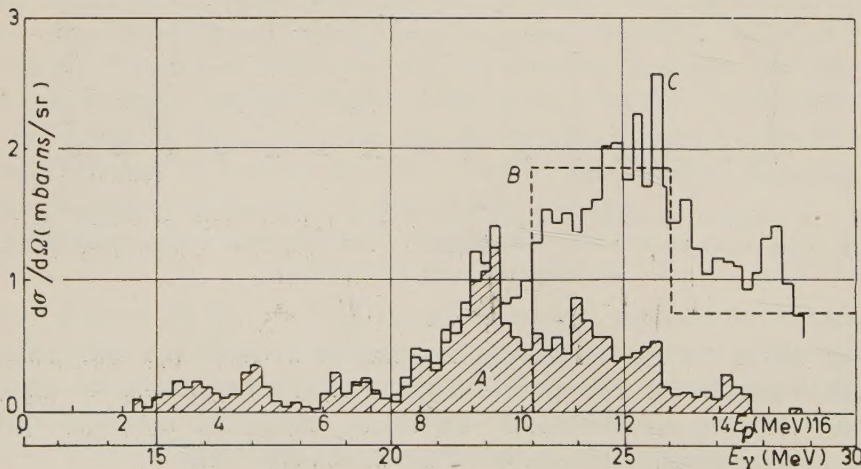


Fig. 7. – Sezione d'urto del processo $\text{O}(\gamma, p)$: A) verso lo stato fondamentale del ^{15}N ; B) sezione d'urto media negli intervalli 23–26 e 26–30 MeV; C) andamento della sezione d'urto nelle ipotesi della Sez. 4.4.1 del testo.

Fig. 7. Il raccordo fra le diverse regioni di tale istogramma era del tutto soddisfacente. La curva *A*) della Fig. 7 rappresenta dunque la sezione d'urto del processo $O(\gamma, p)$ verso lo stato fondamentale. In essa si nota per E_γ fra 15 e 18 MeV la « piccola risonanza » messa in evidenza da altri autori ed attribuita ad assorbimento di dipolo magnetico o di quadrupolo elettrico e una grande risonanza intorno a 22 MeV. La sezione d'urto $d\sigma/d\Omega$ della Fig. 7 si riferisce a protoni emessi con un angolo θ compreso fra 90° e 115° rispetto ai γ .

In ordinate sono riportati i valori

$$\frac{d\sigma}{d\Omega} = \frac{N(E_p)}{I_\gamma(E_s + (16/15)E_p)} \frac{1}{n_0 \Omega},$$

in cui:

$N(E_p)$ = numero di protoni di energia E_p che emessi dalla targhetta di ossigeno vengono rivelati dalla lastra sotto un angolo di accettazione Ω ;

$I_\gamma(E_s + (16/15)E_p)$ = numero di fotoni/cm² aventi energia $E_\gamma = E_s + (16/15)E_p$;

n_0 = numero di atomi della targhetta di ossigeno che contribuiscono a inviare protoni sulla lastra.

4.4.2. – Nella zona di energia che va da 23 a 30 MeV la maggioranza dei processi determina stati eccitati del nucleo residuo. In queste condizioni non esiste più una corrispondenza biunivoca fra E_p ed E_γ cosicchè diventa impossibile un calcolo sicuro della sezione d'urto differenziale.

Si può tuttavia tentare di spingere oltre l'analisi dei risultati. In primo luogo occorre determinare le rese in protoni che lasciano eccitato il nucleo residuo. Ciò può farsi per differenza fra i vari spettri normalizzandoli alle stesse condizioni sperimentali tenendo conto anche dello spettro di bremsstrahlung. Per esempio, la curva della Fig. 8 è stata ottenuta per differenza tra lo spettro sperimentale a 26 MeV e lo spettro a 23 MeV normalizzato da 23 MeV a 26 MeV. L'esame della curva così ottenuta mostra che nell'intervallo di energia E_p compreso tra 2 MeV e 8 MeV c'è un notevole contributo di protoni che sono stati emessi in seguito ad assorbimento di fotoni aventi energia compresa tra 23 e 26 MeV e che pertanto hanno lasciato il nucleo residuo ^{15}N in livelli eccitati.

Si nota in particolare un notevole contributo di protoni intorno a 3.5 e 4.3 MeV i quali permettono di interpretare l'aumento dell'altezza relativa dei picchi *B* e *C* quando si passa dalle irradiazioni a 23 MeV alle irradiazioni ad energie più elevate (Fig. 2, 3, 4).

Si noti che essendo $E_{\gamma_{\max}} = 26$ MeV i protoni che hanno lasciato il nucleo residuo in un livello eccitato non possono avere energia E_p maggiore di 8 MeV:

$$E_p = \frac{15}{16} (E_{\gamma_{\max}} - E_s - E_x) \cong 8 \text{ MeV}.$$

Pertanto ci si aspetta che oltre 8 MeV la differenza fra i due spettri sia nulla, cosa che risulta effettivamente entro gli errori fino a 10 MeV (Fig. 8). Al di sopra di $E_p = 10$ MeV il contributo dello spettro a 23 MeV scompare e resta soltanto nella differenza lo spettro sperimentale a 26 MeV.

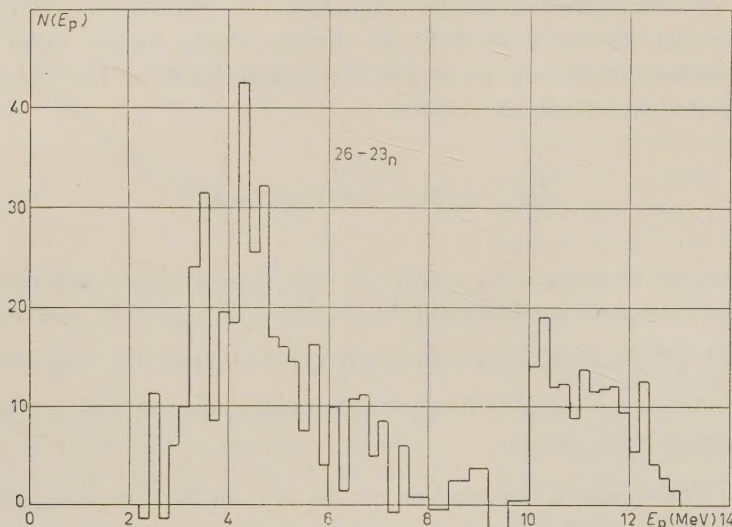


Fig. 8. – Differenza tra lo spettro a 26 MeV e lo spettro a 23 MeV normalizzato da 23 a 26 MeV.

In questa zona di energia i protoni emessi hanno lasciato il nucleo residuo ^{15}N nello stato fondamentale.

L'analogia differenza fra lo spettro a 30 MeV e quello normalizzato da 26 MeV a 30 MeV è riportata nella Fig. 9.

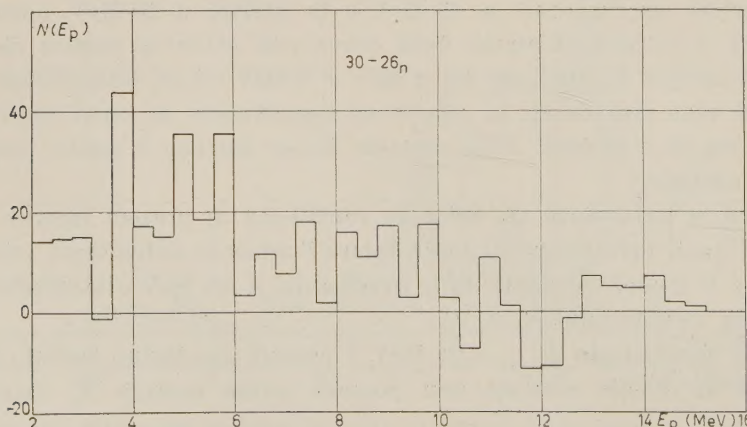


Fig. 9. – Differenza fra lo spettro a 30 MeV e lo spettro a 26 MeV normalizzato da 26 a 30 MeV.

4.4.3. – Nel modo finora esposto ci siamo procurati i valori delle rese in protoni $[N(E_p)]_{\gamma_1}^{6}$ e $[N(E_p)]_{\gamma_1}^{30}$ nei due intervalli di energia considerati.

Ora si ha

$$[N(E_p)]_{E_{\gamma_1}}^{E_{\gamma_2}} = \text{const} \cdot \int_{E_{\gamma_1}}^{E_{\gamma_2}} \sigma(E_{\gamma}) I(E_{\gamma}) dE_{\gamma},$$

con $\sigma(E_{\gamma})$ = sezione d'urto (γ , p);

$I(E_{\gamma})$ = spettro di bremsstrahlung.

In assenza di una corrispondenza biunivoca tra E_p ed E_{γ} si può, a titolo orientativo, valutare sia pure grossolanamente la sezione d'urto integrata ammettendo che la sezione d'urto non vari bruscamente nell'intervallo di energia $E_{\gamma_1} \div E_{\gamma_2}$ considerato. Sotto tale ipotesi si può porre

$$[N(E_p)]_{E_{\gamma_1}}^{E_{\gamma_2}} = \text{const} \sigma(E_{\gamma}) \int_{E_{\gamma_1}}^{E_{\gamma_2}} I(E_{\gamma}) dE_{\gamma},$$

e si ottiene la sezione d'urto media riportata a tratto punteggiato nell'istogramma *B* della Fig. 7 per gli intervalli di energia compresi fra 23 e 26 MeV e fra 26 e 30 MeV. Nel calcolare tale sezione d'urto media alle differenze 26 – 23 normal. e 30 – 26 normal. delle Fig. 8 e 9 è stata apportata una correzione per tenere conto del fatto che la normalizzazione per lo spettro di bremsstrahlung (Fig. 6) nel caso di protoni provenienti da livelli eccitati è diversa che nel caso di protoni che lasciano ^{15}N nello stato fondamentale. Di ciò si è pure tenuto conto nel calcolo riportato nel paragrafo successivo.

4.4.4. – Infine, sempre a titolo orientativo, abbiamo fatto un tentativo di stabilire una corrispondenza fra E_p ed E_{γ} anche per il caso in cui l' ^{15}N non è lasciato nello stato fondamentale. In tale caso, considerato un certo numero di protoni di energia E_p , il quanto γ che ha generato il processo (γ , p) può avere avuto varie energie $E_{\gamma_1}(E_p)$, $E_{\gamma_2}(E_p)$, etc., in corrispondenza dei diversi

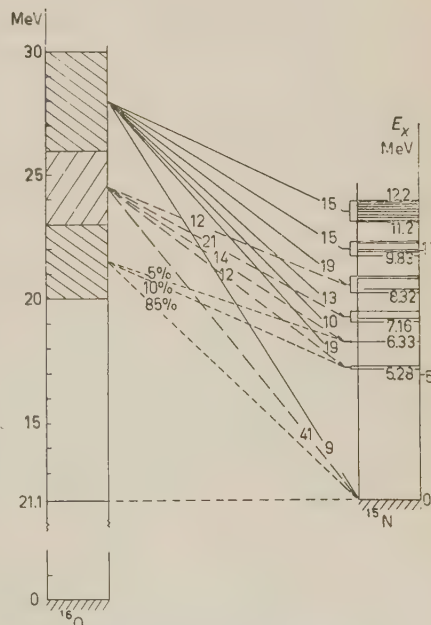


Fig. 10. – Livelli del ^{15}N e percentuale di fotoprotoni che lasciano ^{15}N nello stato fondamentale o in livelli eccitati.

livelli eccitati del ^{15}N ⁽⁹⁾ (Fig. 10). Noi abbiamo adottato l'ipotesi che la frequenza con cui compare ogni $E_{\gamma_i}(E_p)$ sia proporzionale alla corrispondente intensità $I(E_{\gamma_i})$ nello spettro di bremsstrahlung. Con questa ipotesi l'andamento della sezione d'urto diviene quello riportato nell'istogramma C) della Fig. 7 e la percentuale dei protoni che lasciano ^{15}N nello stato fondamentale o nei vari livelli eccitati, in funzione di E_{γ_i} , risulta quella indicata nella Fig. 10.

Questo tipo di analisi è certamente grossolano. Tuttavia esso è il solo possibile ad un'energia di eccitazione così alta che i livelli dei nuclei interessati sono ormai molto fitti. Per l'energia fino a 26 MeV JOHNSSON *et al.* ⁽⁴⁾ hanno fatto un'analisi dello stesso genere ottenendo dei risultati che, nell'intervallo di energia comune, coincidono praticamente con i nostri.

5. — Conclusione.

I risultati ottenuti (Fig. 7) mettono in evidenza il contributo della sezione d'urto $\text{O}(\gamma, p)$ nella zona $E_{\gamma} > 26$ MeV non esaminata da altri autori. In tale regione solo una piccola percentuale dei fotoprotoni emessi lascia il nucleo residuo nello stato fondamentale.

Nelle esposizioni ad $E_{\gamma_{\max}} = 23, 26$ e 30 MeV i fotoprotoni con energia E_p rispettivamente maggiore di $5.2, 8$ e 11.7 MeV hanno lasciato il nucleo residuo nello stato fondamentale ed i massimi nello spettro dei protoni indicano risonanze in assorbimento dei fotoni. Sono evidenti negli spettri a 23 e 26 MeV le risonanze intorno ad $E_{\gamma} = 22.2$ MeV, (21.5), 20.6, 19.3, 18.8 MeV in discreto accordo con i picchi a 22.4, 20.6 e 19.6 MeV trovati da COHEN e altri ⁽³⁾ irradiando con $E_{\gamma_{\max}} = 25$ MeV e con i picchi a 21.9, 20.7 e 19.3 MeV trovati da KATZ e altri ⁽¹⁰⁾ per l'effetto $^{16}\text{O}(\gamma, n)$ irradiando con $E_{\gamma_{\max}} = 22$ MeV.

Lo spettro a 30 MeV — oltre a confermare le precedenti risonanze — mette in evidenza picchi a 24 (e 25.5) MeV.

I due massimi ad $E_p = 3.5$ e 4.3 MeV nella differenza degli spettri $26 - 23 n$ (Fig. 8) derivano invece da assorbimento di fotoni nella regione fra 23 e 26 MeV ed emissione di protoni che lasciano ^{15}N nei primi livelli eccitati (Fig. 10). Tali massimi sono bene evidenti dato l'elevato valore della sezione d'urto fra 23 e 26 MeV e il numero relativamente basso dei livelli eccitati interessati.

⁽⁹⁾ F. AJZENBERG e T. LAURITSEN: *Rev. Mod. Phys.*, **24**, 321 (1952); **27**, 77 (1955); *Amer. Inst. of Phys. Handbook* (New York, 1957), 8, 75.

⁽¹⁰⁾ L. KATZ, R. N. H. HASLAM, R. I. HARSLEY, A. G. W. CAMERON e R. MONTALBETTI: *Phys. Rev.*, **95**, 464 (1954).

* * *

Ringraziamo i prof. R. RICAMO, direttore dell'Istituto di Fisica di Catania, e G. WATAGHIN, direttore dell'Istituto di Fisica di Torino, per aver messo a nostra disposizione i mezzi necessari per eseguire questo lavoro.

Ringraziamo il prof. G. CORTINI per il continuo aiuto prestatoci nella progettazione e nello svolgimento della presente ricerca.

Ringraziamo inoltre i dott. V. EMMA e C. MARCHESE del C.S.F.N. di Catania e tutti i colleghi del gruppo del betatron dell'Istituto di Fisica di Torino per la cordiale assistenza e collaborazione.

S U M M A R Y

The $^{16}\text{O}(\gamma, \text{p})$ reaction has been studied by exposition of an oxygen gas target to the γ -rays of the B.B.C. Betatron of 31 MeV maximum energy. Expositions at 23, 26 and 30 MeV maximum energy have been made with the experimental arrangement shown in Fig. 1a. Good definition in proton energy (about 0.1 MeV) is obtained. The uncertainty for the half thickness of the target (1 mg/cm² equivalent to about 4 μm of nuclear C₂ emulsion) goes from 0.15 MeV for 2 MeV protons to 0.02 MeV for 15 MeV protons. Only tracks having θ angle $90^\circ < \theta < 115^\circ$ with respect to the γ -rays (Fig. 1b) have been examined. The background ($< 2\%$) was $< 0.5\%$ for protons having energy $E_p > 5$ MeV. The spectra at 23, 26 and 30 MeV (Fig. 2, 3 and 4) show the same proton groups *B*, *C*, *D*, *E*, *F*, found by COHEN and others (3) by irradiation with bremsstrahlung of $E_{\gamma\text{max}} = 25$ MeV. Besides our 30 MeV spectrum shows the proton groups *G* and *H* in the region of higher energy. As the first excited level of the residual nucleus ^{15}N is $E_{x1} = 5.3$ MeV (Fig. 10) the protons having energy $E_p > 15/16(E_{\gamma\text{max}} - E_s - E_{x1})$, — where $E_{\gamma\text{max}}$ is the energy of irradiation and $E_s = 12.1$ MeV the threshold of the $\text{O}(\gamma, \text{p})$ process — leave ^{15}N in the fundamental state. Taking account only of these protons, from the experimental spectra (Fig. 2, 3 and 4) the cross-section for decay in the fundamental state of ^{15}N —shown in Fig. 7A—is obtained and a giant resonance in photon absorption at $E_\gamma = 22$ MeV is found. The spectra show a fine structure with well resolved peaks at 18.8; 19.3 (=D); 20.6 (=E); 22.2 (=F); 24 (=G) and 25.5 (=H) MeV. After normalization to the bremsstrahlung spectrum (Fig. 5 and 6) the difference (26 MeV spectrum — 23 MeV spectrum) (Fig. 8) and (30 MeV spectrum — 26 MeV spectrum) (Fig. 9) shows a large contribution of photoprotons leaving ^{15}N in excited states. Taking account also of these protons, the mean cross-section in the interval 23—26 MeV and 26—30 MeV shown in Fig. 7B is derived. The shape of the cross-section (Fig. 7C) is also derived taking account of the excited states of ^{15}N in approximate way. The yield (protons/mole/röntgen) up to 30 MeV is about 20% higher than the yield below 26 MeV. In the $E_\gamma = (26 \div 30)$ MeV region the majority of the photoprotons leave ^{15}N in excited states (Fig. 10). Contribution of protons leaving ^{15}N in the low energy excited states and emitted by absorption of photons in the (23 \div 26) MeV region is shown from difference of the spectra 26 — 23n (Fig. 8).

Propagation of Waves through a Sheet of the Medium with a Cubic Periodic Structure.

P. GOSAR

Institut « Jožef Stefan » - Ljubljana, Yugoslavia

(ricevuto il 28 Settembre 1957)

Summary. — This investigation is concerned with the scattering of plane scalar waves by a planparallel sheet of the medium, whose refractive index $n(\mathbf{r})$ is a periodic function of position vector \mathbf{r} with a cube as the elementary period. A method to obtain an approximate solution of the wave equation is developed for the case of normal and oblique incidence of the ingoing wave in the sheet. In full detail is investigated only the propagation of waves through the media for which the wave equation, written in rectangular co-ordinates, is separable. Two interesting, examples are given. The theory is applicable to the cases, where only a small part of the incident energy is scattered in the waves of higher modes.

1. — Introduction.

This investigation is concerned with the scattering of plane scalar waves by a planparallel sheet of the medium, whose refractive index $n(\mathbf{r})$ is a periodic function of position vector \mathbf{r} with a cube as the elementary period. The problem of propagation of waves through a medium with an internal periodic structure is interesting for optics, acoustics, microwave technique and physics of solid state. In optics we meet a simple example for this type of propagation of waves at the reflection and the transmission of electromagnetic waves through a stack of infinite dielectric plates, made alternatively from different material. The thicknesses of the plates of the same material are equal. In this case, which is very easily to be solved, we have no scattering of waves, as the refractive index of the medium is only a periodic function of the distance from the boundary plane of the sheet. There appears only one reflected wave.

Phase diffraction gratings, which have periodic structure in the plane of the sheet, represent another but degenerate example. Here we obtain several reflected and scattered waves, if the wave length of the incident wave in the surrounding medium is not greater than half the period of the periodic structure. In microwave technique artificial dielectrics, made from metallic plates, cylinders, wires or strips arranged at equal distances one from another to form periodic structures caused great interest for the use as microwave lenses and delay lines. The reflection and the refraction of microwaves at the interface between a homogeneous medium and an artificial dielectric and the dielectric properties of these media have been studied in special cases by different authors ⁽¹⁻⁷⁾. These investigations are chiefly restricted to the case of wave lengths greater than half period of the structure. In physics of solid state we mention only the scattering of fast electrons by thin metallic sheets, where the electron waves propagate in the periodic potential of the crystal lattice. As to the authors knowledge, this problem has yet not been treated from this point of view.

The aim of this paper is to study the propagation of scalar waves through a sheet of the medium with cubic structure. We assume that the boundary planes of the sheet do not cut the elementary cells of the medium and thus these planes are formed by the faces of cubes. We shall develop a method to obtain an approximate solution of the wave equation for the case of normal and oblique incidence of the ingoing wave in the sheet. In full detail we shall investigate only the propagation of waves through the media for which the wave equation, written in rectangular co-ordinates, is separable. Two interesting examples will be given. Here we shall be primarily concerned with the cases, where the wave length of the waves in the medium surrounding the sheet is small in comparison to the edge of the elementary cells.

2. - Statement of the problem.

An incident plane wave, which propagates in the homogeneous medium I in the direction making angles $\alpha_0, \beta_0, \gamma_0$ with the axes x, y, z of the rectangular co-ordinate system, falls upon a planparallel sheet II of the medium with periodic structure. See Fig. 1. The free space wave length of the incident

⁽¹⁾ J. F. CARLSON and A. E. HEINS: *Quart. Appl. Math.*, **4**, 313 (1947).

⁽²⁾ W. E. KOCK: *Bell Syst. Tech. Journ.*, **27**, 58 (1948).

⁽³⁾ S. B. COHN: *Journ. Appl. Phys.*, **20**, 257 (1949).

⁽⁴⁾ F. BERZ: *Proc. Inst. Elec. Engrs. (London)*, Part III, **98**, 47 (1951).

⁽⁵⁾ E. A. N. WHITEHEAD: *Proc. Inst. Elec. Engrs. (London)*, Part III, **98**, 133 (1951).

⁽⁶⁾ J. BROWN: *Proc. Inst. Elec. Engrs. (London)*, Part III, **100**, 51 (1953).

⁽⁷⁾ Z. A. KAPRIELIAN: *Journ. Appl. Phys.*, **27**, 1491 (1956).

wave is λ and the refractive index of the medium I is n_0 . For the refractive index of the homogeneous medium III on the other side of the sheet we choose the same value n_0 . The sheet is bounded by the planes $z = 0$ and $z = d$. The

sheet can be divided in cubic elementary cells of edge a so, that the refractive indices in the points of equal relative position to the faces of the cells are equal. Let the origin of the co-ordinate system be placed in the corner of one cube. The dielectric constant $\varepsilon(\mathbf{r})$ in the sheet is a periodic function of the position vector \mathbf{r} , i.e.

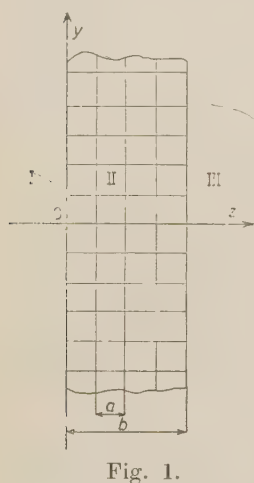


Fig. 1.

$$(1) \quad \varepsilon(\mathbf{r} + m\mathbf{e}_1 + n\mathbf{e}_2 + l\mathbf{e}_3) = \varepsilon(\mathbf{r}),$$

where $\mathbf{e}_1, \mathbf{e}_2, \mathbf{e}_3$ are unit vectors for the directions of the axes x, y, z and m, n, l are integers.

We have now to solve the wave equation

$$(2) \quad \Delta\psi(\mathbf{r}) + \left(\frac{2\pi}{\lambda}\right)^2 \varepsilon(\mathbf{r}) \psi(\mathbf{r}) = 0$$

for the scalar wave function $\psi(\mathbf{r})$. The solution $\psi(\mathbf{r})$ of the wave equation must represent in the field I besides reflected waves only one incident wave. We take for the incident wave

$$(3) \quad \psi_{in}(\mathbf{r}) = \exp[i(k_x x + k_y y + k_z z)],$$

with $k_x = 2\pi n_0 \cos \alpha_0 / \lambda$, $k_y = 2\pi n_0 \cos \beta_0 / \lambda$, $k_z = 2\pi n_0 \cos \gamma_0 / \lambda$. The second boundary condition for the wave function proceeds from the field III, where we can have only outgoing waves from the sheet.

We can deduce some general features of the solution $\psi(\mathbf{r})$ from the fact, that the refractive index is over the whole integration field a periodic function in the directions \mathbf{e}_1 and \mathbf{e}_2 . This periodicity implies, as was shown by BERZ (4) for the two dimensional case, that also the product

$$(4) \quad \varphi(\mathbf{r}) = \psi(\mathbf{r}) \exp[-i(k_x x + k_y y)]$$

is a periodic function of co-ordinates x and y in the whole space with the same period a for both directions. This means, that it is enough to solve the wave equation in a tube of square cross-section a^2 and extending in the direction \mathbf{e}_3 from $-\infty$ to $+\infty$.

The periodic function $\varphi(\mathbf{r})$ can be expanded in the fields I and III in Fourier series of type

$$(5) \quad \sum_{m=-\infty}^{\infty} \sum_{n=-\infty}^{\infty} \{C_{m,n,+} \exp[i k_{m,n} z] + C_{m,n,-} \exp[-i k_{m,n} z]\} \exp[2\pi i (mx + ny)/a],$$

where the propagation constants $k_{m,n}$ for the direction e_3 are equal to

$$(6) \quad k_{m,n} = \sqrt{\left(\frac{2\pi n_0}{\lambda}\right)^2 - \left(k_x + \frac{2\pi m}{a}\right)^2 - \left(k_y + \frac{2\pi n}{a}\right)^2}.$$

For great enough λ and higher modes m and n the propagation constants $k_{m,n}$ become imaginary.

In the field I we have only one incident wave with $m = 0$, $n = 0$ and $k_{0,0} = k_z$. Thus the constants $C_{m,n,+}$ are here zero except $C_{0,0,+} = 1$.

In the field III there are only transmitted waves, i.e. all the constants $C_{m,n,-}$ are zero.

The solution of the wave equation in the sheet can be expressed as a sum of the Bloch functions for the particular periodic structure. Here we must admit also the Bloch functions of the complex wave number vector, as we deal with a one dimension finite medium. Further, the function $\varphi(\mathbf{r})$ thus obtained must be a periodic function of x and y with the period a . This implies, that the only admitted wave number vectors of Bloch functions for a given free space wave length λ are those with the components in the directions e_1 and e_2 equivalent to k_x and k_y , if we use the Brillouin reduced-zone scheme for the wave number vectors.

The task of our calculations is now to determine the coefficients $C_{m,n,+}$ and $C_{m,n,-}$ for the fields I and III and the coefficients of the expansion of the wave function in the sheet so, that the function $\varphi(\mathbf{r})$ and its normal derivative will be continuous on the interfaces $z = 0$ and $z = d$. We shall assume, that the Bloch functions for the particular case are known.

The Bloch functions are not the most appropriate functions for the expansion of the wave function in the sheet when solving our problem. Here we need, as we shall see, a set of functions with postulated properties of periodicity, which satisfy the wave equation in the sheet, which form a complete system and are mutually orthogonal on the faces of elementary cells in the (x, y) plane. The orthogonality is here to be understood so, that the integral of the product of one function with the conjugate value of some other function of the set performed over the face of an elementary cell in the (x, y) plane is zero. The Bloch functions are usually not orthogonal in this sense. But this is true, if the dielectric constant in the sheet can be expressed as a sum of terms, each being only the function of one co-ordinate, i.e.

$$(7) \quad \varepsilon(\mathbf{r}) = \varepsilon_1(x) + \varepsilon_2(y) + \varepsilon_3(z).$$

Functions $\varepsilon_1(x)$, $\varepsilon_2(y)$ and $\varepsilon_3(z)$ are periodic with period a . Now the wave equation is separable and we obtain automatically the solutions of the Bloch type, which are orthogonal in the above sense.

In the following we shall discuss in detail the scattering problem for the medium of type (7). This case is practically important, as it will be seen from the given examples. At the end of this paper we shall give a comment on the general case without restrictions on the refractive index.

3. – The wave equation is separable.

The wave function $\psi(\mathbf{r})$ in the sheet satisfies the equation

$$(8) \quad \Delta\psi(\mathbf{r}) + \left(\frac{2\pi}{\lambda}\right)^2 [\varepsilon_1(x) + \varepsilon_2(y) + \varepsilon_3(z)]\psi(\mathbf{r}) = 0.$$

In order to obtain special solutions with periodic character of type (4) we substitute in (8) $\psi(\mathbf{r})$ by

$$u(x)v(y)w(z) \exp [i(k_x x + k_y y)] ,$$

where $u(x)$, $v(y)$, $w(z)$ are functions of only one variable. $u(x)$, $v(y)$, $w(z)$ are periodic with period a and must solve the following differential equations

$$(9) \quad \frac{d^2u(x)}{dx^2} + 2ik_x \frac{du(x)}{dx} + \left[\left(\frac{2\pi}{\lambda}\right)^2 \varepsilon_1(x) + e\right]u(x) = 0 ,$$

$$(10) \quad \frac{d^2v(y)}{dy^2} + 2ik_y \frac{dv(y)}{dy} + \left[\left(\frac{2\pi}{\lambda}\right)^2 \varepsilon_2(y) + h\right]v(y) = 0 ,$$

$$(11) \quad \frac{d^2w(z)}{dz^2} + \left[\left(\frac{2\pi}{\lambda}\right)^2 \varepsilon_3(z) - k_x^2 - k_y^2 - e - h\right]w(z) = 0 ,$$

where e and h are some real constants. The values of e and h can not be chosen at will, as we wish $u(x)$ and $v(y)$ to be periodic functions with period a . Such solutions are always possible at appropriate real values of e and h due to the periodicity of $\varepsilon_1(x)$ and $\varepsilon_2(y)$. We have to solve the eigenvalue problem in one dimension.

Let e_0 , e_1 , ..., e_m , ... be the eigenvalues of the differential equation (9) and let $u_0(x)$, $u_1(x)$, ..., $u_m(x)$, ... be the eigenfunctions. Similarly we denote the eigenvalues and eigenfunctions of (10) with h_0 , h_1 , ..., h_n , ... and $v_0(y)$, $v_1(y)$, ..., $v_n(y)$, These eigenfunctions are mutually orthogonal. We normalize them so, that

$$(12) \quad \begin{cases} \int_0^a u_m(x) u_m^*(x) dx = 1 , \\ \int_0^a v_n(y) v_n^*(y) dy = 1 . \end{cases}$$

The differential equation (11) for $w(z)$ has at the particular eigenvalues e_m and h_n two independent solutions $w_{m,n,+}(z)$ and $w_{m,n,-}(z)$, which can be written, due to the periodicity of $\varepsilon_3(z)$ as,

$$(13) \quad \begin{cases} w_{m,n,+}(z) = f_{m,n}(z) \exp [i\mu_{m,n}z], \\ w_{m,n,-}(z) = f_{m,n}^*(z) \exp [-i\mu_{m,n}z]. \end{cases}$$

(Theorem of Floquet ⁽⁸⁾). Here $f_{m,n}(z)$ is a periodic function of z with period a . The constant $\mu_{m,n}$ is real or imaginary and depends on the values of e_m and h_n . For real values of $\mu_{m,n}$ the independent solutions of (11) represent running waves. In the other case we obtain as solutions steadily increasing or evanescent waves. The constant $\mu_{m,n}$ has as function of $e_m + h_n$ alternate continuous bands of real and imaginary values and becomes imaginary at great values of $e_m + h_n$. Here can arise also the special case of $\mu_{m,n} = 0$, which needs special consideration. See KRAMERS ⁽⁹⁾.

Special solutions $u_m(x)v_n(y)w_{m,n,\pm} \exp [i(k_x x + k_y y)]$ of the differential equation (8) are of the Bloch type and are besides mutually orthogonal on the faces of elementary cells, which are parallel to the (x, y) plane. The function $\varphi(\mathbf{r})$ of any solution of the wave equation in the sheet, which is periodic in the sense (4), can be expanded into a series

$$(14) \quad \sum_{m=0}^{\infty} \sum_{n=0}^{\infty} [A_{m,n,+} w_{m,n,+}(z) + A_{m,n,-} w_{m,n,-}(z)] u_m(x) v_n(y),$$

where $A_{m,n,+}$ and $A_{m,n,-}$ are expansion coefficients. If we wish the series (14) to represent the solution $\varphi(\mathbf{r})$ in the sheet, the coefficients $A_{m,n,+}$ and $A_{m,n,-}$ must be determined so, that $\varphi(\mathbf{r})$ and its first derivatives are continuous on the planes $z = 0$ and $z = d$ with the solutions $\varphi(\mathbf{r})$ of type (5) and the corresponding derivatives in the field I and III. We obtain from the boundary conditions, that in the field I the coefficients $C_{m,n,+}$ are zero except $C_{0,0,+} = 1$ and that in the field III all $C_{m,n,-}$ are zero, in using orthogonal properties of the solutions

$$\exp [(2\pi i/a)(mx + ny) + ik_{m,n}z] \text{ and } \exp [(2\pi i/a)(mx + ny) - ik_{m,n}z]$$

two infinite sets of linear algebraic equations for the coefficients $A_{m,n,+}$ and $A_{m,n,-}$. It was made no attempt to solve these equations directly.

⁽⁸⁾ E. T. WHITTAKER and G. N. WATSON: *Modern Analysis*, 4-th ed. (Cambridge, 1952), p. 412.

⁽⁹⁾ H. A. KRAMERS: *Physica*, **2**, 483 (1935).

We proceed in another way. First we construct special solutions of the wave equation for the whole space as follows: we search for such solutions of the wave equation, which satisfy the condition (4) for periodicity and which may be represented in the field I only with one mode of propagation. Let $\psi_{\alpha,\beta,+}(\mathbf{r})$ be a solution of this type with the following form in the field I

$$(15) \quad \psi_{\alpha,\beta,+}(\mathbf{r}) = \exp [2\pi i(\alpha x + \beta y)/a] \exp [i(k_x x + k_y y + k_{\alpha,\beta} z)] ; \quad z < 0,$$

where α and β are integers.

The determination of expansion coefficients $A_{m,n,+}^{\alpha,\beta,+}$ and $A_{m,n,-}^{\alpha,\beta,+}$ of $\varphi_{\alpha,\beta,+}$ in the field II is now straightforward. The interface $z=0$ imposes the conditions

$$(16) \quad \left\{ \begin{array}{l} \sum_{m=0}^{\infty} \sum_{n=0}^{\infty} [A_{m,n,+}^{\alpha,\beta,+} w_{m,n,+}(0) + A_{m,n,-}^{\alpha,\beta,+} w_{m,n,-}(0)] u_m(x) v_n(y) = \\ \qquad \qquad \qquad = \exp [2\pi i(\alpha x + \beta y)/a], \\ \sum_{m=0}^{\infty} \sum_{n=c}^{\infty} \left[A_{m,n,+}^{\alpha,\beta,+} \frac{dw_{m,n,+}(z)}{dz} + A_{m,n,-}^{\alpha,\beta,+} \frac{dw_{m,n,-}(z)}{dz} \right]_{z=0} u_m(x) v_n(y) = \\ \qquad \qquad \qquad = ik_{\alpha,\beta} \exp [2\pi i(\alpha x + \beta y)/a]. \end{array} \right.$$

to the values of the expansion coefficients. Multiplying these equations by $u_m^*(x) v_n^*(y)$ and than integrating over x and y from 0 to a we obtain the following equations for $A_{m,n,+}^{\alpha,\beta,+}$ and $A_{m,n,-}^{\alpha,\beta,+}$

$$(17) \quad \left\{ \begin{array}{l} A_{m,n,+}^{\alpha,\beta,+} w_{m,n,+}(0) + A_{m,n,-}^{\alpha,\beta,+} w_{m,n,-}(0) = a^2 a_{m,\alpha}^* b_{n,\beta}^*, \\ A_{m,n,+}^{\alpha,\beta,+} \left[\frac{dw_{m,n,+}(z)}{dz} \right]_{z=0} + A_{m,n,-}^{\alpha,\beta,+} \left[\frac{dw_{m,n,-}(z)}{dz} \right]_{z=0} = ia^2 k_{\alpha,\beta} a_{m,\alpha}^* b_{n,\beta}^*, \end{array} \right.$$

where

$$(18) \quad \left\{ \begin{array}{l} a_{m,\alpha} = \frac{1}{a} \int_0^a u_m(x) \exp [-2\pi i \alpha x/a] dx, \\ b_{n,\beta} = \frac{1}{a} \int_0^a v_n(y) \exp [-2\pi i \beta y/a] dy. \end{array} \right.$$

$a_{m,\alpha}$ and $b_{n,\beta}$ are Fourier coefficients of the functions $u_m(x)$ and $v_n(y)$. Hence,

we have

$$(19) \quad \begin{cases} A_{m,n,+}^{\alpha,\beta,+} = a^2 a_{m,\alpha}^* b_{n,\beta}^* \left[\frac{(\mathrm{d}/\mathrm{d}z) \log w_{m,n,-}(z) - ik_{\alpha,\beta}}{w_{m,n,+}(z) (\mathrm{d}/\mathrm{d}z) \log (w_{m,n,-}(z)/w_{m,n,+}(z))} \right]_{z=0}, \\ A_{m,n,-}^{\alpha,\beta,+} = a^2 a_{m,\alpha}^* b_{n,\beta}^* \left[\frac{(\mathrm{d}/\mathrm{d}z) \log w_{m,n,+}(z) - ik_{\alpha,\beta}}{w_{m,n,-}(z) (\mathrm{d}/\mathrm{d}z) \log (w_{m,n,+}(z)/w_{m,n,-}(z))} \right]_{z=0}. \end{cases}$$

It remains the determination of the expansion coefficients $C_{m',n',+}^{\alpha,\beta,+}$ and $C_{m',n',-}^{\alpha,\beta,+}$ of the function $\varphi_{\alpha,\beta,+}(\mathbf{r})$ in the field III. The continuity of $\varphi_{\alpha,\beta,+}(\mathbf{r})$ and its first derivatives on the interface $z=d$ imposes the conditions

$$(20) \quad \begin{cases} \sum_{m'=-\infty}^{\infty} \sum_{n'=-\infty}^{\infty} \{ C_{m',n',+}^{\alpha,\beta,+} \exp [ik_{m',n'} d] + C_{m',n',-}^{\alpha,\beta,+} \exp [-ik_{m',n'} d] \} \cdot \exp [2\pi i(m'x + n'y/a)] = \\ = \sum_{m=0}^{\infty} \sum_{n=0}^{\infty} [A_{m,n,+}^{\alpha,\beta,+} w_{m,n,+}(d) + A_{m,n,-}^{\alpha,\beta,+} w_{m,n,-}(d)] u_m(x) v_n(y), \\ \sum_{m'=-\infty}^{\infty} \sum_{m'=-\infty}^{\infty} ik_{m',n'} \{ C_{m',n',+}^{\alpha,\beta,+} \exp [ik_{m',n'} d] - C_{m',n',-}^{\alpha,\beta,+} \exp [-ik_{m',n'} d] \} \cdot \exp [2\pi i(m'x + n'y/a)] = \\ = \sum_{m=0}^{\infty} \sum_{n=0}^{\infty} \left[A_{m,n,+}^{\alpha,\beta,+} \frac{\mathrm{d}w_{m,n,+}(z)}{\mathrm{d}z} + A_{m,n,-}^{\alpha,\beta,+} \frac{\mathrm{d}w_{m,n,-}(z)}{\mathrm{d}z} \right]_{z=d} u_m(x) v_n(y) \end{cases}$$

Multiplying these equations by $\exp [-2\pi i(m'x + n'y)/a]$ and integrating over x and y from 0 to a we obtain two linear equations for $C_{m',n',+}^{\alpha,\beta,+}$ and $C_{m',n',-}^{\alpha,\beta,+}$. The solutions of these equations are

$$(21) \quad \begin{cases} C_{m',n',+}^{\alpha,\beta,+} = \frac{1}{2} \exp [-ik_{m',n'} d] \sum_{m=0}^{\infty} \sum_{n=0}^{\infty} a_{m,m'} b_{n,n'} \cdot \\ \cdot \left\{ A_{m,n,+}^{\alpha,\beta,+} w_{m,n,+}(d) \left[1 - \frac{i}{k_{m',n'}} \frac{\mathrm{d}}{\mathrm{d}z} \log w_{m,n,+}(z) \right]_{z=d} + \right. \\ \left. + A_{m,n,-}^{\alpha,\beta,+} w_{m,n,-}(d) \left[1 - \frac{i}{k_{m',n'}} \frac{\mathrm{d}}{\mathrm{d}z} \log w_{m,n,-}(z) \right]_{z=d} \right\}, \\ C_{m',n',-}^{\alpha,\beta,+} = \frac{1}{2} \exp [ik_{m',n'} d] \sum_{m=0}^{\infty} \sum_{n=0}^{\infty} a_{m,m'} b_{n,n'} \cdot \\ \cdot \left\{ A_{m,n,+}^{\alpha,\beta,+} w_{m,n,+}(d) \left[1 + \frac{i}{k_{m',n'}} \frac{\mathrm{d}}{\mathrm{d}z} \log w_{m,n,+}(z) \right]_{z=d} + \right. \\ \left. + A_{m,n,-}^{\alpha,\beta,+} w_{m,n,-}(d) \left[1 + \frac{i}{k_{m',n'}} \frac{\mathrm{d}}{\mathrm{d}z} \log w_{m,n,-}(z) \right]_{z=d} \right\}. \end{cases}$$

Inserting for $A_{m,n,+}^{\alpha,\beta,+}$ and $A_{m,n,-}^{\alpha,\beta,+}$ the values (19) we obtain the finite formulae

$$\left\{ \begin{aligned}
 C_{m',n',+}^{\alpha,\beta,+} &= \frac{a^2}{2ik_{m',n'}} \exp[-ik_{m',n'}d] \sum_{m=0}^{\infty} \sum_{n=0}^{\infty} a_{m,m'} a_{m,\alpha}^* b_{n,n'} b_{n,\beta}^* \cdot \\
 &\cdot \left\{ \frac{w_{m,n,+}(d)}{w_{m,n,+}(0)} \left[\frac{(d/dz) \log w_{m,n,-}(z) - ik_{\alpha,\beta}}{(d/dz) \log(w_{m,n,+}(z)/w_{m,n,+}(0))} \right]_{z=0} \left[\frac{d}{dz} \log w_{m,n,+}(z) + ik_{m',n'} \right]_{z=d} + \right. \\
 &+ \left. \frac{w_{m,n,-}(d)}{w_{m,n,-}(0)} \left[\frac{(d/dz) \log w_{m,n,+}(z) - ik_{\alpha,\beta}}{(d/dz) \log(w_{m,n,+}(z)/w_{m,n,-}(0))} \right]_{z=0} \left[\frac{d}{dz} \log w_{m,n,-}(z) + ik_{m',n'} \right]_{z=d} \right\}, \\
 C_{m',n',-}^{\alpha,\beta,+} &= -\frac{a^2}{2ik_{n',n'}} \exp[ik_{m',n'}d] \sum_{m=0}^{\infty} \sum_{n=0}^{\infty} a_{m,m'} a_{m,\alpha}^* b_{n,n'} b_{n,\beta}^* \cdot \\
 &\cdot \left\{ \frac{w_{m,n,+}(d)}{w_{m,n,+}(0)} \left[\frac{(d/dz) \log w_{m,n,-}(z) - ik_{\alpha,\beta}}{(d/dz) \log(w_{m,n,-}(z)/w_{m,n,+}(0))} \right]_{z=0} \left[\frac{d}{dz} \log w_{m,n,+}(z) - ik_{m',n'} \right]_{z=d} + \right. \\
 &+ \left. \frac{w_{m,n,-}(d)}{w_{m,n,-}(0)} \left[\frac{(d/dz) \log w_{m,n,+}(z) - ik_{\alpha,\beta}}{(d/dz) \log(w_{m,n,+}(z)/w_{m,n,-}(0))} \right]_{z=0} \left[\frac{d}{dz} \log w_{m,n,-}(z) - ik_{m',n'} \right]_{z=d} \right\}.
 \end{aligned} \right. \tag{22}$$

We obtain expansion coefficients of the special solution $\varphi_{\alpha,\beta,-}(\mathbf{r})$, which represents in the field I outgoing wave of the modes of propagation α and β , by substituting in all formulae $k_{\alpha,\beta}$ by $-k_{\alpha,\beta}$.

We can now expand the searched function $\varphi(\mathbf{r})$ in terms of functions $\varphi_{\alpha,\beta,+}(\mathbf{r})$ and $\varphi_{\alpha,\beta,-}(\mathbf{r})$. We put

$$\varphi(\mathbf{r}) = \varphi_{0,0}(\mathbf{r}) + \sum_{\alpha=-\infty}^{\infty} \sum_{\beta=-\infty}^{\infty} B_{\alpha,\beta} \varphi_{\alpha,\beta}(\mathbf{r}), \tag{23}$$

as in the field I we have only one ingoing wave. The coefficients $B_{\alpha,\beta}$ are the amplitudes of the waves reflected by the sheet and must be determined so, that in the field III there are no ingoing waves. We obtain from this condition the following set of linear equations for the coefficients $B_{\alpha,\beta}$

$$\sum_{\alpha=-\infty}^{\infty} \sum_{\beta=-\infty}^{\infty} B_{\alpha,\beta} C_{m',n',-}^{\alpha,\beta,-} = -C_{m',n',-}^{0,0,+}, \tag{24}$$

where m' and n' can have any integer value from $-\infty$ to $+\infty$.

How to solve the equations (24) depends on the particular case, which is examined. The advantage of our way of calculation is in the fact, that in many practically important cases it is possible to obtain approximate solutions of (24) in the form of successive approximations, which converge very quickly. This are the cases, where the transmission of the unscattered wave through the sheet is great and only a part of the incident energy is scattered in waves of higher modes. Here the reflection amplitudes $B_{\alpha,\beta}$ are relatively

small and further the coefficients $C_{m',n',-}^{(\alpha,\beta,-)}$ with $m' = \alpha$ and $n' = \beta$ are absolutely much greater than coefficients with $m' \neq \alpha$ or $n' \neq \beta$. Hence, the most important terms in the equation (24) are those with $m' = \alpha$ and $n' = \beta$. Therefore we can take as a first approximation for $B_{\alpha,\beta}$ the value

$$B_{\alpha,\beta} = - \frac{C_{\alpha,\beta,-}^{0,0,+}}{C_{\alpha,\beta,-}^{(\alpha,\beta,-)}}.$$

Inserting now these approximate value in (24) except in the term with $B_{m',n'}$, which is much greater than the other terms, we obtain by solving these equations a further approximation for the reflection coefficients. The successive approximations thus obtained converge in many cases very quickly.

We propose also an alternate way of calculation. We take as the zero approximation for $\varphi(\mathbf{r})$ the function $\varphi_{0,0,+}(\mathbf{r})$. In this approximation there are no reflected waves and in the field III there appear also ingoing waves. Now we add to $\varphi_{0,0,+}(\mathbf{r})$ such ingoing waves from the field III, that these waves conceal the ingoing waves of the zero approximation. The amplitudes of the added waves are $-C_{m',n',-}^{0,0,+}$. Thus we obtain the first approximation, which satisfies the boundary conditions in the field III. The boundary conditions in the field I are not fulfilled, as we have many ingoing waves due to the added waves in the field III. The amplitudes of these ingoing waves will be small in the above case of great transmission. We can proceed in the same way to obtain further approximations. We add additional functions $\varphi_{\alpha,\beta,+}(\mathbf{r})$ in the field I to conceal ingoing waves, thus obtaining the second approximation, and so on. The rate of the convergence of these approximations is essentially the same as in the case of approximations for $B_{\alpha,\beta}$.

In the following sections we shall give two examples for the application of the theory.

4. – Scattering by a set of planparallel dielectric plates.

We consider the propagation of waves through a sheet made from planparallel plates, which are parallel to the co-ordinate plane (x, y) and have alternatively thickness $2b$ and dielectric constant ϵ_1 or thickness $2c$ and dielectric constant ϵ_2 ($\epsilon_1 > \epsilon_2$). Plates are infinite in the direction \mathbf{e}_2 and wide d in the direction \mathbf{e}_3 . Such a medium has cubic structure and the above theory is applicable to it. We shall discuss in full detail only the case of very small differences of dielectric constants $\Delta\epsilon = \epsilon_1 - \epsilon_2$. If $\Delta\epsilon$ is very small, the evaluation of the amplitudes of reflected and transmitted waves is relatively simple and we obtain a good insight into the mechanism of scattering. Let the thicknesses $2b$ and $2c$ be some wave lengths of the ingoing wave in the surrounding homogeneous medium.

The periodic function $\varepsilon_1(x)$ with a period $a = 2b + 2c$ is here defined by

$$(25) \quad \varepsilon_1(x) = \begin{cases} \varepsilon_1 ; & 0 < x < b , \\ \varepsilon_2 ; & b < x < a - b , \\ \varepsilon_1 ; & a - b < x < a . \end{cases}$$

The functions $\varepsilon_2(y)$ and $\varepsilon_3(z)$ are identically zero.

The solution of the differential equation (9) in the interval $(0, a)$ is

$$(26) \quad u(x) = \begin{cases} A \exp [i(\omega_1 - k_x)x] + B \exp [-i(\omega_1 + k_x)x] ; & 0 < x < b , \\ A_1 \exp [i(\omega_2 - k_x)x] + B_1 \exp [-i(\omega_2 + k_x)x] ; & b < x < a - b , \\ A_2 \exp [i(\omega_1 - k_x)x] + B_2 \exp [-i(\omega_1 + k_x)x] ; & a - b < x < a , \end{cases}$$

where

$$(27) \quad \begin{cases} \omega_1 = \sqrt{\left(\frac{2\pi}{\lambda}\right)^2 \varepsilon_1 + k_x^2 + e} , \\ \omega_2 = \sqrt{\left(\frac{2\pi}{\lambda}\right)^2 \varepsilon_2 + k_x^2 + e} . \end{cases}$$

The coefficients A_1, A_2, B_1, B_2 are determined so, that $u(x)$ and its derivative are continuous in the points $x = b$ and $x = a - b$. The eigenvalues e_m and the coefficients A and B are now obtained from the postulation of normalization and of periodicity of the function $u(x)$, which must have a period a . The constants ω_1 and ω_2 are connected with a trascendental equation and thus the computation of eigenvalues is in the general case a little troublesome.

The determination of eigenvalues e_m and eigenfunctions $u_m(x)$ is in the case of small difference $\Delta\varepsilon$ easier. We obtain approximate solutions by the use of perturbation theory ⁽¹⁰⁾. We substitute in the equation (9) $u(x)$ by

$$(28) \quad u(x) = g(x) \exp [-2\pi i s x/a] ,$$

where $g(x)$ is a periodic function and s such an integer, that the difference $k'_x = k_x - 2\pi s/a$ is absolutely smaller than π/a . The constants k'_x is a reduced value of the wave number vector component k_x . Now we expand $g(x)$ and e

⁽¹⁰⁾ L. I. SCHIFF: *Quantum Mechanics*, 2-nd ed. (New York, 1955), p. 151.

in power series of $\Delta\varepsilon$,

$$(29) \quad \left\{ \begin{array}{l} g(x) = g^{(0)}(x) + \Delta\varepsilon g^{(1)}(x) + (\Delta\varepsilon)^2 g^{(2)}(x) + \dots, \\ e = e^{(0)} + \Delta\varepsilon e^{(1)} + (\Delta\varepsilon)^2 e^{(2)} + \dots, \end{array} \right.$$

where the functions $g^{(0)}(x)$, $g^{(1)}(x)$, ... are periodic and satisfy the following conditions of normalization

$$(30) \quad \left\{ \begin{array}{l} \int_0^a g^{(0)}(x) g^{(0)*}(x) dx = 1, \\ \int_0^a [g^{(0)}(x) g^{(1)*}(x) + g^{(0)*}(x) g^{(1)}(x)] dx = 0, \\ \dots \dots \dots \dots \dots \dots \dots \dots \dots \end{array} \right.$$

We shall calculate only the zero order approximation $g^{(0)}(x)$ and the first order perturbation $g^{(1)}(x)$. We obtain in the usual way the equations

$$(31) \quad \left\{ \begin{array}{l} \frac{d^2 g^{(0)}(x)}{dx^2} + 2ik'_x \frac{dg^{(0)}(x)}{dx} + \left[\left(\frac{2\pi}{\lambda} \right)^2 \varepsilon^{(0)} + e^{(0)} + \left(\frac{2\pi s}{a} \right)^2 + \frac{4\pi s}{a} k'_x \right] g^{(0)}(x) = 0, \\ \frac{d^2 g^{(1)}(x)}{dx^2} + 2ik'_x \frac{dg^{(1)}(x)}{dx} + \left[\left(\frac{2\pi}{\lambda} \right)^2 \varepsilon^{(0)} + e^{(0)} + \left(\frac{2\pi s}{a} \right)^2 + \frac{4\pi s}{a} k'_x \right] g^{(1)}(x) = \\ = - \left[\left(\frac{2\pi}{\lambda} \right)^2 \frac{\varepsilon_1(x) - \varepsilon^{(0)}}{\Delta\varepsilon} + e^{(1)} \right] g^{(0)}(x) \end{array} \right.$$

for $g^{(0)}(x)$ and $g^{(1)}(x)$. Here $\varepsilon^{(0)}$ is the average dielectric constant of dielectric plates, i.e.

$$(32) \quad \varepsilon^{(0)} = 2(b\varepsilon_1 + c\varepsilon_2)/a.$$

The zero approximation is now

$$(33) \quad g_m^{(0)}(x) = \frac{1}{\sqrt{a}} \exp [i(\omega_m - k'_x)x]; \quad m = 0, \pm 1, \pm 2, \dots$$

with

$$(34) \quad \omega_m = \frac{2\pi m}{a} + k'_x.$$

and

$$(35) \quad e_m^{(0)} = \omega_m^2 - k_x^2 - \left(\frac{2\pi}{\lambda}\right)^2 \varepsilon^{(0)}.$$

The eigenvalues $e_m^{(0)}$ increase with the absolute value of m . Further $e_{+m}^{(0)} > e_{-m}^{(0)}$ for $k_x' > 0$ and $e_{+m}^{(0)} < e_{-m}^{(0)}$ for $k_x' < 0$.

Integration of the second equation of (31) gives the following solution $g_m^{(1)}(x)$, which satisfies the conditions of normalization and of periodicity,

$$(36) \quad g_m^{(1)}(x) = g_m^{(0)}(x) \cdot \begin{cases} \left(\frac{2\pi}{\lambda}\right)^2 \frac{ic}{\omega_m a} x + A \exp[-2i\omega_m x] + B; & 0 < x < b, \\ -\left(\frac{2\pi}{\lambda}\right)^2 \frac{ib}{\omega_m a} x + A_1 \exp[-2i\omega_m x] + B_1; & b < x < a-b, \\ \left(\frac{2\pi}{\lambda}\right)^2 \frac{ic}{\omega_m a} x + A_2 \exp[-2i\omega_m x] + B_2; & a-b < x < a, \end{cases}$$

with the values of constants

$$(37) \quad \begin{cases} A = \left(\frac{\pi}{\lambda\omega_m}\right)^2 \frac{\sin 2\omega_m c}{\sin \omega_m a}; & B = -\left(\frac{\pi}{\lambda\omega_m}\right)^2 \frac{2c}{a}, \\ A_1 = -\left(\frac{\pi}{\lambda\omega_m}\right)^2 \frac{\sin 2\omega_m b}{\sin \omega_m a} \exp[i\omega_m a]; & B_1 = \left(\frac{\pi}{\lambda\omega_m}\right)^2 \frac{2b}{a} (1 + i\omega_m a), \\ A_2 = \left(\frac{\pi}{\lambda\omega_m}\right)^2 \frac{\sin 2\omega_m c}{\sin \omega_m a} \exp[2i\omega_m a]; & B_2 = -\left(\frac{\pi}{\lambda\omega_m}\right)^2 \frac{2c}{a} (1 + 2i\omega_m a), \end{cases}$$

From the condition of periodicity of $g_m^{(1)}(x)$ we derive also, that the first order correction $e_m^{(1)}$ of the eigenvalue e_m is zero.

If k_x' approaches the value 0 or $\pm\pi/a$, our approximation fails already in the first order. We see from (37), that in this case the constants A , A_1 , A_2 become infinite. The cause for this is the degeneracy of eigenvalues for the unperturbed case, if $k_x' = 0$ or $\pm\pi/a$. Let us consider the case of k_x' very small. At $k_x' = 0$ the zero order approximations of the eigenvalues e_{+m} and e_{-m} become equal. We remove the degeneracy with the choice of the linear combination of $g_{+m}^{(0)}(x)$ and of $g_{-m}^{(0)}(x)$ for the zero approximation of $g(x)$, if k_x' is very small. We put

$$(38) \quad g_m^{(0)}(x) = c_1 \exp[i\omega_m x] + c_2 \exp[-i\omega_m x],$$

where

$$(39) \quad \omega_m = 2\pi m/a$$

and the constants c_1 and c_2 are functions of k'_x . Note, that the approximation (38) do not satisfy the first differential equation of (31). We determine c_1 and c_2 by using the variation method (11). The differential equation for $g(x)$ is the Euler equation of the variation problem

$$(40) \quad \delta \int_0^a \left\{ \frac{dg(x)}{dx} \frac{dg^*(x)}{dx} + ik'_x \left[g(x) \frac{dg^*(x)}{dx} - g^*(x) \frac{dg(x)}{dx} \right] - \left(\frac{2\pi}{\lambda} \right)^2 \varepsilon_1(x) g(x) g^*(x) \right\} dx = 0.$$

Here only functions $g(x)$, which are periodic and normalized, are admitted. Substituting (38) in (40) and taking variations of c_1 and c_2 so, that the condition of normalization $(c_1 c_1^* + c_2 c_2^*)a = 1$ is fulfilled, we obtain the following relation between c_1 and c_2

$$(41) \quad c_1 \left\{ \omega_m k'_x \pm \sqrt{\left(\frac{\pi}{\lambda} \right)^2 \Delta \varepsilon \frac{\sin 2\omega_m b}{\omega_m a}^2 + (\omega_m k'_x)^2} \right\} = 2c_2 \left(\frac{\pi}{\lambda} \right)^2 \Delta \varepsilon \frac{\sin 2\omega_m b}{\omega_m a}.$$

At the extreme the value of the integral in (40) is equal to $e_m^{(0)} + k_x^2 - k_x'^2$. Hence, we obtain

$$(42) \quad e_m^{(0)} = \omega_m^2 - \left(\frac{2\pi}{\lambda} \right)^2 \varepsilon^{(0)} - k_x^2 + k_x'^2 \mp 2 \sqrt{\left(\frac{\pi}{\lambda} \right)^2 \Delta \varepsilon \frac{\sin 2\omega_m b}{\omega_m a}^2 + (\omega_m k'_x)^2}.$$

We obtain from (41) two solutions for c_1 and c_2 and thus we have two zero approximations with different eigenvalues for each value of m . The split of eigenvalues (42) depends on k'_x and can not be smaller than

$$8 \left(\frac{\pi}{\lambda} \right)^2 \Delta \varepsilon \frac{\sin 2\omega_m b}{\omega_m a}.$$

Now we can calculate the first order perturbation $g_x^{(1)}(x)$ in a similar way as in (31) using the function (38) for the zero order approximation. We put

$$(43) \quad g_m^{(1)}(x) = c_1(x) \exp [i\omega_m x] + c_2(x) \exp [-i\omega_m x],$$

where $c_1(x)$ and $c_2(x)$ are yet unknown functions. Taking an additional condition

$$(44) \quad \frac{dc_1(x)}{dx} \exp [i\omega_m x] + \frac{dc_2(x)}{dx} \exp [-i\omega_m x] = 0$$

(11) L. I. SCHIFF: l. c., p. 171.

we obtain the following differential equations for $c_1(x)$ and $c_2(x)$

$$(45) \quad \left\{ \begin{array}{l} \frac{dc_1(x)}{dx} = -\frac{1}{2i\omega_m} \left\{ \left(\frac{2\pi}{\lambda} \right)^2 \frac{\varepsilon_1(x) - \varepsilon^{(0)}}{\Delta\varepsilon} \mp \frac{2}{\Delta\varepsilon} \sqrt{\left[\left(\frac{\pi}{\lambda} \right)^2 \Delta\varepsilon \frac{\sin 2\omega_m b}{\omega_m a} \right]^2 + (\omega_m k'_x)^2} \right\} \\ \quad \cdot \{ c_1 + c_2 \exp [-2i\omega_m x] \} - \frac{ik'_x}{\Delta\varepsilon} \{ c_1 - c_2 \exp [-2i\omega_m x] \}, \\ \frac{dc_2(x)}{dx} = \frac{1}{2i\omega_m} \left\{ \left(\frac{2\pi}{\lambda} \right)^2 \frac{\varepsilon_1(x) - \varepsilon^{(0)}}{\Delta\varepsilon} \mp \frac{2}{\Delta\varepsilon} \sqrt{\left[\left(\frac{\pi}{\lambda} \right)^2 \Delta\varepsilon \frac{\sin 2\omega_m b}{\omega_m a} \right]^2 + (\omega_m k'_x)^2} \right\} \\ \quad \cdot \{ c_1 \exp [2i\omega_m x] + c_2 \} + \frac{ik'_x}{\Delta\varepsilon} \{ c_1 \exp [2i\omega_m x] - c_2 \}. \end{array} \right.$$

Integrating the equations (45) we choose the integration constants so, that the second condition of normalization (30) is fulfilled. The function $c_1(x)$ and $c_2(x)$ are periodic. We do not give explicitly these functions, as the knowledge of equations (45) is sufficient for the evaluation of Fourier coefficients $a_{m,\alpha}$.

The approximations (38) and (49) fail for $m=0$. In this case the zero and the first approximation are the limits of the zero and the first approximation (33) and (36), if ω_m approaches zero.

Similarly we can obtain solutions for k'_x nearly equal to $\pm\pi/a$. At $k'_x = \pm\pi/a$ the zero order approximations of the eigenvalues e_{m+1} and e_{-m} or e_m and $e_{-(m+1)}$ become equal. This case is equivalent with the former, if we shift the co-ordinate system in the direction e_1 for $\pm a/2$. Therefore we shall not discuss it separately.

The approximations (36) and (43) are allowable, if the difference of dielectric constants is smaller than $(\lambda/a)^2$.

The evaluation of the Fourier coefficients $a_{m,\alpha}$, which we need in calculating the amplitudes of scattered waves by a set of dielectric plates, is now easy. Using the above approximate solutions we obtain

$$(46) \quad \left\{ \begin{array}{l} a_{m,\alpha} = \left(\frac{a}{\lambda} \right)^2 \frac{\Delta\varepsilon}{\pi\sqrt{a}} \frac{\sin [2\pi(\alpha + s - m)b/a]}{(\alpha + s - m)^2(\alpha + s + m + k'_x a/\pi)}; \quad \alpha + s \neq m, \\ a_{m,m-s} = \frac{1}{\sqrt{a}} \end{array} \right.$$

for k'_x sufficiently different from 0 or $\pm\pi/a$. If k'_x is small, we have

$$(47) \quad a_{m,\alpha} = \left(\frac{a}{\lambda} \right)^2 \frac{\Delta\varepsilon}{\pi(\alpha + s + m)(\alpha + s - m)} \cdot \left\{ c_1 \frac{\sin [2\pi(\alpha + s - m)b/a]}{\alpha + s - m} + c_2 \frac{\sin [2\pi(\alpha + s + m)b/a]}{\alpha + s + m} \right\}$$

for $\alpha+s \neq \pm m$ and $m \neq 0$. In the case of $\alpha+s = \pm m$ and $m \neq 0$ we give only the zero approximations of the Fourier coefficients

$$(48) \quad \begin{cases} a_{m,m-s} = c_1, \\ a_{m,-m-s} = c_2. \end{cases}$$

The formula (46) is valid also in the case $m=0$ and k'_x small.

Note, that

$$(49) \quad a_{m,\alpha} = -a_{\alpha+s,m-s}; \quad \alpha+s \neq m,$$

if k'_x is sufficiently different from zero and $\pm \pi/a$ or equal to zero. This relation is also approximately valid in the intermediate case. The result (49) is due to the orthogonality of the eigenfunctions $u_m(x)$.

We have now to solve the equations (10) and (11). The solutions are simple waves as $\varepsilon_2(y) = 0$ and $\varepsilon_3(z) = 0$. Putting $k_y = (2\pi s'/a) + k'_y$, where s' is an integer and $|k'_y| \leq \pi/a$, we obtain

$$(50) \quad v_n(y) = \frac{1}{\sqrt{a}} \exp [i(v_n - k_y)y]; \quad n = 0, \pm 1, \pm 2, \dots,$$

where

$$(51) \quad v_n = \frac{2\pi n}{a} + k'_y.$$

The eigenvalue of this solution is

$$(52) \quad h_m = v_n^2 - k_y^2$$

and the Fourier coefficient is

$$(53) \quad \begin{cases} b_{n,\beta} = 0; \quad \beta + s' \neq n, \\ b_{n,n-s'} = \frac{1}{\sqrt{a}}. \end{cases}$$

Two independent solutions of the equation (11) are

$$(54) \quad \begin{cases} w_{m,n,+}(z) = \exp [i\mu_{m,n}z], \\ w_{m,n,-}(z) = \exp [-i\mu_{m,n}z], \end{cases}$$

where

$$(55) \quad \mu_{m,n} = \sqrt{-k_x^2 - k_y^2 - e_m - h_n}.$$

After this preliminary evaluation of eigenfunctions and Fourier coefficients the calculation of the amplitudes of scattered waves is easy. We shall discuss in full detail only the case of k'_x different from 0 or $\pm\pi/a$. Further we assume only due to the simplicity of finite formulae, that the dielectric constant of the medium surrounding the sheet with periodic structure is $\epsilon^{(0)}$. In this case the formulae for the amplitudes are extremely simple, as $\mu_{m+s,n+s'} = k_{m,n}$. If we neglect in our calculation terms with higher powers of $\Delta\epsilon$ and we retain only first order terms, we obtain substituting (46), (53), (54) in (32) the following formulae for the amplitudes of waves of the zero approximation $\varphi_{0,0,+}(\mathbf{r})$

$$(56) \quad \left\{ \begin{array}{l} C_{m',0,+}^{0,0,+} = \left(\frac{a}{\lambda}\right)^2 \frac{\Delta\epsilon}{2\pi} \frac{\sin(2\pi m' b/a)}{m'^2(m' + k_x a/\pi)} \left(1 + \frac{k_{0,0}}{k_{m',0}}\right) \cdot \{\exp[i(k_{0,0} - k_{m',0})d] - 1\}; \quad m' \neq 0, \\ C_{m',0,-}^{0,0,+} = \left(\frac{a}{\lambda}\right)^2 \frac{\Delta\epsilon}{2\pi} \frac{\sin(2\pi m' b/a)}{m'^2(m' + k_x a/\pi)} \left(1 - \frac{k_{0,0}}{k_{m',0}}\right) \cdot \{\exp[i(k_{0,0} + k_{m',0})d] - 1\}; \quad m' \neq 0, \\ C_{m',n',+}^{0,0,+} = 0; \quad n' \neq 0, \quad C_{0,0,+}^{0,0,+} = 1, \\ C_{m',n',-}^{0,0,+} = 0; \quad n' \neq 0, \quad C_{0,0,-}^{0,0,+} = 0. \end{array} \right.$$

We obtain pretty complicated formulae in the case of k'_x equal or nearly equal 0 or $\pm\pi/a$. But it can be shown, that the difference of these formulae from (56) is small.

The zero approximation $\varphi_{0,0,+}(\mathbf{r})$ is quite good for the transmitted waves. To obtain amplitudes of reflected waves we add to $\varphi_{0,0,+}(\mathbf{r})$ such ingoing waves in the field III, which conceal the ingoing waves of the zero approximation in this field. The amplitudes of these waves are $-C_{m',n'}^{0,0,+}$. As we see from (56), the transmission of waves in the direction of propagation is equal to one to the second order of $\Delta\epsilon$. This means, that in our approximation $-C_{m',n',-}^{0,0,+}$ are the amplitudes of the reflected waves. Thus the zero approximation $\varphi_{0,0,+}(\mathbf{r})$ gives directly the amplitudes of transmitted and reflected waves. We can use also the equation (24) for the determination of the amplitudes of reflected waves. Here the coefficients $C_{m',n',-}^{m',n',-}$ are in a first approximation equal to one and further $C_{m',n',-}^{0,0,+}$ are equal to zero, if $n \neq 0$. Thus we obtain the same result $B_{m',0} = -C_{m',0,-}^{0,0,+}$ and $B_{m',n'} = 0$ if $n \neq 0$.

We have here chosen the dielectric constant of the medium surrounding the sheet equal to $\epsilon^{(0)}$. In a general case the formulae for $C_{m',0,+}^{0,0,+}$ and $C_{m',0,-}^{0,0,+}$ are a little complicated and we shall not cite them. We give only the values of the transmission and reflection coefficients $C_{0,0,+}^{0,0,+}$ and $C_{0,0,-}^{0,0,+}$ for the case of

k'_x different from 0 or $\pm \pi/a$

$$(57) \quad \begin{cases} C_{s,s,+}^{0,0,+} = \left[\cos \mu_{s,s'} d + \frac{i}{2} \left(\frac{k_{0,0}}{\mu_{s,s'}} + \frac{\mu_{s,s'}}{k_{0,0}} \right) \sin \mu_{s,s'} d \right] \exp [-ik_{0,0} d], \\ C_{s,s,-}^{0,0,+} = \frac{i}{2} \left(\frac{k_{0,0}}{\mu_{s,s'}} - \frac{\mu_{s,s'}}{k_{0,0}} \right) \sin \mu_{s,s'} d \exp [ik_{0,0} d]. \end{cases}$$

These formulae are identical with the formulae for the transmission and for the reflection of waves passing through the dielectric plate of the dielectric constant $\varepsilon^{(0)}$.

If the thickness d of the sheet is great, the value $\mu_{m,n}$ obtained from (55) in using the first order approximation for ε_m , is not enough accurate for the use in formulae (22). We must evaluate further approximations for ε_m . The second approximation is easily obtained, as we know the first approximation of the eigenfunction $u_m(x)$.

The scattering of scalar waves by a set of plan-parallel dielectric plates is similar to the scattering of electromagnetic waves by ultrasonic waves in liquids. This problem was examined very completely by E. H. WAGNER (12, 13).

5. – Scattering by centrally symmetrical scatterers arranged in a cubic lattice

In this section we shall give another example for the application of the theory. Let the dielectric constant in the cubic cells, which compose the sheet, be a centrally symmetrical function in reference to the centers of cubes. The only function of this kind with the property (7) is

$$(58) \quad \varepsilon(\mathbf{r}) = \varepsilon^{(0)} - \varrho(\mathbf{r} - \mathbf{r}_0)^2,$$

where \mathbf{r}_0 is the position vector of the center of the chosen cube and $\varepsilon^{(0)}$ and ϱ are constants.

We shall discuss only the case of very small differences of dielectric constants between different points of the medium, i.e. the case of small ϱ . The evaluation of the Fourier coefficients $a_{m\alpha}$ and $b_{n\beta}$ goes here along the same way as in the former example. We put

$$(59) \quad \begin{cases} \varepsilon_1(x) = -\varrho \left(x - \frac{a}{2} \right)^2; & 0 < x < a, \\ \varepsilon_2(y) = -\varrho \left(y - \frac{a}{2} \right)^2; & 0 < y < a, \\ \varepsilon_3(z) = \varepsilon^{(0)} - \varrho \left(z - \frac{a}{2} \right)^2; & 0 < z < a. \end{cases}$$

(12) E. H. WAGNER: *Zeits. f. Phys.*, **141**, 604 (1955).

(13) E. H. WAGNER: *Zeits. f. Phys.*, **141**, 622 (1955).

In solving the differential equations (9) and (10) we assume k'_x and k'_y to be sufficiently different from 0 or $\pm\pi/a$. The other case is easily to be solved in the way shown in the previous section.

Expanding $g(x) = u(x) \exp[2\pi isx/a]$ and e in power series of ϱ we obtain

$$(60) \quad \left\{ \begin{array}{l} g_m^{(0)}(x) = \frac{1}{\sqrt{a}} \exp[i(\omega_m - k'_x)x]; \\ g_m^{(1)}(x) = \frac{1}{2\omega_m} \left(\frac{2\pi}{\lambda} \right)^2 \left\{ \frac{1}{3i} \left(x - \frac{a}{2} \right)^3 + \frac{1}{2\omega_m} \left(x - \frac{a}{2} \right)^2 - \frac{1}{2i\omega_m^2} \left(x - \frac{a}{2} \right) - \frac{a^2}{12i} \left(x - \frac{1}{2i\omega_m} \right) - \frac{1}{4\omega_m^3} + \frac{a}{4\omega_m^2} \frac{\exp[-2i\omega_m(x - (a/2))]}{\sin \omega_m a} \right\} g_m^{(0)}(x), \end{array} \right. \quad m = 0, \pm 1, \pm 2, \dots,$$

where

$$(61) \quad \omega_m = \frac{2\pi m}{a} + k'_x.$$

The first approximation for the eigenvalues is

$$(62) \quad e_m = \omega_m^2 - k_x^2 + \left(\frac{\pi}{\lambda} \right)^2 \frac{\varrho a^2}{3}.$$

The evaluation of Fourier coefficients $a_{m,\alpha}$ gives the following formulae

$$(63) \quad \left\{ \begin{array}{l} a_{m,\alpha} = - \left(\frac{a}{\lambda} \right)^2 \frac{\varrho a^2}{2\pi^2 \sqrt{a}} \frac{1}{(\alpha + s - m)^3 (\alpha + s + m + k'_x a/\pi)}; \quad \alpha + s \neq m, \\ a_{m,m-s} = \frac{1}{\sqrt{a}} \left[1 + i \left(\frac{\pi}{\lambda} \right)^2 \frac{\varrho a^3}{12\omega_m} \right]. \end{array} \right.$$

Note, that the relation (49) between Fourier coefficients is also here valid.

We obtain analogical results for $v_n(y)$, h_n and $b_{n,\beta}$, as the equations (9) and (10) are identical.

The differential equation (11) has solutions of type (3). The functions $f_{m,n}(z)$ are in the zero approximation constants, if $\mu_{m,n}$ is not multiple or nearly multiple of π/a . In this case we have the following equation for $\mu_{m,n}$

$$(64) \quad \mu_{m,n}^2 = \left(\frac{2\pi}{\lambda} \right)^2 \left(\varepsilon^{(0)} - \frac{\varrho a^2}{4} \right) - \omega_m^2 - \nu_n^2.$$

If $\mu_{m,n}$, obtained from the equation (64), has the reduced value $\mu'_{m,n} = \mu_{m,n} - (2\pi s''/a)$, where s'' is such an integer that $|\mu'_{m,n}| \leq \pi/a$, equal or nearly equal to 0 or $\pm \pi/a$, the above approximation fails. Let us consider only the case of $\mu_{m,n}$ small. Here we take for the zero approximation a linear combination

$$(65) \quad \begin{cases} w_{m,n,+}(z) = \{c_1 \exp[2\pi i s'' z/a] + c_2 \exp[-2\pi i s'' z/a]\} \exp[i\mu'_{m,n} z], \\ w_{m,n,-}(z) = \{c_1 \exp[-2\pi i s'' z/a] + c_2 \exp[2\pi i s'' z/a]\} \exp[-i\mu'_{m,n} z], \end{cases}$$

where c_1 , c_2 and $\mu'_{m,n}$ are yet unknown parameters. We determine these parameters by using the variation method, as we made this in the former example. We obtain the following relation between c_1 and c_2

$$(66) \quad c_2 = -c_1 \frac{2\lambda^2 s''^2}{\varrho a^2} \left[\frac{4\pi s'' \mu'_{m,n}}{a} \pm \sqrt{\left(\frac{\varrho a^2}{2\lambda^2 s''^2}\right)^2 + \left(\frac{4\pi s'' \mu'_{m,n}}{a}\right)^2} \right]$$

and the following equation for $\mu'_{m,n}$

$$(67) \quad \mu'_{m,n} + \left(\frac{2\pi s''}{a}\right)^2 + \omega_m^2 + \nu_n^2 - \left(\frac{2\pi}{\lambda}\right)^2 \left(\varepsilon^{(0)} - \frac{\varrho a^2}{4}\right) \mp \sqrt{\left(\frac{\varrho a^2}{2\lambda^2 s''^2}\right)^2 + \left(\frac{4\pi s'' \mu'_{m,n}}{a}\right)^2} = 0.$$

The equation (67) has imaginary solutions for $\mu'_{m,n}$ only in small intervals of values $e_m + h_n$, if $s'' > 0$. The breadth of these intervals is

$$\frac{\varrho a^2}{2\lambda^2 s''^2}.$$

Similarly we can obtain zero approximations, if $\mu'_{m,n}$ is equal or nearly equal to $\pm \pi/a$.

In approximate calculations of the amplitudes of waves, scattered in directions different from the direction of incident wave, it is enough to know zero approximations of $w_{m,n,+}(z)$ and of $w_{m,n,-}(z)$. This case only is interesting and therefore we shall not proceed to the evaluation of first approximations.

We shall give here the formulae for the amplitudes of scattered waves by the sheet only in the case of $\mu'_{m,n}$ different from 0 or $\pm \pi/a$. Further we assume the dielectric constant of the medium surrounding the sheet to be

equal to $\varepsilon^{(0)} - (\varrho a^2/4)$. In this case $\mu_{m+s, n+s'} = k_{m,n}$. Neglecting terms with higher powers of ϱ we obtain the following formulae for the amplitudes of waves of the zero approximation $\varphi_{0,0,+}(\mathbf{r})$

$$(68) \quad \left\{ \begin{array}{l} C_{m',0,+}^{0,0,+} = -\left(\frac{a}{\lambda}\right)^2 \frac{\varrho a^2}{4\pi^2} \frac{1}{m'^3(m' + k_x a/\pi)} \left(1 + \frac{k_{0,0}}{k_{m',0}}\right) \cdot \{\exp[ik_{0,0} - k_{m',0}d] - 1\}; \quad m' \neq 0, \\ C_{0,n',+}^{0,0,+} = -\left(\frac{a}{\lambda}\right)^2 \frac{\varrho a^2}{4\pi^2} \frac{1}{n'^3(n' + k_y a/\pi)} \left(1 + \frac{k_{0,0}}{k_{0,n'}}\right) \cdot \{\exp[ik_{0,0} - k_{0,n'}d] - 1\}; \quad n' \neq 0, \\ C_{m',n',+}^{0,0,+} = 0; \quad m' \neq 0, n' \neq 0, \\ C_{m',0,-}^{0,0,+} = -\left(\frac{a}{\lambda}\right)^2 \frac{\varrho a^2}{4\pi^2} \frac{1}{m'^3(m' + k_x a/\pi)} \left(1 - \frac{k_{0,0}}{k_{m',0}}\right) \cdot \{\exp[i(k_{0,0} + k_{m',0})d] - 1\}; \quad m' \neq 0, \\ C_{0,n',-}^{0,0,+} = -\left(\frac{a}{\lambda}\right)^2 \frac{\varrho a^2}{4\pi^2} \frac{1}{n'^3(n' + k_y a/\pi)} \left(1 - \frac{k_{0,0}}{k_{0,n'}}\right) \cdot \{\exp[i(k_{0,0} + k_{0,n'})d] - 1\}; \quad n' \neq 0, \\ C_{m',n',-}^{0,0,+} = 0; \quad m' \neq 0, n' \neq 0. \end{array} \right.$$

6. – General case.

We give here a comment on the cases, where the wave equation is not separable.

The theory developed in this paper is based on the fact, that we can obtain in the case of separability of the wave equation a complete set of functions, which satisfy the wave equation in the sheet, which have periodic character of type (4) and are mutually orthogonal on the faces of elementary cells in the (x, y) plane. Such a set of functions can be formally obtained also in the case of non-separability of the wave equation by an appropriate linear combination of the Bloch functions for the particular case. The Bloch functions are in general not orthogonal on the faces of elementary cells in the (x, y) plane. If the orthogonalization of the Bloch functions by the choice of linear combinations is really possible, than we can obtain the formulae for the amplitudes of scattered waves essentially in the same way as in the case of separable wave equations. But these formulae will be in general very complicated.

RIASSUNTO (*)

La presente ricerca si occupa dello scattering di onde piane scalari su uno strato pian-parallelo del mezzo il cui indice di rifrazione $n(\mathbf{r})$ è funzione periodica del vettore di sito \mathbf{r} con periodo elementare corrispondente a una terza potenza. Si sviluppa un metodo per ottenere una soluzione approssimata dell'equazione d'onda per i casi di incidenza normale e obliqua dell'onda penetrante nello strato. Si esamina dettagliatamente solo la propagazione delle onde nei mezzi in cui l'equazione d'onda scritta in coordinate cartesiane è separabile. Si danno due interessanti esempi. La teoria è applicabile ai casi in cui solo una piccola parte dell'energia incidente è diffusa in onde di modi superiori.

(*) Traduzione a cura della Redazione.

Legge di moto nell'ultima teoria unitaria einsteiniana.

E. CLAUSER

Istituto Matematico del Politecnico - Milano

(ricevuto il 10 Ottobre 1957)

Riassunto. — Si deduce la legge di movimento di particelle, tra le quali si esercitano azioni gravitazionali ed elettromagnetiche, dalle equazioni di campo della teoria unitaria einsteiniana del 1953; si ritrovano così tutte le forze classiche dei due campi e cioè la gravitazionale newtoniana, la elettrostatica coulombiana e quella elettrodinamica di Lorentz; si hanno in più forze meno rilevanti che rappresentano l'interazione fra i due campi.

1. — Introduzione.

È ben noto che dalle equazioni di campo della sua teoria della gravitazione, EINSTEIN e collaboratori hanno dedotto il movimento di particelle rappresentate da singolarità del campo fondamentale (simmetrico). In prima approssimazione le forze agenti su una particella risultano allora costituite dalla sola forza gravitazionale newtoniana, nelle approssimazioni successive dalla precedente e da forze meno rilevanti ⁽¹⁾.

Lo stesso problema si presenta nella teoria unitaria einsteiniana; tra le forze che governano il movimento di un corpuscolo dotato di massa e di carica elettrica, c'è da aspettarsi di trovare quelle essenziali della Fisica classica, e cioè la forza gravitazionale newtoniana, la forza elettrostatica coulombiana e la forza elettrodinamica di Lorentz, ed eventualmente ulteriori addendi di interazione. Il problema fu affrontato da INFELD, che si avvalse delle equazioni einsteiniane di campo (asimmetrico) formulate nel 1950; questo autore trovò

(1) A. EINSTEIN e L. INFELD: *Can. Journ. Math.*, I, 209 (1949); questo lavoro perfeziona uno precedente di A. EINSTEIN, L. INFELD e B. HOFFMANN: *Ann. Math.*, 39, 66 (1938).

bensì la forza gravitazionale newtoniana, ma non le rimanenti forze classiche (2). Più tardi, CALLAWAY utilizzò allo stesso fine le equazioni del campo unitario formulate nel 1953, ma il suo procedimento non era adeguato e non gli permise di andare al di là del risultato di INFELD (3). Legittimo era dunque il sospetto che dalla attuale formulazione della teoria unitaria einsteiniana non si potessero trarre tutte le forze della Fisica classica; per ovviare a ciò furono anzi proposte opportune modifiche delle equazioni di campo (4).

In questa Nota si dimostra invece che nelle equazioni di movimento di un corpuscolo dedotte dalle equazioni di campo (asimmetrico) della teoria unitaria del 1953, sono presenti le forze più significative della Fisica classica, e cioè la forza gravitazionale newtoniana, la forza elettrostatica coulombiana e la forza elettrodinamica di Lorentz.

A questo risultato sono giunto utilizzando una formula integrale che ho precedentemente stabilito in una Nota lincea (5), valendomi opportunamente di alcune ricerche di P. G. BERGMANN e SCHILLER, e di GOLDBERG (6). La formula citata consegue dalle equazioni di campo della teoria unitaria, ed individua rigorosamente il movimento di particelle, una volta assegnate le singolarità che le rappresentano. Dalla formula precedente si possono ottenere le equazioni di movimento di corpuscoli con qualsivoglia approssimazione, applicando ad essa il procedimento di approssimazioni successive introdotto da EINSTEIN ed INFELD per il caso gravitazionale (7): si sviluppa cioè il tensore fondamentale in una conveniente serie di funzioni, ordinate secondo le potenze intere e positive di λ , reciproco della velocità c della luce nel vuoto rispetto ad un osservatore inerziale; in conseguenza, il vettore integrando della formula trovata risulta sviluppato in una serie di potenze intere e positive di λ ; si ottengono così delle equazioni ricorrenti di movimento. Esse discendono dalle equazioni di campo e dalla natura delle singolarità che rappresentano la carica e la massa del generico corpuscolo; queste singolarità non sono completamente arbitrarie, ma anch'esse sono condizionate dalle equazioni di campo.

La più bassa potenza di λ che inizia lo sviluppo del tensore fondamentale, dopo quella d'ordine zero, si può prefissare ad arbitrio; se essa è λ^2 (come nella teoria gravitazionale), la formula integrale comincia ad essere significativa allorchè non si trascurano i termini in λ^4 ; le equazioni di movimento di prima

(2) L. INFELD: *Acta Phys. Pol.*, **10**, 284 (1950).

(3) J. CALLAWAY: *Phys. Rev.*, **92**, 1567 (1953).

(4) B. KURŞUNOĞLU: *Phys. Rev.*, **88**, 1369 (1952); W. B. BONNOR: *Proc. Roy. Soc. London*, **A 226**, 366 (1954).

(5) *Movimento di particelle nel campo unitario einsteiniano*, in *Rend. Acc. Lincei*, vol. **XXI**, 408 (1956).

(6) P. G. BERGMANN ed R. SCHILLER: *Phys. Rev.*, **89**, 4 (1953); J. GOLDBERG: *Phys. Rev.*, **89**, 263 (1953).

(7) Loco primo citato in (1).

approssimazione risultano pertanto costituite dai termini di quarto grado rispetto a λ , come del resto avviene anche nel caso gravitazionale. In questa Nota, deduco appunto così le equazioni di movimento di prima approssimazione per un sistema di due o più particelle; spingendomi poi fino ai termini in λ^6 , determino una parte significativa delle equazioni di movimento in successiva approssimazione.

Le equazioni di prima approssimazione (tratte dai soli coefficienti di λ^4) individuano il moto di una particella soggetta alla forza gravitazionale newtoniana ed alla forza elettrostatica coulombiana, esercitate dalle restanti particelle, ed in più ad una debole forza che rappresenta l'interazione tra il campo gravitazionale e quello elettromagnetico; si ritrovano così le equazioni che in Fisica classica reggono il movimento di particelle cariche e pesanti rispetto ad un osservatore inerziale, quando si prescinde dalla forza elettrodinamica di Lorentz la quale ha ordine di grandezza inferiore alle precedenti, come è ben noto, e dalla debole forza di interazione. La forza elettrostatica coulombiana non si ottiene però scegliendo come potenziale del campo elettrostatico la funzione armonica elementare, ma una funzione biarmonica, proprio come vogliono le equazioni elettromagnetiche che qui intervengono e che si traggono in prima approssimazione dalle equazioni di campo. Precisamente, ho assunto come potenziale elettrostatico di ciascuna particella la funzione biarmonica, somma del classico potenziale elettrostatico (espresso dalla funzione armonica elementare) con un generico polinomio di secondo grado nella distanza dalla particella potenziante; il termine lineare di questo polinomio è essenziale, perché senza di esso la forza coulombiana non compare nelle equazioni di movimento di prima approssimazione. Attraverso il termine addizionale del potenziale elettrostatico si comincia così a manifestare sia il divario tra lo schema elettromagnetico classico e quello implicitamente contenuto nella formulazione 1953 della teoria unitaria einsteiniana, sia l'interazione tra gravitazione ed elettricità, rappresentata da un coefficiente proporzionale al prodotto della costante di attrazione universale per la carica della particella. Tutto ciò spiega il risultato negativo di CALLAWAY nella ricerca delle equazioni di movimento di prima approssimazione (arrestate cioè ai coefficienti di λ^4) e dedotte dalla formulazione 1953 della teoria unitaria; questo autore assume infatti come potenziale, semplicemente quello coulombiano elementare, prescindendo così dal termine addizionale.

I termini di sesto grado in λ si possono raggruppare in tre addendi: un addendo è la somma di termini di interazione fra gravitazione ed elettricità, un altro addendo è la somma di termini che rappresentano la reazione esercitata su ciascuna particella dal campo gravitazionale ed elettromagnetico creato dalla particella stessa; infine il terzo addendo dà la forza elettrodinamica di Lorentz. La presenza di altre forze accanto a quella totale di Lorentz è ben accetta, almeno a priori, perché una particella carica non può esistere

stabilmente se la forza totale di Lorentz è l'unica forza elettromagnetica che si esercita su di essa⁽⁸⁾. Per avere dunque una adeguata descrizione del movimento di una particella è necessario spingere il calcolo sino ai termini in λ^6 .

Ben diversi risultati si ottengono dalla formulazione 1950 della teoria unitaria: il potenziale elettrostatico che interessa le equazioni di movimento di prima approssimazione è infatti una funzione armonica, sicchè le equazioni di movimento di prima approssimazione si riducono alle equazioni del moto gravitazionale newtoniano di due o più particelle, proprio come aveva già trovato INFELD⁽²⁾. La forza totale di Lorentz è dunque qui assente dalle equazioni di movimento arrestate ai termini in λ^6 .

Questa circostanza contribuisce assieme ad altre, di diversa natura, a preferire la formulazione 1953 della teoria unitaria a quella del 1950.

2. - Le equazioni di movimento di una particella.

Nella Nota citata⁽⁵⁾, ho stabilito la seguente formula rigorosa che permette di determinare il moto di una particella:

$$(1) \quad \int_{\sigma} (\mathbf{U}_{\gamma}^{\frac{\partial}{\partial \sigma}} + \mathbf{t}_{\gamma}^s) n_s d\sigma = 0 \quad (\gamma = 0, 1, 2, 3; s = 1, 2, 3);$$

nella (1), σ è una qualsiasi superficie bidimensionale e regolare che appartiene all'ordinario spazio euclideo tridimensionale e racchiude le singolarità che individuano la particella; n_s è il coseno direttore del versore normale a σ ; sopra σ il vettore integrando è regolare⁽⁹⁾.

Il primo membro della (1) non dipende da σ e sarebbe identicamente nullo se il vettore integrando fosse regolare, oltre che sopra σ , anche internamente a σ ; il primo membro della (1) dipende quindi soltanto dalla natura delle singolarità del vettore integrando che sono racchiuse da σ ; la (1) consegue da tutte le equazioni del campo unitario einsteiniano ed è quindi una condizione imposta

⁽⁸⁾ Cfr., ad esempio, R. BECKER: *Théorie des électrons* (Paris, 1938), § 6.

⁽⁹⁾ In questa Nota, come in quella citata in⁽⁵⁾, si seguono le notazioni adottate da EINSTEIN nella Appendice II di *The Meaning of Relativity* (Princeton, 1953), IV ed., trad. it. Einaudi editore: il punto e virgola indica derivazione tensoriale, la virgola derivazione parziale ordinaria rispetto alle coordinate, le lettere gotiche indicano densità vettoriali e tensoriali; pure con lettere gotiche vengono indicate le pseudodensità, ossia quegli enti che si trasformano come densità soltanto quando la trasformazione delle coordinate è lineare. Infine, anche nelle formule non tensoriali, viene omesso il simbolo di sommatoria relativo ad indici uguali, collocati in basso ed in alto. Le quantità che compaiono nella (1) individuano due pseudodensità dello spazio-tempo unitario einsteiniano, la prima tensoriale e la seconda vettoriale; tuttavia, per brevità, ivi e nel seguito, esse vengono ancora denominate rispettivamente tensore e vettore.

da queste equazioni alle singolarità delle componenti del tensore fondamentale, ed al loro movimento. In tal modo, le equazioni (1) determinano il movimento di ciascuna particella, una volta calcolato il vettore integrando mediante le equazioni di campo; la soluzione di queste equazioni deve contenere quelle singolarità che individuano ciascuna particella; queste singolarità non si possono pertanto prefissare completamente ad arbitrio, ma la loro scelta è condizionata dalle equazioni di campo.

3. - Le equazioni del campo unitario einsteiniano e le corrispondenti equazioni di movimento di una particella.

Le equazioni di campo della teoria unitaria di Einstein nella formulazione del 1953 sono

$$(2) \quad R_{\alpha\beta} = 0 ,$$

$$(3) \quad R_{\alpha\beta,\gamma} + R_{\beta\gamma,\alpha} + R_{\gamma\alpha,\beta} = 0 ,$$

$$(4) \quad \Gamma_{\alpha} \equiv \Gamma_{\alpha\beta}^{\beta} = 0 ,$$

$$(5) \quad g^{\alpha\beta}_{\gamma\sigma} \equiv g^{\alpha\beta}_{\gamma\sigma} + g^{\alpha\sigma} \Gamma_{\sigma\gamma}^{\beta} + g^{\beta\sigma} \Gamma_{\sigma\gamma}^{\alpha} - g^{\alpha\beta} \Gamma_{\sigma\gamma}^{\sigma} = 0 ,$$

dove, come in seguito, gli indici greci assumono i valori 0, 1, 2, 3, gli indici latini assumeranno invece i valori 1, 2, 3, $\Gamma_{\alpha\beta}^{\gamma}$ è il coefficiente di connessione,

$$(6) \quad R_{\alpha\beta} \equiv \Gamma_{\alpha\beta,\gamma}^{\gamma} - \Gamma_{\alpha\sigma,\beta}^{\sigma} + \Gamma_{\alpha\beta}^{\sigma} \Gamma_{\sigma\gamma}^{\gamma} - \Gamma_{\alpha\sigma}^{\sigma} \Gamma_{\gamma\beta}^{\gamma}$$

è il tensore contratto di curvatura, mentre, indicando con g il determinante formato con le componenti $g_{\alpha\beta}$ del tensore fondamentale,

$$g^{\alpha\beta} = +\sqrt{-g} g^{\alpha\beta}$$

è la generica componente della densità tensoriale fondamentale ⁽¹⁰⁾. Il vettore integrando delle equazioni di movimento (1), è allora individuato dalle seguenti quantità

$$(7) \quad U_{\gamma}^{\beta\gamma} \equiv \mathfrak{B}_{\alpha\sigma}^{\gamma} g^{\alpha\sigma} \delta_{\gamma}^{\beta} - \mathfrak{B}_{\alpha\gamma}^{\gamma} g^{\alpha\beta} - \mathfrak{B}_{\gamma\alpha}^{\gamma} g^{\beta\alpha} + \delta_{\gamma}^{\sigma} g^{\beta\sigma}_{\sigma,\sigma} - g^{\beta\gamma}_{\gamma,\gamma} ,$$

$$(8) \quad t_{\gamma}^{\beta} \equiv (\mathfrak{B} + g^{\alpha\sigma}_{\gamma\sigma} R_{\alpha\sigma}^{\beta}) \delta_{\gamma}^{\beta} - (\mathfrak{B}_{\alpha\sigma}^{\beta} g^{\alpha\sigma}_{\gamma,\gamma} + 2g^{\alpha\beta}_{\gamma\gamma} R_{\alpha\sigma}^{\sigma}) ,$$

⁽¹⁰⁾ Cfr. loco citato in ⁽⁹⁾.

nelle quali δ_{γ}^{β} è l'ordinario simbolo di Kronecker ($\delta_{\gamma}^{\beta} = 0$ per $\gamma \neq \beta$, $\delta_{\gamma}^{\beta} = 1$ per $\gamma = \beta$), ed è:

$$\left\{ \begin{array}{l} \mathfrak{B}_{\alpha\beta}^{\nu} = \Gamma_{\alpha\beta}^{\nu} - \delta_{\beta}^{\nu} \Gamma_{\alpha\sigma}^{\sigma}, \\ \mathfrak{B}_{\alpha\beta} = \Gamma_{\alpha\beta}^{\nu} \Gamma_{\nu\sigma}^{\sigma} - \Gamma_{\alpha\sigma}^{\nu} \Gamma_{\nu\beta}^{\sigma}, \\ \mathfrak{B} \equiv \mathfrak{B}_{\alpha\beta} g^{\alpha\beta} \text{ (5).} \end{array} \right.$$

Tenendo conto della (5), le quattro equazioni di movimento (1), si esprimono esplicitamente così, in funzione dei coefficienti di connessione, della densità tensoriale fondamentale e della parte emisimmetrica del tensore contratto di curvatura:

$$(9) \quad \int_{\sigma} \left\{ \frac{\partial}{\partial x_0} [(\mathfrak{g}^{is} \Gamma_{ji}^0 - \mathfrak{g}^{i0} \Gamma_{ji}^s) + (\mathfrak{g}_{\nu}^{is} \Gamma_{ji}^0 - \mathfrak{g}_{\nu}^{i0} \Gamma_{ji}^s) + \mathfrak{g}_{\nu}^{0s} \Gamma_{i0}^{\sigma}] n_s + \right. \\ \left. + \left[\frac{\partial}{\partial x_0} (\mathfrak{g}^{\varrho 0} \Gamma_{\varrho\sigma}^{\sigma} - \mathfrak{g}^{\varrho\sigma} \Gamma_{\varrho 0}^0) + (\mathfrak{B} + \mathfrak{g}_{\nu}^{\varrho\sigma} R_{\varrho\nu}^{\sigma}) \right] n_i + \right. \\ \left. - (2\mathfrak{g}_{\nu}^{\varrho s} R_{\varrho i}^{\nu} + \mathfrak{B}_{\alpha\beta}^s \mathfrak{g}^{\alpha\beta}_{,i}) n_s \right\} d\sigma = 0 \quad (i = 1, 2, 3);$$

$$(10) \quad \int_{\sigma} \left\{ \frac{\partial}{\partial x_0} [(\mathfrak{g}^{is} \Gamma_{i0}^0 - \mathfrak{g}^{i0} \Gamma_{i0}^s) + (\mathfrak{g}_{\nu}^{is} \Gamma_{i0}^0 - \mathfrak{g}_{\nu}^{i0} \Gamma_{i0}^s) + \mathfrak{g}_{\nu}^{0s} \Gamma_{0\sigma}^{\sigma}] + \right. \\ \left. + \frac{\partial}{\partial x_0} (\mathfrak{g}^{\varrho\sigma} \Gamma_{\varrho\sigma}^s - \mathfrak{g}^{\varrho s} \Gamma_{\varrho\sigma}^{\sigma}) - (2\mathfrak{g}_{\nu}^{\varrho s} R_{\varrho 0}^{\nu} + \mathfrak{B}_{\alpha\beta}^s \mathfrak{g}^{\alpha\beta}_{,0}) \right\} n_s d\sigma = 0;$$

nella (9) e nella (10), come in seguito, x_1 , x_2 , x_3 , sono le coordinate spaziali di un punto, x_0 è la sua coordinata temporale.

4. - Il metodo di approssimazione.

I primi membri delle equazioni (9) e (10) vanno calcolati tenendo conto di tutte le equazioni del campo unitario. Conviene allora trattare le equazioni di campo e di movimento con il metodo di approssimazioni successive descritto nell'introduzione: sviluppiamo cioè il tensore fondamentale in una conveniente serie di potenze di $\lambda = c^{-1}$ (reciproco della velocità c della luce nel vuoto rispetto ad un osservatore inerziale), ritenendo inoltre le derivate parziali relative alla coordinata temporale di ordine più elevato (rispetto a λ) delle derivate spaziali. È perciò opportuno identificare x_0 nel tempo römeriano ponendo

$$x_0 \equiv ct \equiv \lambda^{-1}t,$$

ed assumendo dello stesso ordine le derivate rispetto a t ed alle x_i .

La natura di questo procedimento implica valutazioni di ordini di grandezza; d'altra parte il tensore fondamentale congloba quantità che dipendono da azioni gravitazionali e da azioni elettromagnetiche; è pertanto comodo imporre a tutte le sue componenti di essere puri numeri. In conseguenza, alle coordinate x_1, x_2, x_3 competono le dimensioni di una lunghezza, come ad x_0 . Ciò premesso, sviluppiamo le componenti del tensore fondamentale nel modo seguente:

$$(I) \quad \left\{ \begin{array}{l} g_{00} = 1 + \frac{\lambda^2 \alpha^2}{2} g_{00} + \frac{\lambda^4 \alpha^4}{4} g_{00} + \dots, \\ g_{mn} = -\delta_{mn} + \frac{\lambda^2 \alpha^2}{2} g_{mn} + \frac{\lambda^4 \alpha^4}{4} g_{mn} + \dots, \\ g_{0n} = \frac{\lambda^3 \alpha^3}{3} g_{0n} + \frac{\lambda^5 \alpha^5}{5} g_{0n} + \dots, \\ g_{mn} = \frac{\lambda^2 \beta^2}{2} g_{mn} + \frac{\lambda^4 \beta^4}{4} g_{mn} + \dots, \\ g_{0n} = \frac{\lambda^3 \beta^3}{3} g_{0n} + \frac{\lambda^5 \beta^5}{5} g_{0n} + \dots; \end{array} \right.$$

nelle (I), δ_{mn} è l'ordinario simbolo di Kronecker, α e β sono due costanti, di valori a priori arbitrari, che hanno dimensioni di una velocità; in tal modo le componenti del tensore fondamentale risultano sviluppate in serie di potenze di λ o meglio dei puri numeri $\lambda\alpha$ oppure $\lambda\beta$; puri numeri sono pertanto anche i coefficienti dello sviluppo (I), i quali sono individuati dagli indici ordinali ad essi sottostanti. Il precedente sviluppo (I) precisa quello adottato da CALLAWAY ⁽³⁾, il quale lascia indeterminate le dimensioni del tensore fondamentale e non introduce le costanti α e β ; la parte simmetrica dello sviluppo (I) corrisponde sostanzialmente al sottostante sviluppo in serie di potenze di λ , assunto da EINSTEIN ed INFELD nel caso gravitazionale,

$$(II) \quad \left\{ \begin{array}{l} \gamma_{00} = \frac{\lambda^2}{2} \gamma_{00} + \frac{\lambda^4}{4} \gamma_{00} + \dots, \\ \gamma_{0n} = \frac{\lambda^3}{3} \gamma_{0n} + \frac{\lambda^5}{5} \gamma_{0n} + \dots, \\ \gamma_{mn} = \frac{\lambda^4}{4} \gamma_{mn} + \frac{\lambda^6}{6} \gamma_{mn} + \dots, \end{array} \right.$$

relativo alle seguenti combinazioni lineari del tensore fondamentale:

$$(11) \quad \gamma_{\mu\nu} \equiv (g_{\mu\nu} - \eta_{\mu\nu}) - \frac{1}{2} \eta_{\mu\nu} \eta^{\rho\sigma} (g_{\rho\sigma} - \eta_{\rho\sigma}) \quad (\mu, \nu = 0, 1, 2, 3);$$

nella (11), le $\eta_{\mu\nu}$ individuano il tensore fondamentale dello spazio-tempo pseudo-

euclideo

$$(\eta_{00} = \eta^{00} = 1, \eta_{mn} = \eta^{mn} = -\delta_{mn}, \eta_{0i} = \eta^{0i} = 0) \quad (1).$$

La (11) identifica la parte simmetrica degli sviluppi (I) con le (II) se nelle (I) è

(12) $\underline{\underline{g}}_{mn} = \underline{\underline{g}}_{00} \delta_{mn},$

condizione alla quale si può soddisfare grazie alle equazioni di campo, scegliendo opportunamente le coordinate spaziali, come si preciserà nella Sez. 6.

5. – Determinazione dei coefficienti di connessione.

I coefficienti di connessione si possono esprimere mediante le componenti del tensore fondamentale, traendoli dall'equazione

$$(5') \quad \underline{\underline{g}}_{\alpha\beta;\nu} = \underline{\underline{g}}_{\alpha\beta,\nu} - \underline{\underline{g}}_{\alpha\beta} \Gamma_{\alpha\nu}^{\sigma} - \underline{\underline{g}}_{\alpha\sigma} \Gamma_{\nu\beta}^{\sigma} = 0,$$

equivalente alla (5), con un procedimento ricorrente assicurato dallo sviluppo (I) del tensore fondamentale.

Poniamo a tal fine

$$(13) \quad \Gamma_{\alpha\beta}^{\nu} = \left\{ \begin{array}{c} \nu \\ \alpha \beta \end{array} \right\} + M_{\alpha\beta}^{\nu} \quad \text{dove} \quad \left\{ \begin{array}{c} \nu \\ \alpha \beta \end{array} \right\} = \frac{1}{2} l^{\nu\sigma} (\underline{\underline{g}}_{\alpha\sigma,\beta} + \underline{\underline{g}}_{\beta\sigma,\alpha} - \underline{\underline{g}}_{\alpha\beta,\sigma}),$$

con $l^{\nu\sigma}$ definito da

$$l^{\nu\sigma} \underline{\underline{g}}_{\sigma\sigma} = \delta_{\alpha}^{\nu}$$

è il generico simbolo di Christoffel di seconda specie dello spazio-tempo riemanniano di tensore fondamentale $\underline{\underline{g}}_{\alpha\beta}$, associato allo spazio-tempo unitario; $M_{\alpha\beta}^{\nu}$ dà così il divario tra i coefficienti di connessione dello spazio-tempo unitario ed i precedenti simboli di Christoffel ed è quindi un tensore. I coefficienti di connessione non sono puri numeri come le componenti del tensore fondamentale, perchè essi dipendono dalle derivate di queste ultime rispetto alle coordinate dello spazio-tempo, le quali hanno dimensioni di una lunghezza.

Eseguendo opportune combinazioni lineari delle equazioni (5') è facile mostrare che tutte le condizioni imposte dalle (5') al tensore $M_{\alpha\beta}^{\nu}$ sono riasseunte dalla relazione seguente:

$$(14) \quad M_{\alpha\beta}^{\nu} = l^{\nu\sigma} [\frac{1}{2} (\underline{\underline{g}}_{\alpha\beta,\sigma} - \underline{\underline{g}}_{\beta\sigma,\alpha} - \underline{\underline{g}}_{\sigma\alpha,\beta}) - \underline{\underline{g}}_{\alpha\sigma} \Gamma_{\beta\sigma}^{\nu} - \underline{\underline{g}}_{\beta\sigma} \Gamma_{\sigma\alpha}^{\nu}] \quad (11).$$

Sostituendo allora gli sviluppi (I) delle componenti del tensore fondamen-

..(11) Cfr., ad esempio, M. A. TONNELAT: *Compt. Rend. Acad. Sci. Paris*, **231**, 487 (1950).

talè nella parte simmetrica ed emisimmetrica delle (13), i coefficienti di connessione risultano sviluppati in serie di potenze di λ , le quali iniziano con λ^2 oppure con potenze di grado superiore al secondo.

Tutti i fattori di λ^2 diversi da zero, risultano individuati dalle quantità seguenti:

$$(III) \quad \left\{ \begin{array}{l} \frac{I^0}{2} \frac{0s}{2} = \frac{I^s}{2} \frac{00}{2} = \frac{1}{2} \alpha^2 g_{00,s} , \\ \frac{I^s}{2} \frac{im}{2} = \frac{1}{2} \alpha^2 (g_{lm,s} - \frac{g_{ms,l}}{2} - \frac{g_{sl,m}}{2}) , \\ \frac{I^s}{2} \frac{im}{\vee} = - \frac{1}{2} \beta^2 (g_{lm,s} + \frac{g_{sm,l}}{2} + \frac{g_{ls,m}}{2}) ; \end{array} \right.$$

analogamente, tutti i fattori di λ^3 diversi da zero nello sviluppo dei coefficienti di connessione sono i seguenti:

$$(IV) \quad \left\{ \begin{array}{l} \frac{I^0}{3} \frac{00}{2} = \frac{1}{2} \alpha^2 g_{00,4} , \\ \frac{I^0}{3} \frac{im}{2} = \frac{1}{2} (\alpha^3 g_{i0,m} + \alpha^3 g_{m0,i} - \alpha^2 g_{im,4}) , \\ \frac{I^s}{3} \frac{0i}{2} = \frac{1}{2} (\alpha^3 g_{0i,s} - \alpha^3 g_{0s,i} - \alpha^2 g_{is,4}) , \\ \frac{I^0}{3} \frac{im}{\vee} = \frac{1}{2} (\beta^2 g_{lm,4} + \beta^3 g_{0m,i} + \beta^3 g_{i0,m}) , \\ \frac{I^i}{3} \frac{p0}{\vee} = - \frac{1}{2} (\beta^3 g_{p0,i} + \beta^3 g_{i0,p} + \beta^2 g_{pi,4}) ; \end{array} \right.$$

mentre l'indice 0 indica derivazione parziale rispetto al tempo römeriano, qui e nel seguito l'indice 4 indica derivazione parziale rispetto al tempo i . Le (III) e le (IV) interessano le equazioni di movimento di quarto e di quinto grado (rispetto a λ), e quel termine dell'equazione di sesto grado che sarà messo in evidenza.

6. - Le equazioni gravitazionali.

Grazie allo sviluppo dei coefficienti di connessione, le equazioni di campo (2), (3) e (4) risultano espresse in serie di potenze di λ e si spezzano quindi in equazioni di un sistema ricorrente, che diremo equazioni ridotte di campo:

$$\left\{ \begin{array}{l} (15) \quad \frac{R}{n} \frac{\alpha\beta}{\beta} = 0 , \\ (16) \quad \frac{R}{n} \frac{\alpha\beta\gamma}{\gamma} + \frac{R}{n} \frac{\beta\gamma\alpha}{\gamma} + \frac{R}{n} \frac{\gamma\alpha\beta}{\gamma} = 0 , \\ (17) \quad \frac{I}{n} \frac{\beta}{\beta} = 0 \end{array} \right. \quad (n = 2, 3, 4 \dots).$$

Dalla definizione (6) del tensore contratto di curvatura e dalla circostanza che λ^2 è la potenza più bassa che compare negli sviluppi dei coefficienti di connessione, risulta, grazie alle (III), che le equazioni (2) di prima approssimazione sono costituite dalle equazioni ridotte

$$(18) \quad 2 \underline{\underline{R}}_{00} \equiv 2 \underline{\underline{\Gamma}}_{00,s}^s \equiv \alpha^2 \Delta g_{00} = 0,$$

(dove Δ è l'ordinario operatore di Laplace dello spazio euclideo tridimensionale) e

$$(19) \quad 2 \underline{\underline{R}}_{lm} \equiv 2 \underline{\underline{\Gamma}}_{lm,s}^s - (\underline{\underline{\Gamma}}_{l0,m}^0 + \underline{\underline{\Gamma}}_{ls,m}^s + \underline{\underline{\Gamma}}_{0m,l}^0 + \underline{\underline{\Gamma}}_{ms,l}^s) = 0.$$

Esplicitando la (19) mediante le (III), si ottiene:

$$(19') \quad \underline{\underline{\Delta}} g_{lm} - \left\{ \sum_1^3 \left[g_{lp} + \frac{1}{2} (g_{00} - \sum_1^3 \frac{1}{2} g_{ss}) \delta_{lp}^p \right]_{,m} + \right. \\ \left. - \left\{ \sum_1^3 \left[g_{mp} + \frac{1}{2} (g_{00} - \sum_1^3 \frac{1}{2} g_{ss}) \delta_{mp}^p \right]_{,l} \right\} \right\} = 0;$$

con la posizione (12), la (19') si riduce alla (18); la metrica dello spazio-tempo è allora individuata dalla forma quadratica

$$(20) \quad ds^2 \equiv (1 + \lambda^2 \alpha^2 g_{00}) dx_0^2 - (1 - \lambda^2 \alpha^2 g_{00}) (dx_1^2 + dx_2^2 + dx_3^2),$$

nella quale, grazie alla (18), il puro numero $\frac{1}{2} g_{00}$ è una funzione armonica, a priori arbitraria; la parte spaziale della metrica (20) è pertanto in rappresentazione conforme con la metrica dello spazio tridimensionale euclideo; x_1, x_2, x_3 ne costituiscono appunto un sistema di coordinate cartesiane ortogonali.

La (18) e la (19') coincidono con le equazioni gravitazionali di prima approssimazione degli spazi vuoti, e la metrica (20) ne rappresenta la soluzione più generale; nessuna limitazione è infatti imposta dalla (12), poiché essa dà una soluzione particolare delle equazioni lineari (19') ed il termine da aggiungervi a secondo membro per avere l'integrale generale delle (19') è nullo nell'approssimazione considerata, quando la metrica dello spazio tridimensionale euclideo è riferita a coordinate cartesiane ortogonali anziché a generiche coordinate curvilinee, come appunto accade per la (20) (12).

Quale soluzione dell'equazione (18) di Laplace, assumeremo infine, come in relatività generale, la somma dei potenziali gravitazionali elementari relativi a più particelle moltiplicata per -2 , porremo cioè

$$(21) \quad \alpha^2 \underline{\underline{g}}_{00} \equiv -2h \sum_1^p \underline{\underline{m}}^s \dot{r}^{s-1}$$

(12) Vedere, ad esempio, T. LEVI-CIVITA: *Fondamenti di meccanica relativistica* (Bologna, 1928), cap. II, § 6.

con

$$(22) \quad \overset{\circ}{r} = + \sqrt{(x_1 - \overset{\circ}{\xi}_1)^2 + (x_2 - \overset{\circ}{\xi}_2)^2 + (x_3 - \overset{\circ}{\xi}_3)^2} ;$$

nella (21), h è la costante di attrazione universale (costante di Cavendish), $\overset{\circ}{m}$ è la massa della particella esesima; infine, per la (22), $\overset{\circ}{r}$ è la distanza (misurata nell'ordinario spazio tridimensionale euclideo) tra il punto potenziato (di coordinate x_1, x_2, x_3) e la particella esesima, di coordinate $\overset{\circ}{\xi}_1, \overset{\circ}{\xi}_2, \overset{\circ}{\xi}_3$.

Grazie alla (6) ed alle determinazioni (III) e (IV) si ha successivamente:

$$(23) \quad 2 \underline{R}_{3\underline{0}l} = 2 \underline{\Gamma}_{l\underline{0},s}^s + \underline{\Gamma}_{l\underline{0},0}^0 - (\underline{\Gamma}_{00,l}^0 + \underline{\Gamma}_{l\underline{s},0}^s + \underline{\Gamma}_{0\underline{s},l}^s) \equiv \\ \equiv \Delta \alpha^3 g_{0l} - \sum_1^3 (\alpha^3 \underline{g}_{0s,l_s} + \alpha^2 \underline{g}_{ls,s1} - \alpha^2 \underline{g}_{ss,l4}) = 0 \quad (l = 1, 2, 3).$$

È comodo esprimere la (23) mediante le combinazioni lineari (11), di uso corrente in relatività generale. Dagli sviluppi (I) e (II) del tensore fondamentale si ha:

$$(24) \quad \alpha^2 \underline{g}_{00} = \frac{1}{2} \underline{\gamma}_{00} ,$$

$$(25) \quad \alpha^3 \underline{g}_{0l} = \underline{\gamma}_{0l} ;$$

per la (12) e per le precedenti (24) e (25), l'equazione (23) diventa così la seguente:

$$(26) \quad \Delta \underline{\gamma}_{0l} = \left(\sum_1^3 \underline{\gamma}_{0s,s} - \frac{1}{2} \underline{\gamma}_{00,4} \right)_{,l} ;$$

grazie alla (21) ed alla (24), si può assumere quale soluzione della (26)

$$(27) \quad \alpha^3 \underline{g}_{0l} = \underline{\gamma}_{0l} = 4h \sum_1^3 \overset{\circ}{m} \overset{\circ}{r}^{-1} \overset{\circ}{v}_l , \quad \text{dove} \quad \overset{\circ}{v}_l \equiv \frac{d\overset{\circ}{\xi}_l}{dt}$$

è la generica componente cartesiana della velocità della particella esesima, nell'ordinario spazio tridimensionale euclideo.

La (27) possiede le medesime singolarità della (21), ossia poli di primo ordine: è appunto ciò che deve accadere affinché la soluzione delle equazioni gravitazionali in questa approssimazione si comporti asintoticamente come la ben nota soluzione rigorosa di Schwarzschild; proprio questa condizione ha suggerito di scegliere la (27) quale soluzione della (26) ⁽¹⁾.

Rileviamo infine che i risultati di questo paragrafo non sussistono soltanto per la formulazione 1953 della teoria unitaria, ma anche per quella del 1950, poiché riguardano l'equazione (2), comune ad entrambe le formulazioni.

7. - Le equazioni elettromagnetiche.

Dagli sviluppi (III) dei coefficienti di connessione, dalla definizione (6) del tensore contratto di curvatura, risulta che le equazioni ridotte di campo (17) e (16), per $n = 2$, sono le seguenti:

$$(28) \quad -\Gamma_{\frac{2}{2} \frac{1}{\vee}}^s = \beta^2 \sum_1^3 g_{im,m} = 0 ,$$

$$(29) \quad -2(R_{\frac{2}{2} \frac{1}{\vee},p} + R_{\frac{2}{2} \frac{1}{\vee},m} + R_{\frac{2}{2} \frac{1}{\vee},l}) \equiv \beta^2 \Delta (g_{\frac{2}{2} \frac{1}{\vee},p} + g_{\frac{2}{2} \frac{1}{\vee},m} + g_{\frac{2}{2} \frac{1}{\vee},l}) = 0 ;$$

la (28) e la (29) si possono interpretare come equazioni del campo elettromagnetico delle particelle. L'equazione (28) è identicamente soddisfatta ponendo

$$(30) \quad \frac{g_{12}}{2 \vee} = k\varphi_{,3} , \quad \frac{g_{23}}{2 \vee} = k\varphi_{,1} , \quad \frac{g_{31}}{2 \vee} = k\varphi_{,2} ,$$

dove $\varphi(x_1, x_2, x_3)$ è una funzione arbitraria delle coordinate spaziali e k è una costante disponibile, da dimensionare a posteriori in modo che i secondi membri delle (30) siano puri numeri.

Grazie alle (30), la (29) diventa:

$$(31) \quad \Delta \Delta \varphi = 0 ;$$

a soluzione dell'equazione (31) corrispondente al campo di una particella, assumiamo la funzione

$$(32) \quad \varphi = Ar^{-1} + (Br^2 + Cr) ,$$

nella quale A , B e C sono costanti a priori arbitrarie ed r è la distanza tra un punto generico dello spazio ordinario e la particella, situata dove la (32) ha una singolarità polare; la soluzione elementare (32) differisce dalla più generale funzione biarmonica che dipende dalla sola coordinata raggio r , per una costante additiva arbitraria, priva di interesse.

Grazie agli sviluppi (III) e (IV) e alla definizione (6) del tensore contratto di curvatura, le equazioni di campo (16) e (17), per $n = 3$, si riducono alle seguenti:

$$(33) \quad \Delta(\beta^3 g_{10,m} + \beta^3 g_{0m,l} + \beta^2 g_{ml,4}) = 0 ;$$

$$(34) \quad \Gamma_{\frac{3}{3} \frac{0}{\vee}}^s \equiv \beta^3 \sum_1^3 g_{s\frac{1}{\vee},s} = 0 ;$$

per le (30), una soluzione particolare delle precedenti equazioni (33) e (34)

è espressa dalla terna di puri numeri

$$(35) \quad \begin{matrix} g_{0i} \\ 3 \vee \end{matrix} = \beta^{-1} k (\mathbf{v} \wedge \text{grad } \varphi)_i \quad (i = 1, 2, 3),$$

dove \mathbf{v} è la velocità della particella ⁽¹³⁾.

È così completamente individuata la singolarità che rappresenta la particella nelle equazioni elettromagnetiche (28) e (29), (33) e (34): le precedenti equazioni sono lineari ed omogenee; come loro soluzioni, relative a più corpuscoli, assumeremo quindi la somma di altrettanti termini (30) e (35), in ognuno dei quali le costanti A , B e C , le quali provengono dalla funzione (32), si riferiscono ad una particella.

8. - Deduzione delle equazioni di movimento.

Gli integrali che intervengono nei primi membri delle equazioni di movimento (9) e (10) non dipendono dalla superficie di integrazione, qualunque sia l'approssimazione con la quale si valutano i vettori integrandi. Tale proprietà sussiste infatti per la formula rigorosa (1) indipendentemente dalle particolari determinazioni dei secondi membri della (7) e della (8) ⁽⁵⁾. Si può allora semplificare il calcolo di questi integrali scegliendo in primo luogo una sfera come superficie di integrazione, che racchiuda la sola particella considerata ed abbia centro in essa; in secondo luogo, anzichè valutare separatamente tutti gli integrali delle equazioni (9) e (10), conviene dapprima raggruppare opportunamente gli addendi dei vettori integrandi, e calcolare poi i limiti dei corrispondenti integrali quando il raggio della sfera tende a zero. Risultano così nulle tutte quelle quantità che dipendono dal raggio della sfera e che si eliderebbero reciprocamente qualora venissero calcolate e poi sostituite nelle equazioni (9) e (10).

Eseguendo sotto il segno di integrale quelle derivazioni rispetto al tempo che sono indicate esplicitamente dalle (9) e dalle (10), va infine tenuto presente che il raggio ed il versore normale alla sfera non dipendono dal tempo, sicchè le loro derivate temporali sono nulle.

Dalla struttura dei vettori integrandi delle equazioni (9) e (10) risulta che gli integrali da calcolare sono di tre tipi: integrali relativi a prodotti fra quantità che si riferiscono alla sola particella racchiusa dalla superficie di integrazione, integrali che riguardano quantità relative alle restanti particelle, integrali che riguardano prodotti fra quantità relative alla sola particella considerata e quantità relative alle restanti particelle. I limiti degli integrali del secondo tipo sono tutti nulli, poichè i corrispondenti vettori integrandi si mantengono

⁽¹³⁾ Nella (35), come in seguito, una lettera in grassetto (maiuscola o minuscola) indica un vettore, ed il segno \wedge indica un prodotto vettoriale; il segno \times indicherà invece un prodotto scalare.

finiti oltre che sulla superficie di integrazione anche in tutti i punti interni ad essa. Per calcolare i limiti degli integrali del terzo tipo, conviene sviluppare in serie di Taylor, attorno al centro della sfera che racchiude la particella, i fattori del vettore integrando che provengono dalle restanti particelle; l'ipotesi di sviluppabilità che si viene così ad introdurre è assai poco restrittiva, poichè le quantità che si sviluppano sono funzioni regolari all'infuori della posizione occupata dalla particella che rappresentano, ed inoltre l'intorno del centro della sfera nel quale devono sussistere i precedenti sviluppi in serie di Taylor non è prefissato, ma può essere comunque piccolo.

Nessuna semplificazione si può invece prevedere per il calcolo dei limiti degli integrali del primo tipo.

9. - Le equazioni di movimento in prima approssimazione.

La (9) e la (10) cessano di essere delle identità, almeno a priori, quando si comincia a tener conto in esse dei termini di quarto grado rispetto a λ ; ciò risulta dalla struttura medesima della (9) e della (10), grazie agli sviluppi (III) e (IV) dei coefficienti di connessione, agli sviluppi (I) delle componenti del tensore fondamentale ed a quelli delle corrispondenti componenti della densità tensoriale fondamentale.

I termini di quarto grado della (9) e della (10) si calcolano facendo capo alle soluzioni (21) e (27) delle equazioni gravitazionali (18), (19') e (23) ed alla soluzione delle equazioni elettromagnetiche (28) e (29), espressa dalle (30) e dalla (32). Questo calcolo, semplice ma assai laborioso, è stato eseguito riferendosi a due particelle.

Analogamente al caso gravitazionale, la (10) risulta allora identicamente soddisfatta grazie alla (21), mentre la (9), come constateremo, dà effettivamente tre equazioni. Le equazioni di movimento di prima approssimazione sono pertanto costituite dai termini in λ^4 delle (9); quelli non nulli provengono da prodotti che dipendono o dalle sole componenti simmetriche o dalle sole componenti emisimmetriche del tensore fondamentale. In tal modo, nelle equazioni di movimento di prima approssimazione mancano termini di interazione fra campo gravitazionale e campo elettromagnetico.

Le quantità non nulle di quarto grado relative ai primi membri delle tre equazioni (9) sono le seguenti:

$$(36) \quad \lim_{\frac{1}{r} \rightarrow 0} \int_{\sigma} \left\{ \lambda \frac{\partial}{\partial t} [g^{js} I_{ji}^0 - g^{j0} I_{ji}^s] \frac{1}{n_s} + \lambda \frac{\partial}{\partial t} (g^{\varrho\sigma} \Gamma_{\varrho\sigma}^{\sigma} - g^{\varrho\sigma} \Gamma_{\varrho\sigma}^0) \frac{1}{n_i} \right\} d\sigma = 16\pi \lambda^4 h \frac{1}{m} \frac{1}{a_i};$$

$$(37) \quad \lim_{\frac{1}{r} \rightarrow 0} \int_{\sigma} g^{\varrho\sigma} R_{\varrho\sigma}^{\frac{1}{V}} \frac{1}{n_i} d\sigma = - \lim_{\frac{1}{r} \rightarrow 0} \lambda^4 \beta^4 k^2 \int_{\sigma} \sum_{i=1}^3 \varphi_{,i} \Delta \varphi_{,i} \frac{1}{n_i} d\sigma = \frac{4}{3} \pi \lambda^4 \beta^4 k^2 [A \Delta \varphi_{,i} + 2C_{\varphi,i}^2];$$

$$(38) \quad \lim_{\substack{r \rightarrow 0 \\ 1}} \int_{\sigma} g_{\frac{2}{2}}^{\frac{2}{2}} R_{\frac{2}{2}}^{\frac{1}{1}} \dot{n}_s d\sigma = -\frac{8}{3} \pi \lambda^4 \beta^4 k^2 \dot{C} \dot{\varphi}_{,i} ;$$

$$(39) \quad \lim_{\substack{r \rightarrow 0 \\ 1}} \int_{\sigma} \mathfrak{B}_{\alpha\beta}^s g_{,i}^{\alpha\beta} \dot{n}_s d\sigma = -\frac{24}{5} \pi \lambda^4 \beta^4 k^2 A \Delta \dot{\varphi}_{,i} - 4\pi \lambda^4 h \dot{m}_{\frac{2}{2}}^{\frac{2}{2}} \dot{\gamma}_{00,i} + \\ - \frac{1}{4} \lambda^4 \lim_{\substack{r \rightarrow 0 \\ 1}} \int_{\sigma} \sum_{i=1}^3 \dot{\gamma}_{00,i}^{\frac{2}{2}} \dot{\gamma}_{00,i}^{\frac{2}{2}} \dot{n}_s d\sigma ;$$

$$(40) \quad \lim_{\substack{r \rightarrow 0 \\ 1}} \int_{\sigma} \mathfrak{B} \dot{n}_i d\sigma = -\frac{32}{15} \pi \lambda^4 \beta^4 k^2 A \Delta \dot{\varphi}_{,i} - \frac{1}{4} \lambda^4 \lim_{\substack{r \rightarrow 0 \\ 1}} \int_{\sigma} \sum_{i=1}^3 \dot{\gamma}_{00,i}^{\frac{2}{2}} \dot{\gamma}_{00,i}^{\frac{2}{2}} \dot{n}_i d\sigma .$$

In queste formule gli indici sovrapposti 1 e 2 indicano, come nella formula (21) e successive, la particella alla quale si riferisce la quantità così denotata; tutti i limiti precedenti riguardano dunque la particella 1, e quindi le funzioni che li esprimono si intendono valutate nella posizione \dot{O} occupata dalla particella 1; inoltre le $\dot{\varphi}_{,i}$ e le $\Delta \dot{\varphi}_{,i}$ che ivi intervengono, sostituiscono, per comodità, le $\dot{g}_{lm}^{\frac{2}{2}}$ e le $\Delta \dot{g}_{lm}^{\frac{2}{2}}$, le quali si ottengono dal calcolo diretto dei primi membri e sono equivalenti a quelle, grazie alle (30). Infine i due limiti dell'ultimo addendo della (39) e del secondo addendo della (40) non sono stati calcolati, perché si constata facilmente che i due corrispondenti integrali sono uguali e contrari e quindi si elidono reciprocamente nella equazione (9). Dalle formule precedenti (36), (37), (38), (39) e (40) risulta così:

$$(41) \quad 16\pi \lambda^4 h \dot{m}_{\frac{2}{2}}^{\frac{1}{1}} = -4\pi \lambda^4 h \dot{m}_{\frac{2}{2}}^{\frac{2}{2}} - 4\pi \lambda^4 \beta^4 k^2 \dot{A} \Delta \dot{\varphi}_{,i} - 8\pi \lambda^4 \beta^4 k^2 \dot{C} \dot{\varphi}_{,i} ;$$

le variabili indipendenti delle (41) sono le coordinate cartesiane ortogonali x_1, x_2, x_3 e quindi, grazie alle dimensioni di h , di λ , di β ed a quelle di A, k e φ che seguono dalle (30) e (32), le (41) costituiscono tre equazioni adimensionali; dividiamone ambo i membri per il fattore comune $16\pi \lambda^4 h$, che è il doppio della costante di ragguglio tra il tensore gravitazionale ed il tensore energetico nelle equazioni gravitazionali della relatività generale⁽¹⁴⁾; per la (21), per la (24) e per la (32), le tre equazioni (41) si possono allora riassumere nella seguente equazione vettoriale di movimento della particella 1, la quale si riferisce all'ordinario spazio tridimensionale euclideo:

$$(42) \quad \dot{m} \dot{\mathbf{a}} = h \frac{\dot{m}^{\frac{1}{2}} \dot{m}^{\frac{2}{2}}}{r^2} \text{vers}(\dot{O} - \dot{O}) + \frac{1}{2} \frac{\dot{A}^{\frac{1}{2}} \dot{C} + \dot{A}^{\frac{2}{2}} \dot{C}^{\frac{1}{1}}}{h} \beta^4 k^2 \frac{1}{r^2} \text{vers}(\dot{O} - \dot{O}) + \\ - \frac{1}{2} \frac{\dot{C}^{\frac{1}{2}} \dot{C}^{\frac{2}{2}}}{h} \beta^4 k^2 \text{vers}(\dot{O} - \dot{O}) - \frac{\dot{C}^{\frac{1}{2}} \dot{B}^{\frac{2}{2}}}{h} \beta^4 k^2 (\dot{O} - \dot{O}) ;$$

(14) Vedere, ad esempio, loco citato in (12), cap. II, § 5.

nella (42), \dot{m} ed \ddot{m} sono le masse delle particelle, \dot{a} è l'accelerazione della particella 1, h è la costante di Cavendish, mentre le costanti disponibili A , B e C provengono dalla funzione (32) che costituisce con le (30) la soluzione prescelta delle equazioni elettromagnetiche (28) e (29); infine $\dot{\theta}$ ed $\ddot{\theta}$ sono le posizioni occupate rispettivamente dalle particelle 1 e 2 ed r la distanza di $\dot{\theta}$ da $\ddot{\theta}$.

Nella (42), supponiamo per ora diverse da zero le costanti disponibili \dot{A} ed \ddot{A} , \dot{C} e \ddot{C} , rimandando alla Sez. 13 la discussione dell'eventualità opposta; è allora possibile determinare queste costanti in modo che il secondo addendo a secondo membro dell'equazione (42) si riduca all'ordinaria forza elettrostatica coulombiana esercitata dalla particella 2 sulla particella 1. Basta porre a tal fine

$$(V) \quad \left\{ \begin{array}{l} \dot{A} = -\dot{e}, \quad \ddot{A} = -\ddot{e}, \\ \dot{C} = -h\beta^{-4}k^{-2}\dot{e}, \quad \ddot{C} = -h\beta^{-4}k^{-2}\ddot{e}, \\ \dot{B} = h\dot{\mu}, \quad \ddot{B} = h\ddot{\mu}, \end{array} \right.$$

dove \dot{e} ed \ddot{e} sono le cariche delle due particelle in valore e segno, mentre $\dot{\mu}$ e $\ddot{\mu}$ sono due costanti ancora disponibili; con queste determinazioni, ciascuna costante contiene i soli parametri della particella alla quale è riferita, e nessuna delle due particelle risulta privilegiata. L'equazione (42) diventa pertanto:

$$(43) \quad \dot{m}\dot{a} = h \frac{\dot{m}\dot{m}}{r^2} \text{vers}(\ddot{\theta} - \dot{\theta}) + \frac{\dot{e}\dot{e}}{r^2} \text{vers}(\dot{\theta} - \ddot{\theta}) + \\ - \frac{1}{2} h\beta^{-4}k^{-2} \dot{e}\dot{e} \text{vers}(\dot{\theta} - \ddot{\theta}) + h\dot{\mu}\dot{e}(\dot{\theta} - \ddot{\theta});$$

nella prima approssimazione considerata si ottiene così la legge fondamentale che nella dinamica classica individua il movimento della particella 1 per azione della particella 2, rispetto ad un osservatore inerziale. Questa azione è data da quattro forze: la prima è la forza gravitazionale newtoniana, la seconda è la forza elettrostatica coulombiana; le due forze centrali rimanenti provengono dall'interazione fra il campo gravitazionale ed il campo elettromagnetico: la prima ha modulo costante, la seconda, di tipo elastico, è proporzionale alla distanza fra le due particelle; poiché quest'ultima al crescere della distanza diventa tanto grande quanto si vuole (se $h\dot{\mu}\dot{e} \neq 0$), sembra ragionevole riguardare μ come quantità di misura estremamente piccola nel sistema elettrostatico, anzi addirittura nulla. In quanto alla forza centrale di modulo costante (proporzionale al prodotto delle due cariche \dot{e} ed \ddot{e} ed alla costante h di Cavendish), nulla a priori possiamo affermare relativamente al coefficiente $\beta^{-4}k^{-2}$ che vi compare. Soltanto si può osservare che ha le dimensioni $[e^2 l^{-8} t^4]$

e che deve avere ordine di grandezza finito quando è misurato nelle unità elettrostatiche, se si vuole che le g_{lm} siano piccole dell'ordine λ^2 e vi predomini l'addendo colombiano. Lasciando dunque questa sola forza a rappresentare l'interazione fra gravitazione ed elettricità, la (43) diviene più semplicemente:

$$(44) \quad \overset{1}{m} \overset{1}{\dot{a}} = \hbar \frac{\overset{1}{m} \overset{2}{m}}{r^2} \text{vers}(\overset{2}{\dot{O}} - \overset{1}{\dot{O}}) + \frac{\overset{1}{e} \overset{2}{e}}{r^2} \text{vers}(\overset{1}{\dot{O}} - \overset{2}{\dot{O}}) - \frac{1}{2} \hbar \beta^{-4} k^{-2} \overset{1}{e} \overset{2}{e} \text{vers}(\overset{1}{\dot{O}} - \overset{2}{\dot{O}});$$

prescindendo dalla forza di interazione, la (44) coincide con l'equazione vettoriale di movimento di prima approssimazione della Fisica classica, riferita ad un osservatore inerziale.

Naturalmente perchè abbia significato tener conto delle forze gravitazionali accanto a quelle elettrostatiche, perchè cioè il problema unitario abbia interesse, occorre che $\hbar \overset{1}{m} \overset{2}{m}$ sia finito, come è; poichè \hbar è piccolo, è quindi necessario che $\overset{1}{m} \overset{2}{m}$ sia grande.

L'equazione (44) si estende immediatamente a sistemi formati da un numero qualsiasi di particelle, grazie alla struttura delle equazioni (9) e (10) ed alla duplice circostanza che le equazioni ridotte di campo che ivi intervengono, (18), (19) e (23), (28) e (29), sono lineari ed individuano il campo elettromagnetico indipendentemente dal campo gravitazionale.

10. – Le equazioni di movimento sino ai termini in λ^5 .

I termini di quinto grado in λ delle tre equazioni (9) risultano identicamente nulli in qualsiasi riferimento, grazie agli sviluppi (I) delle componenti del tensore fondamentale, alla (13), alla (14) ed alle determinazioni (III) e (IV) dei coefficienti di connessione. Almeno a priori, i termini di quinto grado in λ dell'equazione (10) non sono invece identicamente nulli come gli analoghi di quarto grado, ma riguardano le equazioni di movimento di sesto grado e non quelle di quinto grado poichè in essi intervengono anche componenti del tensore fondamentale di grado superiore al terzo, e queste non compaiono nelle precedenti equazioni di movimento.

In definitiva, come nel caso gravitazionale, le equazioni di movimento sino ai termini in λ^5 coincidono con quelle di quarto grado in λ (e cioè di prima approssimazione), le quali sono riassunte dall'equazione vettoriale (44).

11. – Il campo elettromagnetico.

Grazie alle determinazioni (V) con $\mu=0$, la funzione (32) diventa la seguente:

$$(32') \quad \varphi = -er^{-1} - \hbar \beta^{-4} k^{-2} er;$$

le componenti emisimmetriche (30) del tensore fondamentale moltiplicate per

k^{-1} individuano allora, in corrispondenza a ciascuna carica e , un campo elettrostatico costituito da due forze centrali conservative, di potenziale (32'): una è la classica forza elettrostatica coulombiana della carica puntiforme e , l'altra è una forza di modulo costante, proporzionale alla carica stessa ed alla costante h di Cavendish.

Grazie alla (32'), la (35) diviene

$$(35') \quad \mathop{g_{0i}}_3 = \beta^{-1}k[\mathbf{v} \wedge \text{grad}(-er^{-1})]_i + h\beta^{-1}k(\mathbf{v} \wedge \text{grad } \psi)_i$$

con

$$(45) \quad \psi \equiv -\beta^{-4}k^{-2}er;$$

nella (35'), \mathbf{v} è la velocità della carica e .

Le $\mathop{g_{lm}}_2$ e le $\mathop{g_{0i}}_3$ dell'intero sistema di particelle sono costituite dalla somma delle precedenti (30) e (35'), estesa a tutte le cariche, ed individuano quindi un campo elettromagnetico somma dei campi considerati. Attraverso ai contributi di tutte le cariche relativi agli addendi delle (30) e delle (35') che contengono la costante h di Cavendish, si comincia così a manifestare l'interazione tra il campo gravitazionale ed il campo elettromagnetico complessivi; invece i due rimanenti addendi delle (30) e delle (35') coincidono rispettivamente con il primo termine dello sviluppo in serie di potenze di λ del campo elettrico e del campo magnetico maxwelliani di una carica puntiforme, in movimento rispetto ad un osservatore inerziale, quando si sceglie il potenziale ritardato oppure la semisomma del potenziale ritardato con il potenziale anticipato quale soluzione delle classiche equazioni dei potenziali elettromagnetici nel vuoto, relativi ad una carica puntiforme. È tuttavia più spontaneo ritenere che i due termini considerati appartengano alla soluzione dedotta dal potenziale ritardato poichè, quando gli sviluppi in serie di potenze di λ convergono, questa soluzione coincide con quella ben nota di Wiechert-Liénard; il campo creato da ciascuna carica sussiste quindi senza apporto di energia alla carica stessa; la circostanza opposta si verifica invece per il campo elettromagnetico dedotto dalla semisomma del potenziale ritardato con il potenziale anticipato, poichè a grande distanza dalla carica che lo genera esso si propaga prevalentemente per onde stazionarie⁽¹⁵⁾. Vi è infine coincidenza tra i termini principali elettrico e magnetico dei due precedenti campi, perchè lo sviluppo in serie di potenze di λ del campo elettromagnetico corrispondente alla semidifferenza fra potenziale ritardato e potenziale anticipato, inizia con due potenze di λ di grado superiore a quelle considerate⁽¹⁵⁾.

In definitiva, indicando con \mathbf{E} ed \mathbf{H} i due termini principali dei due citati campi elettromagnetici maxwelliani, le (30), grazie alla (32'), e la (35') si pos-

(15) L. INFELD: *Phys. Rev.*, **53**, 836 (1938). L. PAGE: *Phys. Rev.*, **24**, 296 (1924).

sono esprimere rispettivamente così

$$(46) \quad k^{-1} g_{\frac{1}{2} \frac{1}{2}} = E_3 + h \psi_3 = e r^{-2} \operatorname{vers}(P - O)_3 + h \psi_3; \dots,$$

$$(47) \quad \lambda \beta k^{-1} g_{\frac{3}{2} \frac{3}{2}} = \lambda (\mathbf{v} \wedge \mathbf{E})_i + \lambda h (\mathbf{v} \wedge \operatorname{grad} \psi)_i = H_i + \lambda h (\mathbf{v} \wedge \operatorname{grad} \psi)_i,$$

dove la funzione ψ è individuata dalla (45), mentre P ed O indicano rispettivamente il punto potenziato e la posizione occupata dalla carica potenziante e ed r la reciproca distanza.

In tal modo, ancora una volta nella teoria unitaria einsteiniana è possibile ravvisare il tensore elettromagnetico in una quantità proporzionale al coniugato della parte emisimmetrica del tensore fondamentale.

12. – Le equazioni di movimento di seconda approssimazione e la forza di Lorentz.

Come risulta dalla Sez. 10, le equazioni di movimento di seconda approssimazione non contengono termini in λ^5 e sono pertanto costituite dalla somma dei termini di quarto grado in λ (che danno luogo all'equazione (44) di prima approssimazione) con i termini di sesto grado delle equazioni (9).

Si può constatare che gli integrali di sesto grado delle equazioni (9), nel caso di due particelle, danno luogo al vettore

$$(48) \quad \lambda \dot{e} (\mathbf{v} \wedge \mathbf{H}),$$

il quale costituisce l'addendo elettrodinamico della forza totale di Lorentz

$$(49) \quad \dot{e} [\mathbf{E} + \lambda (\mathbf{v} \wedge \mathbf{H})],$$

nella quale, come nella (48), i vettori \mathbf{E} ed \mathbf{H} sono individuati dalla (46) e dalla (47) e valutati in \dot{O} ⁽¹⁶⁾. Si può però dimostrare l'asserto senza procedere al calcolo, concettualmente semplice, ma assai laborioso, degli integrali precedenti.

(16) Ecco, ad esempio, come l'addendo (48) compare esplicitamente nella parte di sesto grado dei seguenti vettori:

$$\lim_{r \rightarrow 0} \int_{\sigma} R_{\frac{1}{2} \frac{1}{2}} \mathbf{n} \, d\sigma = \lim_{r \rightarrow 0} + \lambda^6 \beta^6 \int_{\sigma} \left(\sum_{i=1}^3 g_{0i} \Delta g_{0i} \mathbf{n} \right) \, d\sigma + \dots = -\frac{16}{3} \pi \lambda^5 h \dot{e} (\mathbf{v} \wedge \mathbf{H}) + \dots;$$

$$\lim_{r \rightarrow 0} \int_{\sigma} \left(\sum_{i=1}^3 R_{\frac{1}{2} \frac{1}{2}} g_{0s}^i \mathbf{n}_s \mathbf{u}_i \right) \, d\sigma = \lim_{r \rightarrow 0} -\lambda^6 \beta^3 \int_{\sigma} \left(\sum_{i=1}^3 R_{0i} g_{0s}^i \mathbf{n}_s \mathbf{u}_i \right) \, d\sigma \dots = +\frac{4}{3} \pi \lambda^5 h \dot{e} (\mathbf{v} \wedge \mathbf{H}) + \dots;$$

in queste formule, \mathbf{u}_i è il versore del generico asse cartesiano x_i , il vettore a terzo membro costituisce la parte maxwelliana del limite in evidenza a secondo membro; i termini rimanenti, rappresentati dai puntini a secondo ed a terzo membro, o non contengono il vettore (48) oppure lo contengono implicitamente grazie alle equazioni ridotte di campo.

A tal fine, riferiamo il movimento del corpuscolo 1, oltre che ad un osservatore O prefissato ad arbitrio, anche ad un osservatore \bar{O} rispetto al quale il corpuscolo 1 ha velocità $\dot{\mathbf{v}} = 0$, in una posizione ed in un istante prefissati ad arbitrio. Le corrispondenti equazioni di movimento di sesto grado in λ si possono allora indicare così:

$$(50) \quad \left\{ \begin{array}{l} \lambda^4 \mathbf{Q}_4 + \lambda^6 \mathbf{Q}_6 = 0 \quad \text{rispetto ad } O, \\ \lambda^4 \bar{\mathbf{Q}}_4 + \lambda^6 \bar{\mathbf{Q}}_6 = 0 \quad \text{rispetto ad } \bar{O}. \end{array} \right.$$

$$(51) \quad \left\{ \begin{array}{l} \lambda^4 \mathbf{Q}_4 + \lambda^6 \bar{\mathbf{Q}}_6 = 0 \quad \text{rispetto ad } O, \\ \lambda^4 \bar{\mathbf{Q}}_4 + \lambda^6 \mathbf{Q}_6 = 0 \quad \text{rispetto ad } \bar{O}. \end{array} \right.$$

La legge di trasformazione fra la (50) e la (51) si può stabilire in modo completo soltanto dopo aver determinato esplicitamente tutti i loro addendi, poichè è a priori ignota la legge di trasformazione delle equazioni (9) e (10) dalle quali provengono la (50) e la (51). Si può tuttavia osservare che l'equazione di movimento di quarto grado in λ riferita ad O , è ancora la (44) di prima approssimazione, poichè la (44) sussiste per un generico osservatore e non contiene la velocità $\dot{\mathbf{v}}$ del corpuscolo 1.

Le coordinate spaziali e temporali di O e di \bar{O} sono legate tra loro dalla corrispondente trasformazione di Lorentz. A quest'ultima è pertanto subordinata la legge di trasformazione fra la (50) e la (51). Il vettore $\lambda^4 \mathbf{Q}_4$ si trasforma allora nella somma di un vettore di quarto grado, indicato con $\lambda^4 \bar{\mathbf{Q}}_4$, con un vettore $\lambda^6 \mathbf{L}_6$ di sesto grado; il contributo del vettore $\lambda^6 \bar{\mathbf{Q}}_6$ rimane invece inalterato. Si ha dunque:

$$(52) \quad \mathbf{Q}_4 = \bar{\mathbf{Q}}_4, \quad \mathbf{Q}_6 = \bar{\mathbf{Q}}_6 + \mathbf{L}_6.$$

Ma per la (44), \mathbf{Q}_4 come \mathbf{Q}_6 non contiene l'addendo elettrodinamico (48) della forza totale di Lorentz (49); neppure lo contiene l'addendo \mathbf{Q}_6 , perchè rispetto ad \bar{O} è nulla la velocità $\dot{\mathbf{v}}$ della particella 1; pertanto \mathbf{L}_6 è il solo vettore dell'equazione (50) che può contenere la forza (48).

La dimostrazione dell'asserto si riduce pertanto a provare che effettivamente $\lambda^2 \mathbf{Q}_4$ è somma della forza elettrodinamica di Lorentz (48) e di altri termini da essa indipendenti. Osserviamo a tal fine che alla forza (48) può dar luogo soltanto, attraverso alla trasformazione di Lorentz, quella parte di \mathbf{Q}_4 che non contiene la costante h di Cavendish, cioè l'addendo elettrostatico che compare a secondo membro della (44), ed è ben noto che una trasformazione di Lorentz muta tale addendo elettrico nella somma della forza elettrodinamica totale con altri addendi che non si elidono con questa; ma constatiamolo direttamente.

L'equazione di movimento di quarto grado valida per l'osservatore O è ancora la (44) ed in questa, moltiplicata per λ^4 , la forza elettrostatica coulombiana è rappresentata (ricordando le (46)) dalla parte indipendente dalla costante h di Cavendish, delle quantità

$$(53) \quad \lambda^4 \dot{e} k^{-1} \frac{2}{2} \bar{g}_{23}, \quad \lambda^4 \dot{e} k^{-1} \frac{2}{2} \bar{g}_{31}, \quad \lambda^4 \dot{e} k^{-1} \frac{2}{2} \bar{g}_{12}.$$

Passiamo da \bar{O} ad O con la trasformazione speciale di Lorentz; si ha allora notoriamente:

$$(VI) \quad \begin{cases} \dot{e} \bar{g}_{12} = \dot{e} (g_{12} + \lambda \dot{v} g_{02}) (1 - \lambda^2 \dot{v}^2)^{-\frac{1}{2}}, \\ \dot{e} \bar{g}_{31} = \dot{e} (g_{31} - \lambda \dot{v} g_{03}) (1 - \lambda^2 \dot{v}^2)^{-\frac{1}{2}}, \\ \dot{e} \bar{g}_{23} = \dot{e} g_{23} \quad (17). \end{cases}$$

Tenendo conto nelle (VI) degli sviluppi (I) delle componenti emisimmetriche del tensore fondamentale, arrestati ai termini in λ^4 , risulta

$$\dot{e} (\lambda^2 \beta^2 \bar{g}_{12} + \lambda^4 \beta^4 \bar{g}_{12}) = \dot{e} (\lambda^2 \beta^2 g_{12} + \lambda^4 \beta^4 g_{12} + \lambda^4 \dot{v} \beta^3 g_{02}) + \frac{1}{2} \dot{e} \lambda^4 (\dot{v})^2 \beta^2 g_{12}$$

e due formule analoghe; si ha quindi, osservando che $\lambda^6 g_{12}$ differisce da $\lambda^6 g_{12}$ per termini di grado superiore al sesto rispetto a λ :

$$(54) \quad \lambda^4 \dot{e} k^{-1} \frac{2}{2} \bar{g}_{12} = \dot{e} k^{-1} [\lambda^4 \frac{2}{2} \bar{g}_{12} + \lambda^6 \dot{v} \beta \frac{2}{3} \bar{g}_{02} + \frac{1}{2} \lambda^6 (\dot{v})^2 \frac{2}{2} \bar{g}_{12}];$$

la (54) precisa la legge con cui si trasforma una componente della forza elettrostatica coulombiana nel passaggio da \bar{O} ad O . Nel secondo membro della (54), il primo addendo dà la componente della forza elettrostatica coulombiana, il secondo (proporzionale alla velocità \dot{v} di \dot{e}) dà la corrispondente componente della forza elettrodinamica di Lorentz, associata alla forza coulombiana, infine il terzo addendo, proporzionale al quadrato della velocità \dot{v} , non può elidere nessuno dei precedenti. Ricordando le (46) e le (47), potremo dare alla considerata forza elettromagnetica maxwelliana la seguente espressione vettoriale:

$$(55) \quad \dot{e} \lambda^4 [\dot{\mathbf{E}} + \lambda (\dot{\mathbf{v}} \wedge \dot{\mathbf{H}})] + \frac{1}{2} \dot{e} \lambda^6 [(\dot{v})^2 \dot{\mathbf{E}} - \dot{\mathbf{v}} (\dot{\mathbf{E}} \times \dot{\mathbf{v}})],$$

dove il secondo addendo è di sesto grado poichè, per le (47), $\dot{\mathbf{H}}$ è di primo grado.

(17) Vedere, ad esempio, B. FINZI e M. PASTORI: *Calcolo tensoriale e applicazioni* (Bologna, 1949), cap. IX, § 3.

La (55) contiene appunto la forza elettrodinamica totale di Lorentz, proprio come era stato annunciato (18).

Dalle tre equazioni (9) discende così la seguente equazione di movimento di seconda approssimazione per la particella 1, sottoposta alla sola azione della particella 2:

$$(56) \quad \dot{\vec{m}}\vec{a} = h \frac{\vec{m}\vec{m}}{r^2} \text{vers}(\vec{O} - \vec{O}) + \vec{e}[\vec{E} + \lambda(\vec{v} \wedge \vec{H})] + \\ - \frac{1}{2} h \beta^{-4} k^{-2} \vec{e} \vec{e} \text{vers}(\vec{O} - \vec{O}) + \dots ;$$

nella (56), \vec{E} ed \vec{H} sono i termini principali del campo elettrico e magnetico maxwelliani della particella 2, i quali sono individuati dalla (46) e dalla (47) (e valutati in \vec{O}); tutti i termini messi in evidenza nella (56), all'infuori del terzo, provengono dalla equazione (44) di quarto grado, mentre i puntini indicano i rimanenti termini di sesto grado; questi termini, per quanto si è già detto, non si possono elidere con quelli messi in evidenza.

L'equazione (56) si estende inalterata nella forma dei termini esplicitati, a sistemi costituiti da quante si vogliano particelle.

Conviene infine rilevare che l'equazione (10) va ora naturalmente valutata sino ai termini di sesto grado; essa interviene, almeno a priori, nella determinazione delle equazioni di movimento di sesto grado, perchè già la sua parte di quinto grado contiene termini che riguardano le equazioni di sesto grado, secondo quanto è stato rilevato nella Sez. 10; tuttavia, come nel caso gravitazionale, l'equazione (10) di sesto grado è una condizione di integrabilità la quale interessa soltanto i termini della (56) indicati con i puntini e precisamente quelli fra essi che contengono componenti di quarto e di quinto grado del tensore fondamentale.

13. - Le equazioni di movimento nella formulazione 1950 della teoria unitaria e la soluzione di Callaway.

La formulazione 1950 della teoria unitaria differisce da quella del 1953 in una sola equazione di campo: precisamente la (3) viene ivi sostituita dall'equazione, più restrittiva,

$$R_{\frac{\nu}{\beta}} = 0 .$$

(18) Si perviene alla stessa conclusione anche se la legge di trasformazione dell'addendo elettrostatico della (51) si desume assumendo la (41) (precisata dalle (V) con $\mu=0$) ad equazione di movimento di quarto grado, ed esprimendo $\Delta \overset{2}{g}_{lm}$ mediante $\overset{2}{g}_{lm}$ (ivi rappresentate dalle $\overset{2}{\varphi}_{,i}$ grazie alle (30)), soltanto dopo aver eseguito la trasformazione di Lorentz, e non prima, come invece accade utilizzando la (44).

Alle equazioni elettromagnetiche (29) e (33) vanno allora sostituite le stesse private dell'operatore di Laplace.

Le posizioni (30), relative alle componenti emisimmetriche di secondo grado del tensore fondamentale, sono ancora possibili, poichè esse discendono dalle equazioni (28) che sussistono inalterate, ed ancora possibili sono le posizioni (35), ma la funzione φ che interviene nelle (30) e nelle (35) non soddisfa più alla (31), ma all'equazione di Laplace

$$\Delta\varphi = 0.$$

Alla (32) va allora sostituita la funzione armonica elementare

$$\varphi = Ar^{-1},$$

con A costante a priori arbitraria.

In definitiva, le soluzioni delle equazioni elettromagnetiche ridotte di secondo e di terzo grado in λ , contenute nella formulazione 1950 della teoria unitaria, possono essere ancora quelle indicate dalle (30) e dalla (35), ma nella (32) va posto:

$$B = C = 0.$$

In conseguenza, le equazioni di movimento (44) di prima approssimazione perdono tutti i termini elettrostatici, e si riducono così alla medesima equazione classica del moto gravitazionale di una particella, che EINSTEIN ed INFELD hanno potuto dedurre in prima approssimazione dalle equazioni gravitazionali ⁽¹⁾.

Si ritrova così un risultato di INFELD ⁽²⁾.

Nelle equazioni di movimento di seconda approssimazione non può quindi comparire la forza elettrodinamica totale di Lorentz perchè essa proviene dalla forza elettrostatica coulombiana, la quale manca nelle equazioni di movimento di prima approssimazione.

Nella Nota citata ⁽³⁾, CALLAWAY, pur ricercando le equazioni di movimento di prima approssimazione dedotte dalla formulazione 1953 della teoria unitaria einsteiniana, si attiene a soluzioni delle equazioni elettromagnetiche analoghe a quelle indicate in questa sezione; queste soluzioni sono possibili anche nell'ambito della formulazione 1953, ma risultano troppo particolari e perciò questo autore ricade nel risultato negativo precedentemente dedotto dalla formulazione 1950 della teoria unitaria.

14. — Conclusioni.

Mi sembra così di poter concludere con tre osservazioni: il problema discusso in questa Nota porta a preferire la formulazione 1953 della teoria unitaria einsteiniana a quella del 1950, come avviene pure muovendo da altre considerazioni (19); lo schema elettromagnetico di prima approssimazione contenuto nelle equazioni 1953 è alquanto più ampio di quello maxwelliano e sembra opportuno tenere conto anche in prima approssimazione di questa circostanza (20), la quale appare legata all'interazione tra gravitazione ed elettricità; infine dalle equazioni del campo unitario si deduce che tutte le forze ponderomotrici della Fisica classica compaiono accanto a quella gravitazionale nella determinazione del movimento di un corpuscolo elettrizzato.

(19) Loco citato in (9), ibidem; cfr. pure, A. EINSTEIN e B. KAUFMAN: *Sur l'état actuel de la théorie de la gravitation généralisée* (*Louis de Broglie, physicien et penseur* (Paris, 1953)).

(20) Loco citato in (9), ibidem, al paragrafo «Osservazioni sulla interpretazione fisica del sistema di equazioni».

SUMMARY

In this paper the author demonstrates that, in the motion equations of a particle, deduced from the asymmetric field equations of Einstein's unified theory of 1953, are present the most significant forces of classical physics, that is the Newtonian force of gravity, the Coulombian electrostatic force and Lorentz's electrodynamic force. The author has reached this result using an integral formula previously found by him. This formula originates from the field equations of the unified theory, and strictly determines the motion of two or more particles, once assumed the singularities representing them. From this formula are obtained the equations of motion of particles to any degree of approximation, applying the subsequent steps method introduced by EINSTEIN and INFELD in the gravitational problem; i.e. the fundamental tensor is expanded into an appropriate series of functions, arranged according to the integer and positive powers of λ which is the reciprocal of the light velocity *in vacuo* as measured by an inertial frame; consequently the vector to be integrated of the found formula is expanded into a series of integer and positive powers of λ ; thus recurrent motion equations are obtained. Assuming that the lowest power of λ which in the expansion of the fundamental tensor follows that of zero degree, is λ^2 (as in the gravitational theory), the integral formula begins to have a meaning when the factors of λ^4 are not left aside; the motion equations of the first step therefore consist in the terms of fourth degree with respect to λ^4 . The author deduces in this way the motion equations of the first

step regarding a system of two or more particles; considering also the factors of λ^6 , he determines a significant part of the equations of motion by subsequent steps. The first step equation (obtained solely by means of λ^4 coefficients) determines the motion of a particle subject to the Newtonian force of gravity and the Coulombian electrostatic force, exerted by the remaining particles, and to a minor force representing the interaction between the gravitational and electromagnetic fields; thus one finds again the equation that in classical physics governs the motion of charged and heavy particles, if one leaves aside the interaction forces and the Lorentz force, which is of a lower magnitude order than the previous forces, as is well known. The Coulombian electrostatic force is not obtained however selecting the elementary harmonic function as potential of the electrostatic field, but a biharmonic function, just as is requested by the electromagnetic equations which ensue in the first step from the field equations. That is, the author has chosen as electrostatic potential of each particle the biharmonic function which is the sum of the classical electrostatic potential (expressed by the elementary harmonic function), with a general polynomial of second degree concerning the distance from the acting particle; the linear term of this polynomial is essential as, without it, the Coulombian force is not present in the motion equations of the first step. This additional term of the electrostatic potential begins to show both the discrepancy between the classical electromagnetic model and that implied in the 1953 formulation of Einstein's unified theory and the interaction between gravity and electricity, thanks to a coefficient proportional to the multiplication of Cavendish constant by the charge of the particle. All the above explains the negative result obtained by Callaway in the research of the equation of motion of the first step, limited to the coefficients of λ^4 and deduced from the 1953 formulation of the unified theory; this author adopts as a potential merely the elementary Coulomb one, leaving thus aside the additional term. The factors of λ^6 can be grouped into three addenda: one is the sum of the interaction terms between gravitation and electricity; another addendum is the sum of terms which represent the reaction exerted on each particle by the gravitational and electromagnetic field produced by the particle itself; finally the third addendum represents Lorentz's electrodynamic force.

An Analysis of the Strong Interaction Data.

P. T. MATTHEWS and A. SALAM

Department of Mathematics, Imperial College of Science and Technology - London, England

(ricevuto l'8 Novembre 1957)

Summary. — An analysis is made of the data on strong interactions based on considerations of phase space and an estimate of matrix elements based on perturbation theory. A consistent picture is obtained for a scalar K-meson with all coupling constants of the order of unity.

1. — Introduction.

In 1950 FERMI (1) gave a broad general analysis of the then existing pion data in terms of an effective scalar pion and using perturbation theory to estimate the matrix element for various processes. There are now sufficient data on the strong interactions to make a similar analysis worthwhile. We will assume the standard three-field interactions (2) allowed by conservation of charge, strangeness, and baryon number, and obtain estimates of the strength of the average coupling between baryons and pions, g_π , and between baryons and K-mesons, g_K : In this way we are able to obtain a consistent picture of these interactions with all coupling constants of the order of unity. In particular we are able to explain the factor of about a hundred between the scattering and production cross-sections, the factor of about six between K^- and K^+ scattering and, to some extent, the rapid rise of K^- absorption near threshold. We do not find it necessary to assume any 4-field interactions coupling π and K fields directly. It is a limitation of the method that the K-meson has to be treated as scalar.

(1) E. FERMI: *Elementary Particles* (Oxford, 1951).

(2) B. d'ESPAGNAT and J. PRENTKI: *Nucl. Phys.*, **1**, 38 (1956).

2. – The method.

Assume the matrix element is independent of angle, then the total cross-section for a process with two particles in the final state is

$$(2.1) \quad \sigma = \frac{|T|^2 p_f^2}{4\pi \omega_i \omega_f v_i v_f},$$

where p_f is the final momentum, v_i , v_f are the initial and final velocities, and ω_i , ω are the energies of the initial and final bosons.

$$(2.2) \quad v = p/M,$$

where M is the reduced mass. Thus

$$(2.3) \quad \sigma = \frac{|T|^2 p_f M_i M_f}{4\pi p_i \omega_i \omega_f}.$$

The T -matrix element, according to perturbation theory, is

$$(2.4) \quad T = g_i g_f / \Delta E,$$

where ΔE is the difference between the initial (or final) energy, and the energy in the intermediate state, and the g 's are the appropriate coupling constants. Thus

$$(2.5) \quad \sigma = 4\pi \left[\left(\frac{g_i^2}{4\pi} \right) \left(\frac{g_f^2}{4\pi} \right) \frac{1}{\Delta E^2} \right] \frac{M_i M_f p_f}{\omega_i \omega_f p_i}.$$

The terms outside the square bracket are statistical factors independent of any assumption about the interaction. Since the value of the coupling constants turn out to be too large to justify a detailed perturbation calculation, only a single typical graph will be used in the estimate of the matrix element given in the square bracket.

3. – K-meson scattering.

3.1. K^+ -nucleon scattering. – The conservation of strangeness allows only crossed graphs, thus at threshold

$$(3.1) \quad \Delta E = K + Y - N = 5m,$$

where m is the pion mass and K , Y , N denote the K-meson, hyperon (Σ or Λ) and nucleon masses, respectively. Thus, by (2.5), at threshold

$$(3.2) \quad \sigma(K^+) = \frac{1}{12} \left(\frac{g_K^2}{4\pi} \right)^2 \sigma_Y ,$$

where

$$(3.3) \quad \sigma_Y = \pi \left(\frac{1}{m} \right)^2 \simeq 60 \text{ mb} .$$

Experimentally (3.4)

$$(3.4) \quad \sigma(K^+) \simeq 10 \text{ mb} ,$$

giving as a rough estimate of the coupling

$$(3.5) \quad \left(\frac{g_K^2}{4\pi} \right) = 1.4 .$$

3.2. K^- -nucleon scattering. – In this case only uncrossed graphs are allowed. Then

$$(3.6) \quad \Delta E = Y - N - K \simeq 2m .$$

The other factors are the same as above. Thus

$$(3.7) \quad \sigma(K^-)/\sigma(K^+) = 25/4 ,$$

which is in reasonable agreement with the data (5).

(3) See summary talks by S. and G. GOLDHABER: *International Conf.* (Padua, 1957).

(4) We remark in passing that the observed predominance of the $T=1$ state is given in Born approximation by

$$g_{K\Lambda}^2 = 3g_{K\Sigma}^2 .$$

This conclusion will survive in any of the standard methods (TAMM-DANCOFF: *One Meson, or Potential Approximations*) which have been applied to pion scattering, since all of them in one way or another, calculate the scattering in the potential given by Born approximation.

(5) The signs of the scattering lengths given by this scalar model are not in agreement with observation. This point will be discussed elsewhere by the authors.

4. – K-absorption. ($K^- + p \rightarrow Y + \pi$).

The main contribution comes from the uncrossed graph. Thus

$$(4.1) \quad \Delta E = E - Y \simeq \omega_K,$$

$$(4.2) \quad \sigma_{\text{abs}} = 4\pi \left[\left(\frac{g_K^2}{4\pi} \right) \left(\frac{g_\pi^2}{4\pi} \right) \frac{1}{\omega_K^2} \right] \frac{2}{\omega_K p_K},$$

Near threshold $w_K \simeq 3\frac{1}{2}m$, giving

$$(4.3) \quad \sigma_{\text{abs}} \sim \frac{1}{p_K},$$

which is the familiar $1/v$ law for exothermic processes. The experimental data (6) appear to follow more closely $1/v^2$ for which we have no explanation.

If $p_K \simeq m$, (50 MeV Lab.), then

$$(4.4) \quad \sigma_{\text{abs}} = \left(\frac{g_K^2}{4\pi} \right) \left(\frac{g_\pi^2}{4\pi} \right) \frac{\sigma_Y}{4},$$

which is slightly larger than the observed value (3) with g_K , determined above and

$$(4.5) \quad \frac{g_\pi^2}{4\pi} \simeq 1.$$

Note that this is the coupling for an «effective» scalar pion and includes an average over both pion-nucleon and pion-hyperon couplings.

5. – Production by pions. ($\pi + p \rightarrow Y + K$).

The intermediate energy is

$$(5.1) \quad \Delta E = E - N.$$

At about 1 GeV in center of mass system

$$(5.2) \quad \sigma = \left(\frac{g_K^2}{4\pi} \right) \left(\frac{g_\pi^2}{4\pi} \right) \frac{\sigma_Y}{200},$$

(6) See summary talk by J. STEINBERGER: *International Conference* (Padua, 1957).

which is again in agreement (6) with experiment with the above values of g_K and g_π .

6 - Conclusions.

A consistent picture of the magnitudes of the observed cross-sections for K-scattering and production by pions is obtained on the assumption that average coupling constants are

$$\frac{g_K^2}{4\pi} \simeq 1, \quad \frac{g_\pi^2}{4\pi} \simeq 1.$$

In particular, the large difference between scattering and production cross-sections is shown to happen quite naturally. This is also consistent with a similar analysis of photoproduction (7) and with the order of magnitude of the hyperon nucleon force observed in hyperfragments (8).

(7) International Conference (Padua, 1957); A. FUJII and R. E. MARSHAK: *Phys. Rev.*, **107**, 570 (1957); M. KAWAGUCHI and M. J. MORAVCSIK: *Phys. Rev.*, **107**, 563 (1957).

(8) N. DALLAPORTA and F. FERRARI: *Nuovo Cimento*, **5**, 3 (1957); M. ROSS and D. LICHTENBERG: *Phys. Rev.*, **103**, 1131 (1956).

RIASSUNTO (*)

Si esegue un'analisi dei dati disponibili sull'interazione forte basata sulla considerazione dello spazio delle fasi; si esegue altresì una valutazione degli elementi di matrice basata sulla teoria della perturbazioni. Si ottiene un quadro attendibile per un mesone K scalare con tutte le costanti d'accoppiamento dell'ordine dell'unità.

(*) Traduzione a cura della Redazione.

On a New Method in the Theory of Superconductivity.

N. N. BOGOLJUBOV

Joint Institute for Nuclear Research - Dubna, USSR

(ricevuto il 14 Novembre 1957)

Summary. — A generalization of the method elaborated by the author for the theory of superconductivity is presented. It is shown that the original Fröhlich model possesses the property of superconductivity. The ground state and its fermion excitations are considered.

After the discovery of the isotope effect it is generally accepted that interaction between electrons and the lattice should play an important role in superconductivity.

We shall show in the present paper that such a system really does exhibit superconductive properties.

Some very interesting investigations of a system of electrons interacting with a phonon field have been performed ⁽¹⁻⁴⁾ along this line. In the present paper it will be shown that by extending the method previously proposed by us for the study of superfluidity one may develop a consistent theory of the superconductive state. In particular this theory yields results which confirm those of Bardeen's theory ⁽³⁾.

For sake of simplicity we shall base our considerations on the model proposed by FRÖHLICH ⁽¹⁾; Coulomb interaction is not introduced explicitly, the

⁽¹⁾ H. FRÖHLICH: *Phys. Rev.*, **79**, 845 (1950); *Proc. Roy. Soc. (London)*, A **215**, 291 (1952).

⁽²⁾ J. BARDEEN: *Rev. Mod. Phys.*, **23**, 261 (1951); *Handb. der Phys.* (Berlin, 1956), **15**, 274; J. BARDEEN and D. PINES: *Phys. Rev.*, **99**, 1140 (1950).

⁽³⁾ J. BARDEEN, L. N. COPPER and J. R. SCHRIEFFER: *Phys. Rev.*, **106**, 162 (1957).

⁽⁴⁾ D. PINES: *Phys. Rev.* (in print).

dynamical system being characterized by the Hamiltonian (*)

$$(1) \quad \begin{cases} H_p = \sum_{k,s} E(k) a_{ks}^+ a_{ks}^- + \sum_q \omega(q) b_q^+ b_q^- + H' \\ H' = \sum_{\substack{k,q,s \\ (k',k)=q}} g \left\{ \frac{\omega(q)}{2V} \right\}^{\frac{1}{2}} a_{ks}^+ a_{ks}^- b_q^+ b_q^- + \text{c. c.} \end{cases}$$

where $E(k)$ is the electron energy, $\omega(q)$ the phonon energy, g a coupling constant and V the volume.

As is now well known, conventional perturbation theory expressed in powers of the coupling constant is not valid due to the circumstance that the electron-phonon interaction, despite its smallness, is very significant near the Fermi surface.

Thus as a preliminary step we shall perform a canonical transformation on the basis of the following considerations.

First of all it will be noted that matrix elements corresponding to virtual « particle » creation in vacuum always involve energy denominators of the form

$$\{\varepsilon(k_1) + \dots + \varepsilon(k_{2s}) + \omega(q_1) + \dots + \omega(q_{2r})\}^{-1}$$

in which $\varepsilon(k) \sim |E(k) - E_F|$ is the particle energy of an electron ($E(k) > E_F$), or of a hole ($E(k) < E_F$) which becomes small near the Fermi surface.

Such denominators are in general not « dangerous » and integration over the momenta $k_1, \dots, k_{2s}, q_1, \dots, q_{2r}$ does not lead to divergences, *an exception being the case of virtual creation of a single pair without phonons*. In virtue of the conservation law the momenta of this pair will be oppositely directed and the energy denominator

$$\{2\varepsilon(k)\}^{-1}$$

will then be « dangerous » during integration.

It may also be mentioned that the particle spins will likewise have opposite directions.

Thus in choosing a canonical transformation one should keep in mind the *necessity of ensuring mutual compensation of graphs leading to virtual creation in vacuum of a pair of particles with opposite momenta and spins* (+).

(*) The unit system in which $\hbar=1$ is employed here.

(+) It is to be stressed that in the ordinary perturbation theory applied directly to the normal state these graphs cannot appear because of conservation of the number of real electrons.

But if we mix electron and hole states by a canonical transformation the conservation principle does not help and such graphs appear.

It might be pertinent to point out the analogy between the present situation and that encountered in our theory of superfluidity (5) of a non-ideal Bose gas; in the latter case the same role was played by virtual creation from the condensate of a pair of particles with momenta $\pm k$. In this theory (5) we employed a linear transformation of Bose amplitudes which « mixes » b_q with \dot{b}_{-q} .

Generalizing this transformation we introduce in the case under consideration new Fermi amplitudes α

$$\begin{aligned}\alpha_{k0} &= u_k a_{k,\frac{1}{2}} - v_k \dot{a}_{-k,-\frac{1}{2}}^+ \\ \alpha_{k1} &= u_k a_{-k,-\frac{1}{2}} + v_k \dot{a}_{k,\frac{1}{2}}^+\end{aligned}$$

or

$$\begin{aligned}a_{k,\frac{1}{2}} &= u_k \alpha_{k0} + v_k \dot{\alpha}_{k1} \\ a_{-k,-\frac{1}{2}} &= u_k \alpha_{k1} - v_k \dot{\alpha}_{k0}\end{aligned}$$

where u_k, v_k are real numbers which are related as follows

$$u_k^2 + v_k^2 = 1.$$

It is not difficult to verify that this transformation retains all commutation properties of Fermi operators and is therefore canonical. It may also be noted that it is a generalization of the usual transformation employed to introduce creation and annihilation operators for holes inside the Fermi surface or for electrons outside this surface.

Indeed, if we put

$$\begin{aligned}u_k &= 1, & v_k &= 0 & (E(k) > E_F) \\ u_k &= 0, & v_k &= 1 & (E(k) < E_F)\end{aligned}$$

we obtain

$$\begin{aligned}\alpha_{k0} &= a_{k,\frac{1}{2}}, & \alpha_{k1} &= a_{-k,-\frac{1}{2}} & (E(k) > E_F) \\ \alpha_{k0} &= -\dot{a}_{-k,-\frac{1}{2}}, & \alpha_{k1} &= \dot{a}_{k,\frac{1}{2}}^+ & (E(k) < E_F)\end{aligned}$$

so that α_{k0} for example, will be the annihilation operator of an electron having momentum k and spin $\frac{1}{2}$ outside the Fermi sphere and the annihilation operator of a hole with a momentum $-k$ and spin $-\frac{1}{2}$ inside it.

(5) N. N. BOGOLJUBOV: *Journ. of Phys. USSR*, **9**, 23 (1947); *Vestnik MGU*, no. 7, 43 (1947).

In the general case, when $(u_k, v_k) \neq (0, 1)$ superposition of a hole and electron is encountered.

Returning to the Fröhlich Hamiltonian we note that for technical reasons it will be more convenient for us not to be tied up with the relation

$$\sum_{k,s} \hat{a}_{ks}^+ a_{ks} = N_0 ,$$

where N_0 is the total number of electrons, but to proceed in a manner which is usual in such cases, and choose a parameter λ which plays the role of a chemical potential.

Thus instead of H_F we shall deal with the Hamiltonian

$$(2) \quad H = H_F - \lambda N .$$

The value of parameter λ will be found from the condition that in the state under consideration

$$(3) \quad \bar{N} = N_0 .$$

Transforming H to new Fermi amplitudes we get

$$H = V + H_0 + H_{\text{int}}$$

$$H_{\text{int}} = H_1 + H_2 + H_3 ,$$

where V is a constant

$$V = 2 \sum E(k) r_k^2 - 2\lambda \sum r_k^2$$

$$H_0 = \sum_{k,k'} (E(k) - \lambda) (u_k^2 - r_k^2) (\dot{\alpha}_{k0} \alpha_{k0} + \dot{\alpha}_{k1} \alpha_{k1})$$

and

$$H_1 = \sum_{\substack{k,k' \\ (k'-k=q)}} g \sqrt{\frac{\omega(q)}{2V}} \left\{ u_k v_{k'} \dot{\alpha}_{k0} \alpha_{k'1} + u_{-k} v_{-k'} \dot{\alpha}_{-k'0} \alpha_{-k1} + u_{k'} v_k \dot{\alpha}_{k1} \alpha_{k'0} + u_{-k'} v_{-k} \dot{\alpha}_{-k'1} \alpha_{-k0} \right\} \dot{b}_q + \text{c. c.}$$

$$H_2 = \sum_{\substack{k,k' \\ (k'-k=q)}} g \sqrt{\frac{\omega(q)}{2V}} \left\{ u_k u_{k'} \dot{\alpha}_{k0} \alpha_{k'0} + u_{-k} u_{-k'} \dot{\alpha}_{-k'1} \alpha_{-k'1} - v_k v_{k'} \dot{\alpha}_{k1} \alpha_{k'1} - v_{-k} v_{-k'} \dot{\alpha}_{-k'0} \alpha_{-k0} \right\} \dot{b}_q + \text{c. c.}$$

$$H_3 = 2 \sum (E(k) - \lambda) u_k v_k (\alpha_{k1} \alpha_{k0} + \dot{\alpha}_{k0} \dot{\alpha}_{k1}) .$$

We now introduce the occupation numbers

$$\nu_{k0} = \dot{\alpha}_{k0} \alpha_{k0} , \quad \nu_{k1} = \dot{\alpha}_{k1} \alpha_{k1} ,$$

for the new quasi particles created by the operators.

Evidently the state

$$C_v = \prod_k \delta(\nu_{k0}) \delta(\nu_{k1}),$$

with zero ν will be a «non-interaction vacuum» that is, a state for which

$$H_0 C_v = 0.$$

It may be pointed out that λ should be close to E_F since in the absence of interaction $\lambda = E_F$. The expression



Fig. 1.

$$\varepsilon(k) = (E(k) - \lambda)(u_k^2 - v_k^2)$$

thus should vanish on a surface close to the Fermi surface.

We can now see that as regards the criterion given above a «dangerous process»

will be one of virtual creation of a pair of quasi-particles ν_{k0} , ν_{k1} in vacuum without phonons since the corresponding energy denominator will be

$$\{2\varepsilon(k)\}^{-1}.$$

The Hamiltonian H_3 directly leads to this type of process; for the vacuum this Hamiltonian yields the graph (*) shown in Fig. 1. The joint action of H_1 , H_2 can also yield this process.

Thus, for example, in the second order in the coupling constant g we have the graphs shown in Fig. 2a.

At higher orders graphs of the type shown in Fig. 2b are obtained; the circle denotes a connected part which cannot be divided into two connected parts linked only by two lines of the single pair under consideration.

In virtue of the principle of compensation of dangerous graphs proposed above we are obliged to equate to zero the sum of

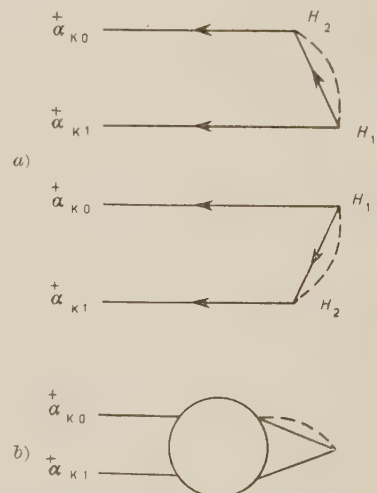


Fig. 2.

(*) Application of the graph technique to the many body problem can be found in a detailed paper by HUGENHOLTZ (6).

(6) N. M. HUGENHOLTZ: *Physica*, **23**, 481 (1957).

the contributions from the graph in Fig. 1 and from those in Fig. 2. An equation for u_k, v_k is thus obtained.

It will now be unnecessary to take into account the graphs in Fig. 1 and 2 (and their conjugates) and hence no expressions involving dangerous energy denominators will appear in the perturbation theory expansions.

We now set up an equation for u_k, v_k in the second order. In this approximation the graphs in Fig. 1 should be compensated by those in Fig. 2.

We get

$$2(E(k) - \lambda) u_k v_k + Q_k = 0,$$

where Q_k is the coefficient of $\dot{\alpha}_{k0} \dot{\alpha}_{k1} C_\nu$ in the expression

$$-H_2 H_0^{-1} H_1 C_\nu.$$

In the expanded form we finally obtain

$$(4) \quad \{\tilde{E}(k) - \lambda\} u_k v_k = (u_k^2 - v_k^2) \frac{1}{2V} \sum_{k'} g^2 \frac{\omega(k - k')}{\omega(k - k') + \varepsilon(k) + \varepsilon(k')} u_k v_{k'},$$

where

$$(5) \quad \tilde{E}(k) = E(k) - \frac{1}{2V} \sum g^2 \frac{\omega(k - k')}{\omega(k - k') + \varepsilon(k) + \varepsilon(k')} (u_{k'}^2 - v_{k'}^2).$$

Without leaving the limits of the chosen approximation we can replace

$$\varepsilon(k) = \{E(k) - \lambda\} (u_k^2 - v_k^2)$$

in the denominator of the right hand part by

$$\tilde{\varepsilon}(k) = \{\tilde{E}(k) - \lambda\} (u_k^2 - v_k^2).$$

Assuming

$$\tilde{E}(k) - \lambda = \xi(k),$$

we may then rewrite the equation obtained in the following form

$$(6) \quad \xi(k) u_k v_k = (u_k^2 - v_k^2) \frac{1}{2(2\pi)^3} \int g^2 \frac{\omega(k - k')}{\omega(k - k') + \tilde{\varepsilon}(k) + \tilde{\varepsilon}(k')} u_k v_{k'} d\mathbf{k}'.$$

This equation evidently possesses the trivial solution

$$uv = 0, \quad (u, v) = (0, 1),$$

which corresponds to the «normal state». However it also possesses a different type of solution which goes over into the trivial one on moving away from the Fermi surface.

Putting

$$C(k) = \frac{1}{(2\pi)^3} \int g^2 \frac{\omega(k - k')}{\omega(k - k') + \tilde{\varepsilon}(k) + \tilde{\varepsilon}(k')} u_k v_{k'} d\mathbf{k}'$$

we find from (6)

$$(7) \quad u_k^2 = \frac{1}{2} \left\{ 1 + \frac{\xi}{\sqrt{C^2 + \xi^2}} \right\}, \quad v_k^2 = \frac{1}{2} \left\{ 1 - \frac{\xi}{\sqrt{C^2 + \xi^2}} \right\},$$

whence

$$u_k v_k = \frac{1}{2} \frac{C(k)}{\sqrt{C^2(k) + \xi^2(k)}}, \quad \tilde{\varepsilon}(k) = \frac{\xi^2(k)}{\sqrt{C^2(k) + \xi^2(k)}}.$$

Thus our equation reduces to the following

$$(8) \quad C(k) = \frac{1}{2(2\pi)^3} \int g^2 \frac{\omega(k - k')}{\omega(k - k') + \tilde{\varepsilon}(k) + \tilde{\varepsilon}(k')} \frac{C(k')}{\sqrt{C^2(k') + \xi^2(k')}} d\mathbf{k}'.$$

It should be noted that this equation possesses a peculiar feature: for $g^2 \rightarrow 0$ the solution C tends to zero like $\exp[-A/g^2]$, A being a positive constant because near the surface, $\xi(k) = 0$ and the integral in the right hand part of (8) becomes logarithmically divergent if $C = 0$.

Under these conditions it is not difficult to derive the asymptotic form of the solution for small values of g :

$$(9) \quad C(k) = \tilde{\omega} \exp \left[-\frac{1}{\varrho} \int_{-1}^1 \frac{\omega \{ k_0 \sqrt{2(1-t)} \}}{\omega \{ k_0 \sqrt{2(1-t)} \} + |\xi(k)|} dt \right],$$

where

$$\varrho = \frac{g^2}{2\pi^2} \left(\frac{d\tilde{E}(k)/dk}{d\tilde{E}(k)/dk} \right)_{k=k_0}, \quad \tilde{E}(k_0) = \lambda,$$

$$(10) \quad \ln \tilde{\omega} = \int_0^\infty \ln \frac{1}{2\xi} \frac{d}{d\xi} \left\{ \frac{1}{2} \int_{-1}^1 \frac{\omega \{ k_0 \sqrt{2(1-t)} \}}{\omega \{ k_0 \sqrt{2(1-t)} \} + \xi} dt \right\}^2 d\xi.$$

Taking into account the auxiliary condition (3) and the expressions (7), (9) found for u , v it may be seen that

$$k_0 = k_F.$$

It is furthermore evident that the corrections to expression (5) which result from the substitution of u_k and v_k with the «normal» values

$$(11) \quad \left\{ \begin{array}{l} u_k = \theta_g(k) = \begin{cases} 1, & |k| > k_F \\ 0, & |k| < k_F \end{cases} \\ v_k = \theta_F(k) = \begin{cases} 0, & |k| > k_F \\ 1, & |k| < k_F \end{cases} \end{array} \right.$$

will be exponentially small.

Thus, without loss of precision we may replace by $\tilde{E}(k)$ in formula (10) the corresponding expression for the normal state and we may interpret the factor

$$\frac{1}{2\pi^2} \left(\frac{k^2}{d\tilde{E}/dk} \right)_{k=k_F} = \frac{1}{V} \left\{ \frac{V}{(2\pi)^3} \frac{4\pi k^2 dk}{dE} \right\}_0$$

as the relative density dn/dE of the number of electron levels in an infinitely narrow energy gap near the Fermi surface. Then

$$(12) \quad \varrho = g^2 \frac{dn}{dE}.$$

We shall now proceed to calculate the ground state energy in a second approximation.

From the total H_{int} only H_1 should now be taken into account. We thus assume that for the eigenvalue of H in the ground state

$$V - \langle C_{\nu}^* H_1 H_0^{-1} H_1 C_{\nu} \rangle = 2 \sum_k \{E(k) - \lambda\} v_k^2 - \frac{1}{V} \sum_{k \neq k'} g^2 \frac{\omega(k - k') \{u_k^2 v_k^2 + u_k v_k u_{k'} v_{k'}\}}{\omega(k - k') + \varepsilon(k) + \varepsilon(k')}.$$

Inserting the expression for u_k , v_k previously found we calculate the difference ΔE between the energy of the ground state and that of the normal state.

We get

$$(14) \quad \frac{\Delta E}{V} = - \frac{dn}{dE} \frac{\tilde{\omega}^2}{2} \exp \left[- \frac{2}{\varrho} \right].$$

It is interesting to note that this result is the same as that of BARDEEN and co-workers (3). This can easily be seen if Bardeen's parameters ω , V are

chosen as follows

$$(15) \quad 2\omega = \tilde{\omega}, \quad V = g^2.$$

We shall now set up in the accepted approximation the formula for the energy of an elementary excitation. For this purpose we consider the excited state

$$C_1 = \tilde{\alpha}_{k_0} C_r$$

and apply to it the perturbation theory in the usual manner. For the energy of an elementary excitation with momentum k we obtain the following expression

$$E_e(k) = \varepsilon(k) - \langle C_1^* H_{\text{int}} (H_0 - \varepsilon(k))^{-1} H_{\text{int}} C_1 \rangle_{\text{connected}}$$

which in the expanded form is

$$(16) \quad E_e(k) = \tilde{\varepsilon}(k) \left\{ 1 - \frac{g^2}{V} \sum_{k'} \omega(k - k') \frac{u_k^2 u_{k'}^2 + v_k^2 v_{k'}^2}{[\omega(k - k') + \varepsilon(k')]^2 - \varepsilon^2(k)} \right\} + \\ + \frac{g^2}{V} 2u_k v_k \sum_{k'} \frac{\omega(k - k')(\omega(k - k') + \varepsilon(k'))}{[\omega(k - k') + \varepsilon(k')]^2 - \varepsilon^2(k)} u_{k'} v_{k'}.$$

The first term which is proportional to $\tilde{\varepsilon}(k)$ does not possess any singular properties and vanishes on the Fermi surface. However on this surface the second term is

$$\frac{g^2}{V} 2u_k v_k \sum_{k'} \frac{\omega(k - k')}{\omega(k - k') + \varepsilon(k')} u_{k'} v_{k'} = 2u_k v_k C(k) = C(k_F) = \tilde{\omega} \exp \left[-\frac{1}{\varrho} \right].$$

Thus the energy values of states with fermion excitations are separated from the energy of the ground state by the gap

$$(17) \quad \Delta = \tilde{\omega} \exp \left[-\frac{1}{\varrho} \right].$$

It should be mentioned that an expression of the same type as (17) is contained in BARDEEN's paper and is interpreted there as the energy required for the destruction of a « pair ».

It is interesting to note that contrary to Bardeen's theory our « vacuum » or the lowest energy state is formed by fermions. These fermions characterized by creation and annihilation amplitudes α^+ and α correspond to a kind of superposition of the electron and the hole.

Consider now the «ground current state», that is, a state possessing the lowest energy among possible estates with a given momentum \mathbf{P} .

Thus our task is to determine the eigenvalue of H with the auxiliary condition

$$\sum_{k,s} \mathbf{k} \bar{a}_{ks} a_{ks}^+ = \mathbf{P}.$$

Instead of doing this we shall introduce in the usual manner not only the scalar parameter λ , but also a vector parameter \mathbf{u} which plays the role of a mean velocity, and take the complete Hamiltonian in the form

$$(18) \quad H = H_{F2} - \lambda \sum_{k,s} \bar{a}_{ks}^+ a_{ks} - \sum_{k,s} (\mathbf{u} \cdot \mathbf{k}) \bar{a}_{ks}^+ a_{ks} = \\ = \sum_{k,s} \{E(k) - (\mathbf{u} \cdot \mathbf{k}) - \lambda\} \bar{a}_{ks}^+ a_{ks} + \sum_{\mathbf{q}} \omega(\mathbf{q}) \bar{b}_{\mathbf{q}} b_{\mathbf{q}} + H_{\text{int}}.$$

The value of \mathbf{k} is determined from the condition

$$\sum_{k,s} \mathbf{k} \bar{a}_k^+ a_{ks} = \mathbf{P}.$$

Since we have been dealing only with a small area in the vicinity of the Fermi surface we may put, for sake of simplicity,

$$E(k) = \frac{k^2}{2m} + \mathcal{D}, \quad \mathcal{D} = E_F - \frac{k_F^2}{2m}$$

and in the final formulae we may assume

$$m = \left(\frac{k}{dE/dk} \right)_{k=k_F}.$$

However in this case

$$E(k) - (\mathbf{u} \cdot \mathbf{k}) = E(k - m\mathbf{u}) - \frac{m\mathbf{u}^2}{2}$$

and therefore if we perform in momentum space the translation

$$(19) \quad \mathbf{k} \rightarrow \mathbf{k} + m\mathbf{u}, \quad a_{ks} \rightarrow a_{k+m\mathbf{u},s}$$

and make the substitution

$$\lambda \rightarrow \lambda - \frac{m\mathbf{u}^2}{2},$$

the hamiltonian (18) will have the same form as (2) and will not contain the vector \mathbf{u} . We again arrive at the case of a ground state with zero momentum. Thus there is no necessity of carrying out a special investigation of the current flow state; it should be sufficient to apply the inverse transformation of (19) to the formulae previously obtained.

In this manner, for example, one may verify that the energy of the ground current state with a mean velocity \mathbf{u} differs from the energy of a ground state with no current by $N(mu^2/2)$.

Excitations are separated from the energy of the ground current state by the gap

$$\Delta_u = \Delta - \mathbf{k}_F \mathbf{u} > \Delta - \mathbf{k}_F |\mathbf{u}|.$$

Hence if

$$\mathbf{k}_F |\mathbf{u}| < \Delta ,$$

the current state will nevertheless be stable with respect to excitations, despite the fact that the energy of this state is greater than that of the non-current state (neglecting the effects of the magnetic field).

We thus see that superconductivity is really an intrinsic property of the considered model.

Some additional remarks may be made.

In order to be able to restrict our considerations to asymptotic approximations it was necessary to assume that the parameter ϱ was small. However V. V. TOLMAČEV and S. V. Tjablikov (?) have shown, by applying a method which does not assume the smallness of ϱ , that for $\varrho > \frac{1}{2}$ the velocity of sound is imaginary. This means that the lattice is unstable. If the lattice is so rigid that the electron-phonon interaction does not appreciably affect the phonon energy, the parameter ϱ should be small. Already for $\varrho = \frac{1}{4}$, $\exp[-1/\varrho]$ equals $1/55$. In our opinion this explains the small magnitude of the energy gap and hence of the critical temperature.

It may also be pointed out that if a Coulomb interaction term is explicitly introduced in the Fröhlich Hamiltonian, summation over electron-hole graphs of the Gell-Mann-Brueckner type should be performed in order to ensure the appearance of screening.

One can thus easily verify that Coulomb interaction counteracts the appearance of superconductivity (*).

(?) V. V. TOLMAČEV and S. V. Tjablikov: *Žu. Exper. Teor. Fiz.* (in print).

(*) *Note added in proof.* — The detailed study of the Coulomb interaction shows (8) that its efficiency is essentially reduced due to its «long range» in momentum space.

(8) N. N. BOGOLJUBOV, D. V. SHIRKOV and V. V. TOLMAČEV: preprint of the Joint Institute for Nuclear Research.

* * *

In conclusion the author considers it a pleasant duty to express his appreciation to D. N. ZUBAREV, V. V. TOLMAČEV, S. V. TJABLIKOV and YU. A. TSERKOVNIKOV for valuable discussions.

RIASSUNTO (*)

Si presenta una generalizzazione del metodo elaborato dall'autore per la teoria della supercondutività. Si dimostra che il modello originale di Fröhlich possiede la proprietà di essere superconduttivo. Si prendono in considerazione lo stato fondamentale e le eccitazioni dei suoi fermioni.

(*) *Traduzione a cura della Redazione.*

Invariants in Muon Decay (*).

R. GATTO (†) and G. LÜDERS (†)

Radiation Laboratory University of California - Berkeley, Cal.

(ricevuto il 15 Novembre 1957)

Summary. — The assumption of vanishing neutrino mass leads to a group of transformations of the neutrino field which leave commutation relations and free-field Hamiltonian invariant but change the interaction into an equivalent one giving the same physical results. This concept, which is attributable to PURSEY and PAULI, is here applied to μ -e decay under the assumption of local non-derivative coupling with no restrictions as to conservation of parity or lepton charge. The physically relevant invariant combinations of coupling constants are derived, and relations between them are discussed. Use is made of a recent paper by KINOSHITA and SIRLIN to express all experimental information on μ -e decay in terms of these invariants.

1. — Construction of the invariants.

It has been shown recently by PAULI (1) that the assumption of vanishing neutrino mass leads to a group of linear transformations of the neutrino field operators which leave both commutation relations and free Hamiltonian

(*) This work was done under the auspice of the U.S. Atomic Energy Commission,
(†) On leave of absence from Istituto di Fisica dell'Università di Roma, Italy.

(†) Fulbright Grantee on leave of absence from Max-Planck-Institut für Physik, Göttingen, Germany.

(1) W. PAULI: *Nuovo Cimento*, **6**, 204 (1957). A similar discussion on the basis of Transformation (II) only was given independently by D. L. PURSEY (to be published). A somewhat more complete analysis of this concept in β -decay can be found in G. LÜDERS: *On the Pursey-Pauli Invariants in the Theory of Beta Decay*, UCRL-3903, Aug. 1957; *Nuovo Cimento* (to be published). A discussion for K-meson decay can be found in R. GATTO: *Invariants in $K_{\mu 3}$ and $K_{e 3}$ Decays*, UCRL-3949, September 1947; *Progress of Theoretical Physics* (to be published).

invariant. The group is generated by the following two commuting subgroups,

$$(I) \quad \psi'_v = a\psi_v + b\gamma_5 C^{-1}\bar{\psi}_v, \quad \bar{\psi}'_v = a^*\bar{\psi}_v + b^*\psi_v C\gamma_5,$$

with

$$(1) \quad |a|^2 + |b|^2 = 1,$$

and

$$(II) \quad \psi'_v = \exp[ix\gamma_5]\psi_v, \quad \bar{\psi}'_v = \bar{\psi}_v \exp[ix\gamma_5],$$

with α real. The symbol C in Transformation (I) denotes the 4-by-4 charge-conjugation matrix. An interaction Hamiltonian containing neutrinos does not stay invariant under this transformation. It is transformed, however, into a Hamiltonian that is equivalent to the original one in the sense that it leads to the same observable effects.

In this paper the concept of equivalent Hamiltonians is studied for the μ -e decay. The interaction is assumed to be invariant under the proper Lorentz group and local, and without derivative couplings but with no restrictions as to conservation of parity or of lepton charge. The most general expression for the interaction then is ⁽²⁾

$$(2) \quad H_{\text{int}} = \sum_i (\bar{\psi}_e \Gamma_i \psi_\mu) \{ (\bar{\psi}_v \Gamma_i (g_i + g'_i \gamma_5) \psi_v) + (\bar{\psi}_v^c \Gamma_i (f_i + f'_i \gamma_5) \psi_v) + (\bar{\psi}_v \Gamma_i (h_i + h'_i \gamma_5) \psi_v^c) \} + \text{Hermitian conj.}$$

with

$$(3) \quad \psi_v^c = C^{-1}\bar{\psi}_v, \quad \bar{\psi}_v^c = -\psi_v C.$$

The sum in Eq. (2) goes over all five covariant combinations of matrices corresponding to scalar (S), vector (V), tensor (T), axial vector (A), and pseudo-scalar (P) coupling. It is well known that other orderings of the field operators in Eq. (2) do not lead to expressions that are not already contained in this equation ⁽³⁾.

The behaviour of the Dirac matrices Γ under charge conjugation and their commutativity or anticommutativity with γ_5 determine whether a particular type of coupling characterized by the subscript i really needs six coupling constants, as in the general expression (2), or less. One finds that only the

⁽²⁾ For the notation we follow a paper by T. KINOSHITA and A. SIRLIN (*Phys. Rev.*, to be published). We also use their definition of the Γ matrices.

⁽³⁾ L. MICHEL: *Proc. Phys. Soc.*, A **63**, 514 (1950); M. FIERZ: *Zeits. f. Phys.*, **104**, 553 (1937).

following coupling constants are multiplied by non-vanishing expressions:

$$(4) \quad g_T, \quad g'_T; \quad g_V, \quad g'_V; \quad f'_V; \quad h'_V; \quad g_A, \quad g'_A; \quad f_A; \quad h_A; \quad \text{all constants for S and P.}$$

Since equivalent Hamiltonians lead to the same observable effects, all physical results can be characterized by combinations of the coupling constants that are invariant under the group of transformations of the neutrino field. In the Appendix the transformation properties of the coupling constants are discussed in detail; there it is also explained how the most general invariant combinations of them can be constructed. For practical purposes, however, only those invariants are needed which can occur in a first-order perturbation treatment, i.e., which are bilinear expressions formed by products of coupling constants and complex conjugate coupling constants. Before such invariants are given we want to discuss which simplifications arise from the fact that, for all practical purposes, the mass of the electron, can be neglected in calculations of the μ -e decay. Putting the mass of the electron formally equal to zero one sees that then also the electron field admits a group of transformations of the type (II):

$$(III) \quad \psi'_e = \exp [ie\gamma_5] \psi_e, \quad \bar{\psi}'_e = \bar{\psi}_e \exp [ie\gamma_5] \quad (e \text{ real}).$$

Because, for the electron the particle and antiparticle are distinguished by their charges, there is, however, no analogue to Transformation (I). Under Transformation (III), electron states with spin parallel or opposite to the direction of motion are only multiplied by a phase factor. Results of experiments in which only the intensity of the decay electrons and their longitudinal polarization is observed can therefore be expressed in terms of combinations of coupling constants that are invariant under this wider group (Class *A* in the following list). Observations of the transversal polarization of an electron beam do not admit the group of transformations of the electron field; they have to be expressed in terms of the Class *B* invariants. The situation is not quite so simple if the electron mass is not neglected ⁽⁴⁾.

⁽⁴⁾ Even for non-vanishing rest mass the electron field admits multiplication by γ_5 connected with the formal substitution $m_e \rightarrow -m_e$. The invariants of Class *A* stay invariant under such a transformation, whereas those of Class *B* take up a minus sign. Therefore in expressions for intensity and longitudinal polarization, terms with an even power of the electron mass appear multiplied by invariants of Class *A*, and those with an odd power of the electron mass appear multiplied by invariants of Class *B*. Similarly, in expressions for transversal polarization, terms with an even (odd) power of the electron mass appear multiplied by invariants of Class *B* (*A*). Compare the similar considerations for β -decay with neutrinos of non-vanishing mass in LÜDERS, l. c. footnote ⁽⁵⁾.

The list of the invariants is as follows:

Class A

$$\begin{aligned}
 K^{(2)} &= |g_T|^2 + |g'_T|^2, \quad L^{(2)} = 2R(g_T g'_T)^* \\
 K^{(1)} &= |g_V|^2 + |g'_A|^2 + 2(|f_V|^2 + |f_A|^2 + |h_V'|^2 + |h_A'|^2) \\
 K_2^{(1)} &= |g_V'|^2 + |g_A'|^2 \\
 L_1^{(1)} &= 2R[g_V g_A'^* + 2(f_V f_A'^* + h_V' h_A'^*)] \\
 L_2^{(1)} &= 2R(g_V' g_A)^* \\
 K_1^{(0)} &= |g_S|^2 + |g'_S|^2 + |g_P|^2 + |g'_P|^2 + 2(|f_S|^2 + |f'_S|^2 + |f_P|^2 + |f'_P|^2 + \\
 &\quad + |h_S|^2 + |h'_S|^2 + |h_P|^2 + |h'_P|^2) \\
 K_2^{(0)} &= 2R[g_S g_P^* + g'_S g_P'^* + 2(f_S f_P^* + f'_S f_P'^* + h_S h_P^* + h'_S h_P'^*)] \\
 L_1^{(0)} &= 2R[g_S g_S^* + g_P g_P^* + 2(f_S f_P^* + f'_S f_P'^* + h_S h_P^* + h'_S h_P'^*)] \\
 L_2^{(0)} &= 2R[g_S g_P'^* + g'_S g_P^* + 2(f_S f_P'^* + f'_S f_P^* + h_S h_P'^* + h'_S h_P^*)].
 \end{aligned} \tag{5}$$

Class B

$$\begin{aligned}
 M^{(2)} &= |g_T|^2 - |g'_T|^2, \quad N^{(2)} = 2I(g_T g'_T)^*; \\
 M_1^{(1)} &= |g_V|^2 - |g'_A|^2 + 2(|f_V|^2 - |f_A|^2 + |h_V'|^2 - |h_A'|^2) \\
 M_2^{(1)} &= |g_V'|^2 - |g_A'|^2 \\
 N_1^{(1)} &= 2I[g_V g_A'^* + 2(f_V f_A'^* + h_V' h_A'^*)] \\
 N_2^{(1)} &= 2I(g_V' g_A)^* \\
 M_1^{(0)} &= |g_S|^2 + |g'_S|^2 - |g_P|^2 - |g'_P|^2 + 2(|f_S|^2 + |f'_S|^2 - |f_P|^2 - |f'_P|^2 + \\
 &\quad + |h_S|^2 + |h'_S|^2 - |h_P|^2 - |h'_P|^2) \\
 N_1^{(0)} &= I2[g_S g_P^* + g'_S g_P'^* + 2(f_S f_P^* + f'_S f_P'^* + h_S h_P^* + h'_S h_P'^*)] \\
 N_2^{(0)} &= 2R[g_S g_S^* - g_P g_P^* + 2(f_S f_P^* - f'_S f_P'^* + h_S h_P^* - h'_S h_P'^*)] \\
 N_3^{(0)} &= I2[g_S g_P'^* + g'_S g_P^* + 2(f_S f_P'^* + f'_S f_P^* + h_S h_P'^* + h'_S h_P^*)]
 \end{aligned} \tag{6}$$

One notices that the invariants fall into three distinct groups (SP, AV, T) so that there are no interference terms between the three groups ⁽⁵⁾.

⁽⁵⁾ PURSEY (*l. c.*) gives only two such groups (STP and AV); there is, however, no interference between T on the one hand SP on the other. This follows for Pursey's interaction Hamiltonian ($f_i = f'_i = h_i = h'_i = 0$) from the observation that both Transformation (II) and charge conjugation of the neutrino field transform the Hamiltonian into an equivalent one.

The particular invariant combination of S and P or of A and V in Class A comes about by the action of Transformation (III) of the electron field, which just mixes the coupling constants in these pairs of types of interactions among themselves. The list contains 20 invariants, but not all of them appear independently in lowest-order expressions for experimental distributions. Rather

$$K_2^{(1)}, \quad L_1^{(0)}, \quad M^{(2)}, \quad N^{(2)} - N_1^{(0)}, \quad N_2^{(0)}$$

do not appear at all, whereas the VA invariants occur only in the combinations

$$K_1^{(0)} + K_2^{(0)}, \quad L_1^{(0)} + L_2^{(0)}, \quad M_1^{(0)} + M_2^{(0)}, \quad N_1^{(0)} + N_2^{(0)}.$$

The reason for this very limited experimental information as compared with β -decay is twofold: there is only one charged—and therefore observable—decay product, and we observe only the decay of the free μ -meson (in contrast to the β -decay of nucleons bound in nuclei).

Radiative corrections ⁽⁶⁾ have to be expressable in terms of the same invariants, since Transformations (I) and (II) of the neutrino field do not affect the interaction between the charged particles involved in the decay, and the electromagnetic field. Furthermore, even radiative corrections in experiments in which only the intensity of longitudinal polarization of the electrons is observed can depend only upon the invariants of Class A , since the electron transformation (III) does not affect the electron current,

$$(7) \quad j_\mu = e\bar{\psi}_e \gamma_\mu \psi_e = e\bar{\psi}_e \exp[i\varepsilon \gamma_5] \gamma_\mu \exp[i\varepsilon \gamma_5] \psi_e,$$

whose interaction with the Maxwell field gives rise to these corrections.

The invariants (5) and (6), in contrast to the invariants given for β -decay ⁽¹⁾, do not form a complete set. Therefore their equality for two different interactions is a necessary but not a sufficient condition for the equivalence of these two interactions in the sense that they can be transformed into each other by a combination of Transformations (I) and (II) of the neutrino field.

2. – Discussions of the invariants.

a) The invariants (5) and (6) are not all independent, but are restricted by a number of relations between them. First of all, all K invariants with the exception of $K_2^{(0)}$ are non-negative: they vanish only if all coupling con-

⁽⁶⁾ Such corrections were calculated for a particular case (two-component theory in the Salam-Lee-Yang-Landau form) by T. KINOSHITA and A. SIRLIN (*Phys. Rev.*, **107**, 593 (1957)).

stants occurring in them vanish separately. Further, one has the following identities and inequalities between the invariants:

$$(8) \quad \left\{ \begin{array}{l} K^{(2)^2} = L^{(2)^2} + M^{(2)^2} + N^{(2)^2}, \\ -K_1^{(1)} \leq (L_1^{(1)}, M_1^{(1)}, N_1^{(1)}) \leq K_1^{(1)}, \\ K_2^{(1)^2} = L_2^{(1)^2} + M_2^{(1)^2} + N_2^{(1)^2}, \\ -K_1^{(0)} \leq (K_2^{(0)}, L_1^{(0)}, L_2^{(0)}, M_1^{(0)}, N_1^{(0)}, N_2^{(0)}, N_3^{(0)}) \leq +K_1^{(0)}. \end{array} \right.$$

b) The necessary condition for conservation of parity is: all L and all N , with the exception of $N_1^{(0)}$ vanish. The necessary condition for invariance with respect to charge conjugation is: all L and $N_1^{(0)}$ as well as $N_2^{(0)}$ vanish. The necessary condition for invariance under time reversal is: all N with the exception of $N_2^{(0)}$ vanish. These conditions are not sufficient, because the list of invariants is not complete; there may be practically unobservable higher-order effects that violate one or several of these invariance properties, and which depend on other invariant combinations of the coupling constants. The conditions are, however, sufficient in the weaker sense that if they are satisfied there are no first-order violation effects.

If one goes over from μ^+ decay to μ^- decay, all observable quantities that are multiplied by invariants that remain invariant under charge conjugation stay unchanged, whereas those which are multiplied by invariants that would have to vanish if charge conjugation were satisfied take up a minus sign.

c) Necessary conditions to be satisfied by an interaction which conserves lepton charge ⁽⁷⁾, in the sense that μ -meson and electron with the same electric charge also carry the same lepton charge, are given by:

No additional condition for

$$(9) \quad \left\{ \begin{array}{l} K^{(2)}, \quad L^{(2)}, \quad M^{(2)}, \quad N^{(2)} \quad \text{and} \quad K_2^{(1)}, \quad L_2^{(1)}, \quad M_2^{(1)}, \quad N_2^{(1)}; \\ K_1^{(1)^2} = L_1^{(1)^2} + M_1^{(1)^2} + N_1^{(1)^2}; \\ \text{S, P identities.} \end{array} \right.$$

Here «S, P identities» refers to complicated relations between the invariants

⁽⁷⁾ The concept of conservation of lepton charge appears to have been put forward first by E. J. KONOPINSKI and H. M. MAHMOUD: *Phys. Rev.*, **96**, 1045 (1953).

Note added in proof: Our results concerning lepton conservation were previously and independently obtained by B. FERRETTI (*Nuovo Cimento*, **6**, 999 (1957)), who gives a more general discussion of the problem.

characteristic for scalar and pseudoscalar coupling which are of the type of 5-by-5 determinants (constructed from the invariants) set equal to zero. The same identities, which we do not give explicitly, will appear at a few other places. These relations are derived by observing that there has to exist an equivalent Hamiltonian with $f_i = f'_i = h_i = h'_i = 0$. Because of the incompleteness of the list of invariants the conditions are again only necessary but not sufficient.

d) Conservation of leptons, when μ -meson and electron with equal electric charge have opposite lepton charge, leads to the necessary conditions:

$$(10) \quad \left\{ \begin{array}{l} K^{(2)} = L^{(2)} = M^{(2)} = N^{(2)} = K_2^{(1)} = L_2^{(1)} = M_2^{(1)} = N_2^{(1)} = 0, \\ K_1^{(1)2} = L_1^{(1)2} + M_1^{(1)2} + N_1^{(1)2}, \\ \text{S, P identities.} \end{array} \right.$$

e) A general two-component theory with no restrictions as to conservation of lepton charge ⁽⁸⁾ leads to the following conditions on the invariants:

$$(11) \quad \left\{ \begin{array}{l} K^{(2)} = L^{(2)} = M^{(2)} = N^{(2)} = 0, \\ K_1^{(1)} = K_2^{(1)}, \quad L_1^{(1)} = L_2^{(1)}, \quad M_1^{(1)} = M_2^{(1)}, \quad N_1^{(1)} = N_2^{(1)}, \\ \text{S, P identities.} \end{array} \right.$$

f) A two-component coupling, with conservation of lepton charge (i.e., a two-component theory in the conventional sense ⁽⁹⁾), leads to the following necessary conditions:

i) equal electric charge of μ -meson and electron implies equal lepton charge:

all invariants with superscript (2) and (10) vanish,

$$(12) \quad K_1^{(1)} = K_2^{(1)}, \quad L_1^{(1)} = L_2^{(1)}, \quad M_1^{(1)} = M_2^{(1)}, \quad N_1^{(1)} = N_2^{(1)};$$

ii) equal electric charge of μ -meson and electron implies opposite lepton charge ⁽¹⁰⁾:

⁽⁸⁾ This possibility has been considered for μ -e decay by M. H. FRIEDMAN: *Phys. Rev.*, **106**, 387 (1957). It was used in the discussion of β -decay by PAULI (*l. c.*).

⁽⁹⁾ A. SALAM: *Nuovo Cimento*, **5**, 299 (1957); T. D. LEE and C. N. YANG: *Phys. Rev.*, **105**, 1671 (1957); L. LANDAU: *Nuclear Physic*, **3**, 127 (1957).

⁽¹⁰⁾ This case is definitely excluded experimentally by the observed spectrum.

all invariants with superscript (2) and (1) vanish:

$$(13) \quad \left\{ \begin{array}{l} K_1^{(0)} = \pm L_1^{(0)}, \quad K_2^{(0)} = \pm L_2^{(0)}, \quad M_1^{(0)} = \pm N_2^{(0)}, \quad N_1^{(0)} = \pm N_3^{(0)}; \\ K_1^{(0)2} = K_2^{(0)2} + M_1^{(0)2} + N_1^{(0)2}. \end{array} \right.$$

The sign (+ or -) in the second line has to be the same in all four cases.

A complete discussion of all observable effects in μ -e decay (without radiative corrections) has been given recently by KINOSHITA and SIRLIN (11). They use an interaction in which they assume

$$(14) \quad f_i = f'_i = h_i = h'_i = 0,$$

i.e., they assume conservation of lepton charge and electric charge equal to lepton charge for μ -meson and electron. The concept of invariants permits us to generalize their results immediately to the interaction Hamiltonian Eq. (2): the coupling constants f_i , f'_i and h_i , h'_i can enter into expressions for observable results only in such a way that the invariants (5) and (6) are obtained. KINOSHITA and SIRLIN express all observable quantities in terms of ten combinations of coupling constants. Their results hold also for the more general interactions (2) if one puts

$$(15) \quad \left\{ \begin{array}{l} a = K_1^{(0)}, \quad b = K_1^{(1)} + K_2^{(1)}, \quad c = K^{(2)}, \\ a' = L_2^{(0)}, \quad b' = L_1^{(1)} + L_2^{(1)}, \quad c' = L^{(2)}, \\ \alpha = M_1^{(1)}, \quad \beta = M_1^{(1)} + M_2^{(1)}, \\ \alpha' = -N_3^{(1)}, \quad \beta' = N_1^{(1)} + N_2^{(1)}. \end{array} \right.$$

One recognizes the result stated in Sect. 1 that some invariants do not occur at all and others in particular combinations.

Especially for the so-called ϱ value (12), they find

$$(16) \quad \varrho = \frac{3b + 6c}{a + 4b + 6c}.$$

(11) T. KINOSHITA and A. SIRLIN: *Phys. Rev.* (to be published).

(12) L. MICHEL: *Proc. Phys. Soc.*, A **63**, 514 (1950); C. BOUCHAT and L. MICHEL: *Phys. Rev.*, **106**, 170 (1957).

Since a measurement of the spectrum does not show violation effects and since one has, neglecting the mass of the electron, invariance with respect to Transformation (III) of the electron field, ϱ can depend only upon K invariants, as is indeed the case. The inequality for ϱ ,

$$(17) \quad 0 \leq \varrho \leq 1,$$

is always fulfilled. The same inequality holds if conservation of lepton charge (μ -mesons and electrons of equal electric charge have equal lepton charge) is postulated (12). For conservation of lepton charge with μ -meson and electrons of equal electric charge having opposite lepton charge, one finds (12)

$$(18) \quad 0 \leq \varrho \leq \frac{3}{4}.$$

This is also true in a general two-component theory with no restriction as to the conservation of lepton charge (1, 14).

In two-component theory with conservation of lepton charge, with μ -meson and electron of equal electric charge having equal lepton charge, one has

$$(19) \quad \varrho = \frac{3}{4}$$

and with μ -mesons and electrons of equal electric charge having opposite lepton charge (9),

$$(20) \quad \varrho = 0.$$

All these relations are found if one applies the restrictions on the K invariants in the particular cases as summarized in Sect. 2.

KINOSHITA and SIRLIN (11) write the general electron spectrum for the decay of (negatively charged) μ -mesons in the form

$$(21) \quad dN = C_0 + C_1(\mathbf{P}_e \cdot \boldsymbol{\sigma}_e)(\mathbf{P}_e \cdot \boldsymbol{\sigma}_\mu) + C_2(\mathbf{P}_e \wedge \boldsymbol{\sigma}_e)(\mathbf{P}_e \wedge \boldsymbol{\sigma}_\mu) + \\ + C_3 \mathbf{P}_e(\boldsymbol{\sigma}_e \wedge \boldsymbol{\sigma}_\mu) + C_4(\mathbf{P}_e \cdot \boldsymbol{\sigma}_e) + C_5(\mathbf{P}_e \cdot \boldsymbol{\sigma}_\mu).$$

(13) M. H. FRIEDMAN: *Phys. Rev.*, **106**, 387 (1957).

(14) In this paper we assume local interaction (cf. Eq. (2)). Possible non-local effects are, however, not unlikely to show up in μ -e decay. LEE and YANG (*Phys. Rev.*, to be published) show that the assumption of a reasonable non-locality permits one to reconcile the observed electron spectrum with the two-component theory, without violation of the conservation of lepton charge.

The relevance of the various terms for violation effects is seen if it is recognized that under reflections in space, one has (15)

$$(22) \quad \mathbf{P} \rightarrow -\mathbf{P}, \quad \boldsymbol{\sigma} \rightarrow \boldsymbol{\sigma},$$

and under time reversal, T , one has (16)

$$(23) \quad \mathbf{P} \rightarrow -\mathbf{P}, \quad \boldsymbol{\sigma} \rightarrow -\boldsymbol{\sigma}.$$

If validity of the TCP theorem is assumed, then violation of charge conjugation C , can be recognized from terms which change sign under the transformation

$$(24) \quad \mathbf{P} \rightarrow \mathbf{P}, \quad \boldsymbol{\sigma} \rightarrow -\boldsymbol{\sigma}.$$

From Eqs. (21) through (23) one sees immediately which terms are characteristic for the various violation effects (Table I). This table, apart from the last column, can also be used for other decay processes if the assumption on test of time reversal (16) is satisfied and if the TCP theorem is assumed to hold. Coefficients characteristic for violation of charge conjugation (i.e., C_4 and C_5)

TABLE I. – *Behaviour of the various terms of Eq. (21) under T , C , P .*

Number of momenta	Number of spins	Violation	Coefficients
even	even	None	C_0, C_1, C_2
odd	any	Parity	C_3, C_4, C_5
any	odd	Charge conjugation	C_4, C_5
even	odd (1)	Time reversal	C_3
odd	even		

(1) A more concise statement would be: number of factors odd.

(15) This rule appears to be more simple than other rules in which a distinction between vectors and pseudovectors as well as between scalars and pseudoscalars is to be made.

(16) The operation of time reversal maps a process into another one which develops with time in the opposite sense; therefore a decay situation is mapped into a built-up situation. The usual tests of time reversal (cf. the above transformation formulae) are possible only if this second process can again be related to the original one, i.e., if the transition matrix is not only unitary but also Hermitian. For this to be true the process need not be strictly of first order. It is, however, important that the contribution from intermediate states that fulfill energy-momentum conservation, and therefore could be real states, be negligible. In μ -e decay there are no such intermediate states, since they would also appear as another (and more frequent) decay channel.

change sign if one goes over to the decay of μ -mesons of the opposite charge; the others stay unchanged. KINOSHITA and SIRLIN make the interesting remark that this behavior of signs could be used for a model-independent test of the *TCP* theorem.

From the table and the discussion in Sect. 2. (ii) it is clear which invariants can occur in the various coefficients. If the mass of the electron is neglected, C_0 , C_1 , and C_4 (describing experiments in which intensity and (or) longitudinal polarization of the electrons is measured) must be expressible in terms of invariants of Class *A* only; it must be possible to express the other coefficients in terms of invariants of Class *B*. From the explicit expressions for the coefficients as given by KINOSHITA and SIRLIN it can be seen that the following invariants or combinations of them appear in the above spectrum:

$$K_1^{(0)}, \quad K_1^{(1)} + K_2^{(1)}, \quad \text{and} \quad K^{(2)} \quad \text{in } C_0 \text{ and } C_1;$$

$$M^{(0)} \quad \text{and} \quad M_1^{(1)} + M_2^{(1)} \quad \text{in } C_2; \quad N_3^{(0)} \quad \text{and} \quad N_1^{(1)} + N_2^{(1)} \quad \text{in } C_3;$$

$$L_2^{(0)}, \quad L_1^{(1)} + L_1^{(1)}, \quad \text{and} \quad L^{(2)} \quad \text{in } C_4 \text{ and } C_5.$$

• • • • • • • • • • • • • • • •

* * *

The authors wish to thank Professor PAULI for his interest in the work and for stimulating correspondence. They also want to acknowledge discussions with Dr. TSUNEYUKI KOTANI on various aspects of the theory of μ -e decay.

APPENDIX

Transformation properties of coupling constants.

The group generated by Transformations (I) and (II) is isomorphic with the unitary group in two dimensions. (G. LÜDERS (1), Sect. 3). The interaction Hamiltonian of β -decay contains only one neutrino operator; the coupling constants therefore transform like vectors in the two-dimensional space. The interaction Hamiltonian of μ -e decay contains in each term two neutrino operators. It is therefore to be expected that the coupling constants will transform like tensors of second rank (17). For the systematic construction

(17) In this connection a remark in a letter by Professor PAULI was of great value to us.

of irreducible representations of the group occurring as transformations of these coupling constants the application of tensor calculus is useful.

The basic transformation is ⁽¹⁸⁾

$$(A.1) \quad (T_{\mu\nu}) = \exp[-i\alpha] \begin{pmatrix} a & -b^* \\ b & a^* \end{pmatrix}.$$

We further introduce the complex conjugate transformation matrix

$$(A.2) \quad (T_{\mu\nu}) = \exp[i\alpha] \begin{pmatrix} a^* & -b \\ b^* & a \end{pmatrix}.$$

Then a two-dimensional vector A_μ with undotted index is defined by the transformation law

$$(A.3) \quad A'_\nu = \sum_\mu A_\mu T_{\mu\nu},$$

And a vector $B_{\dot{\mu}}$ with dotted index by ⁽¹⁹⁾

$$(A.4) \quad B'_\nu = \sum_{\dot{\mu}} B_{\dot{\mu}} T_{\dot{\mu}\nu}.$$

A general tensor with undotted and dotted indices transforms under (A.3) with respect to the undotted indices and under Transformation (A.4) with respect to the dotted indices. The complex conjugate of such a tensor transforms like one for which all undotted indices are replaced by dotted ones and vice versa. Therefore one may define

$$(A.5) \quad (A_{\mu\nu} \dots \dot{\rho}\dot{\sigma} \dots)^* = A_{\dot{\mu}\dot{\nu}} \dots \rho\sigma \dots$$

Because of the unitarity of Transformation (A.1), contraction of tensor indices is possible by summing over one dotted and one undotted index.

A tensor of second rank may contain two indices, either of the same kind (both undotted or both dotted) or of different kind (one undotted and one dotted). Tensors with indices of the same kind can be either symmetrical or antisymmetrical in these indices, a property that is invariant under tensor transformations. Therefore one gets the following two types of irreducible tensors.

a) Antisymmetrical tensors,

$$(A.6) \quad A_{[\mu,\nu]} = -A_{[\nu,\mu]} \quad \text{and} \quad B_{[\dot{\mu},\dot{\nu}]} = -B_{[\dot{\nu},\dot{\mu}]}.$$

⁽¹⁸⁾ W. PAULI, (*l. c.*) Eq. (10).

⁽¹⁹⁾ Examples of such vectors are given by Pauli's coupling constants F and G . One has $A_1 = F_1$, $A_2 = F_2$, $B_1^* = G_2$, $B_2^* = -G_1$. In the sense of this terminology LÜDERS used only vectors with undotted indices ($H_1 = (B_1^*)^*$, $H_2 = (B_2^*)^*$).

These tensors contain only one non-vanishing component $A_{[1,2]}$ or $B_{[1,2]}$; therefore one obtains representations of first degree ⁽²⁰⁾.

b) Symmetrical tensors,

$$(A.7) \quad C_{(\mu,\nu)} = C_{(\nu,\mu)} \quad \text{and} \quad D_{(\dot{\mu},\dot{\nu})} = D_{(\dot{\nu},\dot{\mu})}.$$

These representations are of third degree. On tensors with indices of different kind the operation of contraction can be applied. Therefore one has two types of irreducible representations.

c) The trace of a tensor ⁽²¹⁾,

$$(A.8) \quad E = \sum_{\mu} E_{\mu,\dot{\mu}}.$$

This give a representation which actually is the identical representation: the quantity E is an invariant.

d) Tensor with vanishing trace,

$$(A.9) \quad F_{\mu\dot{\nu}} \quad \text{with} \quad \sum_{\mu} F_{\mu,\dot{\mu}} = 0.$$

This representation is again of third degree. Tensors of Classes *c*) and *d*) are invariant under Transformation (II), whereas tensors of Classes *a*) and *b*) take up factors $\exp[-2i\alpha]$ (for undotted indices) or $\exp[2i\alpha]$ (for dotted indices). The irreducible representations are characterized by the traces of the transformation matrices (characters)

$$(A.10) \quad \left\{ \begin{array}{ll} a) & \exp[-2i\alpha] \text{ and } \exp[2i\alpha], \\ b) & \exp[-2i\alpha]((a+a^*)^2-1) \text{ and } \exp[2i\alpha]((a+a^*)-1), \\ c) & 1, \\ d) & (a+a^*)^2-1, \end{array} \right.$$

where the two alternatives for Classes *a*) and *b*) refer to pairs of undotted or dotted indices.

The construction of invariants is now quite simple. One forms products of tensors with equal numbers of undotted and of dotted indices and contracts over pairs of such indices. In β -decay all invariants were bilinear in the basic quantities (vectors or coupling constants). The situation is different here.

⁽²⁰⁾ Pauli's relative invariants (Ref. (18), Eq. (18)-(18b)) transform according to these representations.

⁽²¹⁾ The symbol \sum_{μ} means here and in some of the following equations that the sum of the two terms with $\mu=1$, $\dot{\mu}=\dot{1}$ and $\mu=2$, $\dot{\mu}=\dot{2}$ has to be taken.

There are linear invariants, i.e., Class *c*) of the tensors; they appear, however, not to be interesting from a physical point of view. Then there are bilinear invariants, i.e., apart from products of quantities of Class *c*), the combinations

$$(A.11) \quad \sum_{\mu\nu} A_{[\mu\nu]} B_{[\dot{\mu}\dot{\nu}]} , \quad \sum_{\mu\nu} C_{(\mu\nu)} D_{(\dot{\mu}\dot{\nu})} , \quad \sum_{\mu\nu} F_{\mu\nu} G_{\dot{\mu}\dot{\nu}} .$$

For physical applications, only those invariants in this group are of interest in which one tensor consists of coupling constants and the other of complex conjugate coupling constants. There are also invariants, not expressible by the ones already given, which consist of more than two tensors, e.g.,

$$(A.12) \quad \sum_{\mu\nu\lambda} A_{[\mu\nu]} C_{\mu\dot{\lambda}} F_{\dot{\nu}\lambda} .$$

But such invariants do not appear in description of experiments that are now possible, because all such experiments can be described by first-order perturbation calculation.

All irreducible tensors of second rank given above do really occur in μ -decay. By performing Transformation (I) and (II) explicitly one finds

$$(A.13) \quad \left| \begin{array}{l} A_{[12]} = g_T - g'_T , \\ B_{[1\dot{2}]} = g_T + g'_T , \\ C_{(12)}^S = g_S - g'_S , \quad C_{(11)}^S = 2(f_S - f'_S) , \quad C_{(22)}^S = 2(h_S - h'_S) , \\ D_{(\dot{1}\dot{2})}^S = g_S + g'_S , \quad D_{(1\dot{1})}^S = 2(f_S + f'_S) , \quad D_{(\dot{2}\dot{2})}^S = 2(h_S + h'_S) , \\ C_{(12)}^P = g_P - g'_P , \quad C_{(11)}^P = 2(f_P - f'_P) , \quad C_{(22)}^P = 2(h_P - h'_P) , \\ D_{(\dot{1}\dot{2})}^P = g_P + g'_P , \quad D_{(1\dot{1})}^P = 2(f_P + f'_P) , \quad D_{(\dot{2}\dot{2})}^P = 2(h_P + g'_P) , \\ E^V = g'_V , \quad E^A = g_A , \\ F_{(1\dot{1})}^V = g_V , \quad F_{2\dot{1}}^V = 2f'_V , \quad F_{1\dot{2}}^A = 2h'_V , \\ F_{\dot{1}\dot{1}}^A = g'_A , \quad F_{2\dot{1}}^A = 2f_A , \quad F_{1\dot{2}}^A = 2h_A . \end{array} \right.$$

When only intensity or longitudinal polarization of the outgoing electrons is observed and the electron mass is neglected also, the electron group (III) is admissible. The following combinations of coupling constants,

$$(A.14) \quad A_{[\mu\nu]} , \quad C_{(\mu\nu)}^S - C_{(\mu\nu)}^P , \quad D_{[\mu\nu]}^S + D_{(\mu\nu)}^P , \quad E^V - E^A , \quad F_{\mu\nu}^V - F_{\mu\nu}^A ,$$

take up an $\exp[+i\varepsilon]$ under this transformation, and

$$(A.15) \quad B_{[\dot{\mu}\dot{\nu}]} , \quad C_{(\mu\nu)}^S + C_{(\mu\nu)}^P , \quad D_{[\mu\nu]}^S - D_{(\mu\nu)}^P , \quad E^V + E^A , \quad F_{\mu\nu}^V + F_{\mu\nu}^A .$$

take up an $\exp[-i\varepsilon]$. The invariants of Class *A* (Eq. (5)) were obtained by use for these tensors, and their combination according to Eq. (A.11); to have

invariance under the electron group only products of tensors and complex conjugate tensors, both from Eq. (A.14) or both from Eq. (A.15), are to be formed. Class *B* (Eq. (6)), which is not invariant under the electron group, is obtained by multiplying a tensor contained in (A.14) by the complex conjugate of a tensor contained in (A.15) or vice versa.

RIASSUNTO (*)

L'ipotesi che il neutrino abbia massa tendente a zero conduce a un gruppo di trasformazioni del campo neutrino che lasciano invarianti le relazioni di commutazione e l'hamiltoniana del campo libero, ma cambiano l'interazione in una equivalente che dà gli stessi risultati fisici. Questo concetto espresso da PURSEY e PAULI si applica qui al decadimento μ -e nell'ipotesi di accoppiamento locale non derivativo senza restrizioni riguardo alla conservazione della parità o alla carica leptonica. Si derivano le combinazioni invarianti delle costanti d'accoppiamento d'importanza fisica e se ne discutono le reciproche relazioni. Si utilizza un recente lavoro di KINOSHITA e SIRLIN per esprimere tutte le risultanze sperimentali sul decadimento μ -e in termini di tali invarianti.

(*) Traduzione a cura della Redazione.

On the Optical Model for Nuclear Reactions.

L. VERLET

Laboratoire de Physique, École Normale Supérieure - Université de Paris

(ricevuto il 18 Novembre 1957)

Summary. — The complex potential for neutrons in an infinite nuclear medium is computed in a perturbation calculation up to the second order, using for the nucleon-nucleon interaction a regular potential which fits the low energy two-body data. It is shown that it is possible to fit simultaneously the real and the imaginary part of the optical potential and the binding energy of the nuclear matter at normal density. Some arguments for the convergence of the theory are given.

1. — Introduction.

The problem of the optical model for scattering of neutrons by complex nuclei may be divided in two steps. Firstly one calculates the scattering cross-sections in terms of a phenomenological complex potential acting on the incoming particle. This program has been successfully carried out in the high energy region by FERNBACH, TAYLOR and SERBER ⁽¹⁾ and extended, with the necessary reinterpretations, in the resonance region by FESHBACH, PORTER and WEISSKOPF ⁽²⁾. Some more recent results ⁽³⁾ of this type of analysis are summarized in Fig. 2 and 3. The second step consists in linking the depth

⁽¹⁾ S. FERNBACH, R. SERBER and T. B. TAYLOR: *Phys. Rev.*, **75**, 1352 (1949).

⁽²⁾ H. FESHBACH, C. E. PORTER and V. F. WEISSKOPF: *Phys. Rev.*, **96**, 448 (1954).

⁽³⁾ H. L. TAYLOR: *Phys. Rev.*, **92**, 831 (1953); H. L. TAYLOR, O. LÖNSNÖ and T. W. BONNER: *Phys. Rev.*, **100**, 174 (1956); F. MANDL and T. H. SKYRME: *Phil. Mag.*, **44**, 1028 (1953); M. A. MELKANOFF, S. A. MOZKOWSKI, J. NODVIK and D. S. SAXON: *Phys. Rev.*, **101**, 57 (1956); R. JASTROW and R. M. STERNHEIMER: *Phys. Rev.*, to be published.

of this phenomenological potential to the more fundamental 2-body interactions. The formal solution to this problem has been amply discussed by WATSON and his collaborators ⁽⁴⁾, who express the complex potential in terms of the scattering amplitude calculated in the nuclear matter. When one is only interested in relating directly the complex potential to the two-body potentials, its expression is straightforwardly given as a series of successive Born approximations. There is some hope that this series ⁽⁵⁾ converges if one simulates the nucleon-nucleon potential by a regular two-body potential. In the present work, we shall suppose that this is the case, and we shall perform the calculation of the complex potential including the two first Born approximations. We shall moreover make two simplifying assumptions, which are natural if we keep only the first and the second order in the interaction:

- a) We shall consider an infinite nuclear medium described by an uncorrelated Fermi gas.
- b) We shall assume that the nuclear particles are imbedded in a constant potential. This potential will also be used to define, in zero order approximation the wave function of the incoming neutron.

A calculation of the imaginary potential in the limit of a zero energy incoming particle has been already carried out along these lines by CINI and FUBINI ⁽⁶⁾ on the one hand, and by BRUECKNER, EDEN and FRANCIS ⁽⁷⁾ on the other. These last authors, however, take into account the variation of the real part of the well felt by the incoming particle as a function of its energy in the approximation of the effective mass. The absorption is then reduced by a factor $(M^*/M)^3$, where M^* is the effective mass, usually taken of the order of $0.6 M$, and no agreement with the experiment can be obtained. BRUECKNER ⁽⁸⁾ shows, however, that if one abandons assumption a) by introducing a non-degenerate Fermi gas to describe the nuclear medium, the value of the absorption potential rises again by a factor 5. Although it is not quite clear whether this procedure is consistent with the general theory of nuclear structure, this result may be considered as an indication that the errors introduced by approximations a) and b) may be compensating each other.

We shall show in this work that, with the approximation afore-mentioned, it is possible to reproduce the experimental results for the complex potential

⁽⁴⁾ K. M. WATSON: *Phys. Rev.*, **89**, 575 (1953); G. TAKEDA and K. M. WATSON: *Phys. Rev.*, **97**, 1336 (1955); N. C. FRANCIS and K. M. WATSON: *Phys. Rev.*, **92**, 291 (1953).

⁽⁵⁾ W. SWIATECKI: *Phys. Rev.*, **101**, 1321 (1956); H. A. BETHE: *Phys. Rev.*, **103**, 1353 (1956).

⁽⁶⁾ M. CINI and S. FUBINI: *Nuovo Cimento*, **10**, 75 (1955).

⁽⁷⁾ K. A. BRUECKNER, R. J. EDEN and N. C. FRANCIS: *Phys. Rev.*, **100**, 891 (1955).

⁽⁸⁾ K. A. BRUECKNER: *Phys. Rev.*, **100**, 36 (1956).

up to 200 MeV with a regular two-body potential which fits the low energy data (singlet and triplet scattering length and effective range). This potential, which is consistent with those used in shell model calculations, gives also the correct value for the binding energy when the density is kept fixed and induces a configuration mixing, the smallness of which is a further indication of the convergence of the method.

2. – Calculation of the complex potential.

We shall choose, as a two-body interaction, a potential of the form:

$$(1) \quad V(r) = \mathcal{O}A \exp[-\alpha^2 r^2],$$

where:

$$(2) \quad \mathcal{O} = -\frac{1}{4}[(1 + P_\sigma)(1 + P_M) + q(1 - P_\sigma)(1 + P_M) + p_3(1 + P_\sigma)(1 - P_M) + p_1(1 - P_\sigma)(1 - P_M)]$$

P_σ and P_M being the spin and space exchange operators respectively.

By fitting the singlet and triplet scattering length and the triplet effective range, we determine the three parameters belonging to the S -state of the two-nucleon system. Their values are:

$$A = 72 \text{ MeV},$$

$$\alpha = 0.86 \cdot 10^{13} \text{ cm}^{-1},$$

$$q = 0.65.$$

Then, the value of the singlet effective range turns out to be $2.3 \cdot 10^{-13}$ cm, a value which is in agreement with the experiment.

The first Born approximation gives only a contribution to the real part of the potential. Its expression, which has often been given in the past, will be recalled for the sake of completeness. It is the sum of a direct term and of an exchange term:

$$(3) \quad \mathcal{O}^{(1)} = \frac{\text{Tr } \mathcal{O}}{24} \left(\frac{k_0}{\alpha} \right)^3 \frac{A}{\sqrt{\pi}} - \frac{\text{Tr } \mathcal{O} P_\sigma P_\tau}{32} \frac{1}{\pi^2 k_N} \int_{k_N - k_0}^{k_N + k_0} J(K) [k_0^2 - (K - k_N)^2] K dK,$$

where k_0 and k_N are the momenta of the top of the Fermi gas and of the incoming particle, respectively, P_τ is the isotopic spin exchange operator, and

$J(K)$ is the Fourier transform of the potential:

$$(4) \quad J(K) = A \left(\frac{\sqrt{\pi}}{\alpha} \right)^3 \exp \left[- \frac{K^2}{4\alpha^2} \right].$$

The direct part of the second order term is immediately written as:

$$(5) \quad \mathcal{O}^2(D) = - \frac{\text{Tr } \mathcal{O}^2}{2} \frac{M}{(2\pi)^6} \int \underset{<}{\text{d}^3 k} \int \underset{>}{\text{d}^3 k'} \int \underset{>}{\text{d}^3 k'_N} \frac{J^2(k'_N - k_N) \delta(k'_N + k' - k_N - k)}{(k'^2_N + k'^2 - k_N^2 - k^2 - i\epsilon)}.$$

If one keeps $|k'_N - k_N| = K$ fixed, it is possible to perform all the other integrations appearing in (5), and cast it into the form:

$$(6) \quad \mathcal{O}^2(D) = - \frac{M}{(2\pi)^3} \frac{\text{Tr } \mathcal{O}^2}{48\pi k_N} \int_{\omega} J^2(K) f(K) K \text{d}K,$$

ω is the K -integration domain which may be separated into several regions to each of which corresponds a definite form of $f(K)$.

The real part of $f(K)$ is a very lengthy expression; it will not be given here ⁽⁹⁾. The imaginary part of $f(K)$ is much simpler. If we suppose that $k_0 < k_N < 3k_0$, we have:

— for $0 < K < k_N - k_0$

$$\text{Im } f(K) = \pi \left(3k_0^2 K - \frac{K^3}{4} \right),$$

— for $k_N - k_0 < K < 2k_0$

1) if $k_N < \sqrt{2} k_0$,

$$\text{Im } f(K) = \pi \left(\frac{3}{4K} [k_N^2 - k_0^2]^2 \right);$$

2) if $k_N > \sqrt{2} k_0$,

$$\text{Im } f(K) = \pi \left[\frac{3}{4K} (k_N^2 - k_0^2)^2 - \frac{(k_0^2 + 2k_0 K - K^2 - k_N^2)^2 (-k_0^2 + 4k_0 K + K^2 + k_N^2)}{8K^3} \right],$$

— for $2k_0 < K < k_N + k_0$

$$\text{Im } f(K) = \pi \frac{(k_0^2 + 2k_0 K - K^2 - k_N^2)^2 (k_0^2 + 4k_0 K + K^2 - k_N^2)}{8K^3},$$

⁽⁹⁾ L. VERLET: *Thesis*, to be published in the *Ann. Phys.*

SIMPOSIO INTERNAZIONALE SULLE UNITÀ E SUI METODI DI MISURA DELLE RADIAZIONI IONIZZANTI

ROMA, 14-15 APRILE 1958

Nei giorni 14 e 15 Aprile 1958 si terrà in Roma, presso l'Istituto Superiore di Sanità (Viale Regina Elena, 299), un Simposio Internazionale sulle unità e sui metodi di misura delle radiazioni ionizzanti organizzato dalla Società Italiana di Radiologia Medica e di Medicina Nucleare, con la collaborazione della Organisation Mondiale de la Santé e dell'Istituto Superiore di Sanità, sotto il patronato dell'Alto Commissariato per l'Igiene e la Sanità Pubblica, del Consiglio Nazionale delle Ricerche, del Comitato Nazionale per le Ricerche Nucleari, e dell'Istituto Nazionale Assicurazione Infortuni sul Lavoro.

Il Comitato Organizzatore è così costituito : *Presidente* : Prof. LUIGI TURANO, Presidente della S.I.R.M.N. (Roma); *Segretario Generale* : Prof. FRANCO FOSSATI, Segretario del Comitato per le Unità e le Misure Radiologiche della S.I.R.M.N. (Milano); *Segretario Aggiunto* : Dott. CARLO POLVANI, Capo Servizio del Servizio Biologico del C.N.R.N. (Roma); *Segretario Tesoriere* : Dott. MARIO GUTTADAURO, Istituto di Radiologia dell'Università, Policlinico Umberto I, Roma.

Al Simposio hanno aderito numerosi membri della International Commission on Radiological Units and Measurements.

Coloro che desiderano partecipare al Simposio sono pregati di iscriversi il più presto possibile e comunque non oltre il 6 Aprile, segnalandosi al Segretario Tesoriere Dott. M. GUTTADAURO, Istituto di Radiologia dell'Università, Policlinico Umberto I, Roma. L'iscrizione al Simposio è gratuita.

Il Comitato Organizzatore si trova nella necessità di informare che l'accesso alla sala del Simposio sarà consentita — data la limitatezza dei posti — soltanto a chi presenterà l'apposita tessera d'iscrizione rilasciata dalla Segreteria.

La corrispondenza riguardante l'organizzazione del Simposio e qualsiasi richiesta di informazione devono essere indirizzate al Segretario Generale Prof. FRANCO FOSSATI, Istituto di Radiologia dell'Ospedale Maggiore, Milano.

DOMUS GALILÆANA

PISA - VIA S. MARIA, 18

On June 19 1957 the tercentenary of the first reunion of the Accademia del Cimento took place and to celebrate this occasion the Domus Galilæana in Pisa and the Museo di Storia della Scienza in Florence, with the financial support of the National Council for Research — to which they are both much indebted — have published in a single large-sized volume (27 cm × 36 cm) the photolithographic reproduction of the *Saggi di Naturali Esperienze* (taken from the *editio princeps*) as well as the presentation written by Dr. Maria Luisa Bonelli of the instruments and fittings of the Accademia which are kept in the above mentioned Museum.

The Volume, in laid paper similar to the original one, has been printed in a limited number of copies and is on sale both at the Domus Galilæana (Via S. Maria, 18, Pisa) and at the Museo di Storia della Scienza (Piazza dei Giudici, 1, Florence) at the price of Lit. 14.000 for the bound edition and at Lit. 12.000 for the paper cover edition.

$$(7) \quad \text{if } k_N + k_0 < K < +\infty \quad \text{Im } f(K) = 0.$$

When the energy of the incident particle is very low, one can make an expansion in $(k_N - k_0)$. Keeping the lowest order term, one obtains:

$$(8) \quad \lim_{k_N \rightarrow k_0} \text{Im } \mathcal{O}^{(2)}(D) = \frac{M}{(2\pi)^3} (k_N - k_0)^2 k_0 \frac{\text{Tr } \mathcal{O}^2}{16} \int_0^{2k_0} J^2(K) dK,$$

This expression is the same as the one given by CINI and FUBINI, except for terms of higher order in $(k_N - k_0)$ which should be left out in a consistent expansion. Out of the validity range of this very simple expression, which is unfortunately rather small, the complete expression (6) has to be used.

The exchange part of the second order term is most conveniently calculated by going to the relative co-ordinates:

$$(9) \quad \begin{cases} 2\mathbf{p} = \mathbf{k}_N - \mathbf{k} , \\ 2\mathbf{q} = \mathbf{k}'_N - \mathbf{k}' . \end{cases}$$

Expressed in these new variables, the exchange term analogous to (5) is:

$$(10) \quad \mathcal{O}^{(2)}(E) = \frac{M}{(2\pi)^6} \frac{\text{Tr } \mathcal{O}^2 P_\sigma P_\tau}{16} \int d^3\mathbf{p} d^3\mathbf{q} \frac{J(|\mathbf{p} - \mathbf{q}|) J(|\mathbf{p} + \mathbf{q}|)}{q^2 - p^2 - i\epsilon}.$$

The integration domain (Fig. 1) is such that the Pauli principle is obeyed in the intermediate state. The imaginary part of $\mathcal{O}^{(2)}(E)$ is, in this way, easily reduced to a single integral which has been computed numerically ⁽⁹⁾. Since we are going to show in the next section that the imaginary part of the potential as calculated here agrees best with experiment when $\text{Tr } \mathcal{O}^2 P_\sigma P_\tau = 0$, we do not need to go into the trouble of calculating $\text{Re } \mathcal{O}^{(2)}(E)$. This exchange term could be in principle reduced to a single integral, but this would imply a lengthy calculation.

The traces entering into $\mathcal{O}^{(1)}$ and $\mathcal{O}^{(2)}$ can be easily performed ⁽¹⁰⁾. If one puts $\lambda = (9p_3 + p_1)/16$ and $\mu = (9p_3^2 + p_1^2)/16$, it is seen that the two traces

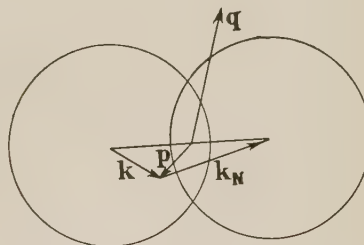


Fig. 1. – Integration domain for Eq. (10). \mathbf{q} is to be kept outside the two spheres, \mathbf{p} is integrated inside the left sphere.

⁽¹⁰⁾ L. ROSENFELD: *Nuclear Forces* (Amsterdam, 1948).

appearing in $\mathcal{O}^{(1)}$

$$(11) \quad \begin{cases} \text{Tr } \mathcal{O} & = -3(1+q) - 16\lambda \\ \text{Tr } \mathcal{O} P_\sigma P_\tau & = 3(1+q) - 16\lambda \end{cases}$$

imply only the parameter λ , when the two traces coming from $\mathcal{O}^{(2)}$

$$(12) \quad \begin{cases} \text{Tr } \mathcal{O}^2 & = 3(1+q^2) + 16\mu \\ \text{Tr } \mathcal{O}^2 P_\sigma P_\tau & = -3(1+q^2) + 16\mu \end{cases}$$

can be expressed as a function of μ only.

We shall fit μ from the comparison of the imaginary part of the potential with experiment; the real part will then be a function of λ only, which will be determined by a comparison with experiment.

3. – Numerical results and discussion.

For the numerical calculations, we have chosen $k_0 = 1.12 \cdot 10^{13} \text{ cm}^{-1}$ (which corresponds to $r_0 = 1.27 \cdot 10^{-13} \text{ cm}$, a compromise between the radii of the

nuclear matter and of the nuclear potential) and a gap of 10 MeV between the top of the Fermi gas and the outside. The zero order well is thus 40 MeV deep. In Fig. 2 we have plotted $\text{Im } \mathcal{O}^{(2)}$ for $\mu = 0.267$, that is for $\text{Tr } \mathcal{O}^2 P_\sigma P_\tau = 0$ (curve 1); and also for $\mu = 0.07$, a value which corresponds roughly to the Serber mixture (curve 2). One sees that curve 1 ($\mu = 0.267$) fits unexpectedly well the experimental results. The low energy results may as well be fitted with lower values of μ . This is due to the near equality of the direct and the exchange term

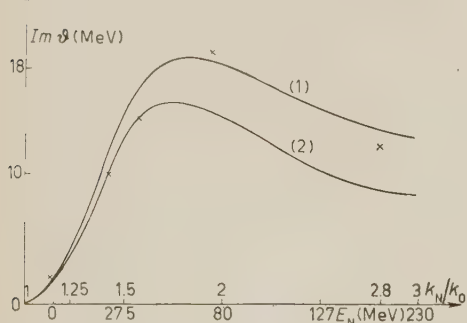


Fig. 2. – Imaginary part of the potential as given by Eqs. (6) and (10). The experimental points (crosses) are taken from ref. (3). Curve 1: $\mu = 0.267$; curve 2: $\mu = 0.07$.

when k_y is near k_0 . As is well known, the Pauli principle is essential in this type of calculation: it cuts out more and more the intermediate states when the incident energy is decreasing so as to bring the imaginary potential to zero when k_y tends to zero.

In Fig. 3 we have plotted the real part of the potential for $\mu = 0.267$ and $\lambda = -0.21$ (curve 1). It is seen that the theoretical curve fits fairly well the experimental points (3). Some other analyses of the experiments (11) give lower values for the real potential. According to these, the real potential should go to zero for a neutron energy of 270 MeV. We can also fit these results by modifying λ (curve 2 where $\lambda = -0.31$).

We could think of testing the convergence of the method by computing the ratio $\text{Re } \mathcal{V}^{(2)}/\mathcal{V}^{(1)}$, which is, for $\mu = 0.267$, $\lambda = -0.21$, $k_N = k_0$, equal to 0.35. But such a ratio is probably misleading because, as is well known, the exchange properties of the interaction make $\mathcal{V}^{(1)}$ artificially small, and because the higher order terms of the perturbation series may have a quite different structure than the two first ones (12).

A better indication of the validity of the Born approximation in nuclear matter is provided by the smallness of the configuration mixing calculated up to the second approximation. The state considered in zero order approximation, namely the antisymmetrized product of the nuclear wave function in its ground state and the wave function of the neutron is mixed into other states by the residual interaction (13). Let us call N the probability that, due to the residual interaction, the system is not in the zero order state, and expand N as an ascending series in the residual interaction. The zero order potential can always be defined so that the diagonal term of the residual interaction is zero. Then the first non-vanishing term is $N^{(2)}$. It is easily seen that it is equal to the second order part of the real potential, and by using (5) and (6), that:

$$(13) \quad N^{(2)} = -2M \frac{\partial}{\partial k_N^2} \text{Re } \mathcal{V}^{(2)}.$$

$N^{(2)}$, for $\mu = 0.267$ and $k_N = k_0$, is equal to 0.11 and it is decreasing with energy. The role of the Pauli principle is essential to obtain such a small

(11) J. A. DE JUREN: *Phys. Rev.*, **80**, 27 (1950); S. FERNBACH, W. HECKROTTE and J. V. LEPORE: *Phys. Rev.*, **97**, 1059 (1955); A. KIND: *Nuovo Cimento*, **1**, 318 (1957).

(12) N. M. HUGGENHOLTZ: *Physica*, **23**, 543 (1957).

(13) We define the residual interaction as the sum of the interactions between the incident nucleon and the incident nucleus minus the zero order potential.

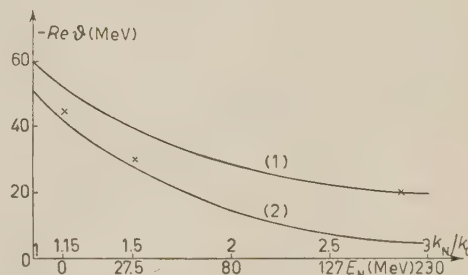


Fig. 3. — Real part of the potential as given by Eqs. (3) and (6). The experimental data (crosses) are given by ref. (3). Curve 1: $\mu = 0.267$, $\lambda = -0.21$; curve 2: $\mu = 0.267$, $\lambda = -0.31$.

value of $N^{(2)}$. When the Pauli principle is neglected, $N^{(2)}$ is multiplied by 14 for $k_n = k_0$, and the approximation scheme breaks down completely.

Another quantity, the binding energy, is a characteristic of the nuclear matter. We have calculated its value by using, like other authors (14) have recently done, the old EULER (15) calculations which include the two first orders in the interaction. We find, with our value of the nuclear radius which is held fixed, a binding energy for nuclear matter of — 13.5 MeV for $\lambda = -0.21$ and of — 9.5 MeV for $\lambda = -0.31$ (we have, as above, taken $\mu = 0.267$). These values should be compared with the «experimental» value (16) which is of — 16 MeV.

Finally, we wish to point out that our fits are quite sensitive to the precise form of the two-body potential that we have used. The various fits (low energy two-body data, complex potential, binding energy of nuclear matter) do not turn at all as good when a Yukawa potential is used (9).

I am indebted to Dr. B. JANCOVICI for numerous discussions.

(14) C. DE DOMINICIS and P. MARTIN: *Phys. Rev.*, **105**, 1417 (1957), and ref. (5).

(15) H. EULER: *Zeits. Phys.*, **105**, 553 (1937).

(16) A. E. S. GREEN: *Phys. Rev.*, **95**, 1006 (1954).

RIASSUNTO (*)

Con un caleolo delle perturbazioni fino al secondo ordine si calcola il potenziale complesso per i neutroni in un mezzo nucleare infinito, assumendo per l'interazione nucleone-nucleone un potenziale regolare soddisfacente i dati dell'interazione a bassa energia fra due corpi. Si dimostra che è possibile soddisfare contemporaneamente le parti reale e immaginaria del potenziale ottico e l'energia di legame della materia nucleare di densità normale. Si danno alcuni argomenti a favore della convergenza della teoria.

(*) Traduzione a cura della Redazione.

Analytical Theory of the Behaviour of Ferromagnetic Materials.

G. BIORCI and D. PESCETTI (*)

*Istituto Elettrotecnico Nazionale « Galileo Ferraris » - Torino
Centro Studi per l'Elettrofisica del C.N.R.*

(ricevuto il 23 Novembre 1957)

Summary. — It is shown that every transformation in the J - H plane of a ferromagnetic specimen can be computed from the magnetization curve and saturation loop of the material. This is based on the assumption that each volume element is characterized by a rectangular loop of sides a and b (Preisach model). Also, it must be assumed that a distribution function $\varphi(a, b)$, related to the probability density of finding a loop with given (a, b) , exists and is unique. Then, given an arbitrary path of H , $\varphi(a, b)$ permits the computation of the corresponding path of J . The function $\varphi(a, b)$ can be computed numerically by manipulation of the magnetization curve and saturation loop. Experiments have been carried out on two materials, magnetically quite different. The theoretical curves fit the experimental data quite well.

1. - Introduction.

The theoretical prediction of the properties ⁽¹⁾ of a ferromagnetic material is impossible to-day; and also in principle so complicated as to verge on the absurd. In fact one should know not only the crystallographic structure of the material, but also the form and orientation of each grain, the distribution of impurities, and so on. In addition, one should compute the initial domain configuration, for instance, after cooling through the Curie point. But experimental observations show that such configuration is not determined uniquely.

(*) Present address of D.P.: I.T.I. Amedeo Avogadro, Torino.

⁽¹⁾ With the term « properties » of a ferromagnetic material we mean here the ensemble of all the possible transformations in the $(J \cdot H)$ plane, which the material can undergo.

In fact it is different even for the same cooling process at different times. Therefore, it seems that even an excellent knowledge of the properties of each point in the specimen, would not determine uniquely the initial domain configuration, and therefore the magnetic behavior.

On the other hand it is well known that the experimental curves of a given specimen can be repeated to within a few percent, even starting from initial configurations completely different. Also, two specimens, made from the same raw materials, and identically treated, have magnetization curves and loops quite similar, even if their structures, point by point, are extremely different. This means that the average behavior of the material, although influenced by several infinite sets of parameters, does not vary much with the variation of a large number of these parameters (for instance the initial domain configurations in the case of several measurements on the same specimen, or the spacial distribution of grains in the case of two specimens macroscopically identical). The problem of foreseeing the magnetic behavior of the material by an extremely precise description of its structure therefore appears hopeless. It is reasonable to ask, instead, whether the magnetic behavior is deducible from a few macroscopic magnetic experiments on the material itself.

In this paper ⁽²⁾ we indicate a procedure to obtain this result. The basic experiments are the measuring of the magnetization curve and the saturation loop. From the knowledge of these, a function $\varphi(a, b)$ is obtained, from which every magnetization path ⁽³⁾ can be deduced. As shown in the following, this procedure is a generalization of the representation of hysteresis due to PREISACH ⁽⁴⁾ with the formalism introduced by NÉEL ⁽⁵⁾.

2. - General considerations.

Let us divide the volume of the material into infinitesimal parts, by means of a cubic lattice. Then let us assume that each volume element be magnetically characterized by a rectangular loop of sides a and b ; the sides parallel to the H -axis being $+J$ and $-J$. That is, the loop is symmetrical with respect to the H -axis, but of arbitrary height (Fig. 1a). Two different volume elements, taken at random, have in general different loops, in particular dif-

⁽²⁾ Previous notice of this research has been given in *Nuovo Cimento*, **6**, 242 (1957).

⁽³⁾ The problem of deducing the form of hysteresis loops, or at least of their analytical expression has been widely studied, but with little success: See for instance: C. MACMILLAN: *Gen. El. Rev.*, **39**, 225 (1936); I. KUNZ: *Phys. Zeits.*, **13**, 591 (1912); M. S. PROCOPIN: *Compt. Rend.*, **228**, 457 (1949).

⁽⁴⁾ F. PREISACH: *Zeits. f. Phys.*, **94**, 277 (1935). See also BECKER und DÖRING: *Ferromagnetismus* (1939), p. 221.

⁽⁵⁾ L. NÉEL: *Cahier de Physique*, No. 12 (1942).

ferent values for a and b . The ensemble of all the couples of values (a, b) which correspond to the loops existing in some volume elements, cover a surface in the (a, b) plane, Fig. 1b. It is evident that only the half plane where $a > b$ contains real loops, since the energy associated with a loop must be lost.

It has been shown (5) that, when the specimen is demagnetized in an a-c decreasing field, the volume elements go to positive magnetization if their representative points fall between OA and OB , and to negative magnetization if their points fall between OB and OC (Fig. 1b). If, starting from this condition, a field strength $H > 0$ is applied to the specimen, all the volume elements negatively magnetized which have $a \leq H$ turn to positive magnetization, whereas all the others remain in the previous condition (Fig. 2a). Now, if the field strength is reduced from H to H_1 , all the volume elements

positively magnetized which have $b \geq H_1$, turn to negative magnetization (Fig. 2b).

Then we can recognize that every arbitrary path of H is reducible to a sequence of variations ΔH , each having the opposite sign of the preceding. In fact, two variations in the same sense produce the same effect as a single variation, having intensity equal to the sum of the two variations. Now it is easily understood that the sequence of ΔH 's defines a surface S , which con-

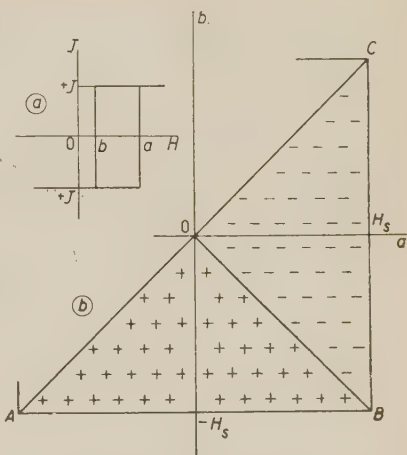


Fig. 1. - a) The elemental loop;
b) Preisach plane.

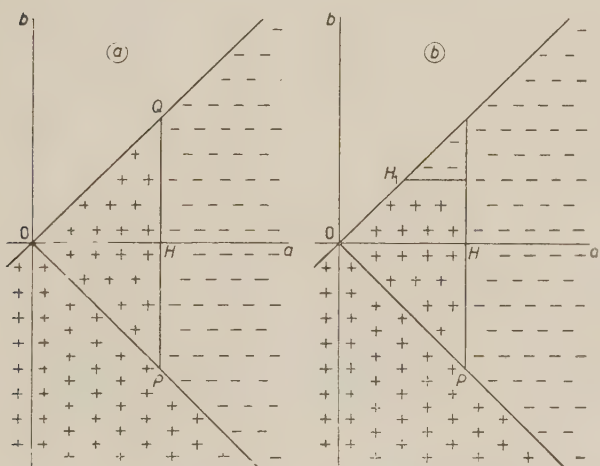


Fig. 2. - a) Representation of hysteresis along the magnetization curve. b) Representation of hysteresis along the path: from $h = 0$ to $h = H$; from $h = H$ to $h = H_1$ ($H_1 < H$).

contains all the points representative of volume elements which have undergone an odd number of magnetization inversions. If the statistical weight of

each loop were known, the magnetization intensity would be derivable from the knowledge of S . The function $\varphi(a, b)$, which will be defined in the next paragraph, is actually related to the statistical weight of the elemental loop.

Before going into the detailed theory we can observe that the described model reduces to the original representation given by PREISACH (4) under the assumption that each elemental loop extends from $-J_s$ to J_s , being J_s the saturation magnetization.

NÉEL (5), LLIBUTRY (6) *et al.* used Preisach model for the study of magnetic phenomena at low field strength (Rayleigh region). In that region one can assume that the number of volume elements, having given values of (a, b) , is independent of a and b . This case falls in the present theory assuming that $\varphi(a, b) = \text{const.}$ in a region close to the origin.

3. - The distribution function $\varphi(a, b)$.

Let us consider a small area $\delta a \cdot \delta b$ in the (a, b) plane (Fig. 3). Starting from the condition of material demagnetized by a decreasing a-c field, let the field strength H describe the following path:

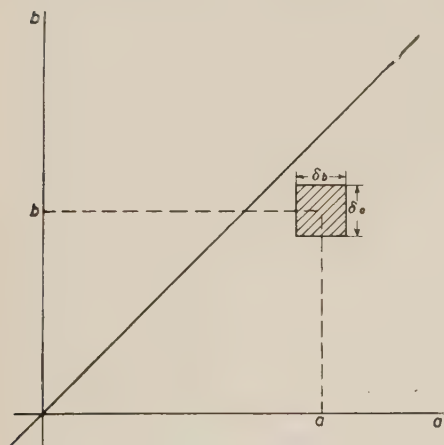


Fig. 3. - Definition of $\varphi(a, b)$.

- 1) from zero to $\left(a + \frac{\delta a}{2}\right)$;
- 2) from $\left(a + \frac{\delta a}{2}\right)$ to $\left(b + \frac{\delta b}{2}\right)$
($b < a$);
- 3) from $\left(b + \frac{\delta b}{2}\right)$ to $\left(b - \frac{\delta b}{2}\right)$;
- 4) from $\left(b - \frac{\delta b}{2}\right)$ to $\left(a - \frac{\delta a}{2}\right)$;
- 5) from $\left(a - \frac{\delta a}{2}\right)$ to $\left(b - \frac{\delta b}{2}\right)$.

If we consider the surfaces S_i corresponding to the various steps of the path of H , we observe that:

$$(1) \quad S_5 - S_2 = \delta a \cdot \delta b,$$

where the subscript of S indicates how many steps of H a given S accounts

(6) L. LLIBUTRY: *Thèses* 17, Univ. de Grenoble (1950).

for. The intensities of magnetization after the fifth step and after the second differ by a small amount δJ , going to zero when the area $\delta a \cdot \delta b$ goes to zero. Then we can define a function $\varphi(a, b)$ such that

$$(2) \quad \delta J = J_s \cdot \varphi(a, b) \cdot \delta a \cdot \delta b .$$

From this definition it follows that the intensity of magnetization at the end of a given path of H , is

$$(3) \quad J = 2J_s \int_S \varphi(a, b) da db ,$$

where S is the surface corresponding to that path of H , that is the surface which contains all the points (a, b) representing volume elements which have undergone an odd number of inversions, during the sequence of the ΔH 's.

Not all of the half plane where $a \geq b$ is interesting, but only the triangle ABC (Fig. 1) limited by

$$a = H_s ,$$

$$b = H_s ,$$

H_s being the field strength corresponding to saturation magnetization ⁽⁷⁾. In fact, $\varphi(a, b)$ is zero everywhere outside ABC .

When the material is brought to saturation, all the volume elements have positive magnetization. Hence, from eq. (3) we have easily:

$$(4) \quad \int_{OBC} \varphi(a, b) da db = \frac{1}{2} .$$

The function $\varphi(a, b)$ is positive (or zero) in all point of ABC . This property follows from the definition itself. Furthermore, since the great majority of the ferro-magnetic materials behave in the same way if all variations of H are changed in sign (an exception has been discovered recently ⁽⁸⁾), we can easily find that

$$(5) \quad \varphi(a, b) = \varphi(-b, -a) ,$$

that is $\varphi(a, b)$ is symmetric with respect to the line OB (Fig. 1).

⁽⁷⁾ In other words, an arbitrary increase of field strength above H_s produces a negligible increase in intensity of magnetization.

⁽⁸⁾ W. H. MEIKLEJOHN and C. P. BEAN: *Phys. Rev.*, **105**, 904 (1957).

4. - Meaning of $\varphi(a, b)$.

The knowledge of the function $\varphi(a, b)$ is sufficient to determine the macroscopic behavior of the material. More specifically, for every path of H , the intensity of magnetization at the end of that path can be computed. In fact, at first the path of H can be expressed as a sequence of ΔH 's, each ΔH having a sign opposite to that of the preceding one. Then the sequence of ΔH 's is transformed into a sequence of displacements along a (for $\Delta H > 0$) or along b (for $\Delta H < 0$). The displacements define the surface S . Finally, eq. (3) determines J .

If all the elemental loops extended from $-J_s$ to J_s , the function $\varphi(a, b)$, apart from a factor 2, would be the statistical weight mentioned above. In that case one could say that $\varphi(a, b) \cdot da \cdot db$ is the probability of finding an elemental loop having one side falling between a and $(a + da)$, and the other falling between b and $(b + db)$; or that $\varphi(a, b) \cdot da \cdot db$ is the fraction of the total volume having elemental loops with these a and b . According to our definition of $\varphi(a, b)$, which does not specify the heights of the elemental loops, those meanings have to be modified, in the sense that here each elemental loop with a given a and b has another statistical weight, which is the ratio between its J and J_s .

From the preceding assumptions it follows that the function $\varphi(a, b)$ exists and is unique, that is, it depends only on the nature and structure of the material. It is worth recalling that the only hypothesis on which the function $\varphi(a, b)$ has been built, and its existence and uniqueness have been deduced, is (Sect. 2) that every infinitesimal part of the volume be characterized by a rectangular loop. Perhaps it is more satisfactory not to locate in given positions the elemental volumes having a given loop. If this is done, the theory remains valid, but the existence and uniqueness of the function $\varphi(a, b)$ has to be assumed as a postulate.

5. - Determination of $\varphi(a, b)$. General considerations.

Once we have assumed that $\varphi(a, b)$ exists and is unique, the problem is to determine $\varphi(a, b)$ by simple experiments which, as mentioned before, must be sufficiently general to allow the deduction of as many transformations as possible in the (J, H) plane. At this point we can specify that these experiments must cover the whole field of definition of $\varphi(a, b)$, that is, the field strength must range from H_s to H_s . Therefore, the fundamental experiments to determine $\varphi(a, b)$ are the measuring of the magnetization curve, and the saturation loop, that is, the loop having the positive vertex at (H_s, J_s) .

Along the magnetization curve, the field strength is increasing. Hence the independent variable is a (equal to H). As it was explained before, when the field strength is a , the surface S is (Fig. 2a):

$$S = OPQ.$$

Then the intensity of magnetization, considered as a function of a is:

$$J(a) = 2J_s \int_{OPQ} \varphi(a, b) da db$$

or, since the lines OP and OQ have equation $b = a$ and $b = -a$ respectively,

$$(6) \quad \frac{J(a)}{2J_s} = \int_0^a da \int_{b=-a}^{a=b} \varphi(a, b) db.$$

If we put

$$(7) \quad f(a) = \frac{d}{da} \left[\frac{J(a)}{2J_s} \right]$$

and differentiate eq. (6) with respect to a , we have

$$(8) \quad f(a) = \int_{-a}^a \varphi(a, b) db.$$

That is, the intensity of magnetization due to an infinitesimal increase of field da along the magnetization curve is proportional to the integral of $\varphi(a, b)$ on the infinitesimal strip parallel to the b -axis.

In the preceding, we have tacitly assumed that the field has positive sign. For the mentioned symmetry of the magnetic curves with respect to the sign of the field strength, we can conceive an expression entirely similar to eq. (8), if a magnetization curve with negative field strength is considered. Therefore we have also

$$(9) \quad f(b) = \int_{-b}^b \varphi(a, b) da.$$

Let us consider now the saturation loop, and define J' as the difference

between J_s and J (Fig. 4a). In this experiment the field strength is decreasing: hence the variable is b (Fig. 4b). With the same procedure used above we have

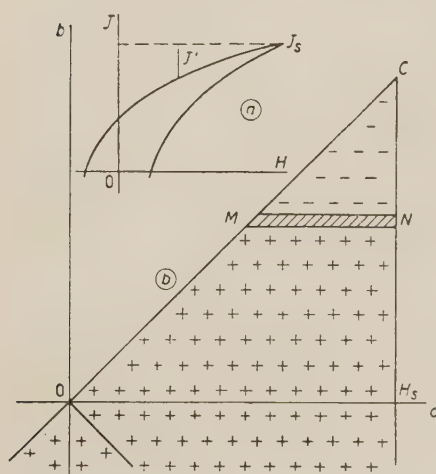


Fig. 4. - a) Definition of J' . b) Representation of the saturation loop in the Preisach plane.

experimental data. If the set (8), (11) could be solved for $\varphi(a, b)$, the latter would be known in all points of OBC , and therefore in the whole field of definition ABC , for reasons of symmetry. However, it is intuitive that in general equations (8), (11) do not uniquely determine $\varphi(a, b)$. But, if we assume that separation of variables is possible for $\varphi(a, b)$, i.e.

$$(12) \quad \varphi(a, b) = \varphi_1(a) \cdot \varphi_2(b),$$

the set of integral equations can be solved uniquely.

If the interpretation of $\varphi(a, b)$ as probability density is recalled, hypothesis (12) can be, in general, justified. In fact eq. (12) says that the probability that an elemental loop has the a -side falling in a given da and the b -side in a given db is equal to the product of the probabilities of the two events. This means that in an infinitesimal volume of the material, the event that the a -side is in a given da is independent of the event that b -side is in a given db . This statement seems plausible, and is consistent with the theories of irreversible magnetization processes (5).

6. - Numerical determination of $\varphi(a, b)$.

Let us divide the triangle OBC in small squares of side H_s/N . If N is sufficiently large, $\varphi(a, b)$ can be considered a constant in each square. Equa-

$$(10) \quad J'(b) = 2J_s \int_{CMN} \varphi(a, b) da db,$$

which leads to

$$(11) \quad g(b) = - \int_{|b|}^{H_s} \varphi(a, b) da,$$

where

$$g(b) = \frac{d}{db} \left[\frac{J'(b)}{2J_s} \right] \quad \text{for } b \geq 0,$$

$$g(b) = \frac{d}{db} \left[\frac{J'(b)}{2J_s} \right] - f(b) \quad \text{for } b < 0.$$

Equations (8) and (11) form a set of two integral equations for $\varphi(a, b)$, the functions $f(a)$ and $g(b)$ being known from

tion (12) being supposed to be valid, $\varphi_1(a)$ is defined by N values, and $\varphi_2(b)$ by $2N$ values. Now equation (8) gives rise to N relationships, and eq. (11) to $2N$ relationships. Hence, we have $3N$ equations and $3N$ unknowns, which can be determined uniquely. Actually the $3N$ equations are not independent: in fact $\sum_i f(a_i)$ is equal to $\sum_i g(b_i)$, since both sums are equal to the integral of $\varphi(a, b)$ over the whole triangle. Therefore the $2N$ unknowns can be determined as functions of one of them, for instance $\varphi_1(a_N)$, which remains arbitrary.

It turns out that the solutions take the form:

$$(13) \quad \varphi_1(a_i) = k_i \varphi_1(a_N); \quad \varphi_2(b_i) = h_i / \varphi_1(a_N).$$

Hence the values $\varphi(a_i, b_j) = \varphi_1(a_i) \cdot \varphi_2(b_j)$ are unambiguously determined (N being any finite number).

The detailed calculation of the coefficients k_i and h_i is given in the Appendix.

7. - Results.

Following the indicated procedure and taking $N = 30$, the functions $\varphi(a, b)$ has been deduced for two materials, magnetically quite different, i.e. having very different ratio J_s/J_r . The functions $\varphi(a, b)$ have been determined from the magnetization curve and the loop having maximum induction of 1.5 Wb/m^2 (15 000 G). From the knowledge of the $\varphi(a, b)$'s we have computed symmetrical loops with maximum induction of the order of 0.5 Wb/m^2 and 1.0 Wb/m^2 . For one of the specimens the curve of residual induction of symmetrical loops vs. their maximum field strength has been computed. Fig. 5

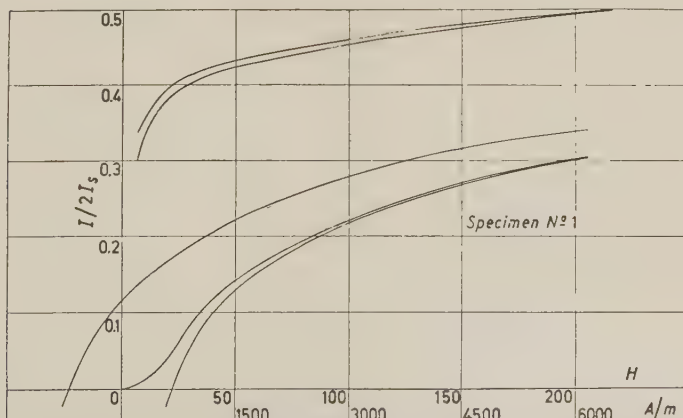


Fig. 5. - Specimen No. 1 (3.5% Si-Fe alloy). Magnetization curve and saturation loop.

and 6 show the magnetization curves and the 1.5 Wb/m^2 loops of the two specimens. Specimen No. 1 is a 3% Si-Fe alloy; specimen No. 2 is commercial

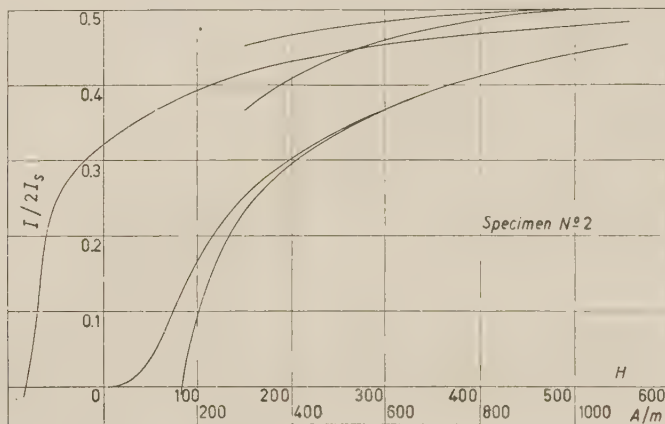


Fig. 6. – Specimen No. 2 (commercial iron). Magnetization curve and saturation loop.

iron. Fig. 7 and 8 show the computed and measured curves. The agreement is very satisfactory, and in many places the curves coincide within the limits of experimental error.

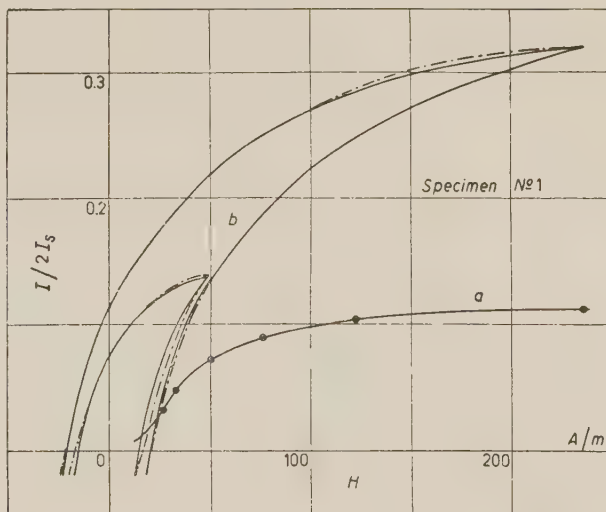


Fig. 7. – Specimen No. 1. Computed (broken line) and measured (solid line) loops. Curve a : residual induction of symmetrical loops vs. their max. field strength (solid line: theoretical curve; solid points: experimental observation). Curves b : symmetrical loops (broken line: theoretical curve; solid lines: experimental observations).

The numerical solution could be refined by considering that the squares falling on the straight lines OB and OC should actually be triangles. We have deduced the solutions for this better approximation and found that the correction is appreciable only if N is of the order of 10.

8. - Conclusion.

It has been shown that from the knowledge of the magnetization curve and saturation loop of a given material, it is possible to deduce the distribution function $\varphi(a, b)$, which in turn permits the calculation of the intensity of magnetization along an arbitrary static path of H (°). The agreement with experimental data, taken on two materials magnetically very different, is satisfactory.

This representation of magnetic hysteresis is based on the fundamental hypothesis which states that the macroscopic behavior of the material can be reduced to a conveniently chosen sum of an infinite number of rectangular loops. No assumption is necessary on the heights of the loops, nor on the distribution of their sides. Therefore we are inclined to believe that the fundamental hypothesis is nothing but a mathematical tool to deal with static hysteresis, having no connection with the nature of the phenomena giving rise to the hysteresis itself. Naturally, to carry the method to its final conclusions, it is necessary to introduce the hypothesis of uniqueness of $\varphi(a, b)$, which has physical meaning, and hypothesis (12).

It seems useful to say a few more words about the fundamental hypothesis. A first remark is that time does not appear in this representation. Therefore all time-dependent magnetic effects cannot be treated by this method, unless other hypotheses are introduced, such as the equivalence of a given effect to a fictitious magnetic field. Furthermore, since the elemental loop is a typically irreversible process, reversible phenomena cannot, in general, be represented by this model. However, if the elemental loops having $a = b$ are

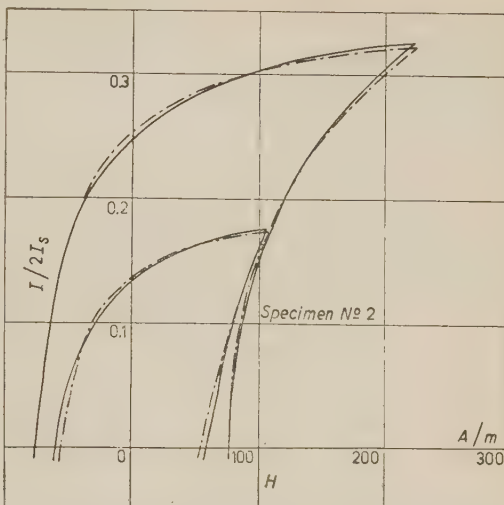


Fig. 8. - Specimen No. 2. Computed (broken lines) and measured (solid lines) loops.

(°) At the T.H. of Stuttgart, Germany, where similar research is being done, they assume that $\varphi(a, b)$ has a simple mathematical expression. See R. FELDTKELLER and H. WILDE: *ETZ-A*, **1**, 7 (1956), p. 499.

considered, reversible processes could be included in the model, but in a somewhat inconvenient form. For instance, it could be shown that in the Rayleigh region $\varphi(a, b)$ is constant at all points where $a \neq b$, and becomes infinite where $a = b$.

* * *

We wish to thank Profs. G. MONTALENTI and R. SARTORI for helpful discussions.

APPENDIX

Numerical determination of $\varphi_1(a)$ and $\varphi_2(b)$.

To treat the numerical solution in the most general way, let us draw a set of vertical straight lines, at arbitrary distances $\alpha_1, \alpha_2, \dots, \alpha_N$ from 0 to H_s .

Then let us draw a set of horizontal straight lines crossing the vertical lines on points falling on OC and OB (Fig. 9). Let us call (a_i, b_j) the co-ordinates of the centre of a rectangle. Finally let us put:

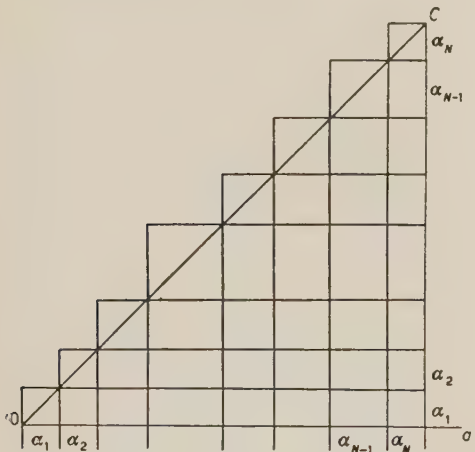


Fig. 9. - Numerical determination of $\varphi(a, b)$.

$$F_i = \frac{1}{2J} \int_{a_{i-1}}^{a_i} f(a) da ;$$

$$G_j = \frac{1}{2J} \int_{b_{j-1}}^{b_j} g(b) db .$$

Eq. (8) gives the following set of equations:

$$F_1 = \alpha_1 \cdot \varphi_1(a_1) \cdot [\alpha_1 \cdot \varphi_2(b_N) + \alpha_1 \cdot \varphi_2(b_{N+1})] ,$$

$$F_2 = \alpha_2 \cdot \varphi_1(a_2) \cdot [\alpha_2 \cdot \varphi_2(b_{N-1}) + \alpha_1 \cdot \varphi_2(b_N) + \alpha_1 \cdot \varphi_2(b_{N+1}) + \alpha_2 \cdot \varphi_2(b_{N+2})] ,$$

$$\dots$$

$$F_N = \alpha_N \cdot \varphi_1(a_N) \cdot [\alpha_N \cdot \varphi_2(b_1) + \alpha_{N-1} \cdot \varphi_2(b_2) + \dots + \alpha_1 \cdot \varphi_2(b_N) + \alpha_1 \cdot \varphi_2(b_{N+1}) + \dots + \alpha_{N-1} \cdot \varphi_2(b_{N-1}) + \alpha_N \cdot \varphi_2(b_{N+1})] .$$

Similarly, eq. (11) gives rise to the following set:

$$\begin{aligned}
 G_1 &= \alpha_N \cdot \varphi_2(b_1) \cdot \alpha_N \cdot \varphi_1(a_N), \\
 G_2 &= \alpha_{N-1} \cdot \varphi_2(b_2) \cdot [\alpha_N \cdot \varphi_1(a_N) + \alpha_{N-1} \cdot \varphi_1(a_{N-1})], \\
 &\dots \dots \dots \\
 &\vdots \\
 G_N &= \alpha_1 \cdot \varphi_2(b_N) \cdot [\alpha_N \cdot \varphi_1(a_N) + \alpha_{N-1} \cdot \varphi_1(a_{N-1}) + \dots + \alpha_1 \cdot \varphi_1(a_1)], \\
 G_{N+1} &= \alpha_1 \cdot \varphi_2(b_{N+1}) \cdot [\alpha_N \cdot \varphi_1(a_N) + \alpha_{N-1} \cdot \varphi_1(a_{N-1}) + \dots + \alpha_1 \cdot \varphi_1(a_1)], \\
 &\dots \dots \dots \\
 &\vdots \\
 G_{2N-1} &= \alpha_{N-1} \cdot \varphi_2(b_{2N-1}) \cdot [\alpha_N \cdot \varphi_1(a_N) + \alpha_{N-1} \cdot \varphi_1(a_{N-1})], \\
 G_{2N} &= \alpha_N \cdot \varphi_2(b_{2N}) \cdot \alpha_N \cdot \varphi_1(a_N).
 \end{aligned}$$

Among the $3N$ equations we have the relationship $\sum F_i = \sum G_i$. A simple look at the equations shows that the α_i 's can be associated with the $\varphi_1(a_i)$'s or $\varphi_2(b_i)$'s. For instance $\varphi_1(a_1)$ appears multiplied by α_1 everywhere, and so on. Therefore, if we put

$$\begin{aligned}
 \psi_1(a_i) &= \alpha_i \cdot \varphi_1(a_i), \\
 \psi_2(b_i) &= \alpha_{N+1-i} \cdot \varphi_2(b_i) \quad [1 \leq i \leq N], \\
 \psi_2(b_i) &= \alpha_{i-N} \cdot \varphi_2(b_i) \quad (N+1 < i \leq 2N),
 \end{aligned}$$

the set of equations becomes:

$$\begin{aligned}
 F_1 &= \psi_1(a_1) \cdot [\psi_2(b_N) + \psi_2(b_{N+1})], \\
 F_2 &= \psi_1(a_2) \cdot [\psi_2(b_{N-1}) + \psi_2(b_N) + \psi_2(b_{N+1}) + \psi_2(b_{N+2})], \\
 &\dots \dots \dots \\
 &\vdots \\
 F_N &= \psi_1(a_N) \cdot [\psi_2(b_1) + \psi_2(b_2) + \dots + \psi_2(b_{2N})], \\
 G_1 &= \psi_2(b_1) \cdot \psi_1(a_N), \\
 G_2 &= \psi_2(b_2) \cdot [\psi_1(a_N) + \psi_1(a_{N-1})], \\
 &\dots \dots \dots \\
 &\vdots \\
 G_N &= \psi_2(b_N) \cdot [\psi_1(a_N) + \psi_1(a_{N-1}) + \dots + \psi_1(a_1)], \\
 G_{N+1} &= \psi_2(b_{N+1}) \cdot [\psi_1(a_N) + \psi_1(a_{N-1}) + \dots + \psi_1(a_1)], \\
 &\dots \dots \dots \\
 &\vdots \\
 G_{2N-1} &= \psi_1(b_{2N-1}) \cdot [\psi_1(a_N) + \psi_1(a_{N-1})], \\
 G_{2N} &= \psi_2(b_{2N}) \cdot \psi_1(a_N).
 \end{aligned}$$

If we take $\psi_1(a_N)$ as the arbitrary unknown, the solutions are:

$$(14) \quad \left\{ \begin{array}{l} \psi_1(a_i) = \frac{G_{N-i} \cdot F_i}{P_{N-i}} \frac{1}{\psi_2(b_{N-i})} \cdot \psi_1(a_N) \quad [i = 1, 2, \dots, N-1], \\ \psi_2(b_i) = \frac{G_i \cdot F_{N+1-i}}{Q_{i-1}} \frac{1}{\psi_1(a_{N+1-i})} \quad [i = 1, 2, \dots, N], \\ \psi_2(b_i) = \frac{G_i}{G_{2N+1-i}} \cdot \psi_2(b_{2N+1-i}) \quad [i = N+1, N+2, \dots, 2N], \end{array} \right.$$

where

$$P_i = \sum_{k=1}^{2N-i} G_k - \sum_1^{N-i} F_k \quad [i = 1, 2, \dots, N-1],$$

$$Q_i = P_i + F_{N-i} \quad [i = 0, 1, 2, \dots, N-1],$$

Equations (14) permit the determination of the ψ_1 's and ψ_2 's one after the other. That is, first we take a value for $\psi_1(a_N)$ (for instance 1), then we determine $\psi_2(b_1)$, then $\psi_1(a_{N-1})$, etc. Of course it is possible, but less convenient for actual numerical computation, to express the ψ_1 's and ψ_2 's directly as functions of the known quantities. These expressions are:

$$\psi_1(a_i) = \psi_1(a_N) \cdot \frac{F_i}{P_{N-i}} \cdot \prod_{k=1}^{k=N-1-i} \frac{Q_k}{P_k} \quad [i = 1, 2, \dots, N],$$

$$\psi_2(b_i) = \frac{1}{\psi_1(a_N)} \cdot G_i \prod_{k=1}^{k=i-1} \frac{P_k}{Q_k} \quad [i = 1, 2, \dots, N],$$

$$\psi_2(b_i) = \frac{1}{\psi_1(a_N)} \cdot G_i \prod_{k=1}^{k=2N-i} \frac{P_k}{Q_k} \quad [i = N+1, N+2, \dots, 2N].$$

RIASSUNTO

Viene mostrato che ogni trasformazione nel piano $J-H$ di un campione ferromagnetico può essere calcolata dalla curva di magnetizzazione e dal ciclo di saturazione del materiale. Questa possibilità si fonda sull'ipotesi che ogni elemento di volume sia caratterizzato da un ciclo rettangolare di lati a e b (modello di Preisach). Si deve inoltre ammettere che esista e sia unica una funzione di distribuzione $\varphi(a, b)$, legata alla probabilità di trovare un ciclo con una certa a e una certa b . Allora, assegnato un qualsiasi percorso di H , $\varphi(a, b)$ consente di calcolare il corrispondente percorso di J . La funzione $\varphi(a, b)$ può essere calcolata numericamente partendo dalla curva di magnetizzazione e dal ciclo di saturazione. Sono state fatte esperienze su due materiali, magneticamente assai diversi. Le curve teoriche sono in buon accordo con quelle sperimentali.

Comments on the Theory of Superconductivity.

J. G. VALATIN

Department of Mathematical Physics - University of Birmingham

(ricevuto il 23 Dicembre 1957)

Summary. — Some ideas of the new theory of Bardeen, Cooper and Schrieffer are expressed in a more transparent form. New collective fermion variables are introduced which are linear combinations of creation and annihilation operators of electrons, and describe elementary excitations. They lead to a simple classification of excited states and a great simplification in the calculations. The structure of the excitation spectrum is investigated without equating the matrix element of the interaction potential to a constant at an early stage, and new relationships and equations are derived. The temperature dependent problem is described by means of a statistical operator, and its relationship to that of the grand canonical ensemble is established. Simple new relationships are obtained for the correlation function.

1. — Introduction.

In a recent paper BARDEEN, COOPER and SCHRIEFFER ⁽¹⁾ have developed a new approach to the theory of superconductivity. Their model assumes a simple attractive two body interaction between the electrons which expresses the effect of the interactions through the phonon field and of screened Coulomb interactions. It gives a good quantitative account of the thermodynamic and electromagnetic properties of superconductors.

The aim of the present paper is to simplify the conceptual background of the new theory and to obtain a clearer insight into the ideas involved. Improved mathematical tools are introduced which are related to simple physical concepts, and some simple new relationships are brought out.

⁽¹⁾ J. BARDEEN, L. N. COOPER and J. R. SCHRIEFFER: *Phys. Rev.*, **108**, 1175 (1957).

The important problem of obtaining the two body forces from the phonon interaction will not be touched here, so that the starting point will be a theory with a Hamiltonian containing two body interactions. It will be pointed out that the trial ground state vector introduced by BARDEEN, COOPER and SCHRIEFFER which expresses long range correlations between particles of opposite spin, is related in a natural way to new collective fermion variables which lead to a simple description of the excited states. The calculations are much simplified by the introduction of the new variables, and it can be hoped that they will be of help also in making further progress in the theory.

The structure of the excitation spectrum will then be investigated by expressing the Hamiltonian in terms of the new variables. The error involved by neglecting a non-diagonal part of the Hamiltonian will not be discussed, but the new expressions obtained also make the mathematical formulation of this problem easier. Various relationships will be established without replacing the matrix element of the interaction by an average value at an early stage. This brings out more clearly those features of the theory which are independent of the assumption of a constant matrix element. Equations are obtained for the investigation of more general interactions.

To describe temperature dependent phenomena, BARDEEN, COOPER and SCHRIEFFER formulate a variational problem with two independent functions to be varied. One describes the elementary excitations; the other, a statistically independent distribution of these excitations. This problem will be expressed here in terms of a statistical operator and it will be pointed out that this can be considered as the trial approximation for the statistical operator of the grand ensemble.

Finally, simple expressions will be obtained for the correlation functions which make the interpretation of the relationships of the theory more transparent.

2. – Collective fermion variables.

The Hamiltonian

$$(1a) \quad H = T + V$$

of the theory is the sum of the Bloch energy

$$(1b) \quad T = E_0 + \sum_{k,\sigma} \varepsilon_k a_{k\sigma} a_{k\sigma}^* ,$$

$$(1c) \quad E_0 = -2 \sum_{k < k_F} \varepsilon_k ,$$

and of a non-local two-body interaction energy

$$(1d) \quad V = \frac{1}{2} \sum_{\substack{k, k', q \\ \sigma, \sigma'}} V_{k k'} a_{k\sigma} a_{q-k, \sigma'} a_{q-k', \sigma'}^* a_{k', \sigma}^*.$$

The energy ε_k of a Bloch electron with momentum k is counted from the Fermi level. The index σ stands for a definite \uparrow or \downarrow spin direction. The index \varkappa will be used to indicate both momentum k and spin σ , whenever this simplifies the notation. In this case, $-\varkappa$ will stand for opposite momentum and opposite spin. Creation operators are denoted by a_{\varkappa} and annihilation operators by a_{\varkappa}^* . (This is in accordance with Dirac's notation ⁽²⁾ and with the geometric interpretation ⁽³⁾ of these operators, unstarred quantities representing the unit vectors and the stars being reserved for the basis elements of the dual vectors). It will be found convenient to write $a_{\varkappa_1} \dots a_{\varkappa_j}$ for the state vector with electrons in the one particle states $\varkappa_1, \dots, \varkappa_j$, replacing by unity the state $|0\rangle$ in which no particles are present.

The trial ground state vector of Bardeen, Cooper and Schrieffer can be written as a product of commuting factors in the form

$$(2a) \quad \Phi_0 = \prod_{\varkappa} \frac{1 + g_{\varkappa} a_{\varkappa} a_{-\varkappa}}{(1 + |g_{\varkappa}|^2)^{\frac{1}{2}}},$$

with

$$(2b) \quad g_{k\uparrow} = g_{-k\uparrow} = g_k = -g_{k\downarrow} = -g_{-k\downarrow}.$$

This corresponds to an indeterminate number of particles, but with a sharp peak in the probability distribution of the particle number for the actual values of g_{\varkappa} . The choice of such a state vector exploits the advantages of the fact that the Hamiltonian (1a, b, d) is valid for any number of particles and the quantum field equations of the problem are independent of the special value of the number operator $N = \sum_{\varkappa} a_{\varkappa} a_{\varkappa}^*$. The projection operator of the state (2a) can be considered as a trial approximation for the statistical operator of the grand ensemble in the limit of temperature $T = 0$.

Separating the state vectors and operators by a stroke, whenever this seems convenient, equations can be written like $a_{\varkappa}^* |a_{\varkappa} a_{\varkappa}| = a_{\varkappa}$, $a_{\varkappa}^* |1 = 0$ or $a_{\varkappa} |1 = a_{\varkappa}$. One obtains the simple relations

$$(2c) \quad a_{\varkappa}^* |(1 + g_{\varkappa} a_{\varkappa} a_{-\varkappa}) = g_{\varkappa} a_{-\varkappa},$$

$$(2d) \quad a_{-\varkappa} |(1 + g_{\varkappa} a_{\varkappa} a_{-\varkappa}) = a_{-\varkappa}.$$

⁽²⁾ P. A. M. DIRAC: *The Principles of Quantum Mechanics*, 3rd ed. (Oxford, 1947), p. 249.

⁽³⁾ J. G. VALATIN: *Journ. Phys.*, **12**, 131 (1951).

Accordingly, it is rather natural to introduce the new variables

$$(3a) \quad \xi_{\kappa}^* = \frac{a_{\kappa}^* - g_{\kappa} a_{-\kappa}}{(1 + |g_{\kappa}|^2)^{\frac{1}{2}}}, \quad \xi_{\kappa} = \frac{a_{\kappa} - g_{\kappa}^* a_{-\kappa}^*}{(1 + |g_{\kappa}|^2)^{\frac{1}{2}}},$$

since from (2a, c, d) one sees immediately that

$$(3b) \quad \xi_{\kappa}^* |\Phi_0 = 0 \quad \text{for all } \kappa.$$

The anticommutation relations of a_{κ} , a_{κ}^* give with (3a)

$$(3c) \quad \xi_{\kappa'}^* \xi_{\kappa} + \xi_{\kappa} \xi_{\kappa'}^* = \delta_{\kappa \kappa'}, \quad \xi_{\kappa} \xi_{\kappa'} + \xi_{\kappa'} \xi_{\kappa} = 0, \quad \xi_{\kappa'}^* \xi_{\kappa}^* + \xi_{\kappa}^* \xi_{\kappa'}^* = 0.$$

The equations (3a) represent a canonical transformation, and the products

$$(3d) \quad \Phi_{\kappa_1 \dots \kappa_j} = \xi_{\kappa_1} \dots \xi_{\kappa_j} \Phi_0$$

form a complete orthonormal set of state vectors.

From

$$(4a) \quad \xi_{\kappa} \left| \frac{1 + g_{\kappa} a_{\kappa} a_{-\kappa}}{(1 + |g_{\kappa}|^2)^{\frac{1}{2}}} \right. = a_{\kappa},$$

$$(4b) \quad \xi_{\kappa} \xi_{-\kappa} \left| \frac{1 + g_{\kappa} a_{\kappa} a_{-\kappa}}{(1 + |g_{\kappa}|^2)^{\frac{1}{2}}} \right. = \frac{a_{\kappa} a_{-\kappa} - g_{\kappa}^*}{(1 + |g_{\kappa}|^2)^{\frac{1}{2}}},$$

one can see that the states

$$\xi_{\kappa} \Phi_0 \quad \text{and} \quad \xi_{\kappa} \xi_{-\kappa} \Phi_0$$

are the excited states of Bardeen, Cooper and Schrieffer with a « single particle » and a « real pair » excited. They appear here on the same footing; and the set of products $\xi_{\kappa_1} \dots \xi_{\kappa_j} \Phi_0$ gives a natural description of their system of excited states. As seen from (4a), though the state $\xi_{\kappa} \Phi_0$ contains an explicit particle creation operator factor a_{κ} , at the same time a « virtual pair » factor $(1 + |g_{\kappa}|^2)^{-\frac{1}{2}} (1 + g_{\kappa} a_{\kappa} a_{-\kappa})$ of Φ_0 is missing. The operation of ξ_{κ} on Φ_0 corresponds to a collective excitation of all the particles; ξ_{κ} creates an elementary excitation, or a « quasi-particle », with the properties of a fermion ⁽⁺⁾.

(+) Analogous phonon variables for a boson system were introduced by BOGORLOBOV ⁽⁴⁾ in 1947. At the time of writing this paper a preprint of a recent work by BOGORLOBOV arrived in which essentially the same fermion variables as given here are used independently in investigating the interacting electron-phonon system.

(4) N. BOGORLOBOV: *Journ. Phys. U.S.S.R.*, **11**, 23 (1947).

From (3a) one can write

$$(5) \quad a_{\kappa} = \frac{\xi_{\kappa} + g_{\kappa}^* \xi_{-\kappa}^*}{(1 + |g_{\kappa}|^2)^{\frac{1}{2}}}, \quad a_{\kappa}^* = \frac{\xi_{\kappa}^* + g_{\kappa} \xi_{-\kappa}}{(1 + |g_{\kappa}|^2)^{\frac{1}{2}}},$$

and any operator expressed in terms of a_{κ} , a_{κ}^* can be transformed into an expression in the collective variables ξ_{κ} , ξ_{κ}^* . Ordering the factors in each term in such a way that creation operators ξ_{κ} stand at the left of the annihilation operators ξ_{κ}^* , the constant term of the expression represents the expectation value of the operator in the ground state Φ_0 .

For the number of particles in state κ ,

$$(6a) \quad n_{\kappa} = a_{\kappa} a_{\kappa}^*$$

one obtains

$$(6b) \quad n_{\kappa} = \frac{(\xi_{\kappa} + g_{\kappa}^* \xi_{-\kappa}^*)(\xi_{\kappa}^* + g_{\kappa} \xi_{-\kappa})}{1 + |g_{\kappa}|^2}.$$

The ground state expectation value

$$(6c) \quad \bar{n}_{\kappa} = h_{\kappa}$$

results from ordering the term with $\xi_{-\kappa}^* \xi_{-\kappa}$, and one obtains

$$(6d) \quad h_{\kappa} = \frac{|g_{\kappa}|^2}{1 + |g_{\kappa}|^2}.$$

From (2b) one concludes that

$$(6e) \quad h_{k\uparrow} = h_{k\downarrow} = h_{-k\uparrow} = h_{-k\downarrow} = h_k.$$

For real g_k , this gives

$$(6f) \quad (h_k)^{\frac{1}{2}} = \frac{g_k}{(1 + |g_k|^2)^{\frac{1}{2}}}, \quad (1 - h_k)^{\frac{1}{2}} = \frac{1}{(1 + |g_k|^2)^{\frac{1}{2}}}, \quad (h_k(1 - h_k))^{\frac{1}{2}} = \frac{g_k}{1 + |g_k|^2},$$

which establishes the connection with the expressions of Bardeen, Cooper and Schrieffer.

The expression (6b) of n_{κ} contains a term with $\xi_{\kappa} \xi_{-\kappa}$ and one with $\xi_{-\kappa}^* \xi_{\kappa}^*$ which have vanishing expectation values for states $\xi_{\kappa_1} \dots \xi_{\kappa_j} \Phi_0$. The remaining

terms can be written in the form

$$(6g) \quad (n_{\kappa})_0 = (1 - h_{\kappa}) \mathcal{N}_{\kappa} + h_{\kappa} (1 - \mathcal{N}_{-\kappa}) ,$$

where

$$(6h) \quad \mathcal{N}_{\kappa} = \xi_{\kappa} \xi_{\kappa}^*$$

represents the number of elementary excitations in state κ .

In a similar way, the substitution (5) gives for the « diagonal part » of the pair creation and annihilation operators $a_{\kappa} a_{-\kappa}$ and $a_{-\kappa}^* a_{\kappa}^*$,

$$(7a) \quad (a_{\kappa} a_{-\kappa})_0 = \chi_{\kappa}^* (1 - \mathcal{N}_{\kappa} - \mathcal{N}_{-\kappa}) ,$$

$$(7b) \quad (a_{-\kappa}^* a_{\kappa}^*)_0 = \chi_{\kappa} (1 - \mathcal{N}_{\kappa} - \mathcal{N}_{-\kappa}) ,$$

with

$$(7c) \quad \chi_{\kappa} = \frac{g_{\kappa}}{1 + |g_{\kappa}|^2} .$$

One particle operators $B = \sum_{\kappa, \kappa'} B_{\kappa \kappa'} a_{\kappa} a_{\kappa'}^*$ are transformed with (5) into a form, from which the matrix elements between states $\xi_{\kappa_1} \dots \xi_{\kappa_j} \Phi_0$ which are tabulated in a section of the paper by BARDEEN, COOPER and SCHRIEFFER can be immediately obtained.

3. – Structure of the excitation spectrum.

The Hamiltonian (1a, b, c, d) is separated through (5) into two parts,

$$(8a) \quad H = H_0 + H_1 ,$$

where H_1 has a vanishing expectation value for states of the form $\xi_{\kappa_1} \dots \xi_{\kappa_j} \Phi_0$ which are the eigenstates of H_0 . The diagonal operator H_0 can be written as

$$(8b) \quad H_0 = E_0 + \sum_{k, \sigma} \epsilon_k (n_{k\sigma})_0 + \frac{1}{2} \sum_{k' \sigma} (n_{k'\sigma})_0 \sum_{k, \sigma} V_{kk'} (n_{k\sigma})_0 - \\ - \frac{1}{2} \sum_{kk' \sigma} V_{kk'} (n_{k\sigma})_0 (n_{k'\sigma})_0 + \frac{1}{2} \sum_{kk' \sigma} V_{kk'} (a_{k\sigma} a_{-k, -\sigma})_0 (a_{-k', -\sigma}^* a_{k', \sigma}^*)_0 ,$$

where $(n_{\kappa})_0$ and $(a_{\kappa} a_{-\kappa})_0$, $(a_{-\kappa}^* a_{\kappa}^*)_0$ are given by (6g) and (7a, b). Accordingly, H_0 is of the form

$$(8c) \quad H_0 = W_0 + \sum_{\kappa} \tilde{E}_{\kappa} \mathcal{N}_{\kappa} + \sum_{\kappa \neq \kappa'} \mathcal{V}_{\kappa \kappa'} \mathcal{N}_{\kappa} \mathcal{N}_{\kappa'} ,$$

in which the ground state expectation value W_0 is given by

$$(8d) \quad W_0 = E_0 + 2 \sum_k \varepsilon_k h_k + 2 \sum_{k'} h_{k'} \sum_k V_{kk'} h_k - \sum_{kk'} V_{kk'} h_k h_{k'} + \sum_{kk'} V_{kk'} \chi_k^* \chi_{k'} = \\ = E_0 + \sum_k (\varepsilon_k h_k + v_k h_k - \mu_k^* \chi_k)$$

and the excitation energy $\tilde{E}_{k\uparrow} = \tilde{E}_{k\downarrow} = \tilde{E}_k$ of states $\xi_k \Phi_0$ is

$$(8e) \quad \tilde{E}_k = v_k (1 - 2h_k) + (\mu_k^* \chi_k + \chi_k^* \mu_k).$$

The quantities v_k , μ_k occurring in (8d, e) are defined by

$$(8f) \quad v_k = \varepsilon_k - \sum_{k'} \bar{V}_{kk'} h_{k'},$$

$$(8g) \quad \bar{V}_{kk'} = \frac{1}{2} (V_{kk'} + V_{k'k}) - (V_{kk} + V_{k'k'}),$$

$$(8h) \quad \mu_k = - \sum_{k'} V_{kk'} \chi_{k'}.$$

Considering W_0 as a function of g_k^* , g_k given by (8d), (6d), (7c) and minimizing it with respect to g_k^* , the equation $\partial W_0 / \partial g_k^* = 0$ reads

$$(9a) \quad \mu_k^* g_k^2 + 2v_k g_k - \mu_k = 0.$$

In referring directly to $\partial W_0 / \partial g_k^* = 0$ it is assumed that the density of states is symmetric about the Fermi level and ε_k is given with respect to it. Otherwise one would have to add a Lagrangian multiplier to v_k in (9a), corresponding to the supplementary condition of a constant average number of particles.

The solution of the second order algebraic equation (9a) gives

$$(9b) \quad g_k = \frac{1}{\mu_k^*} (-v_k + (v_k^2 + |\mu_k|^2)^{\frac{1}{2}}),$$

or with

$$(9c) \quad E_k = + (v_k^2 + |\mu_k|^2)^{\frac{1}{2}},$$

$$(9d) \quad g_k = \frac{1}{\mu_k^*} (E_k - v_k).$$

The root with the plus sign is chosen in (9b) in order to minimize the energy W_0 .

From (9c, d), (6d), (7c) one obtains

$$(10a) \quad |g_k|^2 = \frac{(E_k - \nu_k)^2}{|\mu_k|^2},$$

$$(10b) \quad 1 + |g_k|^2 = \frac{2E_k(E_k - \nu_k)}{|\mu_k|^2} = \frac{2E_k}{E_k + \nu_k},$$

$$(10c) \quad h_k = \frac{1}{2} \left(1 - \frac{\nu_k}{E_k} \right),$$

$$(10d) \quad \chi_k = \frac{\mu_k}{2E_k}.$$

With these values of h_k , χ_k the expression (8d) of W_0 gives

$$(10e) \quad W_0 = E_0 + \sum_k \left\{ \varepsilon_k h_k + \frac{1}{2} \left(\nu_k - \frac{\nu_k^2}{E_k} - \frac{|\mu_k|^2}{E_k} \right) \right\} = \\ = E_0 + \sum_k \left\{ \varepsilon_k h_k + \frac{1}{2} (\nu_k - E_k) \right\},$$

and from (8e) one obtains

$$(10f) \quad \tilde{E}_k = \frac{\nu_k^2}{E_k} + \frac{|\mu_k|^2}{E_k} = E_k;$$

that is, (9c) gives the energy of an elementary excitation (*).

The quantities ν_k , μ_k are to be determined from the non-linear equations obtained from (8f, g, h) with (10c, d) and (9c),

$$(11a) \quad \nu_k = \bar{\varepsilon}_k + \frac{1}{2} \sum_{k'} \bar{V}_{kk'} \frac{\nu_{k'}}{(\nu_{k'}^2 + |\mu_{k'}|^2)^{\frac{1}{2}}},$$

$$(11b) \quad \bar{\varepsilon}_k = \varepsilon_k - \frac{1}{2} \sum_{k'} \bar{V}_{kk'},$$

$$(11c) \quad \mu_k = -\frac{1}{2} \sum_{k'} \bar{V}_{kk'} \frac{\mu_{k'}}{(\nu_{k'}^2 + |\mu_{k'}|^2)^{\frac{1}{2}}}.$$

(*) Formally very similar expressions to those obtained here, though with a rather different physical content, can be derived for a boson system. They include those of Bogolubov's 1947 method (4) as their low density limit. An investigation of this problem in collaboration with D. BUTLER is still in progress.

In the case of a factorisable potential $V_{kk'} = v_k v_{k'}$ these equations can be reduced to integrations and algebraic equations, by introducing quantities of the type

$$\lambda = \frac{1}{2} \sum_{k'} \frac{v_{k'} \mu_{k'}}{(v_{k'}^2 + |\mu_{k'}|^2)^{\frac{1}{2}}}, \quad \mu_k = -\lambda v_k.$$

The approximations involved in the form of the trial state vector Φ_0 are such that better approximations are obtained by excluding the occupation (or emptiness) of electron states outside a definite energy region $|\varepsilon_k| \leq \hbar\omega$ about the Fermi level. This can be done on the ground of physical considerations, where $\hbar\omega$ is a characteristic phonon energy. The trial state vector is chosen accordingly with $h_k = 0$ for $\varepsilon_k > \hbar\omega$ and $h_k = 1$ for $\varepsilon_k < -\hbar\omega$. The equations obtained by minimizing W_0 are unchanged, though the summation extends only over a restricted energy region. Replacing in this region V_{kk} by an average value $V_{kk'} = -V$, and replacing by their average a part of the terms in H_0 which depend only on the total number N of particles, one obtains $v_k \simeq \varepsilon_k$, and $\mu_k = \text{constant} = \varepsilon_0$. The relationships (9c), (10c), (10d) then reduce to those given by BARDEEN, COOPER and SCHRIEFFER, and the equation for the energy gap ε_0 can be solved explicitly.

The equations (11a, b, c) for determining v_k , μ_k can be put into a simpler linearized form. They can be obtained by minimizing the expression (8d) of W_0 which is a quadratic form in h_k , χ_k with respect to the independent variables h_k , χ_k under the supplementary conditions $|\chi_k|^2 + h_k^2 = h_k$, or $|\chi_k|^2 + (1 - 2h_k)^2 = 1$.

4. – Statistical operator and grand ensemble.

With the simplified classification of states, the ensemble of states considered by BARDEEN, COOPER and SCHRIEFFER corresponds to a statistical operator of the form

$$(12a) \quad U_0 = C_0^{-1} \sum_{j=0}^{\infty} \sum_{\kappa_1 < \dots < \kappa_j} w_{\kappa_1} \dots w_{\kappa_j} P_{\kappa_1 \dots \kappa_j},$$

where $P_{\kappa_1 \dots \kappa_j}$ is the projection operator on the state $\xi_{\kappa_1} \dots \xi_{\kappa_j} \Phi_0$ and C_0 is the trace of the operator sum,

$$(12b) \quad C_0 = \text{tr} \sum_{j=0}^{\infty} \sum_{\kappa_1 < \dots < \kappa_j} w_{\kappa_1} \dots w_{\kappa_j} P_{\kappa_1 \dots \kappa_j} = \prod_{\kappa} (1 + w_{\kappa}),$$

so that $\text{tr } U_0 = 1$. The average number of elementary excitations in the

state \varkappa is

$$(12e) \quad \langle \mathcal{Q}_\varkappa \rangle = \text{tr } \mathcal{Q}_\varkappa U_0 = \frac{w_\varkappa}{1 + w_\varkappa} = f_\varkappa,$$

and it is assumed that

$$(12d) \quad f_{k\uparrow} = f_{k\downarrow} = f_{-k\uparrow} = f_{-k\downarrow} = f_k.$$

This form of the statistical operator implies that the elementary excitations are statistically independent because, for $\varkappa \neq \varkappa'$ one has

$$\langle \mathcal{Q}_\varkappa \mathcal{Q}_{\varkappa'} \rangle = \langle \mathcal{Q}_\varkappa \rangle \langle \mathcal{Q}_{\varkappa'} \rangle = f_\varkappa f_{\varkappa'}.$$

U_0 is determined by the two independent functions g_\varkappa and f_\varkappa both of which will be obtained as temperature dependent. From (6g) and (7b) one has the average values

$$(13a) \quad \langle n_\varkappa \rangle = (1 - h_\varkappa) f_\varkappa + h_\varkappa (1 - f_\varkappa) = h_\varkappa^{(T)},$$

$$(13b) \quad \langle a_{-\varkappa}^* a_\varkappa^* \rangle = \chi_\varkappa (1 - 2f_\varkappa) = \chi_\varkappa^{(T)}.$$

The average value of the energy $\langle H \rangle = \langle H_0 \rangle = W_0^{(T)}$ results from (8b) as

$$(13c) \quad \begin{aligned} W_0^{(T)} = E_0 + 2 \sum_k \varepsilon_k h_k^{(T)} + 2 \sum_{k'} h_{k'}^{(T)} \sum_k V_{kk'} h_{\varphi}^{(T)} - \\ - \sum_{kk'} V_{kk'} h_k^{(T)} h_{k'}^{(T)} + \sum_{kk'} V_{kk'} \chi_k^{*(T)} \chi_{k'}^{(T)}, \end{aligned}$$

which is of the same form as (8d) with h_k , χ_k replaced by $h_k^{(T)}$, $\chi_k^{(T)}$. In connection with the quantities (13a, b) the relationship

$$(13d) \quad |\chi_\varkappa^{(T)}|^2 = h_\varkappa^{(T)} (1 - h_\varkappa^{(T)}) - f_\varkappa (1 - f_\varkappa)$$

might be mentioned.

With the standard entropy expression for a system of independent fermions given by

$$(14a) \quad TS_0 = -2\beta \sum_k \{f_k \log f_k + (1 - f_k) \log (1 - f_k)\},$$

one can form an approximate free energy expression

$$(14b) \quad W_0^{(T)} - TS_0$$

and minimize it independently with respect to the functions g_k and f_k .

The minimization with respect to f_k for a given g_k leads to the fermion distribution

$$(15a) \quad f_k = \frac{1}{\exp[\beta \tilde{E}_k^{(T)}] + 1},$$

$$(15b) \quad w_k = \exp[-\beta \tilde{E}_k^{(T)}],$$

with

$$(15c) \quad \tilde{E}_k^{(T)} = \frac{1}{2} \frac{\partial W_0^{(T)}}{\partial f_k} = \nu_k^{(T)}(1 - 2h_k) + \mu_k^{(T)*}\chi_k + \chi_k^*\mu_k^{(T)},$$

where in analogy to (8f, h)

$$(15d) \quad \nu_k^{(T)} = \varepsilon_k - \sum_{k'} \bar{V}_{kk'} h_{k'}^{(T)},$$

$$(15e) \quad \mu_k^{(T)} = - \sum_{k'} V_{kk'} \chi_{k'}^{(T)}.$$

With (15b), the statistical operator (12a) can be, therefore, written in the form

$$(16a) \quad U_0 = \exp[\beta A_0] \exp[-\beta \mathcal{H}_0],$$

$$(16b) \quad \exp[-\beta A_0] = \text{tr} \exp[-\beta \mathcal{H}_0].$$

with

$$(16c) \quad \mathcal{H}_0 = \bar{W}^{(T)} + \sum_{\kappa} \tilde{E}_{\kappa}^{(T)} \mathcal{N}_{\kappa},$$

where $\tilde{E}_{k\uparrow}^{(T)} = \tilde{E}_{k\downarrow}^{(T)} = \tilde{E}_k^{(T)}$, and $\bar{W}^{(T)}$ is defined by

$$(16d) \quad W_0^{(T)} = \bar{W}^{(T)} + \sum_{\kappa} \tilde{E}_{\kappa}^{(T)} f_{\kappa},$$

so that the additive Hamiltonian \mathcal{H}_0 has the same average value in U_0 as H_0 or H .

In the limit of $T=0$, that is $\beta \rightarrow \infty$, (15b) gives $w_k = 0$, and the statistical operator (12a) reduces to the projection operator P_0 of the state Φ_0 given by (2a). The consideration of the mixture of states (12a) includes, therefore, this special case.

The operator (12a) can be considered as the trial approximation of the theory for the statistical operator of the grand ensemble

$$(17a) \quad U = \exp[\beta A] \exp[-\beta(H - \mu N)],$$

$$(17b) \quad \exp[-\beta A] = \text{tr} \exp[-\beta(H - \mu N)].$$

A theorem due to PEIERLS⁽⁵⁾, which as shown by SCHULTZ can be extended to include the case of the grand ensemble, shows that, with the diagonal operators H_0 and $N_0 = \sum_{\kappa} (n_{\kappa})_0$, the grand potential \bar{A}_0 defined by

$$(17c) \quad \exp[-\beta \bar{A}_0] = \text{tr} \exp[-\beta(H_0 - \mu N_0)],$$

is an upper bound for the grand potential A ,

$$(17d) \quad \exp[-\beta A] \geq \exp[-\beta \bar{A}_0].$$

The effect of the chemical potential μ in (17a) is to replace ε_k by $\varepsilon_k - \mu$ in the Hamiltonian, as can be seen from the expressions $T \simeq \sum_{\kappa} \varepsilon_{\kappa} n_{\kappa}$ and $\mu N = \sum_{\kappa} \mu n_{\kappa}$. Assuming a density of states for the electrons which is an even function of ε_k about the Fermi level, and a constant average number of electrons, one obtains that μ is equal to the Fermi energy. The counting of ε_k from the Fermi level means, therefore, $\mu = 0$. In this case, the grand potential A reduces to the free energy. For any other choice of the zero of the energy scale, however, the role of the chemical potential μ becomes essential.

The grand potential \bar{A}_0 defined by (17c) still differs from the expression A_0 given by (16b) which with (15a) and (14a) is equal to (14b). By an argument due to SCHULTZ, one can, however, show that A_0 is an upper bound for \bar{A}_0 and consequently for A ,

$$(17e) \quad A_0 \geq A.$$

As the expression of the entropy given by (14a) does not depend explicitly on g_k , the minimization of the free energy (14b) with respect to g_k , for fixed f_k , is equivalent to the minimization of $W_0^{(T)}$. This leads to an equation analogous to (9a) and to the relationships

$$(18a) \quad h_k = \frac{1}{2} \left(1 - \frac{v_k^{(T)}}{E_k^{(T)}} \right),$$

$$(18b) \quad \chi_k = \frac{\mu_k^{(T)}}{2E_k^{(T)}},$$

with

$$(18c) \quad E_k^{(T)} = (v_k^{(T)2} + |\mu_k^{(T)}|^2)^{\frac{1}{2}}.$$

(5) R. E. PEIERLS: *Phys. Rev.*, **54**, 918 (1938)

With (18a, b) one obtains from (15c)

$$(18d) \quad \tilde{E}_k^{(T)} = E_k^{(T)}.$$

From (18a, b, c) and (15d, e) one can deduce equations analogous to (11a, c). For constant $V_{kk'}$, with $|\varepsilon_k| \leq \hbar\omega$, these equations are still of the factorizable type and can be solved exactly. One obtains the temperature dependent energy gap $|\mu_k^{(T)}| \sim \varepsilon_0$ which vanishes at the critical temperature T_c . The free energy calculated as a function of temperature gives the specific heat curve of BARDEEN, COOPER and SCHRIEFFER which explains correctly a great number of experimental facts.

For a system with a large number of particles, the statistical operator U_0 corresponds to a probability distribution for the number N of particles with a sharp peak. This can be seen by comparing the average values $\langle N^2 \rangle$ and $\langle N \rangle^2$ in U_0 . A simple calculation gives

$$(19a) \quad \langle N^2 \rangle - \langle N \rangle^2 = 2 \sum_{\varepsilon} h_{\varepsilon}^{(T)} (1 - h_{\varepsilon}^{(T)}) - \sum_{\varepsilon} f_{\varepsilon} (1 - f_{\varepsilon}).$$

Since one has $0 \leq h_{\varepsilon}^{(T)} (1 - h_{\varepsilon}^{(T)}) \leq \frac{1}{4}$ and $0 \leq f_{\varepsilon} (1 - f_{\varepsilon}) \leq \frac{1}{4}$, and both expressions vanish outside an energy region $|\varepsilon_k| \leq \hbar\omega$, (19a) gives

$$(19b) \quad \langle N^2 \rangle - \langle N \rangle^2 \leq \sum_{\varepsilon} \frac{1}{2} \simeq 2N(0)\hbar\omega,$$

where $N(0)$ is the density of states near the Fermi level. With $2N(0)\hbar\omega \sim \sim 10^{-3} \langle N \rangle$, this leads to an estimate

$$(19c) \quad \frac{\langle N^2 \rangle - \langle N \rangle^2}{\langle N \rangle^2} \leq 10^{-3} \frac{1}{\langle N \rangle}.$$

5. – Long range correlations.

Some of the previous expressions obtain a simple physical interpretation by considering the correlation function of the particles, which is the most important quantity from the point of view of collective behaviour. The two-particle correlations are given by the expectation values of the operator

$$(20a) \quad \varrho_{\sigma\sigma'}(x, x') = \Psi_{\sigma}^*(x) \Psi_{\sigma'}^*(x') \Psi_{\sigma'}(x') \Psi_{\sigma}(x).$$

Expressing the quantized field operators $\Psi_{\sigma}^*(x)$, $\Psi_{\sigma}(x')$ by means of creation and annihilation operators of plane wave states $\psi_k(x) = \Omega^{-\frac{1}{2}} \exp[-ikx]$ in the form

$$(20b) \quad \Psi_{\sigma}^*(x) = \sum_k \psi_k^*(x) a_{k\sigma}, \quad \Psi_{\sigma'}(x') = \sum_k \psi_k(x') a_{k'\sigma'}^*,$$

the expectation value of $\varrho_{\sigma\sigma}(x, x')$ in the ground state Φ_0 can be obtained with the help of the relations (6a, c), (7a, b, c). For the correlation functions of particles with parallel and anti-parallel spin

$$(20c) \quad \varrho_p = \varrho_{\uparrow\uparrow} + \varrho_{\downarrow\downarrow}, \quad \varrho_a = \varrho_{\uparrow\downarrow} + \varrho_{\downarrow\uparrow},$$

a simple calculation gives

$$(21a) \quad \bar{\varrho}_p(r) = \frac{1}{2} \varrho_0^2 - 2h^*(r)h(r),$$

$$(21b) \quad \bar{\varrho}_a(r) = \frac{1}{2} \varrho_0^2 + 2\chi^*(r)\chi(r),$$

where $r = x - x'$, $\varrho_0 = \bar{N}/\Omega$ is the average density, $h(r)$ is the Fourier transform of the number distribution h_k given by (6c, d, e) and $\chi(r)$ is the Fourier transform of the quantity χ_k defined by (7c). This throws new light on the role of the quantities h_k , χ_k in the equations. The last two interaction terms in the expression (8d) of W_0 for instance correspond to the contributions from parallel and anti-parallel spin correlations.

At temperature T , the average values of ϱ_p and ϱ_a in the mixture of states (12a), (16a) are in an analogous way

$$(22a) \quad \langle \varrho_p(r) \rangle = \frac{1}{2} \varrho_0^2 - 2h^{(T)*}(r)h^{(T)}(r),$$

$$(22b) \quad \langle \varrho_a(r) \rangle = \frac{1}{2} \varrho_0^2 + 2\chi'^{(T)*}(r)\chi'^{(T)}(r),$$

where $h^{(T)}(r)$ and $\chi^{(T)}(r)$ are the Fourier transforms of the quantities $h_k^{(T)}$, $\chi_k^{(T)}$ defined by (13a), (13b).

The long range correlations are between particles with antiparallel spin and are related to the function χ_k : For $V_{kk'} = \text{constant}$, with $|\varepsilon_k| < \hbar\omega$, they have been calculated by BARDEEN, COOPER and SCHRIEFFER. In the same model, (22b) gives the temperature dependence of the long range correlations, the amplitude of which tends to zero with the square of the energy gap near the critical temperature. The integrations carried out explicitly for small values of $\varepsilon_0 \sim \mu_k^{(T)}$, that is near the critical temperature, show that the form of the correlation function is practically the same as at $T = 0$, with a correlation length of the order of 10^{-4} cm.

* * *

This paper is the outcome of numerous discussions with members of the Department of Mathematical Physics at the University of Birmingham, and thanks are due to many of them. It is a pleasure to express my thanks espe-

cially to Dr. J. R. SCHRIEFFER and Dr. T. D. SCHULTZ, for stimulating discussions, for suggestions and contributions. Thanks are due to D. BUTLER for helpful co-operation.

RIASSUNTO (*)

Si esprimono in forma più accessibile alcuni significati della nuova teoria di Bardeen, Cooper e Schrieffer. Si introducono nuove variabili fermioniche collettive che sono combinazioni lineari di operatori di creazione e di distruzione di elettroni e descrivono eccitazioni elementari. Essi conducono a una semplice classificazione degli stati eccitati e a grande semplificazione dei calcoli. Si esamina la struttura dello spettro di eccitazione senza eguagliare dapprincipio a una costante l'elemento di matrice del potenziale d'interazione e si derivano nuove relazioni ed equazioni. Il problema dipendente dalla temperatura si descrive per mezzo di un operatore statistico e si stabilisce la sua relazione con quella del grande insieme canonico. Si ottengono nuove semplici relazioni per la funzione di correlazione.

(*) Traduzione a cura della Redazione.

On Gamma-Ray Astronomy.

P. MORRISON

Department of Physics, Cornell University - Ithaca, N. Y.

(ricevuto il 22 Dicembre 1957)

Summary. — Photons in the visible range form the basis of astronomy. They move in straight lines, which preserves source information, but they arise only very indirectly from nuclear or high-energy processes. Cosmic-ray particles, on the other hand, arise directly from high-energy processes in astronomical objects of various classes, but carry no information about source direction. Radio emissions are still more complex in origin. But γ -rays arise rather directly in nuclear or high-energy processes, and yet travel in straight lines. Processes which might give rise to continuous and discrete γ -ray spectra in astronomical objects are described, and possible source directions and intensities are estimated. Present limits were set by observations with little energy or angular discrimination; γ -ray studies made at balloon altitudes, with feasible discrimination, promise valuable information not otherwise attainable.

1. — The nature of the problem.

Astronomy is based on information carried by incoming radiation of optical frequencies. The photons in this channel retain the momentum with which they were originally emitted: with precision in direction, subject only to a rather easily interpreted Doppler shift in magnitude. On the other hand, such photons are very indirectly related indeed to the processes, generally nuclear in nature, which form the ultimate source of the radiated energy.

Insofar as energy-releasing processes are thermonuclear in nature, they proceed deep in stellar interiors, screened by dense layers of matter. We cannot hope to obtain direct signals from such regions (except by way of the still unexploited neutrino channel). But it is increasingly clear that energy-releasing processes of quite different type are also of importance for the evolution of

stars and of galaxies. These latter processes are not screened within stellar interiors, but may take place in stellar atmospheres, in expanding nebular shells more or less near stars, in the interstellar space, and even outside in the galactic haloes.

One source of information about such novel processes is the primary cosmic-ray beam. It is an enigmatic one, for charged particles cannot store precise information of how and where they were produced, since interaction with weak but large-scale magnetic fields in space constantly changes their momenta, certainly in direction and very probably even in order of magnitude. For this reason, most of our present information about processes producing relativistic particles has reached us in a very low-energy channel, the radio continuum, plus the *polarized* optical continuum. Both of these channels pretty surely depend upon interaction between the primary radiating particles of high energy and magnetic fields; radiation in these channels, too, is an entirely secondary consequence of the main processes of energy release.

There is a form of radiation which is more directly related to high-energy and nuclear processes than is optical or radio emission, and yet does not share with high-energy charged particles the complete loss of information about the position of its source. It is γ -radiation, particularly in the region of quantum energy extending from a few tenths MeV to a few hundreds of MeV. Quanta of lower energies are both less directly related to the original processes of energy release and so little penetrating that they demand extra-atmospheric stations of observation. Those of higher energies are probably secondary to cosmic-ray particles, and thus again bear a distant relationship to their origins. Moreover, they represent a rather small fraction of the particle flux of similar energy, which forms a troublesome background. The γ -ray region defined above seems to contain the most direct information with the least objectionable background, and to be relatively accessible to observation. This energy range, alone, from $\simeq 0.2$ MeV to $\simeq 400$ MeV per photon, will be discussed here.

For such γ -radiation, the atmosphere is a screen, and observations cannot be made without a reduction in screen thickness. For the most penetrating portion of this range, near 100 MeV, the highest mountain altitudes might prove barely adequate; for more of the range, high performance aircraft make possible stations; for the whole of it, reasonable balloon altitudes, beneath say 25 g/cm² of air (or 25 km above sea level), would be wholly satisfactory.

It is possible to set upper limits on the primary flux in this energy region. Rather high values follow from indirect arguments using the energy balance of ionization in the atmosphere, or using the primary cosmic-ray charge spectrum to set limits on the photonuclear effect arising from collisions between cosmic ray nuclei and γ -ray photons. Much more strict limits follow from the few direct experimental studies.

Ionization chamber (1) and cloud chamber (2) balloon flights agree in showing that the entering quanta with energies beyond 0.5 GeV, in the cosmic-ray range proper, amount to under one percent of the particle flux, or to few times 10^{-3} photons $\text{cm}^{-2}\text{-s}$. In the energy range of present interest, measurements have been made both at balloon (3) and at rocket altitudes (4) with wide angular and energy acceptance.

The rocket results, obtained around 1950, appear to set an upper limit to the incoming γ -ray flux. These results were obtained using Geiger counters, of rather low efficiency for photons, and the observed fluxes can best be interpreted in terms of energy flux, rather than photon flux. For photons between about 3 and 100 MeV energy, a flux of energy was observed beyond the atmosphere amounting to $1.5 \text{ MeV}\cdot\text{cm}^{-2}\cdot\text{s}^{-1}$. This measurement sampled a solid angle of a steradian or two, centered north of the zenith at the time of the experiment. (This is more or less about the constellation Cygnus.) The flux is calculated assuming an isotropic distribution in the upper hemisphere. At lower energies, the observed result was about $1 \text{ MeV cm}^{-2} \text{ s}^{-1}$ for photons between 0.1 MeV and 15 MeV energy, using the same assumed angular distribution. The lower-energy result was found on several flights; it may be regarded as sampling most of the sky. In both cases the sun's direction was included.

There is little doubt that a substantial fraction of this observed γ -ray flux is nothing but the γ -ray splash albedo from the charged cosmic-ray beam incident on the atmosphere. The original experimenters themselves saw no reason to conclude that there was any other contribution; the estimate of the expected albedo contribution is of the same order of magnitude as the flux observed, but such estimates are plainly not enough to justify such a quantitative conclusion. We wish to point out that within these observed limits, but in particular energy ranges and times, and coming from particular directions in the sky, there is likely to be a still undetected but entirely measurable flux of γ -rays bearing astronomical information of the highest interest.

2. - γ -ray emission processes and spectra.

Both continuous γ -radiation and line spectra are to be expected.

Three processes which might emit such a continuum can be listed:

(1) B. ROSSI and R. HULSIZER: *Phys. Rev.*, **76**, 164 (1949).

(2) C. CRITCHFIELD, E. NEY and S. OLEKSA: *Phys. Rev.*, **85**, 461 (1952).

(3) T. BERGSTRAHL and C. SCHROEDER: *Phys. Rev.*, **81**, 244 (1951); L. REIFFEL and G. M. BURGWALD: *Phys. Rev.*, **95**, 1294 (1954).

(4) The rocket results are summarized in *Rocket Exploration of the Upper Atmosphere*, R. BOYD and M. SEATON, editors (London, 1954), p. 306, by C. JOHNSON, L. DAVIES and J. SIRY.

a) Synchrotron radiation. In strong magnetic fields, particles of sufficient energy can radiate a continuous spectrum within this region. The intensity of radiation by fast electrons will far outweigh that of nuclei, particle for particle, roughly by the factor $(M/m)^2 \approx 10^6$. The electron energy E and the ambient magnetic field B in gauss must satisfy the relation

$$(E/mc^2)B > 10^{14},$$

if quanta with energy above 1 MeV are to be emitted in some abundance. The ordinary fields (up to ten kilogauss at most) suspected in astronomical objects cannot satisfy this condition, for plausible electron energies, anywhere except perhaps in magnetic variable stars. Though the radio continuum probably derives largely from synchrotron radiation sources, the γ -ray continuum is not likely to show any appreciable flux from such sources.

b) Ordinary bremsstrahlen. Here the process is plainly a secondary one, arising whenever relativistic electrons are slowed in matter. In the hydrogen-rich plasma of space or of stellar atmospheres, the radiation length is near 75 g/cm^2 . γ -rays in our energy range are most likely to arise from the radiative collisions of electrons with energies in the same region, or an order of magnitude higher. Beyond that, the spectrum of electrons probably falls off with the familiar sort of power law, and the total radiation also falls, at a lower power. Below 100 MeV, radiation takes away only a small fraction of the collision losses. Very roughly one may estimate a quantum yield per slowed electron per radiation length of about 0.1 quantum having from about 0.9 to the full electron energy, about one quantum, with energy between half and quarter of the electron energy, several quanta, with energy a few percent of the original, and so on, following the spectral distribution $dN_\gamma/dE \propto 1/E$.

c) Radiative decay of neutral pions. Such mesons can arise as secondaries to cosmic-ray particle collisions, or possibly in collisions between nucleons and anti-nucleons. If such matter is present, and moves with velocities like those of normal galactic constituents, the gammas released will extend in energy from about 50 MeV to 200 or 300 MeV, and will amount to about 500 MeV in total γ energy per nuclear annihilation ⁽⁵⁾. Such a source might be detectable in high-flying aircraft, or possibly on mountain tops.

Discrete γ -ray lines can be expected between 0.5 MeV and 15 MeV. They may arise in these ways:

d) De-excitation of nuclei formed by radioactive decay,

⁽⁵⁾ W. H. BARKAS *et al.*: *Phys. Rev.*, **105**, 1037 (1957).

by fission, or, probably most importantly, by neutron capture. Neutrons are bound to be important products of nearly any nuclear interactions above some 10 MeV; such neutrons, if released in regions of density above 10^{-9} or 10^{-10} g/cm², will be captured before β -decay, and yield the proton capture γ -ray, at 2.23 MeV, with probability near 1 in material of ordinary composition.

e) **Electron-positron annihilation.** Here the quantum, energy is pretty sharply 0.51 MeV, apart from motional Doppler effects. The yield is two per annihilation.

3. – Sources of γ -rays and their intensities.

It is possible to suggest very tentatively some objects which might be sources of γ 's arising from the processes listed in Sect. 2, and to estimate roughly the order of magnitude of the expected fluxes.

First, the active sun. Solar flares sometimes yield even at the earth a large flux of cosmic-ray particles. Various models, and especially the so-called Type IV radio outbursts seen by the Meudon group (6) suggest the presence of relativistic electrons as well. If such a picture is correct, γ -rays from sources of types *b*) and *d*) above must be present, very possibly even in flares whose cosmic-ray product does not reach the earth. If we estimate (i) that the number of relativistic electrons produced is the same as that of cosmic-ray particles, but that the energy per electron is reduced by a factor of M/m , and (ii) that the electrons move through matter of various densities, all less than the chromospheric value of 10^{11} protons/cm³, during the 10^3 s of a flare of intensity class 2, we may expect a γ -ray flux at the top of the earth's atmosphere, after the optical peak of flare emission, which amounts to between 0.1 and a few gammas/cm²-s, with energies between 10 and 100 MeV. Likewise, if fast protons are present in flare events which do not produce cosmic-rays on earth, and if such protons are directed in part downwards into the photosphere, one must expect a flux of the specific neutron-proton capture γ 's, at 2.23 MeV, as intense as 1 to 10^2 gammas/cm²-s at the earth.

Observation of flare-created gammas in the continuum would verify the presence of fast electrons; in the line spectrum, that of fast nuclei, even though no cosmic-ray effects were seen on earth. Unlike radio emission, the gammas are unaffected by coronal material. If any are observed, evidently their number, energy spectrum, and time course would be sharp tests for any model of flare events.

(6) A. BOISCHOT: *Compt. Rend.*, **244**, 1326, and Professor DENISSE: private communication.

Second, the Crab Nebula. There is little doubt that the expanding gas shell contains radioactive debris from the original explosion. An estimate of the «fall-out» based on the abundance of ^{254}Cf suggests that a flux of specific nuclear γ -rays, mainly those of ^{226}Ra , should be detectable from the direction of Taurus, with an incoming flux of about 10^{-2} gammas/cm 2 -s.

Third, anomalous extragalactic radio sources, particularly the galaxy M87, and the colliding pair of the Cygnus A radio source. It would be possible to test the bizarre but attractive possibility (?) that the high radio intensity of such objects is associated with matter-anti-matter collisions. If one assumes that the collision partners of the Cygnus source are charge-conjugate galaxies, one expects a flux of incoming annihilation gammas, both in a line at 0.5 MeV, and in a continuous distribution from a few tens of MeV to a few hundreds of MeV. The flux of the line spectrum should be about 0.1 to 1 gamma/cm 2 -s; that of the continuum, about the same.

Fourth, an isotropic flux of annihilation gammas is implied by cosmological models involving the creation of matter and antimatter. If such creation goes on in our own galaxy, we may estimate that the rocket observations of γ -ray flux up to 90 MeV limit the creation rate to $\simeq 10^{-22}$ particles cm $^{-2}$ s $^{-1}$ or even a factor of a few less. This seems to set a limit on this postulated process lower than any other observations known (?). The value of more complete γ -ray measurements in the testing of cosmological speculations is evident.

4. - Observational requirements.

The longest exposures with the great Palomar telescope can barely yield an image for stars of photographic magnitude 23. Translating this statement into units of some physical significance, one finds that the limiting incident photon flux amounts to about $6 \cdot 10^{-3}$ quanta cm $^{-2}$ s $^{-1}$. Such a flux limit can be more or less easily reached by instruments exploiting the high quantum energy in the γ -ray region, but still light enough to be capable of high-altitude flight within relatively inexpensive vehicles.

In the optical region, however, great angular discrimination is taken for granted. If an optical detector were to accept visible photons over a full steradian of solid angle, even the brightest star, Sirius, would produce in it a barely noticeable signal, only a few percent above the general sky background; with such detectors, which would be rather more directional than the γ -ray detectors so far used, optical astronomy could hardly exist. The analogue to the light of the night sky is the γ -ray splash albedo of cosmic radiation. This background, coming mainly from below, can be very much reduced by reason-

(?) G. R. BURBIDGE and F. HOYLE: *Nuovo Cimento*, **4**, 558 (1956).

able angular collimation; it gives about the same flux intensity over a hemisphere as the stronger signals estimated in Sect. 3

Energy resolution on the level of optical spectroscopy cannot be hoped for; but «spectroscopic» results as good as the very important four-color techniques of photographic astronomy are entirely feasible with γ -ray. Energy acceptance channels such that the ratio of mean energy to channel half-width is 3 to 1, say, are not impractical.

Measurement of such γ -ray fluxes as those estimated in Sect. 3, even in the presence of the background produced by the incoming particle flux and by the secondary γ -ray it generates in the atmosphere, is within reach of present techniques. Flights of several hours' duration are adequate, and the altitudes required are not extreme. Telemetering of data, or even recovery of the apparatus with stored data, is commonplace. Reasonable angular discrimination can perhaps be obtained in the low-energy region at least by using lead collimation, should balloon loads permit. Otherwise, the use of scintillation counters, possibly taking advantage of coincidences with the Compton-scattered photons to help define angles, seems capable of adequate energy and angular discrimination below 1 or 2 MeV. The dominance of pair-production makes counting techniques even more satisfactory, and angular discrimination easier, in the energy region from 10 MeV to a few hundred MeV. Here emulsions might be of value.

All experience suggests that such speculative estimates of what is present in a novel field of enquiry rarely prove reliable; but it suggests no less strongly that the extension of observations to such a new domain will in the end repay considerable effort. This note is intended mainly to attract to this problem the attention of those experimenters skilled in the required arts.

* * *

It is a pleasure to acknowledge many and indispensable discussions with Professors G. COCCONI and K. I. GREISEN here at Cornell.

RIASSUNTO

L'Astronomia si basa sull'osservazione dei fotoni dello spettro visibile; questi fotoni si propagano in linea retta, quindi forniscono informazioni sulla direzione delle sorgenti; essi tuttavia sono prodotti solo molto indirettamente dai processi nucleari o di alta energia che hanno luogo nei corpi celesti. Le particelle dei raggi cosmici, d'altra

parte, sono prodotte direttamente da processi di alta energia che hanno luogo in oggetti astronomici di vario tipo, ma non forniscono informazione alcuna circa la direzione delle sorgenti. I raggi γ , invece, sono creati in modo più diretto in processi nucleari o di alta energia, e si propagano in linea retta. Si descrivono vari processi che possono dar luogo a spettri continui e discreti di raggi γ in oggetti astronomici e si valutano possibili direzioni e intensità di sorgenti. Si fa infine notare che le poche misure sin qui eseguite sui raggi γ nell'alta atmosfera soffrono di inadeguata risoluzione angolare ed energetica, ma che misure fatte con apparati di ragionevole potere risolutivo ad altezze raggiungibili con palloni, potrebbero fornire informazioni preziose, non ottenibili per altra via.

Ultrasonic Absorption in Anilin and in Mixtures.

M. CEVOLANI and S. PETRALIA

Istituto di Fisica dell'Università - Bologna

(ricevuto il 3 Gennaio 1958)

Summary. — The ultrasonic absorption, at frequencies between 9 and 27 MHz, has been measured in anilin and in anilin- CCl_4 mixtures; the measures to investigate the causes which determine the anomalous absorption were made within a wide temperature range. It appears, according to a recent theory by R. E. NETTLETON, that at high temperatures, anilin behaves like a non-associated liquid, with anomalous absorption of molecular origin. At low temperature another contribution was found to the absorption, which probably indicates the formation of aggregates in anilin and mixtures show a clear absorption maximum for a given molecular anilin concentration; the lower the temperature, the clearer the maximum, its height varying with ultrasonic frequency.

1. — Experimental results.

Till now the chemical physical researches on anilin (1-3) did not already show if it behaves like an associated liquid or not; the eventual association could be caused by hydrogen bonds. If we consider the classification of liquids set up by J. M. M. PINKERTON (4), according to their ultrasonic absorption, we may hope to find some conclusions about the behaviour of anilin by measures of ultrasonic absorption and by analysis of the dependence of the absorption on temperature. In our previous researches (5), that, on the other

(1) M. DAVIES: *Zeits. f. Naturfor.*, **9a**, 474 (1954).

(2) E. FISCHER: *Zeits. f. Naturfor.*, **9a**, 904 (1954).

(3) N. FUSON, M. L. JOSIEN, R. L. POWELL and E. UTERBACK: *Journ. Chem. Phys.*, **2h**, 145 (1952).

(4) J. M. M. PINKERTON: *Proc. Phys. Soc.*, B **62**, 129 (1949).

(5) M. CEVOLANI and S. PETRALIA: *Nuovo Cimento*, **2**, 495 (1955).

side, we were carrying on for a different purpose, we had already suspected that anilin might be somewhat associated; to give a contribution to the solution of this problem, we have thought it advisable to continue the ultrasonic absorption measures in pure anilin and in mixture of anilin with a non-associated liquid like CCl_4 .

Measures were carried out by means of a pulse device previously described (5), at frequencies of 9, 15, 21 and 27 MHz. The temperature of the ultrasonic cell was varied between 80°C and -5°C for anilin (freezing point at -6.2°C) and between 42°C and -20°C for anilin- CCl_4 mixtures; the lowest temperature, at which we worked was always sufficient far from the freezing temperature of the mixtures, at least valid for anilin molecular concentrations lower than 65%. This results from the data obtained by J. TIMMERMANS (6).

To calculate the classical absorption coefficient, we also measured density (ρ), shear viscosity coefficient (η) and ultrasonic velocity (v) in the different mixtures; some values of shear published by E. FISCHER and R. FESSLER (7), were compared with ours.

Most results are in Tables I and III: Table I deals with pure anilin and Table III with mixtures studied at different temperatures. Fig. 1 shows the ratio between the absorption coefficient of ultrasonic

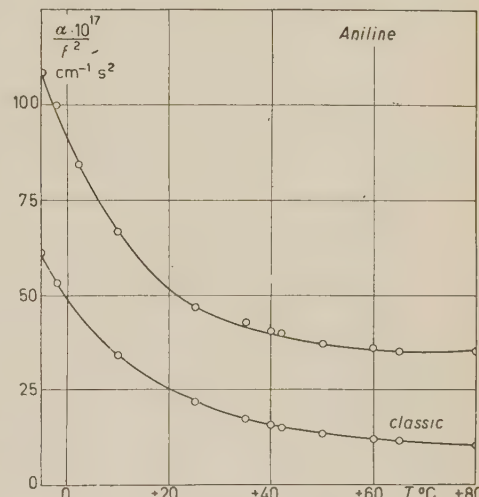


Fig. 1.

TABLE I.

t °C	ρ g/cm ³	v m/s	$10^{12}\beta$ cm ² /dyne	$10^2\eta$ c. poise	$10^{17}\alpha_{\text{cl}}/f^2$ s ² /cm	$10^{17}\alpha_{\text{exp}}/f^2$ s ² /cm	$\alpha_{\text{exp}}/\alpha_{\text{cl}}$
-5	1.043	1752.5	31.2	13.1	61.4	109	1.78
-2	1.041	1741.0	31.7	11.2	53.6	100	1.87
2.5	1.036	1724.1	32.5	9.06	44.9	84	1.87
10	1.030	1695.5	33.8	6.50	34.1	67	1.97
25	1.017	1637.9	36.6	3.71	21.9	47	2.15
40	1.004	1579.7	39.9	2.37	15.7	40	2.53
60	0.987	1502.9	44.9	1.51	11.9	36	3.03
80	0.970	1425.0	50.8	1.09	10.2	35	3.43

(6) J. TIMMERMANS: *Bull. Soc. Chim. Belg.*, **37**, 409 (1928).

(7) E. FISCHER and R. FESSLER: *Zeits. f. Naturfor.*, **8a**, 177 (1953).

TABLE II.

t °C	$10^{-8}\alpha^*$ em ⁻¹	$10^2 p_1 \rightarrow 0$	$10^{-11}Z_c$ s ⁻¹	$10^{10}\tau$ s	$10^2 c_i$ cal/g °C	c_p cal/g °C	$10^3\theta$ °C ⁻¹	γ	$10^{17}\alpha_i/f^2$ s ² /cm	$10^{17}(\alpha_{\text{exp}} - \alpha_{\text{cl}})/f^2$ s ² /cm
1	6.367	1.795	1.957	2.202	1.884	0.47(6)	0.8191	1.276	27.4	41.0
2	6.364	1.801	2.023	2.121	1.886	0.4874	0.8210	1.271	25.4	39.2
25	6.301	1.889	2.153	1.858	1.920	0.4967	0.8644	1.287	24.9	25.1
40	6.261	1.952	2.240	1.705	1.938	0.5024	0.8938	1.297	24.4	24.2
60	6.210	2.040	2.386	1.506	1.960	0.5148	0.9344	1.305	23.0	24.1
80	6.159	2.133	2.545	1.330	1.978	0.5288	0.9764	1.309	21.3	24.8

amplitude and the square of the frequency f as obtained in our measures, and the same ratio, classically calculated for anilin, plotted against temperature.

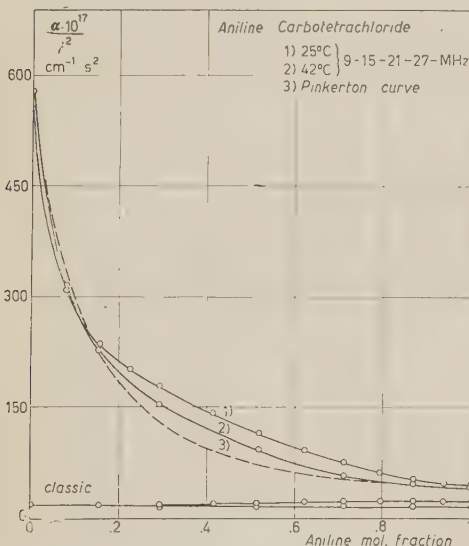


Fig. 2.

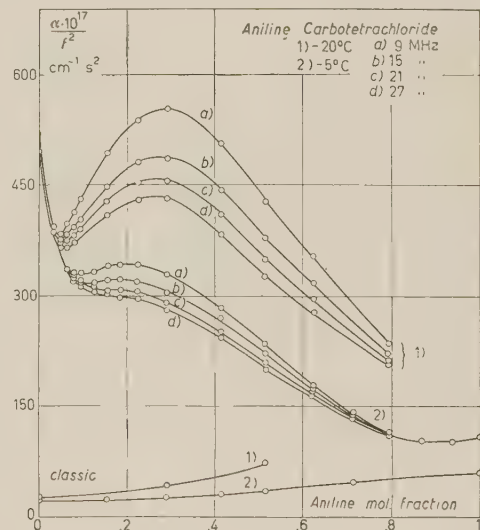


Fig. 3.

Fig. 2 shows this parameter for anilin- CCl_4 mixtures plotted against molecular concentration of anilin; temperatures are 42 °C and 25 °C. Fig. 3 shows the same curves for the lower temperatures of -5 °C and -20 °C.

2. - Discussion of results.

2.1. Anilin. - In pure anilin the experimental ratio α/f^2 rises when temperature diminishes and at -5 °C is $109 \cdot 10^{-17} \text{ cm}^{-1} \text{ s}^2$; this is a low value, of the order of that of water; it is also independent of frequency. The ratio

TABLE III.

t °C	γ mol. conc.	ρ g/cm ³	v m/s	$10^{12}\beta$ cm ² /dyne	$10^2 \eta$ poise	$10^{17}\alpha_{\text{cl}}/f^2$ s ² /cm	$10^{17}\alpha/\text{epx}f^2 \text{cm}^{-1} \text{s}^2; f = \text{MHz}$				$\alpha_{\text{exp}}/\alpha_{\text{cl}}$ (15f)
							9f	15f	21f	27f	
42	0.000	1.551	868.4	85.5	0.72	18.7	580	581	580	581	31.1
	0.080	—	902.5	—	0.79	—	315	316	317	316	—
	0.155	—	937.5	—	0.84	—	228	230	230	227	—
	0.292	1.403	1006.4	70.4	0.95	17.5	154	155	154	155	8.9
	0.524	1.277	1149.0	59.3	1.23	16.7	94	91	91	92	5.5
	0.713	1.173	1288.6	51.3	1.59	16.7	58	56	58	59	3.4
	0.869	1.082	1432.2	45.0	1.98	16.4	47	48	46	47	2.9
	1.000	1.003	1571.9	40.1	2.29	15.5	41	40	41	40	2.6
25	0.000	1.584	921.2	74.4	0.90	19.2	550	555	560	554	28.9
	0.080	1.543	956.5	—	0.96	—	310	308	312	314	—
	0.155	1.504	990.5	67.8	1.03	18.5	238	238	237	237	12.9
	0.292	1.430	1061.0	62.1	1.21	18.6	178	179	177	177	9.6
	0.524	1.301	1205.0	52.9	1.76	20.4	115	115	115	115	5.6
	0.713	1.191	1350.6	46.0	2.54	22.7	75	77	75	76	3.4
	0.869	1.099	1496.2	40.6	3.20	22.9	54	52	54	53	2.3
	1.000	1.018	1637.9	36.6	3.75	22.1	47	47	47	46	2.1
-5	0.000	1.642	1015.2	59.1	1.47	22.5	517	520	518	521	23.1
	0.033	—	—	—	—	—	395	393	391	394	—
	0.064	—	—	—	—	—	338	334	337	334	—
	0.095	—	—	—	—	—	330	320	319	313	—
	0.155	1.553	1086.6	54.5	1.84	24.3	340	320	307	303	13.2
	0.226	—	—	—	—	—	342	320	305	296	—
	0.292	1.476	1156.3	50.7	2.34	27.0	329	305	290	282	11.3
	0.415	1.403	1229.4	47.2	3.19	32.2	284	270	251	243	8.4
	0.524	1.339	1304.8	43.9	4.06	35.9	235	222	209	200	6.2
	0.623	—	1380.3	—	—	—	179	174	168	165	—
	0.713	1.225	1452.2	38.7	6.85	48.0	142	141	136	134	2.9
	0.794	—	1529.9	—	—	—	115	116	113	113	—
	0.869	—	1603.6	—	—	—	105	105	104	104	—
	0.937	—	1677.3	—	—	—	103	103	103	103	—
	1.000	1.403	1752.5	31.2	13.10	61.4	106	110	109	108	1.8
-20	0.000	1.670	1062.3	53.1	1.95	25.6	492	495	500	497	19.3
	0.033	—	—	—	—	—	386	386	388	384	—
	0.049	—	—	—	—	—	384	376	372	366	—
	0.064	—	—	—	—	—	398	383	375	366	—
	0.095	—	—	—	—	—	432	404	390	379	—
	0.155	—	—	—	—	—	494	448	428	409	—
	0.226	—	—	—	—	—	540	482	454	430	—
	0.292	1.500	1206.9	45.8	4.23	42.2	554	487	456	433	11.5
	0.415	—	—	—	—	—	507	445	412	384	—
	0.524	1.359	1357.6	39.9	9.40	72.7	428	379	349	326	5.2
	0.623	—	—	—	—	—	355	319	296	278	—
	0.794	—	—	—	—	—	237	222	213	208	—

$\alpha_{\text{exp}}/\alpha_{\text{cl}}$ between the measured and classical absorption coefficients has a variable value between 2 and 3; that is, little enough but, on the other side, it seems to be not entirely independent of temperature, since it assumes higher values at higher temperatures. The behaviour of anilin seems, therefore, to be similar to the one of water and alcohols, with a clearer dependance of $\alpha_{\text{exp}}/\alpha_{\text{cl}}$ on temperature. The ultrasonic anomalous absorption should be prevailingly attributed to the structural equilibrium perturbation of the liquid. According to T. KISHIMOTO and O. NOMOTO (8), however, a contribution of molecular vibration to the absorption should not be excluded.

Since anilin is chemically unstable, measures become difficult at high temperatures; on the other hand, measures which we repeated in different conditions clearly showed that the absorption coefficient remains constant above 50 °C when temperature rises, and above 80 °C, tends perhaps to increase. (These last results were not reported on our Table I because of their uncertainty). Then we thought to eliminate the molecular contribution to the absorption in the range where the curve α/f^2 falls more rapidly with temperature: we subtracted from the measured absorption at various temperatures the difference between the value of the measured absorption coefficient and the corresponding classical one both at 50 °C; the remaining absorption is partly classical and partly must be attributed to a 'bulk viscosity' and if α_K is the absorption coefficient corresponding to this contribution, we have:

$$(1) \quad \alpha_K = \alpha_{\text{exp}} - (\alpha_{\text{cl}} + \alpha_{\text{mol } 50^\circ\text{C}}) = 2\pi^2 K f^2 / (\rho v^2),$$

where K is the bulk viscosity coefficient, and $\alpha_{\text{mol } 50^\circ}$ refers to the above difference ($23.6 \cdot 10^{-17} f \text{ cm}^{-1}$).

Suppose now to apply to the term α_K the two states theory formulated by L. HALL (9) to explain the anomalous absorption of water. According to the phenomenological point of view of that theory, the relaxation time τ of the processes involved in the absorption is given by:

$$(2) \quad \tau = K \beta_0,$$

where β_0 is the static compressibility which may be deduced from the values of ρ and v already measured, and K may be deduced from (1). τ is therefore determined at different temperatures; at 25 °C $\tau = 1.2 \cdot 10^{-11} \text{ s}$. Knowing the value of τ we can do the calculation of the free energy variation ΔF , which happens when the liquid goes from an initial configuration 1 to a final config-

(8) T. KISHIMOTO and O. NOMOTO: *Journ. Phys. Soc. Japan*, **10**, 933 (1955).

(9) L. HALL: *Phys. Rev.*, **73**, 775 (1948).

guration 2, by the formula:

$$(3) \quad \tau = \frac{\eta V}{RT(1 + \exp[\Delta F/RT])},$$

where V is the molar volume.

If we write the values of $\lg[V\eta/(\tau RT) - 1]$ against $1/T$, we can draw a straight line, from the slope of which we can calculate ΔF ; we find $\Delta F = 7$ kcal/mole. This value appears to be rather high if compared with the free energy variations which happen in other structural processes, like, for instance, the breaking of hydrogen bonds; Hall calculates that the hydrogen bonding energy per mole of half-bond in water is 0.5 kcal/mole; for ethyl alcohol it is of the same order. Therefore we think that Hall's theory is not applicable to the anomalous absorption represented by α_x .

Recently R. E. NETTLETON (10) applied Hall, R. N. SCHWARZ and K. F. HERZFELD's theories (11) to calculate the ultrasonic anomalous absorption in water and in ethyl alcohol; these liquids are, notoriously, associated by hydrogen bonds. He showed that, while the anomalous absorption may be at all justified for water by Hall's theory, in the case of ethyl alcohol the Hall absorption is negligible in the temperature range between 25 °C and 60 °C in which measures were made; the measured absorption is caused for one half by the shear viscosity and for the remainder by the processes concerning the energy exchange between translation degrees of freedom and the internal vibrational modes, processes that we contemplated in Schwarz-Herzfeld theory. Here the ratio α_i/f^2 is given by:

$$(4) \quad \frac{\alpha_i}{f^2} = \frac{2\pi^2}{v} \tau \frac{c_i}{c_p} (\gamma - 1),$$

where c_i is the contribution to the specific heat coming from the molecular vibration (if we suppose only a vibrational state to be excited, the one with the lowest frequency, v), c_p is the total specific heat at constant pressure, γ the the ratio c_p/c_v and τ the relaxation time. The calculation of this time is tedious; it is derived from the effective collision frequency Z_c and from the disexcitation probability $p_1 \rightarrow 0$ from the first excited state to the fundamental one, 0. It is:

$$(5) \quad 1/\tau = Z_c p_{1 \rightarrow 0} (1 + \exp[-hv/RT]).$$

(10) R. E. NETTLETON: *Phys. Rev.*, **106**, 631 (1957).

(11) R. N. SCHWARZ and K. F. HERZFELD: *Journ. Chem. Phys.*, **22**, 767 (1954).

Approximately, the collision frequency Z_e is given by:

$$(6) \quad Z_e = 8\varrho kT \cdot c_v / (3\pi\lambda m),$$

where m = molecular mass, c_v = specific heat per gram at constant volume, k = Boltzmann constant and λ = thermal conductivity coefficient. The transition probability $p_{1 \rightarrow 0}$ is expressed from SCHWARZ and HERZFELD by:

$$(7) \quad p_{1 \rightarrow 0} = \frac{0.716}{[\frac{1}{2}(1 - \chi kT/\varepsilon)^{\frac{1}{2}} + \frac{1}{2}]^{\frac{1}{2}}} \left(\frac{\pi}{3} \right)^{\frac{1}{2}} \left(\frac{8\pi^3 \mu h\nu}{\alpha^{*2} h^2} \right)^2 (V_1 \rightarrow 0)^2 \cdot \chi^{\frac{1}{2}} \exp \left[- \left(3\chi - \left(\frac{h\nu}{2kT} + \frac{\varepsilon}{kT} \right) \right) \right].$$

where $\mu = \frac{1}{2}m$ reduced molecular mass, ε = depth of minimum Lennard-Jones potential, h = Planck constant and:

$$(8) \quad \chi = \left[\frac{2\pi^4 \mu (h\nu)^2}{a^{*2} h^2 k T} \right]^{\frac{1}{2}},$$

$$(9) \quad \alpha^* = \frac{12}{r_0 D} \left[\frac{1}{2} + \frac{1}{2} (1 + D)^{\frac{1}{2}} \right]^{\frac{1}{2}} [1 + (1 + D)^{\frac{1}{2}} + D],$$

$$(10) \quad D = (\frac{1}{2}kT + \varepsilon)/\varepsilon,$$

where r_0 is the zero of Lennard-Jones potential, while $V_{1 \rightarrow 0}$ is the matrix element of the factor of the intermolecular potential involving the internal vibration co-ordinates.

We have extended the calculations of Nettleton to the case of anilin to find how much the anomalous absorption in anilin is caused by intramolecular processes. Unfortunately there do not exist numerical data for some of the involved constants like, ε , r_0 , c_i ; for others (12), like λ and c_v we have imprecise data (like for c_v under 5 °C) or data known only for a limited temperature range. Values given for c_v by H. R. LANG (13) show a quick and uncertain fall under 5 °C; I.C.T. (1929, Vol. V) report a value for c_v at 0 °C that is nearly equal to that given by LANG at 1 °C.

The ratio γ has been calculated according to the relation:

$$(11) \quad \gamma - 1 = \frac{v^2 \theta^2 T}{4.186 c_v \cdot 10^7}.$$

(12) G. W. C. KAYE and W. F. HIGGINS: *Proc. Roy. Soc.*, A **117**, 459 (1927).

(13) H. R. LANG: *Proc. Roy. Soc.*, A **448**, 138 (1928).

and the expansivity θ has been obtained from density as a function of the temperature.

The force constant ϵ has been calculated by the method indicated by J. O. HIRSCHFELDER, C. F. CURTISS e R. B. BIRD (14), starting from vapour viscosity or from the II virial coefficient. Since we have not found experimental determinations of viscosity and of the II virial coefficient for anilin vapours, we have been obliged to use, for viscosity, values calculated from an equation reported by J. R. PARKINGTON (15) and for the II virial coefficient, values obtained from Berthelot's equation. Values obtained for ϵ/k by the two methods disagree, the ones calculated from the virial being smaller than the ones obtained from the viscosity. We considered advisable to use $\epsilon/k = 450 \text{ }^{\circ}\text{K}$; then $r_0 = 5.74 \text{ \AA}$.

The specific heat c_i has been calculated from Plank-Einstein's formula; we choose the frequency of the vibrational mode (which is supposed to be excited), the lowest among those reported by LANDOLT-BÖRNSTEIN (16) (234 cm^{-1}).

The matrix element, for the anilin molecule, $V_{1 \rightarrow 0}$ has been calculated by the Nettleton criterium, who takes the expression of $V_{1 \rightarrow 0}$ valid for a symmetric diatomic molecule:

$$(12) \quad V_{1 \rightarrow 0} = \frac{\alpha^*}{2\beta} \exp[\alpha^{*2}/8\beta^2] \quad \beta = 4\pi^2\mu'/\hbar.$$

According to HERZFELD it seems that this expression gives the right order of magnitude for the more complicated molecules; $\mu' = m/4$ is the oscillator reduced mass.

The results of calculations and the available experimental data are given in Table II. In the two last columns the values of α_i/f^2 and of $(\alpha_{\text{exp}} - \alpha_{\text{cl}})/f^2$ are given; from a comparison of these, we can see that the anomalous absorption may be thought of as being entirely of molecular origin till the temperature of $25 \text{ }^{\circ}\text{C}$. Below this temperature another term adds, that is probably due to structural processes; to this term Hall's theory is not applicable as we showed above.

It must be observed that the molecular term increases when temperature diminishes, contrary to what experience gives for liquids with exclusively molecular anomalous absorption, like, for instance, CCl_4 . It is possible that the increase of α_i/f^2 , when temperature falls below $0 \text{ }^{\circ}\text{C}$, may become more

(14) J. O. HIRSCHFELDER, C. F. CURTISS and R. B. BIRD: *Molecular Theory of Gases and Liquids* (New York, 1954), pp. 166, 562.

(15) J. R. PARTINGTON: *An Advanced Treatise on Physical Chemistry*, vol. I (London, 1949), p. 874, eq. (21).

(16) LANDOLT-BÖRNSTEIN: *I Band 2. Teil, Moleküle I* (Berlin, 1951).

accentuated than it may result from the table because of the specific heat's c_p anomaly at low temperatures.

We must also emphasize that our calculations at high temperatures corresponding to the values chosen for the force constants and for the molecular oscillation frequency are in good agreement with the experimental results; it is not to be excluded, as NETTLETON observed for ethyl alcohol, that the agreement might be casual; worthy of note is, however, the fact that the method gives good results for two so different substances as anilin and ethyl alcohol.

2.2. Anilin-carbon tetrachloride mixtures. — The ultrasonic absorption curves in anilin-carbon tetrachloride mixtures, at temperatures of 25 °C and 42 °C (see Fig. 2), go regularly from the value belonging to CCl_4 , to that belonging to anilin, with the characteristic initial fall caused by the effect that impurities—in this case anilin—have on the molecular origin absorption of a non-associated liquid. In the frequency range in which measures were made the values of α/f^2 are independent of frequency. Measures recently made by K. EPPLER (1) on this mixture until an anilin molecular concentration of about 6%, at the temperature of 23 °C, showed values for α/f^2 perfectly analogous to those we found.

In Fig. 2 is represented a dotted curve, which has been calculated for the temperature of 42 °C, according to the expression given for α/f^2 by PINKERTON (4) for mixtures of two non-associated liquids *A* and *B*:

$$(13) \quad \left(\frac{\alpha}{f^2}\right)_y = \frac{(\alpha/f^2)_B}{(v_A/v_B)(1-y) + 1} \left\{ \frac{1-y}{(\alpha_B v_B / \alpha_A v_A)(1-y) + y} + y \right\},$$

y is the molecular concentration of *B*, v_A and v_B the ultrasonic velocity in *A* and in *B*. Here *A* and *B* are respectively CCl_4 and anilin: this is supposed to be completely non-associated at the temperature of 42 °C, as it seems to result from our precedent discussion. The resulting curve is somewhat different, for middle anilin concentrations, from the one that describes the experimental results at that temperature; differences are not very great; it nearly preludes the successive behaviour of mixtures at low temperatures.

At temperatures of —5 °C and —20 °C absorption presents a clear maximum, corresponding to a molecular anilin concentration of 22% at —5 °C and of 29% at the lower temperature. Around the maximum the ratio α/f^2 depends on frequency: it diminishes when frequency rises and this effect is more accentuated at 20 °C. It results from the tabulated values that the tem-

(17) K. EPPLER: *Zeits. f. Naturfor.*, **10a**, 744 (1955).

perature coefficient of α/f^2 , which initially is positive, changes its sign for an anilin molecular concentration of about 4% and afterwards remains negative. The ratio $\alpha_{\text{exp}}/\alpha_{\text{cl}}$ varies with temperature and concentration.

Mixtures here studied present, therefore, at low temperature, the characteristic behaviour of water-ethyl alcohol mixtures; the absorption excess seems to be caused by a perturbation of an equilibrium existing among different structural states in the mixtures. This perturbation may be caused by pressure and temperature fluctuations accompanying the ultrasonic wave passage and it is difficult to separate the two different contributions.

L. R. O. STOREY (18) thinks that, for water-alcohol mixtures, the anomalous absorption derives mainly from an interaction among the molecules of water and alcohol which form a complex structure which contributes to the specific heat with a finite relaxation time. He deduces from the position of the absorption maximum that the aggregates must be formed from four molecules of water around an alcohol one. Here, however, both liquids are polar. If we want to extend this model to anilin- CCl_4 mixtures and if we suppose that the maximum of absorption happens for a molecular anilin concentration of 30%, then we should admit the existence of aggregates of two molecules of CCl_4 with one of anilin. We don't understand how this could happen, since CCl_4 is an inert liquid, which cannot interact with other molecules. For the same reason it seems that the model, recently elaborated by O. NOMOTO (19) for water-alcohol mixtures cannot be applied to our mixture. It is most probable that we have an association of anilin molecules among themselves, which could occur at the temperature we used.

Because of the remarkable variation of α/f^2 with frequency, the characteristic relaxation frequency may be calculated from experimental data, by the formula of H. O. KNESER (20), that is valid for any process determining the absorption:

$$(14) \quad \frac{\alpha}{f^2} = \frac{A}{1 + (f/f_m)^2} + B,$$

where B includes the classical absorption and the residual absorption, measurable at very high frequencies compared with f_m . We tried to calculate roughly this term in various ways. First, for a mixture concentration near the absorption maximum, we extrapolated the experimental curves obtained in the region of high dilution as far as the concentration of the maximum. Secondly we thought of using the formula of Pinkerton (13) for a mixture, at -5°C or at -20°C , in which CCl_4 is present with its effective absorption

(18) L. R. O. STOREY: *Proc. Phys. Soc.*, B **65**, 943 (1952).

(19) O. NOMOTO: *Journ. Phys. Soc. Japan*, **11**, 827 (1956).

(20) H. O. KNESER: *Ann. d. Phys.*, **32**, 277 (1938).

coefficient and anilin with an absorption coefficient measured at high temperature, where anilin is surely dissociated. Then we subtracted from α/f^2 the term B and calculated $\alpha' = f^2(\alpha_{\text{exp}}/f^2 - B)$; plotting $1/\alpha'$ against $1/f^2$ we draw a straight line which gives the values of relaxation parameters A and f_m . At -20°C and for the anilin concentration that gives the maximum of absorption, taking $B = 107 \cdot 10^{-17} \text{ cm}^{-1} \text{ s}^2$, results $A = 470 \cdot 10^{-17} \text{ cm}^{-1} \text{ s}^2$, $f_m = 44 \text{ MHz}$. From f_m the relaxation time τ may be obtained, because:

$$(15) \quad f_m = \frac{1}{2\pi\tau}.$$

For this mixture $\tau = 3.6 \cdot 10^{-9} \text{ s}$.

3. - Conclusions.

The interpretation of the ultrasonic absorption measures in anilin and in anilin- CCl_4 mixtures at various temperatures, by Nettleton's theory shows that at temperatures higher than the ordinary one, anilin behaves like a non-associated liquid with an ultrasonic absorption which is partly of molecular origin and partly of classical origin. A term, that probably is of structural origin, adds, at low temperatures, to the absorption; this term is due to the formation of particular molecular configurations in liquids and mixtures.

Theoretical knowledge on ultrasonic absorption in liquids, however is not so advanced to surely indicate the anomalous absorption origin here measured at low temperatures.

RIASSUNTO

È stato misurato l'assorbimento di ultrasuoni, di frequenza compresa tra 9 e 27 MHz, nell'anilina e in miscele di questa con tetracloruro di carbonio entro un ampio intervallo di temperatura, allo scopo di vedere quali fattori determinano l'assorbimento anomalo. Sembra potersi concludere, al lume di una recente teoria di R. E. NETTLETON, che a temperatura elevata l'anilina si comporta come liquido non associato, con assorbimento anomalo di origine molecolare. A temperatura bassa compare un altro contributo all'assorbimento, che probabilmente sta a indicare la formazione nell'anilina di complessi. In corrispondenza le miscele mostrano un netto massimo di assorbimento per una certa concentrazione molecolare di anilina; il massimo è tanto più marcato quanto più bassa è la temperatura e ha un'altezza variabile con la frequenza degli ultrasuoni.

Elastic Scattering of Polarized Photons.

D. BRINI, E. FUSCHINI, L. PELI and P. VERONESI

Istituto di Fisica dell'Università - Bologna

Istituto Nazionale di Fisica Nucleare - Sezione di Bologna

(ricevuto l'8 Gennaio 1958)

Summary. — Rayleigh's cross-section for a partially polarized photon beam may be expressed as: $d\sigma/d\Omega = d\sigma_0/d\Omega + \xi(d\sigma_1/d\Omega)$, where $d\sigma_0/d\Omega$ is the term resulting from the non-polarized component and $d\sigma_1/d\Omega$ that due to polarization, ξ being the beam polarization degree in respect to the scattering plane. By polarizing a photon beam through a Compton scattering, a given Rayleigh scattering angle θ being fixed, an asymmetry ratio may be defined by: $R = (d\sigma_0/d\Omega + \xi_{\parallel}(d\sigma_1/d\Omega)) / (d\sigma_0/d\Omega + \xi_{\perp}(d\sigma_1/d\Omega))$, where the numerator is Rayleigh's cross-section for the angle θ in the Compton scattering plane, and the denominator is the same cross-section in the plane perpendicular to the Compton scattering one. R has been measured in the polarized photon elastic scattering, by using photons with a $0.64mc^2$ energy scattered on Hg with a $\theta \sim 90^\circ$ angle. The experimental results appear to be in conformity with the theoretical previsions.

1. — Introduction.

It is known that photon elastic scattering takes place through the following four processes, which depend on the different mechanisms of interaction with matter:

- a) Rayleigh scattering or « electron resonance scattering », resulting from interaction with the atom electrons;
- b) Thomson scattering due to interaction with the electric charge of the nucleus;
- c) Delbrück scattering due to interaction with the electric field of the nucleus;
- d) Nuclear resonance scattering resulting from absorption and successive re-emission of the incident photon by the nucleus.

At energies lower than 0.5 MeV, Rayleigh scattering only is of any significance, the cross-sections of the other processes being very small.

Different theories have been proposed for calculating the cross-section of Rayleigh scattering.

A first calculation was made by FRANZ⁽¹⁾, using the Thomas-Fermi model of the atom. He considered the intermediate states as free and used, moreover, a non-relativistic approximation, assuming that the momentum q transferred to the electron is $\ll mc$.

BETHE⁽²⁾ made the same calculation considering only the K shell of Pb, assuming relativistic wave functions for the electrons of this shell. Following Bethe's criterium, LEVINGER⁽³⁾ made the calculations for the K shell of Sn disregarding the non-relativistic condition $q \ll mc$. Finally a calculation which completely considers the great momentum exchanges, the effect of binding in the intermediate states and an atomic model based on the effective relativistic wave functions of the K orbit electrons has been made for Hg by BRENNER, BROWN and WOODWARD⁽⁴⁾ for photons of energy $0.32mc^2$ and by BROWN and MAYER⁽⁵⁾ for photons of energy $0.64mc^2$, making use of a mathematical formalism suggested by BROWN, PEIERLS and WOODWARD⁽⁶⁾.

Various experiments have been carried out with non-polarized photons to determine the elastic scattering cross-sections at the different energies⁽⁷⁻²³⁾.

⁽¹⁾ W. FRANZ: *Zeits. Phys.*, **98**, 314 (1936).

⁽²⁾ Private communication to WILSON (see ref. ⁽¹¹⁾).

⁽³⁾ J. S. LEVINGER: *Phys. Rev.*, **98**, 656 (1952).

⁽⁴⁾ S. BRENNER, G. E. BROWN and J. B. WOODWARD: *Proc. Roy. Soc.*, A **227**, 59 (1954).

⁽⁵⁾ G. E. BROWN and D. F. MAYER: *Proc. Roy. Soc.*, A **234**, 387 (1956).

⁽⁶⁾ G. E. BROWN, R. E. PEIERLS and J. B. WOODWARD: *Proc. Roy. Soc.*, A **227**, 51, (1954).

⁽⁷⁾ E. C. POLLARD and D. E. ALBURGER: *Phys. Rev.*, **74**, 926 (1948).

⁽⁸⁾ A. STORRUSTE: *Proc. Phys. Soc.*, A **63**, 1197 (1950).

⁽⁹⁾ W. G. DAVEY: *Proc. Phys. Soc.*, A **66**, 1059 (1953).

⁽¹⁰⁾ T. D. STRICKLER: *Phys. Rev.*, **92**, 923 (1953).

⁽¹¹⁾ R. R. WILSON: *Phys. Rev.*, **90**, 720 (1953).

⁽¹²⁾ L. GOLDZAHL and P. EBERHARD: *Compt. Rend. Acad. Sci.*, **240**, 965 (1955).

⁽¹³⁾ L. GOLDZAHL and P. EBERHARD: *Compt. Rend. Acad. Sci.*, **240**, 2304 (1955).

⁽¹⁴⁾ J. L. BURKHADT: *Phys. Rev.*, **100**, 192 (1955).

⁽¹⁵⁾ J. R. COOK: *Proc. Phys. Soc.*, A **68**, 1170 (1955).

⁽¹⁶⁾ A. K. MANN: *Phys. Rev.*, **101**, 4 (1956).

⁽¹⁷⁾ P. EBERHARD, L. GOLDZAHL, E. HARA and J. MEY: *Compt. Rend. Acad. Sci.*, **242**, 484 (1956).

⁽¹⁸⁾ P. EBERHARD, L. GOLDZAHL, E. HARA and E. ALEXANDRE: *Compt. Rend. Acad. Sci.*, **243**, 1862 (1956).

⁽¹⁹⁾ P. EBERHARD, L. GOLDZAHL, E. HARA and J. MEY: *Phys. Rad.*, **17**, 573 (1956).

⁽²⁰⁾ S. MESSELT and A. STORRUSTE: *Proc. Roy. Soc.*, A **69**, 381 (1956).

⁽²¹⁾ H. SCHOPPER: *Zeits. Phys.*, **147**, 253 (1957).

⁽²²⁾ L. GOLDZAHL and P. EBERHARD: *Journ. Phys. Rad.*, **18**, 33 (1957).

⁽²³⁾ E. HARA, J. BANAIGS and J. MEY: *Compt. Rend. Acad. Sci.*, **244**, 2155 (1957).

The measurements at energies greater than 1 MeV were made in order to bring out the eventual existence of Delbrück scattering, while those performed at energies lower than 0.5 MeV were for the purpose of verifying the theoretical values foreseen for Rayleigh scattering. Even if the results of the measurements made by other authors for photons with an energy $h\nu = 1.33$ MeV on Pb are affected by considerable errors and, moreover, fail to show any satisfying mutual agreement, it seems that there is a slight tendency in favour of a qualitative experimental demonstration of Delbrück scattering.

Nevertheless, recent calculations by BROWN and MAYERS (24) for 1.305 MeV energies have produced values for the Rayleigh scattering cross-sections which for Sn have been verified experimentally by HARA, BANAIGS and MEY (23), and would seem to preclude the existence of potential scattering. This situation shows that to be able to give a quantitatively correct figure of this effect there is need of a correct theoretical knowledge of Rayleigh scattering. Here in lies the importance of this effect.

The experimental control of the theories on Rayleigh scattering can be made only at energies considerably lower than 1 MeV, because, as has already been pointed out, at low energies the Rayleigh scattering is the only evident significant elastic process.

The only experiments which have been made at low energies are Mann's (16) at 0.41 MeV and 0.66 MeV on Sn and Pb, Storruste's (8) at 0.41 MeV on Pb, Schopper's (21) at 0.325 MeV and 0.66 MeV on Pb, Cu and Al and, lastly, Burkhardt's (14) at 0.5 MeV and 0.59 MeV on Pb, In, Cd, Cu and Al. The results of these measurements, which are sufficiently coherent one with another, are in general agreement, within the considerable experimental errors, with Franz's forecasts, at least for angles $< 90^\circ$, except in the case of Sn in Mann's experiments, where the agreement seems to be better with Bethe's calculations.

The possibility of comparing any experimental results with Brown and Mayers' recent calculations does not exist, because the only measurement which has been carried out at an energy of about $0.64mc^2$ is Schopper's, which, however, is limited to small angles ($5^\circ < \theta < 20^\circ$), where the contributions of the different atom shells are comparable one with the other, while the theoretical calculations of the above-mentioned authors give no more the K shell contribution.

We have made a measurement on the elastic scattering by using a partially-polarized photon beam of energy corresponding to that considered by BROWN and MAYERS in their calculations. In this way it has been possible to subject also the contribution of the terms depending on the photon polarization state

(24) Referred to under (23) above.

to experimental verification. The following sections contain a detailed description of the criterium we adopted, which is somewhat different from that used by other authors.

2. - Theoretical considerations.

As is known, the term polarization degree of a radiation beam defines a quantity ξ which represents the difference between the intensities of two component beams, with orthogonal polarization states, which may be used to represent the total beam, its intensity being normalized to unity.

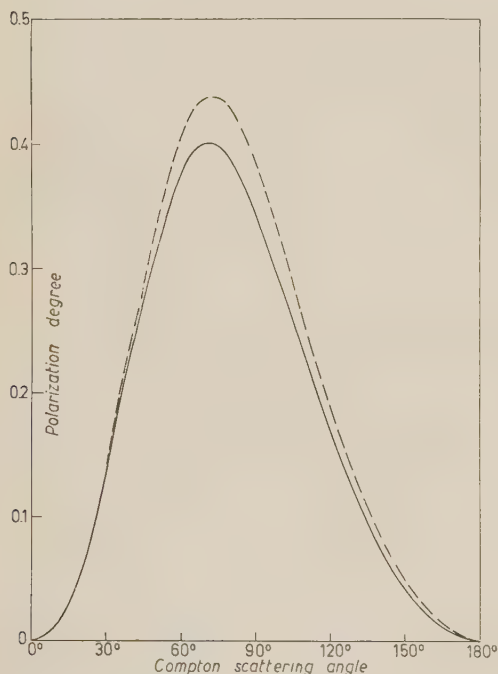


Fig. 1.

For a photon beam, polarized by means of a Compton scattering, ξ may be written using the formalism of Stokes' parameter and Fano's matrix ⁽²⁵⁾ immediately as

$$\xi = \frac{-\sin^2 \theta_c}{1 + \cos^2 \theta_c + (k_0 - k)(1 - \cos \theta_c)},$$

where the component beams were chosen the one parallel to the Compton scattering plane and the other orthogonal, and where

θ_c = Compton scattering angle,

k_0 = incident photon energy in mc^2 units,

k = diffused quantum energy in mc^2 units.

If the component beams, instead of being related to the Compton scattering plane, are related to a generic plane, forming an angle φ therewith, the use of Stokes' parameters immediately furnishes:

$$\xi_\varphi = \frac{-\sin^2 \theta_c}{1 + \cos^2 \theta_c + (k_0 - k)(1 - \cos \theta_c)} \cos 2\varphi.$$

The behaviour of ξ as a function of θ_c , for $\varphi = 0$, in relation to the energies of 1.33 MeV and 1.17 MeV of ^{60}Co is shown in Fig. 1.

⁽²⁵⁾ W. H. McMMASTER: *Amer. Journ. Phys.*, **22**, 351 (1954).

Rayleigh's cross-section for partially-polarized photons is given by

$$(1) \quad \frac{d\sigma}{d\Omega} = \frac{d\sigma_0}{d\Omega} + \xi \frac{d\sigma_1}{d\Omega},$$

where $d\sigma_0/d\Omega$ is Rayleigh's cross-section for a non-polarized photon beam, ξ the polarization degree of the incident beam, the component beams being related to the scattering plane; and $d\sigma_1/d\Omega$ the term sensitive to polarization.

In the paper of FRANZ the cross-section for a totally linearly polarized incident wave is represented by

$$(2) \quad \frac{d\sigma}{d\Omega} = r_0^2 |\mathbf{a} \wedge \mathbf{e}'|^2 \cdot A^2,$$

where r_0 = classic radius of electron,

\mathbf{a} = direction of the incident wave potential vector,

\mathbf{e}' = diffusion direction,

A = form factor.

Bearing (2) and the meaning of ξ in mind, it is possible, by means of simple formal transformations, to express the cross-section in the form (1). One finds, explicitly

$$\frac{d\sigma}{d\Omega} = r_0^2 A^2 [(1 + \cos^2 \theta) + \xi(\cos^2 \theta - 1)],$$

where θ is the Rayleigh scattering angle.

Fig. 2 represents the behaviour of $d\sigma_0/d\Omega$ and $-d\sigma_1/d\Omega$ in r_0^2 units limited to angles greater than 40° for the energy of $0.64 mc^2$.

The explicit expression of (1), as may be deduced from Brown and Mayer's calculations, is given by

$$\frac{d\sigma}{d\Omega} = r_0^2 [(AA^* + BB^*) + \xi(AB^* + A^*B)],$$

where

$$A = M(1', 1) + M(2', 2)$$

$$B = M(1', 2) + M(2', 1),$$

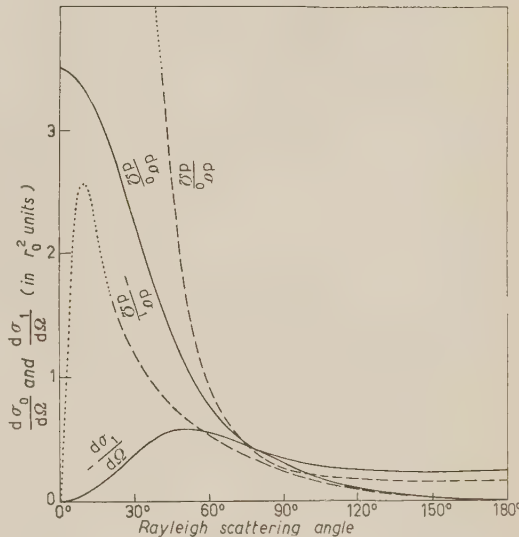


Fig. 2.

the functions $M(1', 1)$, $M(2', 2)$, $M(1', 2)$ and $M(2', 1)$ being the transition amplitudes between leftspinning and rightpinning circular polarization states of the incident and diffused photons. Their expression defined as a function of the θ scattering angle is given in the above-mentioned article by BROWN and MAYER. The behaviour of $d\sigma/d\Omega$ and $-d\sigma_1/d\Omega$ resulting from these calculations is shown in Fig. 2 in r_0 units for $0.64 mc^2$ energy.

Let us now suppose we have a partially-polarized beam, and let a generic reference plane be fixed. Let us consider the Rayleigh scattering of this beam at a given θ angle in respect to the incidence direction, once on the chosen reference plane and once on the orthogonal plane. It is then possible to define a ratio between the intensities scattered on the two planes. Such a ratio is obviously expressed by

$$R = \frac{(d\sigma_0/d\Omega) + \xi_{\parallel} (d\sigma_1/d\Omega)}{(d\sigma_0/d\Omega) + \xi_{\perp} (d\sigma_1/d\Omega)},$$

where ξ is the polarization degree of the incident beam calculated by relating the component beams to the chosen reference plane and ξ_{\perp} is the polarization degree calculated by relating the component beams to the plane perpendicular to the reference plane. The definition of ξ implies that $\xi_{\parallel} = -\xi_{\perp}$.

We planned and carried out an experiment leading to a measurement of R in a particular case.

Starting from γ radiations of a ^{60}Co source of 1.33 MeV and 1.17 MeV, one may obtain, by means of Compton scattering at an angle $\theta_0 = 100^\circ$, a beam of partially polarized photons, of $0.64 mc^2$ mean energy. Taking the Compton scattering plane as the reference plane, the polarization degree of this polarized beam has the value $\xi_{\perp} = 0.307$, $\xi_{\parallel} = -0.307$. A successive Rayleigh scattering of the partially polarized beam on Hg allowed to measure the previously defined R ratio for $\theta = 90^\circ$. At this angle such a ratio has the theoretical values,

$$R = 1.886 \quad (\text{FRANZ}),$$

$$R = 1.813 \quad (\text{BROWN and MAYER}).$$

3. — Experimental arrangement.

Adequately collimating a ^{60}Co source, of about 2 Curie, we sent a photon beam on to a cylindrical Cu target of 3 cm height and 2.54 cm diameter. A second collimation, obtained by means of a hole of 2.5 cm diameter in a 25 cm thick Pb wall, along a direction forming an angle $\theta_c = 100^\circ$ with that of the incident beam, gave us a beam of partially-polarized photons with a

mean energy $h\nu = 0.64 mc^2$. This beam was directed on to a Hg target, consisting of a thin-walled plexiglas container holding the liquid.

We could rotate the target around its axis made to coincide with that of the second collimator. The form of the target was so chosen as to permit a just compromise between intensity diffused through Rayleigh scattering, self-absorption and angular dispersion. Detection of the elastically-scattered photons was carried out by means of a scintillation counter consisting of a 1 in. \times 1 in. NaI(Tl) crystal, mounted on a Du Mont 6292 photomultiplier, set up in such a manner that the crystal centre was at a distance of 15 cm from the centre of the target on the normal to the direction of the polarized incident beam. Measurements were carried out once on the Compton scattering plane and once on the normal one through contemporaneous target and counter rotation. Fig. 3 shows a to-scale drawing of the experimental set-up. The electronic detection system consisted of a conventional chain formed of a cathode follower, an amplifier, a wide channel differential pulse analyzer, counting circuit and power supplies. For the calibration of the equipment, as will be described hereafter, we used a single channel differential discriminator of the kind described by JOHNSTONE (26), with slight modifications.

4. - Measurement calibration and control.

The radiation energy spectrum scattered at $\theta_c = 100^\circ$ through Compton scattering and constituting the partially-polarized beam, is shown in Fig. 4, together with that of a ^{51}Cr source which emits monochromatic rays with an energy $h\nu = 0.323$ MeV. Since our detection system had an 11% energy re-

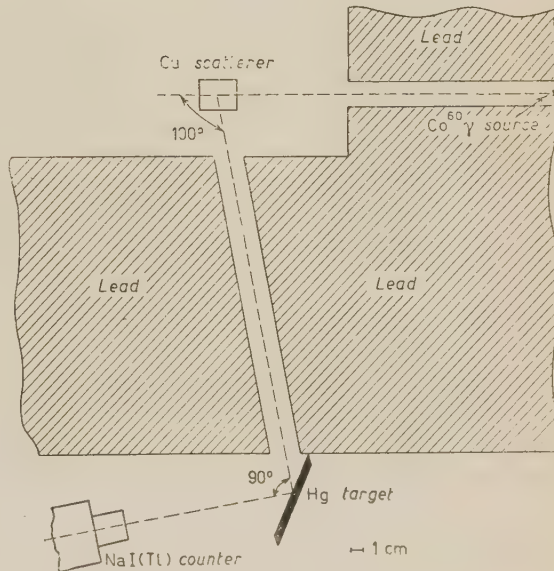


Fig. 3.

(26) C. W. JOHNSTONE: *Nucleonics*, **11** (1), 36 (1953).

solving power at half maximum for the ^{51}Cr line and the scattered radiation spectrum showed a 22% dispersion at half maximum, we may conclude that the polarized radiation beam had an energy dispersion of about 5% around the mean value of 0.64 mev^2 . That means that the energy band of the photons used was included, roughly speaking, between 0.308 MeV and 0.344 MeV, the mean value being at 0.326 MeV.

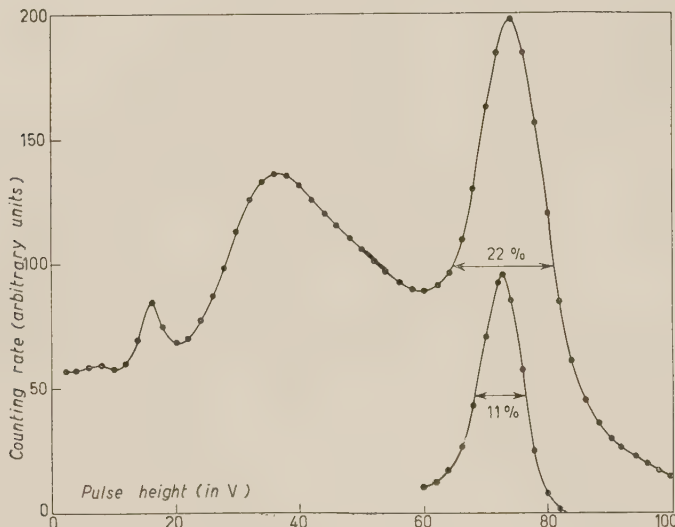


Fig. 4.

A check of the whole detection arrangement was made by a systematic extraction of the ^{51}Cr spectrum and a correction of the gains so that the photoelectric peak was always included within the same channel. Particular attention was given to this check, since it is known that, in measurements of this kind which are rather lengthy, one of the major difficulties is exactly that of gain stability.

Great care was, moreover, dedicated to the separation of the events arising from the elastic scattering on the Hg from other events which were concomitant though of different origin.

From an observation of the experimental disposition figure, it may be seen that the possible events to be detected by the counter are the following ones:

1) Photons which have undergone Compton scattering on the first Cu target and elastic scattering on the Hg. This is the event which is of interest to us.

2) Photons which have undergone elastic scattering on the Cu and Compton scattering on the Hg; the final mean energy of such photons appears to be comparable with that of the photons resulting from the events of interest to us. Nevertheless, their frequency has been estimated at about 0.5% of the frequency of the events under study, and, in consequence, we ignore them.

3) Photons which have undergone double elastic scattering on the Cu and Hg. The probability of detecting an event of this kind is extremely small and quite negligible.

4) Photons which have undergone a Compton scattering on both the first Cu target and the second Hg one. The frequency of this events is considerably higher than that corresponding to the events under consideration and has been estimated at about two orders of magnitude higher.

It is clear then that on no account must any event of the Compton-Compton type be included in the measurement of the elastically-scattered intensity. When the effective geometry of the experiment is borne in mind, we can see that, in the most unfavourable conditions, Compton-Compton photons with an energy of about 0.220 MeV may arise. With the introduction of dispersion in the detection, these photons may be registered as if they had a 0.240 MeV energy. From the same geometry, as well as from the spectrum in Fig. 5, we have deduced a lower limit value of about 0.3 MeV for the energy of the Compton scattered beam. Considering also the energy resolution, these photons may be registered (in relation to the photoelectric line) as if they had an energy of about 0.285 MeV. From these valuations, therefore, there arises the possibility, through a well-chosen analyzer channel, of an absolute separation of the elastic events from the inelastic ones.

Nevertheless, we carried out an experimental test to verify the validity of these considerations. For this purpose we substituted the Hg target with an Al target with the same geometry.

The elastic scattering cross-section at 90° for 0.326 MeV energy photons in Al appeared about 250 times less than for Hg, for which reason a negligible elastic scattering frequency in the Al was to be expected. Prearranging the discriminator's cut-off according to the valuations previously made and measuring count frequencies, once with the second collimation shut (in order to deduct background) and once with open collimator, the eventual differences would have put the existence of any Compton-Compton contribution into evidence. By increasing the precision of these measurements to the limit of sensitivity of the small elastic scattering contribution, we found that the frequencies measured with open and closed collimators to be the same. This confirmed the absence of a Compton-Compton contribution.

5) Other events, as for example, electrons from photoelectric scattering, were neglected owing to the very slight probability of our being able to verify them.

In the measurement, the background consisted of:

- a) cosmic rays;
- b) radioactivity characteristic of the material used (27);
- c) radiation scattered through the ^{60}Co source container walls.

Using suitable screens, we reduced the background which, nevertheless, remained considerable. The measuring of the background was carried out according to the criterium already mentioned, i.e. by closing the hole of the second collimator.

We made three measurement runs, in the second and third of which we further restricted the energetics selection channel of the events in comparison to that used in the first measurement. This allowed us to verify the constancy, within the errors, of the ratio measured under different experimental conditions. Table I reports the results of the three runs of measurements. The R_0 ratio measured taking the weighted mean of the individual measurements, appears as

$$R_0 = 1.600 \pm 0.059.$$

TABLE I.

		$\varphi = 0^\circ$ plane		$\varphi = (\pi/2)^\circ$ plane		R_0 value
		Total number of events	Background	Total number of events	Background	
1 ^o run	Total number of counts	34 288	23 399	48 320	39 947	1.614 ± 0.075
	Time in minutes	4 785	4 499	6 415	6 326	
2 ^o run	Total number of counts	14 339	10 709	27 728	24 297	1.593 ± 0.126
	Time in minutes	3 120	3 130	4 655	4 655	
3 ^o run	Total number of counts	19 822	14 036	25 440	24 245	1.561 ± 0.144
	Time in minutes	4 430	4 031	4 125	4 385	

The mean value of R_0 results, $R_0 = 1.600 \pm 0.059$.

(27) E. C. MILLER, L. D. MARINELLI, R. E. ROWLAND and J. E. ROSE: *Nucleonics*, **14** (4), 40 (1956).

This result must evidently be corrected for the inevitable presence of a geometric asymmetry connected with the experimental arrangement. The amount of this geometric asymmetry was measured directly in the following way. The primary beam of non-polarized photons was directed through the second collimator straight at the Hg target. In the two positions of the experiment, we measured the elastic scattering frequencies of the 1.33 MeV and 1.17 MeV photons, the analyzer channel having been fixed in such a manner as to receive only photoelectric peaks. Thus the frequencies measured depended only on the geometry, since the fixed bias cut-off excluded any contribution resulting from scattering on the screen and collimator walls.

The background in the measurement was measured by closing the first collimator. Two measurement runs were made, the results of which will be found in Table II. The weighted mean of these shows that the ratio between the perpendicular plane frequencies and those in the Compton scattering one, appears as:

$$R_g = 1.069 \pm 0.006 .$$

TABLE II.

	$\varphi = 0^\circ$ plane		$\varphi = (\pi/2)^\circ$ plane		R_g value
	Total number of events	Background	Total number of events	Background	
1 ^o run	Total number of counts	10 585	1 789	10 485	1 864
	Time in minutes	395	720	360	700
2 ^o run	Total number of counts	65 268	5 004	55 291	4 910
	Time in minutes	2 070	2 070	1 636	1 776

The mean value of R_g results, $R_g = 1.069 \pm 0.006$.

It follows therefore that the true asymmetry ratio referring to the elastic scattering of the partially-polarized photon beam is given by:

$$R = R_0 R_g = 1.711 \pm 0.064 ,$$

with a relative error of 3.72%.

5. – Comparison with the theories and conclusions.

To compare the experimental results with the theoretical previsions one must take very precise account of the effective geometry of the experimental set up.

The values of the ratio R calculated with Franz's and Brown and Mayers' theories, obviously referred to an ideal geometry, where the sources and targets were considered as punctiform; moreover, for the primary beam photons a mean energy of 1.25 MeV was assumed. An exact valuation for R taking target's and counter's finite dimensions into account appears to be extremely complicated. It is absolutely necessary to introduce some schematizations to simplify the calculation without sensibly altering the value of R to be calculated. Since such a calculation is important for a comparison with the experimental results, it may be of interest to report its fundamental criteria. We set about through an individual analysis of the causes which, in the experimental arrangement adopted, might raise or lower the value of R in respect to that calculated in the ideal geometry.

1) Causes which may rise the ratio. Through primary absorption in the Cu polarizer the photons scattered in the first strata of the material are greater in number than those scattered in the last one. Moreover, to the first strata there corresponds a mean Compton scattering angle which is smaller than the one corresponding to the last ones. This circumstance is important for the calculation of the effective polarization degree which appears greater than that calculated under ideal conditions.

2) Causes which may lower the ratio.

a) Since the counter has finite dimensions, it detects scattered photons with azimuthal angles φ_{\parallel} and φ_{\perp} included respectively in the intervals:

$$-\psi \leq \varphi_{\parallel} \leq \psi; \quad \frac{\pi}{2} - \psi \leq \varphi_{\perp} \leq \frac{\pi}{2} + \psi,$$

where ψ indicates the maximum azimuthal angular dispersion in our geometry.

Since $\xi_{\varphi_{\parallel}} = \xi_{\varphi=0} \cos 2\varphi_{\parallel}$ and $\xi_{\varphi_{\perp}} = \xi_{\varphi=\pi/2} \sin 2\varphi_{\perp}$ and $\cos 2\varphi_{\parallel} < 1$, $\sin 2\varphi_{\perp} < 1$ this fact tends to lower the ratio R .

b) The photons elastically-scattered on Hg are diffused around the angle $\theta = 90^\circ$. Since the Rayleigh cross-section is still sufficiently sensitive to the scattering angle in this area, an examination of the curves in Fig. 2 shows that this circumstance contributes to lowering the ratio R .

Considering these effects in bulk the final theoretical values obtained from the two theories appear as:

$$R = 1.84 \quad (\text{FRANZ}),$$

$$R = 1.76 \quad (\text{BROWN and MAYERS}).$$

For a comparison of the experimental result with these values, it is necessary to make some further reservations.

The comparison with Franz's theory may be made at once, owing to the atom model used in this theory and since, for photons of $0.64 mc^2$ energy we may have no hesitation in excluding the existence of a slight quasi-elastic scattering contribution (28).

The comparison with Brown and Mayers' theory is less direct, since, as we have already pointed out, these authors went no further than the valuation of the K -shell contribution only. In effect, however, the other shells also contribute to Rayleigh scattering. At large scattering angles, to which there corresponds a considerable momentum transferred to the electron, the L -shell alone makes a still-appreciable contribution. According to BROWN and WOODWARD (29) such a contribution corresponds approximately to $\frac{1}{8}$ of the K -shell contribution at the same angle. Since we were unable to find in the literature any indication about influence of the L -shell on Rayleigh scattering azimuthal anisotropy we took the two following limiting possibilities into account:

- 1) The L -shell contribution may be isotropic in the azimuthal distribution. In this case the theoretical ratio calculated for the effective geometry of the experiment results to be $R = 1.65$.
- 2) The L -shell contribution may show the same anisotropy as for the K -shell. In this case the ratio R does not suffer L -shell influence, and the experimental result may be directly compared with Brown and Mayer's theoretical one, disregarding the exact value of the L -shell contribution.

Since we deem it reasonable to consider the true situation as representing an intermediate case between the limiting cases considered, it may be deduced that the theoretical value of R is, in any case, included between 1.76 and 1.65.

In conclusion it may be affirmed that, whatever the effect of the L -shell contribution, the experimental value of R we have found agrees with Brown and Mayers' previsions, within only one statistical error, while, in the case of Franz's theory, agreement was only obtained within thrice the statistical error. This fact points to a preference for Brown and Mayers' theory.

(28) J. RANDLES: *Proc. Phys. Soc.*, A **70**, 337 (1957).

(29) G. E. BROWN and J. WOODWARD: *Proc. Phys. Soc.*, A **65**, 977 (1952).

* * *

We should like to thank Professor A. BORSELLINO and his co-workers, Dr. G. PASSATORE and Dr. G. BÖBEL, for the help given us in the examination of the theoretical questions, and Mr. R. DEGLI ESPOSTI for the setting up of the electric circuits.

Note added in proof.

After the conclusion of this experiment we received from Drs. BROWN and MEYERS preprints and private communications about their calculations concerning the energies of 1.28 and $2.50mc^2$. We wish to acknowledge their kindness in doing so.

RIASSUNTO (*)

La sezione d'urto Rayleigh, per un fascio di fotoni parzialmente polarizzati, può mettersi nella forma: $d\sigma/d\Omega = d\sigma_0/d\Omega + \xi(d\sigma_1/d\Omega)$, dove $d\sigma_0/d\Omega$ è il termine dovuto alla componente non polarizzata e $\xi(d\sigma_1/d\Omega)$ è il termine dovuto alla polarizzazione, ξ essendo il grado di polarizzazione del fascio rispetto al piano dello scattering. Polarizzando un fascio di fotoni con uno scattering Compton e fissato un certo angolo di scattering Rayleigh θ , si può definire un rapporto di asimmetria ponendo $R = (d\sigma_0/d\Omega + \xi_{\parallel}(d\sigma_1/d\Omega))/(d\sigma_0/d\Omega + \xi_{\perp}(d\sigma_1/d\Omega))$, dove il numeratore è la sezione d'urto Rayleigh per l'angolo θ nel piano di scattering Compton ed il denominatore la stessa sezione d'urto nel piano perpendicolare a quello di scattering Compton. È stata eseguita una misura di R nello scattering elastico di fotoni polarizzati usando fotoni di energia $0.64 mc^2$ scatterati su Hg con un angolo di scattering $\theta \simeq 90^\circ$. I risultati sperimentali si mostrano in buon accordo con le previsioni teoriche.

LETTERE ALLA REDAZIONE

(La responsabilità scientifica degli scritti inseriti in questa rubrica è completamente lasciata dalla Direzione del periodico ai singoli autori)

Circular Polarization of γ -Rays Emitted Opposite to β -Particles. Results on ^{46}Sc .

A. LUNDBY, A. P. PATRO and J. P. STROOT

CERN - Geneva

(ricevuto il 15 Novembre 1957)

In a previous paper ⁽¹⁾ we have reported results on ^{60}Co , ^{22}Na and calibration measurements with Bremsstrahlung from ^{90}Y and ^{32}P β -particles. The circular polarization of the γ -rays was measured by transmission through 15 cm magnetized iron.

In the present experiment a total amount of 0.5 mg fine Sc_2O_3 powder ^(*) was spread over a surface of 0.6 cm^2 on a backing of 5 μm Al. The source was mounted in a lucite housing as previously ⁽¹⁾. The strength of the source was about 300 μm C. The decay scheme of ^{46}Sc is believed to be $4^+ (\beta^- 360)$ $4^+ (\gamma 1120)$ $2^+ (\gamma 890)$ 0^+ (2) . In order to obtain a reasonable coincidence rate between β - and γ -rays (5 \div 10 per minute) we had to accept the photopeaks from both γ -rays in the $\text{NaI}(\text{Ti})$ -crystal ⁽⁺⁾. β -rays with energy above about 50 keV were accepted by the coincidence circuit.

Denoting the $\beta\gamma$ coincidence rates with the magnetic field pointing towards and away from the source by C_{down} and C_{up} respectively we have

$$(1) \quad \begin{cases} R = \frac{C_{\text{down}} - C_{\text{up}}}{\frac{1}{2}(C_{\text{down}} - C_{\text{up}})} = P \cdot 2 \cdot \tgh(N\nu\sigma T), \\ P = \frac{W_{-1} - W_{+1}}{W_{-1} + W_{+1}}, \end{cases}$$

where $W_{\mathcal{H}}$ is the number of γ -rays with helicity \mathcal{H} ^(\text{c}) registered in coincidence

⁽¹⁾ A. LUNDBY, A. P. PATRO and J. P. STROOT: *Nuovo Cimento*, **6**, 745 (1957).

^(*) Obtained from CEA, Saclay.

⁽²⁾ *Nuclear Level Schemes and Nuclear Data Cards*, National Research Council, Washington, D.C.

⁽⁺⁾ Initial experiments where only the highest energy photopeak was accepted indicated a different result from the present. However, the statistical errors were very large. We are therefore repeating this experiment with higher counting rates.

^(\text{c}) \mathcal{H} is $+1$ or -1 for γ -rays of right and left helicity respectively. Right helicity indicates that linear and angular momentum vectors are parallel.

with the β -rays. The ratio R for γ -rays with left helicity is plotted as a function of the γ -ray energy in Fig. 1. Calibration points from ^{20}Y and ^{32}P are indicated.

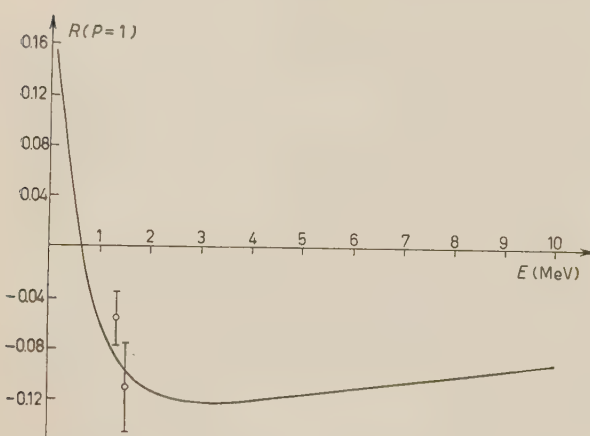


Fig. 1. — Ratio R of difference to half the sum of β - γ coincidence rates with magnetic field pointing towards and away from the source as a function of γ -ray energy ($P=1$).

statistical analysis of the data divided into 100 groups of consecutive runs which confirms the quoted error and checks the reliability of the data.

From (1) and Fig. 1 we find $P=+(18.8 \pm 7.3)\%$, which leads to an asymmetry coefficient (using $(v/c)=0.65$ in Eq. (2))

$$A=+0.29 \pm 0.11.$$

BOEHM and WAPSTRA⁽³⁾ and STEFFEN⁽⁴⁾ have determined A for ^{46}Sc using differential scattering of γ -rays against a magnetized iron cylinder in order to find the circular polarization of the γ -rays. They find

BOEHM and WAPSTRA	$A=+0.33 \pm 0.04$,
STEFFEN	$A=+0.23 \pm 0.06$.

The average is $+0.28$ with an estimated error of $(15 \div 20)\%$ to take into account systematic errors.

Discussion.

The correlation between the direction of β -particles with velocity v and γ -rays with helicity \mathcal{H} is given by

$$(2) \quad W_{\mathcal{H}}\left(\theta, \frac{v}{c}\right) = 1 + \mathcal{H} \cdot \frac{v}{c} \cdot A \cdot \cos \theta,$$

⁽³⁾ F. BOEHM and A. H. WAPSTRA: *Phys. Rev.*, **107**, 1202 (1957).

⁽⁴⁾ R. M. STEFFEN: private communication.

Individual readings of coincidence, γ - and β -counting rates were recorded automatically every 5 minutes with the magnetic field reversed between the readings⁽¹⁾.

The results for ^{46}Sc give

$$R=-(1.11 \pm 0.43)\%$$

where the error is the mean square deviation,

$$\varepsilon_R = \frac{(1 - (1/4) \cdot R)^{1/2}}{\frac{1}{2}(C_{\text{down}} + C_{\text{up}})^{1/2}}.$$

We have also made a

statistical analysis of the data divided into 100 groups of consecutive runs which

confirms the quoted error and checks the reliability of the data.

where A can be derived using techniques developed for the calculation of angular correlation of nuclear radiations. ALDER, STECH and WINTHER⁽⁵⁾ have published extensive calculations of A . For allowed β -transitions $J_a \rightarrow J_b$ followed by an electric quadrupole γ -transition $J_b \rightarrow J_c$ one obtains

$$(3) \quad A = -\frac{2}{3} F_1(2, 2J_c, J_b) \frac{F_1(1, 1, J_a, J_b) \frac{I_{GT-GT}}{(C_{GT})^2} + 2F_1(0, 1, J_a, J_b) \frac{(\int \beta)}{(\int \beta \sigma)} \frac{I_{GT-F}}{(C_{GT})^2}}{\frac{(\int \beta)^2}{(\int \beta \sigma)^2} \frac{(C_F)^2}{(C_{GT})^2} + 1},$$

where the functions F_1 are familiar from the theory of angular correlations⁽⁵⁾, and

$$(4) \quad \begin{cases} I_{GT-GT} = 2 \operatorname{Re} \left[(C_T C'_* - C_A C'_*) + i \frac{Z\alpha}{p} (C_A C'_* + C'_A C_T) \right], \\ I_{GT-F} = \operatorname{Re} \left[(C'_T C_S^* + C_T C'_S^* - C'_A C_V^* - C_A C'_V^*) + \right. \\ \quad \left. + i \frac{Z\alpha}{p} (C'_A C_S^* + C_A C'_S^* - C'_T C_V^* - C_T C'_V^*) \right]. \end{cases}$$

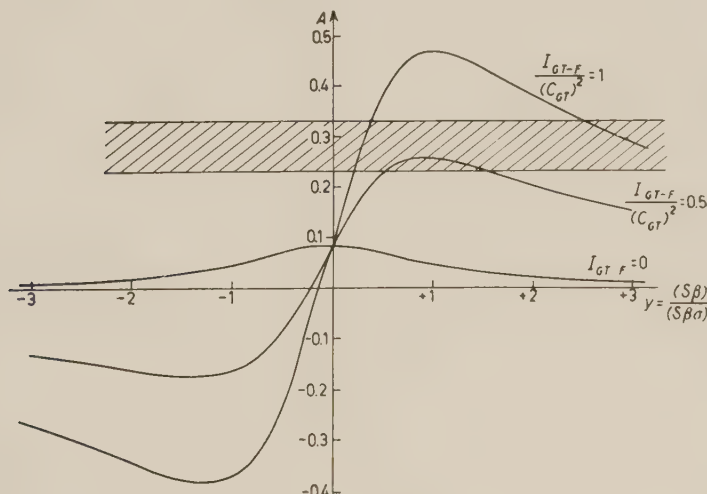


Fig. 2. — Relation between the asymmetry coefficient A and the ratio of Fermi to Gamow-Teller matrix elements. Curves are drawn for different values of the interference term I_{GT-F} . The experimental result is indicated by the shaded band.

The Fierz interference terms have been neglected in (3). Parity measurements for pure GT transitions give for $((I_{GT-GT})/(C_{GT})^2) = -1 \pm 0.1$. We have set the error to 10% due to experimental uncertainties besides statistical errors in the results.

⁽⁵⁾ K. ALDER, B. STECH and A. WINTHER: *Phys. Rev.*, **107**, 728 (1957).

Inserting in (3) numerical values for the coefficients F_1 we obtain

$$A = \frac{0.0834 + 0.745 \cdot y \cdot \frac{I_{\text{GT-F}}}{(C_{\text{GT}})^2}}{\frac{(C_F)^2}{(C_{\text{GT}})^2} y^2 + 1},$$

where $y = (\int \beta) / (\int \beta \sigma)$.

In Fig. 2 we have plotted A as a function of y for $(C_F/C_{\text{GT}})^2 = 0.8$ and for different values of $I_{\text{GT-F}}/(C_{\text{GT}})^2$. The experimental result is indicated in the figure. It is apparent that $I_{\text{GT-F}}$ has the same sign as y .

Since $I_{\text{GT-GT}} < 0$ and $I_{\text{F-F}} < 0$ (6), we conclude that $C_F(\int \beta)$ and $C_{\text{GT}}(\int \beta \sigma)$ have opposite signs if they are real. Furthermore

$$I_{\text{GT-F}} = -C_F/C_{\text{GT}} = +0.9 \quad \text{for} \quad C'_T = -C_T, \quad C'_A = C_A, \quad C'_S = -C_S$$

and $C'_V = C_V$ if we accept ST or VA combinations only (*). This contradicts recoil experiments on ${}^6\text{He}$ (7) and ${}^{35}\text{A}$ (8) which favor T and V respectively.

(6) M. DEUTSCH *et al.*: in press; F. BOEHM *et al.*: in press.

(*) We have chosen the relative sign of the coupling constants in agreement with experiments on polarized neutrons. (V. L. TELEGDI: private communication).

(7) B. M. RUSTAD and S. L. RUBY: *Phys. Rev.*, **97**, 991 (1955); A. SZALAY and J. CSIKAI: *Padua Conference* (Sept. 1957).

(8) W. B. HERRMANNSFELDT, D. R. MAXON, P. STÄHELIN and J. S. ALLEN: *Phys. Rev.*, **107**, 641 (1957).

On the Rosenblum Spark Counter in Air.

L. DADDI and L. DE FRANCESCHI

*Laboratorio di Fisica dell'Accademia Navale - Livorno**Laboratorio di Fisica del C.A.M.E.N. - Livorno*

(ricevuto il 12 Dicembre 1957)

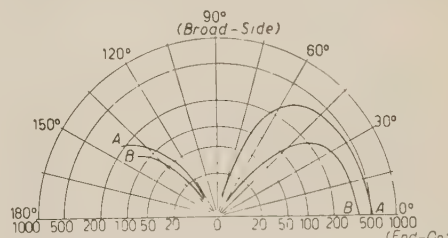
The Rosenblum spark counters in air still need a systematic study account to fix their limits of actual utilization and to clear the reasons for the existence of some contradictions in the mechanism of their performance (1-4).

We have adopted the rod-wire geometry, as done by CONNOR, EICHHOLZ *et al.* Wire and rod are mounted on a plexiglass support, in such a way as to make it possible to use wires and rods with various diameters. Micrometric screws allow, with useful foresight, to stretch the wire and to realize a gap width of up to three millimeters.

The wire is directly connected to the high positive voltage and the rod is grounded through a resistance in the order of a few, or of a few tenths of megohms, with a hundred picofarad shunt capacitor. This network serves to extinguish the sparks and a resistance

divider reduces conveniently the pulses to be handled by a scaler. A microammeter between the RC circuit and the ground can be utilized to read the corona current, by working the counter essentially in the corona region.

The insensitivity to β and γ radiation and cosmic rays, the very small sensitive volume to α -particles and the absence of spurious counts make nearly zero the background of these counters. Using α -particles the counting rate depends strongly on the arrival direction on the sensible volume.



(1) W. Y. CHANG and S. ROSENBLUM: *Phys. Rev.*, **67**, 222 (1945).

(2) R. D. CONNOR: *Proc. Phys. Soc.*, **64** B, 30 (1951).

(3) G. G. EICHHOLZ: *Nucleonics*, **10**, 10, 46 (1952).

(4) N. R. SAHA and N. NATH: *Nucleonics*, **15**, 6, 94 (1957).

Fig. 1. — Variation of efficiency with angle; (Count - min^{-1} , for Spacing wire, rod 2 mm) Curve A; \varnothing wire 100 μm ; Curve B: \varnothing wire 50 μm .

The results of these observations are reported in a polar coordinate plot in Fig. 1, where the angle $\varphi=0$ indicates

the direction perpendicular to the parallel axes of the wire and of the rod, in their plane (« end-on » for CONNOR) and the angle $\varphi = \pi/2$ the normal direction to that and to the wire (« broad side »).

The values have been obtained with a collimated ^{210}Po source arranged at a distance less than the range of the α -particles in air; as it can be seen we have found a counting-rate of nearly zero in the broad-side direction, compared to the end-on one. A different behaviour, but not always well reproducible, is verified when the α -particles reach the counter near the end of their path.

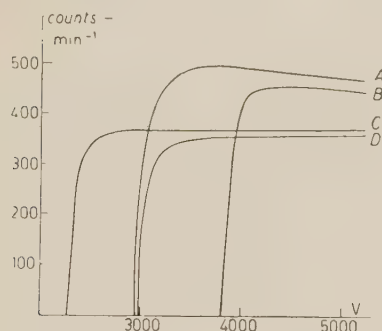


Fig. 2. — Voltage characteristic.

Curve A: \varnothing wire 100 μm Spacing wire-rod 1 mm.
 Curve B: \varnothing wire 100 μm Spacing wire-rod 2 mm.
 Curve C: \varnothing wire 50 μm Spacing wire-rod 1 mm.
 Curve D: \varnothing wire 50 μm Spacing wire-rod 2 mm.

In Fig. 2 are reported the counting rate versus the applied voltage diagrams in different conditions, but all obtained under end-on irradiation. The very good plateau is evident: it, of course, starts from lower voltages with fine wires, while it reaches higher values with large wires, and depends moreover strongly on wire-rod spacing, because of the influence that these elements exercise on the field intensity in the gap and on the onset value of the corona current.

The shape of the diagrams is more similar to that found by Connor than that by Eichholz, which are quite different between them.

In these diagrams the abscissae are the applied voltages V , but really an effective voltage $V' = V - RI$ is established to the counter, R being the external resistance and I the corona current in absence of gap irradiation. V' is a linearly increasing function of V , with the slope decreasing for the greatest values of R . Therefore we have not verified the existence of a « critical resistance » and of the negative slope as found by others (4).

Generally V' will depend also on the wire diameter and the gap width.

We have verified that these counters have the doubtless advantages already remarked by other authors. It appears that their main features are generally good and well reproducible, because they are not critically dependent on less controllable work conditions.

We can understand the sparking mechanism if we consider that the electrostatic field is strongly non-uniform and that the counter operates in the air. If the applied potential is a little smaller to onset of corona current, the field configuration allows the avalanche formation only in a region near enough the wire, extended not more than one third of the gap.

In this region the electrostatic field E_0 is greater than 30 kV/cm, so that the α Townsend coefficient in the air is appreciable and the attachment is negligible. For these conditions the electric field E_s due to the space charge of an avalanche can be found to be

$$E_s = \frac{4\epsilon\alpha \exp[\int \alpha dx]}{3r},$$

where ϵ is the electronic charge, r is the average radius of the avalanche and the integral is extended over the whole path travelled by it.

E_s always results several hundred times less than E_0 , and therefore the Meek criterion insures that a transition from a single avalanche to a streamer, that is the spark formation, is not possible. The contrary occurs in certain parallel plate counters, filled with special mixtures (5).

When the self-sustaining corona is established, a space charge is stationary near the wire, by which the electrostatic field is altered. Nevertheless E_s always remains less than $E_0/10$ and the Meek criterion is not satisfied, as the counter insensibility under the slightly ionizing radiations confirms.

An α , or another heavily ionizing particle, incident from end-on direction,

delivers along a field tube so great deal of neighbouring electrons that their avalanches do not independently increase. The sum of the space charges and the strong electric fields among the consecutive avalanches can make easy the development of a collective streamer. The probability of such a mechanism is clearly decreasing as the angle of the ionized track with the field lines increases. The fact justifies the least verified efficiency for the broad side direction.

A most detailed exposition of all experimental results and a most complete theoretical interpretation will be the subjects of a next paper.

* * *

We thank Prof. T. FRANZINI for the helpful discussions and Mr. R. BOTTAI for technical assistance.

(5) F. BELLA and C. FRANZINETTI: *Nuovo Cimento*, **10**, 1461 (1953).

Mass Selection Rules in the Bilocal Theory - II.

E. MINARDI

*Società Nazionale Cogne - Aosta
Istituto Nazionale di Fisica Nucleare - Sezione di Torino*

(ricevuto il 18 Dicembre 1957)

It is the purpose of this letter to show that the strangeness quantum number S of the elementary particles follows in a very simple way from the bilocal theory of the elementary particles previously developed ⁽¹⁾ and that the majority of the unobserved particles predicted in the last work ⁽²⁾ are excluded because strangeness is not conserved in their production in a $\pi + N$ reaction.

Let us consider the particles at rest and let us define the following internal operator

$$(1) \quad J_{\lambda\mu} = i \left(\eta_\mu \frac{\partial}{\partial \eta_\lambda} - \eta_\lambda \frac{\partial}{\partial \eta_\mu} \right),$$

from which the two vectors

$$(2) \quad \mathbf{M} = (J_{23}, J_{31}, J_{12}),$$

$$(3) \quad \mathbf{N} = (J_{01}, J_{02}, J_{03}) =$$

$$= \left(\frac{1}{i} J_{41}, \frac{1}{i} J_{42}, \frac{1}{i} J_{43} \right),$$

⁽¹⁾ E. MINARDI: *Nuovo Cimento*, **11**, 694 (1954); **12**, 950 (1954); **3**, 968 (1956); **4**, 1127 (1956).

⁽²⁾ E. MINARDI: *Nuovo Cimento*, **7**, 715 (1958). Hereafter referred as I.

can be obtained. It is well known from the theory of the representation of the homogeneous Lorentz group ⁽³⁾ that the three operators M_3 , \mathbf{M}^2 , \mathbf{N}^2 can be simultaneously diagonalized. In our bilocal theory \mathbf{M} is the total internal angular momentum and we shall now see that \mathbf{N}^2 can be very closely related with the strangeness quantum number.

The \mathbf{N}^2 operator is:

$$(4) \quad \mathbf{N}^2 = -\eta_0^2 \Delta \eta - \sum_1^3 \eta_k \frac{\partial^2}{\partial \eta_0^2} - \sum_1^3 \eta_k \frac{\partial}{\partial \eta_k} - 3\eta_0 \frac{\partial}{\partial \eta_0} - 2\eta_0 \sum_1^3 \eta_k \frac{\partial^2}{\partial \eta_k \partial \eta_0},$$

$$(\eta_0 = -i\eta_4).$$

In order to discuss the properties of the \mathbf{N}^2 -eigenvalues we must remember that in the bilocal theory previously developed the supplementary condition

$$(5) \quad \sum_\nu \frac{\partial^2}{\partial x_\nu \partial \eta_\nu} \psi(x, \eta) = 0,$$

must be added to the fundamental bi-

⁽³⁾ See for example: W. PAULI: *Continuous Groups in Quantum Mechanics*, CERN 56-31, Theoretical Study Division.

local equations, so that if $\psi(x, \eta) = f(x)\varphi(\eta)$, one must have in the rest system of the particle

$$(6) \quad \frac{\partial \varphi}{\partial \eta_0} = 0.$$

In order to satisfy conditions (5) or (6) we have considered the solutions of the bilocal equation in an iperplane $\eta_0=0$, so that the internal function does not depend on η_0 .

However, condition (5) or (6) can be likewise satisfied if one puts $\eta_0=A$, where A is an arbitrary real constant. Due to the arbitrariness of this constant, the eigenvalues of the \mathbf{N}^2 operator, which depend on η_0 as it is seen from (4), are not fixed by the theory, unless a further condition is introduced to fix the constant A . In order to give this condition we remind that the \mathbf{N}^2 -eigenvalues can be obtained with the relation

$$(7) \quad \mathbf{N}^2 = -2F + \mathbf{M}^2.$$

In the above formula \mathbf{M}^2 is the square of the internal angular momentum operator and $2F$ is an invariant given by the relation (3)

$$(8) \quad 2F = j_0^2 - 1 - \nu^2,$$

where j_0 is the minimum j value of the j representation, i.e. $j_0=0$ for bosons and $j_0=\frac{1}{2}$ for fermions; ν is an arbitrary constant which, in order to obtain an hermitian representation, must be real. However, we note that in the case $j_0=0$ the representation remains hermitian even with a purely imaginary ν , provided that ν^2 satisfies the condition

$$(9) \quad \nu^2 \geq -1 - j(j+1).$$

The \mathbf{N}^2 -eigenvalues corresponding to a particle with a given j value are:

$$(10) \quad \langle \mathbf{N}^2 \rangle = -j_0^2 + 1 + \nu^2 + j(j+1).$$

Now our condition is the following:

we put

$$(11) \quad \nu^2 = \pm (2n - 1)^2 + B,$$

where the positive or negative sign corresponds to the Bessel functions of positive or negative order respectively and $n (=1, 2, \dots)$ is the position number of the zero corresponding to the considered mass in the increasing succession of all zeros of the $J_{k+\frac{1}{2}}$ Bessel function of the particle (with $k=j$ in the case of bosons and $k=j-\frac{1}{2}$ in the case of fermions). The constant B must be determined in such a way that the \mathbf{N}^2 -eigenvalue of the first allowed boson or fermion (by the selection rule proposed in I) with lowest mass and internal angular momentum, i.e. the pion and the nucleon, is normalized to zero. Then, as it can be readily seen, we get $B=0$ for bosons and $B=-53/2$ for fermions.

The \mathbf{N}^2 -eigenvalues of the particles allowed by the mass selection rule given in I, are listed in Tables I and II of this work.

The relation between $\langle \mathbf{N}^2 \rangle$ and the usual strangeness S is:

$$(12) \quad S = \pm \left(\frac{\langle \mathbf{N}^2 \rangle}{8} \right)^{\frac{1}{2}}.$$

The positive sign must be attributed to antiparticles, in order to be in accordance with the conventional definition of S .

Let us now calculate the value of \mathbf{N}^2 for a given system of particles. For this purpose we note first that the N_1 , N_2 , N_3 operators, which give the components of the \mathbf{N} vector, cannot be diagonalized simultaneously with the \mathbf{M}^2 , \mathbf{N}^2 and M_3 operators. Then the direction and the sense of the \mathbf{N} vector of a particle is not determined and only its intensity $\sqrt{\langle \mathbf{N}^2 \rangle}$ is given. It follows that, when a many particle system is considered, the \mathbf{N} vector of this system, i.e. the sum of the \mathbf{N} vectors of the single particles of the system, is not determined, not only in direction and sense, but even in intensity, unless an

additional hypothesis is made on the way for summing up together the N vectors of the single particles of the system. We introduce now the hypothesis that the N vectors of all particles are parallel and the N vectors of all antiparticles

necessary to fix the first allowed boson or fermion with lowest mass and internal angular momentum, i.e. to fix the normalization constant B . Conservation of strangeness does not contradict this selection rule at least as far as the part-

TABLE I. — *Bosons.*

Mass	n	j	$\langle N^2 \rangle$	Conservation of strangeness in the production with a $\pi + N$ reaction
972	1	2	8	possible
2390	2	6	52	impossible
2975	3	6	68	impossible
2615	4	2	56	impossible

TABLE II. — *Fermions.*

Mass	n	j	$\langle N^2 \rangle$	Conservation of strangeness in the production with a $\pi + N$ reaction
1578	1	9/2	0	possible (with associated π)
1965	1	13/2	24	impossible
2185	2	9/2	8	possible (with one associated K)
2600	2	13/2	32	possible (with two associated K)
2310	3	5/2	8	possible (with one associated K)
2860	4	5/2	32	possible (with two associated K)

are antiparallel to the N vectors of particles. With this hypothesis the direction and the sense of the N vector of a system of particles remain obviously undetermined, but his modulus is given by the absolute value of the sum of the moduli of the N vectors of the particles minus the sum of the moduli of the N vectors of the antiparticles.

With the preceding hypothesis one has that conservation of the modulus of N leads to the same results as conservation of strangeness; moreover the unobserved particles predicted in I, with the exception of a 2360 m_e hyperon with $S=-2$ and of a very unpleasant 1578 m_e fermion with $S=0$, are excluded by non-conservation of the modulus of N , as possible products of a $\pi + N$ reaction.

The mass selection rule given in I is

icles listed in Tables I and II of I are concerned; once the normalization constant is fixed all particles excluded in Tables I and II of I by the mass selection rule, can be also excluded by conservation of strangeness only.

The existence of the strangeness quantum number appears in such a natural way in the present bilocal theory that the author is now inclined to drop the reserves on the physical content of the theory suggested at the end of previous works: he is now rather inclined to express the opinion (4) that the theory has something to do with the physical reality.

(4) This opinion is also supported by the fact that in a further refinement of the bilocal theory of the electron, the mass of the electron can be calculated with a remarkable accuracy, as it will be shown in a successive work.

E M E N D A T I O N

J. M. COOK. — On the Vanishing of the Interaction Hamiltonian: *Nuovo Cimento*, **4**, 1585 (1956).

A. S. WIGHTMAN has pointed out that the commutator $[H, G]$ was incorrectly evaluated. The following is a derivation not using that expression.

For simplicity, take the interaction Hamiltonian density to be

$$H(\mathbf{x}_1, \mathbf{x}_2) = A(\mathbf{x}_1) \otimes \psi^+(\mathbf{x}_2) \psi(\mathbf{x}_2),$$

with $A(\mathbf{x}_1) = a^+(\mathbf{x}_1) + a(\mathbf{x}_1)$ an (improper) operator on \mathfrak{F}_1 , and $\psi^+(\mathbf{x}_2) \psi(\mathbf{x}_2)$ such an operator on \mathfrak{F}_2 .

In the n -particle subspace $\mathfrak{R}_1^{(n)}$ of \mathfrak{F}_1 ,

$$a^+(\mathbf{x}_1) f_1(\mathbf{y}_1, \dots, \mathbf{y}_n) = \frac{1}{\sqrt{n+1}} \sum_{i=1}^n \delta(\mathbf{y}_i - \mathbf{x}_1) f_1(\mathbf{y}_1, \dots, \mathbf{y}_{i-1}, \mathbf{y}_{i+1}, \dots, \mathbf{y}_{n+1}).$$

In the m -particle subspace $\mathfrak{R}_2^{(m)}$ of \mathfrak{F}_2 ,

$$\psi^+(\mathbf{x}_2) \psi(\mathbf{x}_2) f_2(\mathbf{z}_1, \dots, \mathbf{z}_m) = \sum_{j=1}^m \delta(\mathbf{z}_j - \mathbf{x}_2) f_2(\mathbf{z}_1, \dots, \mathbf{z}_m).$$

Let F_A be some form factor such that $F_A(\mathbf{x}) = 0$ if $|\mathbf{x}| > A^{-1}$. Then

$$\begin{aligned} & \left(\iint_{\sigma_1 \sigma_2} F_A(\mathbf{x}_1 - \mathbf{x}_2) a^+(\mathbf{x}_1) \otimes \psi^+(\mathbf{x}_2) \psi(\mathbf{x}_2) d\mathbf{x}_1 d\mathbf{x}_2 f_1 \otimes f_2 \right) (\mathbf{y}_1, \dots, \mathbf{y}_{n+1}, \mathbf{z}_1, \dots, \mathbf{z}_m) = \\ & = \frac{1}{\sqrt{n+1}} \sum_{i=1}^n \sum_{j=1}^m \iint_{\sigma_1 \sigma_2} F_A(\mathbf{x}_1 - \mathbf{x}_2) \delta(\mathbf{y}_i - \mathbf{x}_1) f_1(\mathbf{y}_1, \dots, \mathbf{y}_{i-1}, \mathbf{y}_{i+1}, \dots, \mathbf{y}_{n+1}) \cdot \\ & \quad \cdot \delta(\mathbf{z}_j - \mathbf{x}_2) f_2(\mathbf{z}_1, \dots, \mathbf{z}_m) d\mathbf{x}_1 d\mathbf{x}_2 = \\ & = \frac{1}{\sqrt{n+1}} \sum_{i=1}^n \sum_{j=1}^m F_A(\mathbf{y}_i - \mathbf{z}_j) f_1(\mathbf{y}_1, \dots, \mathbf{y}_{i-1}, \mathbf{y}_{i+1}, \dots, \mathbf{y}_{n+1}) f_2(\mathbf{z}_1, \dots, \mathbf{z}_m). \end{aligned}$$

Now define a projection $P_{i,j,A'}^{(n+1,m)}$ on the subspace $\mathfrak{N}_1^{(n+1)} \otimes \mathfrak{N}_2^{(m)}$ of $\mathfrak{F}_1 \otimes \mathfrak{F}_2$ by

$$(P_{i,j,A'}^{(n+1,m)} g)(\mathbf{y}_1, \dots, \mathbf{y}_{n+1}, \mathbf{z}_1, \dots, \mathbf{z}_m) = \begin{cases} g(\mathbf{y}_1, \dots, \mathbf{y}_{n+1}, \mathbf{z}_1, \dots, \mathbf{z}_m) & \text{if } |\mathbf{y}_i - \mathbf{z}_j| > A'^{-1}, \\ 0 & \text{if } |\mathbf{y}_i - \mathbf{z}_j| \leq A'^{-1}. \end{cases}$$

Then $P_{i,j,A'}^{(n+1,m)} F_A(\mathbf{y}_i - \mathbf{z}_j) f_1(\mathbf{y}_1, \dots, \mathbf{y}_{i-1}, \mathbf{y}_{i+1}, \dots, \mathbf{y}_{n+1}) f_2(\mathbf{z}_1, \dots, \mathbf{z}_m) = 0$ when $A' < A$.

If $P_{A'}^{(n+1,m)} = \prod_{i,j=1}^{n+1,m} P_{i,j,A'}^{(n+1,m)}$, then, a fortiori,

$$P_{A'}^{(n+1,m)} F_A(\mathbf{y}_i - \mathbf{z}_j) f_1(\mathbf{y}_1, \dots, \mathbf{y}_{i-1}, \mathbf{y}_{i+1}, \dots, \mathbf{y}_{n+1}) f_2(\mathbf{z}_1, \dots, \mathbf{z}_m) = 0,$$

so

$$P_{A'}^{(n+1,m)} \left(\int_{\sigma_1} \int_{\sigma_2} F_A(\mathbf{x}_1 - \mathbf{x}_2) a^+(\mathbf{x}_1) \otimes \psi^+(\mathbf{x}_2) \psi(\mathbf{x}_2) \psi(\mathbf{x}_2) d\mathbf{x}_1 d\mathbf{x}_2 \right) f_1 \otimes f_2 = 0,$$

if f_1 is in $\mathfrak{N}_1^{(n)}$ and f_2 in $\mathfrak{N}_2^{(m)}$, and $A' < A$.

Define $P_{A'} = \sum_{n,m=0}^{\infty} \bigoplus P_{A'}^{(n,m)}$. Then

$$P_{A'} \int_{\sigma_1} \int_{\sigma_2} F_A(\mathbf{x}_1 - \mathbf{x}_2) a^+(\mathbf{x}_1) \otimes \psi^+(\mathbf{x}_2) \psi(\mathbf{x}_2) d\mathbf{x}_1 d\mathbf{x}_2 = 0 \quad \text{for } A' < A.$$

Taking adjoints,

$$\int_{\sigma_1} \int_{\sigma_2} F_A(\mathbf{x}_1 - \mathbf{x}_2) a(\mathbf{x}_1) \otimes \psi^+(\mathbf{x}_2) \psi(\mathbf{x}_2) d\mathbf{x}_1 d\mathbf{x}_2 P_{A'} = 0 \quad \text{for } A' < A.$$

Thus, if we define

$$H_A = \int_{\sigma_1} \int_{\sigma_2} F_A(\mathbf{x}_1 - \mathbf{x}_2) A(\mathbf{x}_1) \otimes \psi^+(\mathbf{x}_2) \psi(\mathbf{x}_2) d\mathbf{x}_1 d\mathbf{x}_2,$$

we have shown $P_{A'} H_A P_{A''} = 0$ for $A' < A > A''$.

Now assume that $\lim_{A \rightarrow \infty} H_A = H_\infty$ exists, in some sense. Then $P_{A'} H_\infty P_{A''} = 0$. But $P_{A'} \rightarrow I$ as $A' \rightarrow \infty$ (since the set of all $(\mathbf{y}_1, \dots, \mathbf{y}_{n+1}, \mathbf{z}_1, \dots, \mathbf{z}_m)$ with $\mathbf{y}_i = \mathbf{z}_j$ is of Lebesgue measure zero), so $H_\infty P_{A''} = 0$.

We also assume that H_∞ is self-adjoint. Let g be any vector in $\mathfrak{F}_1 \otimes \mathfrak{F}_2$. Then $P_{A'} g$ is in the domain of H_∞ (since $H_\infty(P_{A'} g) = 0$) and $H_\infty(P_{A'} g) \rightarrow 0$ as $A'' \rightarrow \infty$. Further, $P_{A'} g \rightarrow Ig = g$, so g is the domain of H_∞ and $H_\infty g = 0$ (since H_∞ is closed).

Therefore, $H_\infty = 0$.

LIBRI RICEVUTI E RECENSIONI

Annual Review of Nuclear Science.
Vol. 6 (1956). Published by Annual Reviews, Inc., Palo Alto, California U.S.A., pp. 471.

Il volume contiene 13 monografie di diversi autori ciascuna delle quali costituisce una rassegna aggiornata ed abbastanza completa del soggetto trattato. Utili sono anche le bibliografie riferite ai termini di ciascuna delle 13 rassegne.

— La prima monografia riguarda le « Variazioni temporali della radiazione Cosmica Primaria », ed è scritta da V. SARABHAI e N. W. NERURKAR, del Physical Research Laboratory, Ahmedabad, India. È un aggiornamento fino alla fine del 1955 della rassegna fatta sullo stesso soggetto da H. ELLIOT nel 1952 nel noto libro « *Progress in Cosmic Ray Physics* ».

— La seconda monografia di L. WOLFENSTEIN, Departement of Physics, Carnegie Institute of Technology, Pittsburgh, Pennsylvania, riguarda la « Polarizzazione dei nucleoni veloci ». L'interesse crescente che hanno nel campo delle alte energie e fasci di particelle polarizzati, rende particolarmente utile la lettura di questa rassegna. In essa si trova descritto il formalismo teorico usato per analizzare tali fasci polarizzati, nonchè i risultati sperimentali ottenuti tra i 100 e i 400 MeV sino all'Aprile 1956.

— La terza monografia di N. P. HEYDENBURG e G. M. TEMMER (Departement of Terrestrial Magnetism, Car-

negie Institute of Washington, D. C.) riguarda la « Eccitazione di nuclei da parte di particelle cariche ». Vi vengono discusssi i processi di eccitazione di nuclei in livelli bassi di energia (< 1 MeV) da parte del campo Coulombiano dovuto a particelle cariche in movimento, in particolare da parte di particelle pesanti. La bibliografia è aggiornata al Marzo 1956.

— J. G. MACK (Dep. of Physics, Univ. Wisconsin, Madison USA) e H. ARROE (Dep. of Physics, Montana State College, Bozeman, USA) nella quarta monografia passano brevemente in rassegna gli « Spostamenti isotopici negli spettri atomici ».

— La quinta monografia a cura di un gruppo di ricercatori del Nuclear Data Group, National Research Council, Washington (i nomi sono: K. WAY, D. N. KUNDU; C. L. MC GINNIS; R. VAN LIESHOUT) contiene una rassegna sulle « Proprietà nucleari dei nuclei di peso medio ($40 < A < 140$) ». Per questi nuclei sono riportati i valori degli: « Spin nello stato fondamentale »; « Momenti magnetici »; « Momenti di quadrupolo »; « Livelli »; « Vite medie comparative per quanti gamma »; ed una appendice sui modelli nucleari.

— La sesta monografia riguarda la « Acidità generalizzata nelle separazioni radiochimiche » ed è dovuta a R. A. HOME; C. D. CORYELL (Dep. of Chemistry and Lab. Nuclear Science, Massachusetts Inst. for Technology Cambridge).

ed a L. S. GOLDRING (Radiochemistry Section, Nuclear Developement Co. of America, White Plains, New York).

— I valori delle « Masse dei Nuclidi leggeri » sono riportati criticamente nella settima monografia, dovuta a J. MATTAUCH, L. WALDMANN, R. BIERI, F. EVERLING (Max. Planck Institut fur Chemie, Mainz, Germania).

— Nella ottava monografia H. BROOKS (Division of Engineering and Applied Physics, Harvard University, Cambridge, Massachusetts) fa una ampia rassegna degli « Effetti sui solidi delle radiazioni Nucleari ». Vengono considerati in particolare gli effetti sulla grafite, uranio, semiconduttori, metalli in generale.

La rassegna è completata da una ampia bibliografia.

— La nona monografia dovuta a H. TAUBE (Dep. of Chemistry, University of Chicago, Illinois) riguarda la « Applicazione degli isotopi dell'ossigeno negli studi di chimica », con particolare riguardo allo studio dei fenomeni chimici nelle soluzioni omogenee.

— I « Recenti progressi nelle tecniche di conteggio a basso livello » sono riferiti nella decima monografia di E. C. ANDERSON e F. N. HAYES (Biomedical Research Group, Los Alamos Scientific Lab. — New Mexico). Il problema di conteggi di eventi nucleari ad un livello molto basso rispetto al livello del fondo si presenta in molti campi come: studi in biologia e chimica mediante traccianti; datazione archeologica e geologica; ricerche sulla radioattività naturale ed artificiale; studio delle particelle elementari. Nella rassegna vengono discussi alcuni problemi particolari come: conteggio di radiazione beta da Carbonio 14, e da Trizio, conteggi di gamma da Berillio 7; doppio decadimento beta; rivelazione del neutrino.

— La undicesima monografia è dedicata ad una ampia rassegna aggiornata al Giugno 1956 dei reattori di potenza in costruzione o progetto nei vari paesi del mondo, con una breve descrizione

delle caratteristiche peculiari di ciascun progetto. La rassegna è scritta da L. DAVIDSON, W. L. LOEB, G. YOUNG della Nuclear Development Corporation of America, White Plains, New York.

— La dodicesima e tredicesima monografia sono dedicate a problemi di radiobiologia. La prima riguarda la « Radiobiologia cellulare » ed è dovuta a L. H. GRAY del British Empire Cancer Campaign Research Unit in Radiobiology — Northwood, Middlesex — England. La seconda riguarda la « Radiobiologia dei vertebrati: ambiologia » ed è dovuta a J. P. O'BRIEN del Departement of Biology, Marquette University, Milwaukee, Wisconsin. Entrambe le rassegne sono dotate di una ampia bibliografia.

I. FEDERICO QUERCIA

D. R. HARTREE — *The Calculation of Atomic Structures*, New York, John Wiley & Sons, Inc., London, Chapman & Hall, Ltd, 1957, — III, 181, \$ 5.00.

Questo volume di D. R. HARTREE è basato su una serie di lezioni date dall'autore all'Haverford College nel 1955 e successivamente ripetute all'Università di Princeton.

Lo scopo del volume è di presentare una trattazione dettagliata dei metodi numerici per il calcolo delle strutture atomiche. Finora non esisteva alcuna opera di tale genere.

Occorre precisare subito che il volume è scritto all'unico fine pratico di suggerire i metodi di approssimazione ritenuti più convenienti per il calcolo dei livelli e delle funzioni d'onda atomiche. Questioni fisiche fondamentali o considerazioni a carattere formale sono quindi deliberatamente evitate.

Il primo capitolo, introduttivo, riprende l'equazione di Schrödinger, lo spin, il principio di Pauli, e descrive

l'approssimazione a particelle indipendenti ed il concetto di configurazione.

Il secondo capitolo tratta del metodo variazionale per lo stato fondamentale e per gli stati eccitati e ne contiene l'applicazione all'atomo di elio con una funzione d'onda separabile nei due elettroni.

Il terzo capitolo contiene la derivazione dell'energia totale per configurazioni di gruppi completi. Per il caso particolare in considerazione di strutture atomiche viene riportata la riduzione degli integrali secondo Slater e sono anche riportate tavole dei principali coefficienti di Slater. Il principio variazionale permette quindi la derivazione delle equazioni di Fock, che vengono anche esibite sotto forma integrodifferenziale. Vengono accennate le varie approssimazioni di tali equazioni con e senza termini di scambio.

Il capitolo quarto è dedicato ai procedimenti numerici per integrazione di equazioni differenziali: le varie formule per quadratura, ed in particolare il procedimento di Numerov per equazioni lineari del secondo ordine e quello di Fox-Goodwin per equazioni lineari del primo ordine.

L'applicazione dei metodi descritti nel capitolo quarto alle equazioni già ricavate per le funzioni d'onda radiali è descritta nel capitolo quinto, che contiene numerosi suggerimenti pratici per l'effettiva computazione.

Il capitolo sesto è dedicato al caso formalmente più complesso delle configurazioni che comprendono gruppi incompleti. Viene svolto l'accoppiamento di Russel-Saunders ed illustrata la gerarchia in termini, livelli e stati. La derivazione dei vari termini (LS) provenienti da una configurazione e la derivazione dell'espressione dell'energia per i vari termini (LS) è svolta secondo il metodo di Slater. Vengono quindi ricavate le equazioni di Fock per gruppi incompleti.

Il capitolo settimo sviluppa procedi-

menti per discutere la variazione delle funzioni d'onda e dei campi atomici al variare di Z . Inoltre viene discusso il comportamento delle soluzioni per $Z \rightarrow \infty$. L'approssimazione di Thomas-Fermi è solo accennata.

Nel capitolo ottavo vengono ricavate espressioni per le differenze di energia per i vari termini e discusse nel caso speciale di un gruppo incompleto ed, in particolare, consistente di una sola funzione d'onda.

Il capitolo nono tratta molto brevemente della estensione relativistica, mediante l'equazione di Dirac.

Infine il capitolo decimo intitolato « Approssimazioni migliori », accenna agli altri metodi che partendo direttamente dal principio variazionale e da considerazioni di invarianza rigettano il concetto di configurazione. Viene discusso con maggiore dettaglio il tentativo di superare le limitazioni del concetto di configurazione introducendo superposizioni di configurazioni, che porta al « configuration mixing », tanto importante nel caso dei modelli a shell nucleari.

Le tre appendici contengono riferimenti bibliografici, tabelle di funzioni d'onda e cenni su alcuni nuovi sviluppi.

In conclusione vorremmo dire che è fuori discussione che questo volume sarà molto utile a tutti coloro, fisici, chimici, astrofisici che dovranno calcolare per un motivo o per l'altro particolari strutture atomiche. Non è pertanto un volume da suggerire allo studente che voglia arricchire la sua cultura di fisica o di matematica. Dato il suo fine eminentemente pratico sarà però presumibilmente di grande aiuto a coloro che eseguono calcoli in questo campo.

Dovendo recensire da un punto di vista critico vorremmo dire che ci ha recato un certo disagio il fatto che alcune notazioni sono diverse da quelle usuali (per esempio le armoniche sferiche sono designate con la lettera S , il numero atomico con N). Inoltre riteniamo comunque un difetto del volume quello di

non riportare il metodo algebrico di Racah per ricavare l'energia dei vari termini (L, S) per una data configurazione. È noto che il metodo di Racah permette tra l'altro di superare alcune limitazioni del metodo di Slater dando per esempio espressioni separate per l'energia di due possibili termini con stesso (LS) originanti da una data configurazione. È vero che il metodo di Racah è più complicato formalmente. Poichè d'altra parte esso costituisce un definitivo contributo alla fisica matematica, difficilmente ignorabile in problemi in cui intervengono simmetrie rispetto al gruppo di rotazione, riteniamo che l'aggiunta di alcuni capitoli dedicati ad esporre la necessaria algebra avrebbe reso il volume molto più utile e completo.

R. GATTO

J. L. DESTOUCHES — *La quantification en théorie fonctionnelle des corpuscules* — Paris, Gauthier Villars, 1956 pag. vi-141.

In questo volume l'autore discute in forma preliminare una possibile teoria quantistica inspirata ad idee originariamente dovute a L. DE BROGLIE. L'esigenza che spinge l'autore in questo tentativo è quella di introdurre una rappresentazione del sistema che sia « obbiettiva » e non « soggettiva », quale quella fornita nella ordinaria — a tutt'oggi valida — meccanica quantistica in cui la ψ esprime la conoscenza che noi abbiamo del sistema mediante le nostre misure. L'autore propone pertanto di rappresentare un corpuscolo con una funzione u , detta onda fisica. Previsioni sul sistema possono ottenersi mediante un funzionale della u e del tempo, detto onda funzionale. La quantificazione si dovrà esprimere a partire dagli elementi « obbiettivi ». Però, una volta portata a termine la quantificazione, si trova che ciò

che ne risulta è la solita meccanica ondulatoria. Ove allora si prendano in considerazione le possibili soluzioni non quantizzate si ha uno schema più ampio della ordinaria meccanica quantistica. Questo fa sperare all'autore che sia possibile superare mediante la teoria funzionale dei corpuscoli « l'inadeguatezza delle teorie quantistiche usuali ai fini di una corretta e dettagliata descrizione dei fenomeni nucleari ». Naturalmente, le ragioni di tale inadeguatezza, del resto ben nota, non vengono meglio identificate nel volume.

R. GATTO

B. ROSSI — *Optics* Addison-Wesley, Reading (Mass.) pp. 510, fig. 361.

In questo libro vengono descritti i fenomeni ottici secondo uno schema molto proficuo dal punto di vista didattico.

Fin dall'inizio l'Autore sceglie il modello ondulatorio senza entrare però nei particolari della natura della luce: dopo una rapida digressione sui fenomeni ondulatori (ampliata nell'App. 2), introduce il principio di Huygens ed il concetto di onda e di raggio luminoso (cap. I) descrivendo così i tre fenomeni fondamentali dell'ottica geometrica (propagazione rettilinea, riflessione, rifrazione).

Nei capitoli II, III, IV e VI vengono descritti, con le loro applicazioni, i fenomeni ottici classici dovuti alla riflessione, rifrazione e propagazione della luce nei mezzi omogenei e non omogenei, isotropi ed anisotropi con i relativi fenomeni di diffrazione, interferenza e polarizzazione. Nel cap. IV meritano un particolare rilievo lo studio dei reticolati spaziali, come ampliamento dei normali reticolati di diffrazione ad una e due dimensioni, e la microscopia in contrasto di fase. Nel cap. V sono delineate nelle loro linee essenziali le questioni sulla velocità della luce sia nel vuoto, dalla determinazione

di Roemer fino all'esperienza di Michelson, che nella materia con la determinazione sperimentale della velocità di fase e di gruppo.

Nei capitoli VII e VIII si riconosce la natura e.m. della luce: dalle equazioni di Maxwell si dimostra l'esistenza di onde e.m. e si studia la radiazione emessa da una carica elettrica accelerata. Infine si riportano i principali fenomeni della emissione, propagazione e assorbimento delle onde e.m., dagli spettri atomici e molecolari alla rifrazione, dalla risonanza agli effetti elettrico e magneto-ottici.

Nell'ultimo capitolo si descrivono quei particolari fenomeni (effetto fotoelettrico, Compton, ecc.) che sono la giustificazione sperimentale del modello quantistico della luce.

Il libro termina infine con un rapido cenno alla meccanica ondulatoria.

Le due appendici (la A1 sulle formule matematiche adoperate nel testo e la A2 sulle onde meccaniche) si possono considerare come una premessa necessaria ad una corretta interpretazione dei fenomeni ottici descritti secondo lo schema dell'Autore: esse potrebbero perciò costituire un'ottima introduzione al libro.

L'appendice A3 sul campo e.m. di una carica puntiforme in moto assume un particolare aspetto attuale, benchè forse essa sia troppo rapidamente accennata.

Nell'appendice A4 sono riportati alcuni dati numerici, ovviamente limitati; essi sono stati scelti in modo da concretare quantitativamente i principali fenomeni descritti nel testo.

Il libro è completato da numerosi problemi alla fine di ogni capitolo. Ciascun problema è stato accuratamente risolto dall'Autore e le soluzioni sono riportate in parte alla fine del libro ed in parte in un fascicolo separato, e ciò per uno scopo evidentemente didattico.

L'esposizione risulta dovunque chiara e semplice ed anche nei punti dove la trattazione matematica sembra dover

prevale, l'Autore non fa dimenticare mai che si tratta di fenomeni fisici.

I disegni, molto numerosi nel testo, sono particolarmente curati; la rappresentazione prospettica e l'uso continuo di tratteggi diversi per le diverse parti contribuiscono ad una rapida visualizzazione dei fenomeni.

In definitiva questo libro risulta un ottimo testo dal punto di vista didattico: nello stesso tempo si può ritenere come un manuale veramente prezioso per chi desidera avere a portata di mano un trattato che compendi, nelle loro linee essenziali, i principali fenomeni ottici.

R. CIALDEA

F. G. TRICOMI - *Equazioni a derivate parziali*. Edizione Cremonese, Roma 1957 pag. XII-392. L. 5500.

Questo nuovo volume di TRICOMI è una rielaborazione di un corso di lezioni tenute dall'autore all'Università di Torino, ed a suo tempo pubblicate in edizione litografica.

La trattazione è suddivisa in quattro capitoli, il primo dedicato alle equazioni del primo ordine ed alla teoria delle caratteristiche ed i tre successivi alle equazioni di tipo iperbolico, ellittico e parabolico rispettivamente. L'ultimo capitolo contiene anche una sufficiente discussione delle equazioni di tipo misto.

Il primo capitolo parte dalla rappresentazione geometrica delle equazioni del primo ordine a derivate parziali mediante i coni di Monge e tutta la discussione successiva viene svolta essenzialmente su queste basi intuitive allo scopo di rendere familiare l'importante concetto di caratteristica per equazione a derivate parziali. Il capitolo contiene anche la discussione della teoria di Hamilton-Jacobi, degli equivalenti principi variazionali, delle parentesi di Poisson e di Jacobi, e contiene come applicazione l'esempio del problema dei due corpi.

Il capitolo secondo contiene la discussione del metodo di integrazione in catena di Laplace che viene applicato alla equazione di Euler-Poisson. Vengono quindi discussi l'equazione delle onde ed i diversi metodi di integrazione (con purtroppo solo breve cenno al metodo della trasformazione di Laplace). Sono esaurientemente trattati il problema di Goursat, il metodo d'integrazione di Riemann, il metodo delle differenze finite. Il moto dei fluidi compressibili viene preso come esempio di applicazione della teoria. Viene anche discussa l'equazione delle onde in spazi a più dimensioni.

Le equazioni di tipo ellittico sono studiate nel capitolo terzo. Vengono mostrati gli importanti teoremi di unicità, la formula di Green assieme a brevi cenni sulla proprietà delle funzioni di Green, il problema di Dirichlet (risolto nel caso dell'ipersfera). Notevole per semplicità la dimostrazione del teorema di esistenza per il problema di Dirichlet mediante le funzioni subarmoniche (le cui proprietà vengono più completamente esaminate in un paragrafo successivo). Naturalmente il capitolo contiene anche una sufficiente trattazione della teoria del potenziale (svolta anche col metodo delle

equazioni integrali), dei vari problemi al contorno, ed una applicazione al moto dei fluidi incompressibili.

Una prima metà del capitolo quarto descrive i teoremi di unicità per le equazioni di tipo iperbolico, il teorema di Green per l'equazione del calore, con le solite applicazioni alla barra infinita e con un cenno al metodo delle differenze finite. La seconda metà è dedicata alle equazioni di tipo misto, alla cui teoria l'autore ha dedicato importanti contributi. Vengono esaminate in dettaglio le proprietà della equazione di Tricomi, importante nella aerodinamica transsonica.

Riteniamo che questo libro di TRICOMI riuscirà molto gradito ai fisici, sperimentali e teorici. Non è probabilmente un libro adatto per consultazioni. Possibilmente va letto invece di seguito, dalla prima all'ultima pagina. La sua lettura è facile e sostanziosa, assolutamente lontana da ogni forma di formalismi e soprattutto schiva di quella specie di compiacimento per il patologico, che è peraltro utile in molti casi, ma che rende spesso non conveniente per un fisico la lettura di tanti interessanti lavori di analisi.

R. GATTO